

School of Doctoral Studies in Biological Sciences
University of South Bohemia in České Budějovice
Faculty of Science

**Coordination of growth and cell cycle progression in
green algae**

Ph.D. Thesis

Ivan Nedyalkov Ivanov

Supervisor: **RNDr. Kateřina Bišová, Ph.D.**

Institute of Microbiology, Academy of Sciences of the Czech Republic

České Budějovice 2020

This thesis should be cited as:

Ivanov I. N., 2020: Coordination of Growth and cell cycle progression in green algae, Ph.D. Thesis Series No. 17. University of South Bohemia, Faculty of Science, School of Doctoral Studies in Biological Sciences, České Budějovice, Czech Republic, 172 pp.

Annotation:

Within the past century microalgae have gained importance both as model organisms in cell cycle research and as a biotechnological platform for the production of a variety of economically important compounds. This thesis examines the coordination of growth and cell cycle progression in green algae and attempts to explore the biotechnological relevance of some of the findings. Furthermore, the applicability of confocal Raman microscopy for both quantitative and qualitative analysis of storage biomolecules during the course of the cell cycle of *Desmodesmus quadricauda* is also investigated.

Temperature and light shift experiments showed that there is no direct correlation between growth and cell cycle progression in *D. quadricauda*. Further analysis revealed that supraoptimal temperature has a profound effect on the cell cycle of *Chlamydomonas reinhardtii* causing a block in cell division, increase of cell size and over accumulation of starch. Starch production through supraoptimal temperature was successfully demonstrated in pilot scale experiments, however it was estimated that light availability within the culture poses a major limiting factor. Confocal Raman microscopy was successfully applied for the quantitative and qualitative analysis of storage biomolecules including starch, lipids, polyphosphates and guanine.

Declaration [in Czech]

Prohlašuji, že svoji disertační práci jsem vypracoval samostatně pouze s použitím pramenů a literatury uvedených v seznamu citované literatury. Prohlašuji, že v souladu s § 47b zákona č. 111/1998 Sb. V platném znění souhlasím se zveřejněním své disertační práce, a to v úpravě vzniklé vypuštěním vyznačených částí archivovaných Přírodovědeckou fakultou elektronickou cestou ve veřejně přístupné části 3ale3ase STAG provozované Jihočeskou univerzitou v Českých Budějovicích na jejích internetových stránkách, a to se zachováním mého autorského práva k odevzdanému textu této kvalifikační práce. Souhlasím dále s tím, aby toutéž elektronickou cestou byly v souladu s uvedeným ustanovením zákona č. 111/1998 Sb. zveřejněny posudky školitele a oponentů práce i záznam o průběhu a výsledku obhajoby kvalifikační práce. Rovněž souhlasím s porovnáním textu mé kvalifikační práce s databází kvalifikačních prací Theses.cz provozovanou Národním registrem vysokoškolských kvalifikačních prací a systémem na odhalování plagiátů.

České Budějovice, 13.07.2020

Ivan N. Ivanov

This thesis originated from a partnership of Faculty of Science, University of South Bohemia, and Centre Algatech, Institute of Microbiology, Academy of Sciences of the Czech Republic, supporting doctoral studies in the Physiology and Developmental Biology study programme.



Přírodovědecká
fakulta
Faculty
of Science



Financial support

This work was supported by the Grant Agency of the Czech Republic (grant nos. 15-09231S, 19-12607S), by the Grant Agency of the University of South Bohemia (grant no. 036/2016/P), and the Ministry of Education, Youth and Sports of the Czech Republic (project no. EF16_027/0007990)

Acknowledgements

First and foremost, I would like to express my deep and sincere gratitude to my research supervisor and mentor, **Dr. Kateřina Bišová**. She allowed me to make my own mistakes and learn from them. She provided encouragement and consolation in my times of doubt. And lastly, she taught me what it means to be part of the constant pursuit of knowledge we call Science. For all of this, I am forever grateful.

I am also extremely grateful to **Dr. Vilém Zachleder**. I will always remember his sincerity, wisdom, patience, and never ending enthusiasm.

My appreciation also extends to **Dr. Maria J. Barbosa** and **Rick Wieggers**, who welcomed me in their group at Wageningen University and Research and made me feel at home.

I am also ineffably indebted to **Dr. Shigeyuki Kawano**, **Dr. Tsuyoshi Takeshita** and their whole group at Tokyo University for their outstanding hospitality during my stay in the land of the rising sun.

I would like to thank **Klára Kochtová** and **Kamila Ondrejmišková** for their indispensable help and technical assistance in my daily work.

A special mention goes to **Jana Sýkorová**, **Martín P. Caporgno**, **Veronika Kselíková**, **Vitali Bialevich**, **Vít Náhlík**, and **Zoltan Turoczy** who were always there for me when I needed a friendly advice or simply to have a chat.

Lastly, I would like to express my gratitude to my best friend and life partner, **Valentyna Kuznetsova**. She has been a constant source of unconditional love, support, inspiration and strength during all these years. Without her I wouldn't be who I am.

To all of you: thank you

На Мајка и Мамко

List of papers and author's contributions

The thesis is based on the following papers and manuscripts:

- I. **Ivanov I. N.**, Vítová M., Bišová K. (2019) Growth and the cell cycle in green algae dividing by multiple fission. *Folia Microbiologica* 64, 663-672, doi:10.1007/s12223-019-00741-z. (IF: 1.450)
I. N. Ivanov participated in writing of the manuscript.
- II. Zachleder V., **Ivanov I. N.**, Vítová M., Bišová K. (2019) Effects of cyclin-dependent kinase activity on the coordination of growth and the cell cycle in green algae at different temperatures. *Journal of Experimental Botany* 70 (3), 845-858, doi:10.1093/jxb/ery391. (IF: 5.090)
I. N. Ivanov participated in laboratory experiments, data evaluation and manuscript writing.
- III. Zachleder V., **Ivanov I. N.**, Vítová M., Bišová K. (2019) Cell cycle arrest by supraoptimal temperature in the alga *Chlamydomonas reinhardtii*. *Cells* 8 (10), 1237, doi:10.3390/cells8101237. (IF: 4.366)
I. N. Ivanov participated in laboratory experiments, data evaluation and manuscript writing.
- IV. **Ivanov I. N.**, Vítová M., Zachleder V., Barbosa M. J., Bišová K.: Starch production in *Chlamydomonas reinhardtii* through supraoptimal temperature treatment cultivated in a pilot-scale photobioreactor. (Manuscript in preparation)
I. N. Ivanov participated in laboratory experiments, data evaluation and manuscript writing.

- V. Moudříková Š., **Ivanov I. N.**, Nedbal L., Zachleder V., Bišová K., Mojzeš P.: Raman microscopy shows the distribution of starch, lipids, polyphosphate and guanine during the cell cycle of *Desmodesmus quadricauda*. (Manuscript in preparation)
I. N. Ivanov participated in laboratory experiments, data evaluation and manuscript writing.

Kateřina Bišová, the corresponding author of papers I, II, III, IV and the co-author of paper V, approves the contribution of Ivan N. Ivanov in these papers as described above.

RNDr. Kateřina Bišová, Ph.D.

Table of contents

Foreword		i
Chapter 1	General introduction	1
Chapter 2	Goals and hypotheses	45
Chapter 3	Growth and the cell cycle in green algae dividing by multiple fission	49
Chapter 4	Effects of cyclin-dependent kinase activity on the coordination of growth and the cell cycle in green algae at different temperatures	61
Chapter 5	Cell cycle arrest by supraoptimal temperature in the alga <i>Chlamydomonas reinhardtii</i>	77
Chapter 6	Starch production in <i>Chlamydomonas reinhardtii</i> through supraoptimal temperature treatment cultivated in a pilot-scale photobioreactor	97
Chapter 7	Raman microscopy shows the distribution of starch, lipids, polyphosphate and guanine during the cell cycle of <i>Desmodesmus quadricauda</i>	123
Chapter 8	Summary	163
About the author		171

List of abbreviations

cdc	cell division control
CDK	cyclin dependent kinase
CEO	chief executive officer
CH	carbon-hydrogen bonds
CP	commitment point
DAPI	fluorochrome 4',6-diamidine-2'-phenylindole dihydrochloride
DNA	deoxyribonucleic acid
DNSA	dinitrosalicylic acid
DM	dry matter
EDTA	ethylenediaminetetraacetic acid
EMS	ethyl methane sulfonate
EUR	Euro
GNU	GNU's not unix
G1	gap 1
G2	gap 2
HS	high salt
M	mitosis
MNNG	methylnitronitrosoguanidine
mRNA	messenger ribonucleic acid
S	synthesis
PhAR	photosynthetically active radiation
polyP	polyphosphates
PUFA	poly unsaturated fatty acid
RNA	ribonucleic acid
r. u.	relative units
T-DNA	transfer deoxyribonucleic acid
total P	total phosphates
USD	United States Dollar

Foreword

Dear reader,

I still remember the first time I saw microalgae being cultivated in a photobioreactor. The bright green colour of the *Scenedesmus* sp. culture that was cradled in the bottle, the uniform melody of the air pump and the dance of the air bubbles as they rose to the surface – it all seemed so beautiful to me. It was a simple system, it was teeming with life and in my eyes it held the potential to change the world. As a young (and maybe naive) student I immediately knew that this was what I wanted to do for the rest of my life. This is how my love story with microalgae began.

I soon realised that it took a multidisciplinary approach, if you wanted to study and understand the full potential of microalgae. You had to be in the same time a plant physiologist and a mechanical engineer. You had to have some knowledge of molecular biology and simultaneously grasp the fundamentals of economics. You had to be able to spend long hours meticulously analysing rows of samples in the lab and you also shouldn't shy away from dirty work in the hot sun.

While I consider it far from perfect, this thesis was comprised through the same multidisciplinary approach – it encompasses work in the lab, some hours under the hot sun and a considerable amount of time spent in front of the computer screen. An inherent property of such multidisciplinary approach is that the text at times feels uneven, leaping from one major topic to another. I did my best to smooth it all out; however I cannot help but feel that this sense of roughness is still lingering through some of the pages.

In the introductory chapter I attempt to provide the reader with a comprehensive theoretical overview of the concepts that are later to be examined. However, because of the large number and sometimes the complexity of topics, this overview is in the form of a concise summary. Because sometimes this lack of detail might feel like an oversimplification and in order to encourage further reading, whenever possible, I refer to

the works of other authors that treat the topic more thoroughly. In chapter II I summarize the goals of the experimental work in the form of four individual hypotheses that are tested in the research section of the thesis. In the course of my doctoral studies it was felt that the results of this thesis hold enough merit to be made available to the scientific community. Thus far, one theoretical and two of the experimental research papers have been published in peer reviewed journals and are presented in the form of article excerpts. The other two experimental chapters are in the form of article manuscripts that are yet to be submitted for publication. In the final chapter I make an effort to summarize the results of the individual experimental chapters and comment on the outcome of the hypotheses set in chapter II.

While I can take responsibility for a major share of the text hereafter, I cannot claim complete credit for all sections. This is especially true for work which originated through collaborations with both national and international partners. To help the reader with my involvement in a certain body of work and to pay rightfully deserved tribute to my colleagues and mentors, I have provided a complete list of co-authors in the beginning of each chapter. Furthermore, I need to recognize the invaluable input of my supervisor, Dr. Kateřina Bišová, who supported my efforts throughout the numerous revisions of this text and John D. Brooker who assisted with the language corrections and proof reading of the final draft.

Ivan N. Ivanov

České Budějovice, 13.07.2020

Coordination of growth and cell cycle progression in green algae

Chapter I

General introduction

Ivan N. Ivanov



1.1 Landmarks in eukaryotic cell cycle research

The cell cycle can be commonly defined as a regular sequence of cell growth and cell division events that dividing cells pass through (Curtis 1983). This, at first glance, simple notion is rooted within a set of concepts that can be dated as far back as the early days of cell theory. It should be pointed out that, as often stated, discoveries are not made in isolation and our current understanding of the eukaryotic cell cycle is based upon the foundations laid by countless pioneering individuals. However, the discoverer who is remembered by history is the one who presents his contribution in such a way that the discovery becomes accepted by the scientific world. Hence, the purpose of this section is to illustrate the pivotal moments of cell cycle research and some of the important names associated with them rather than to provide an extensive review of the literature on the topic. Other authors have produced more detailed works documenting different aspects of the history of the eukaryotic cell cycle research (Cvrckova 2018; Hajdu 2002; Hartwell 1991; Hunt et al. 2011; Nurse 2000).

The origins of modern cell cycle research can be traced back to the beginning of 19th century when cell theory was first established by M. Schleiden and T. Schwann stipulating that all living organisms are constituted by structural units called cells (Hajdu 2002). Several decades later R. Virchow building upon the works of others was the first to elucidate and publish the theory that every cell originated from another pre-existing cell (Cvrckova 2018). This was opposed to, the until then, prevailing notion of *de novo* generation according to which organisms arose from non-living matter (Paweletz 2001). At those early stages the first observations of cell division were made in plants, algae and mosses which is attributed to the fact that plant cell boundaries are easier to observe than in animal tissues (Cvrckova 2018).

In spite of the fact that plant cell nuclei were observed to disappear and reappear prior to cell division, a detailed description of mitosis was only possible with the advancements in microscopy techniques. During the

second half of the 19th century A. Schneider and W. Flemming were the first to describe in detail and publish their observations on the duplication of chromosomes and their distribution to daughter cell nuclei (Cvrckova 2018; Paweletz 2001).

Nuclear and cellular division, however, represents only a fraction of the lifetime of the cell. Cells spend the larger proportion of it accumulating macromolecules and cellular components, which ultimately leads to an increase in cytoplasm and results in growth of the cell as a whole (Harashima et al. 2013; Sablowski and Dornelas 2014; Pringle and Hartwell 1981). Further explanations about the processes that lead to cell division were therefore needed.

The next major landmark in the history of the cell cycle came shortly after World War II with the discovery of the structure of DNA by J. Watson and F. Crick (Watson and Crick 1953). During that time A. Howard and S. Pelc (Howard and Pelc 1953) used radioactive isotopes to label DNA in order to find out the exact time point during the lifetime of the cell when replication of genetic material took place. Their results showed that synthesis of DNA occurred well before mitosis and was both preceded and succeeded by periods of growth in which replication of the genetic material did not occur. This discovery led to the development of the now widely accepted model of the binary fission cell cycle (also known as the Howard and Pelc cell cycle model), which describes one of the most common ways of proliferating living cells in nature (Howard and Pelc 1953).

In the period between 1970 and 1971 L. Hartwell discovered a number of mutations in the genes of *Saccharomyces cerevisiae*, commonly known as budding yeast, which were responsible for control of the cell cycle. He pinpointed more than one hundred such genes and named them „cell division control“ genes or “cdc” genes for short. In the course of his work he identified the *cdc28*, or „start“ gene in *S. cerevisiae* that controls a crucial point at which cell cycle progression is regulated by extra- and intra-cellular signals. L. Hartwell also described checkpoints, i. e. control points that ensure the order of cell cycle events (Hartwell and Weinert 1989). One

such checkpoint ensures dependence of mitosis on DNA replication so that arrest of DNA synthesis by inhibitors or DNA damage will prevent mitosis (Bruce 2001; Hartwell and Weinert 1989). A mutation in *rad9* gene abolished this checkpoint and the cells continue through mitosis independent on DNA synthesis (Bruce 2001; Hartwell and Weinert 1989; Johnston and Singer 1978).

Inspired by L. Hartwell's discovery of the *cdc* genes in *S. cerevisiae*, Paul Nurse ran similar genetic screens in the fission yeast *Schizosaccharomyces pombe*. He identified a number of cell cycle control genes including the *cdc2* gene (Nurse 1975; Nurse and Thuriaux 1980), which later proved to be a homolog of *cdc28* in *S. cerevisiae* (Beach et al. 1982). He and V. Simanis characterized the product of *cdc2* and demonstrated that it belonged to a family of protein kinases (Simanis and Nurse 1986). Soon after, Nurse and his collaborators identified human gene with the same function and thus uncovered the amazing functional conservation of cell cycle control elements within the eukaryotic domain (Lee and Nurse 1987; Norbury and Nurse 1989; Elledge 1992; Ferreira et al. 1991).

The last piece of the puzzle of cell cycle regulation was uncovered by R. T. Hunt who identified a protein being periodically destroyed during the cell cycle which he called „cyclin“ (Evans et al. 1983; Poon et al. 1993). Later on, he recognized that the protein kinases discovered by Nurse were activated through binding to that very regulatory protein (Meijer et al. 1989). Thus, the name „Cyclin Dependent Kinase“ or „CDK“ was born (Norbury and Nurse 1991). Together Hartwell, Nurse and Hunt were able to show that the progression of the eukaryotic cell cycle is controlled by a combination of constant CDK units and fluctuating levels of varying cyclins. Moreover, disruptions in this precisely equilibrated machinery can lead to the development of certain types of tumors. For their contributions to our understanding of the regulation of the eukaryotic cell cycle and the arising implications for cancer research Hartwell, Nurse and Hunt were awarded the Nobel Prize in Physiology or Medicine in 2001 (Bruce 2001).

As demonstrated above, in the past two centuries of scientific research we have made unprecedented progress in uncovering the basic principles

that govern the life of the cell. In the following sections, we will explore in detail, some of those key concepts of our modern view of the eukaryotic cell cycle.

1.2 Cells can have different cell cycle patterns

In order to multiply and proliferate, both prokaryotic and eukaryotic cells have to go through a series of precisely controlled events that are commonly described as the cell cycle. While recent advances in prokaryotic genome sequencing have revealed some surprising similarities with eukaryotes in terms of cell cycle mechanics, prokaryotes have cell cycle patterns that are fundamentally different from those in eukaryotes (Bramhill 1997; Samson and Bell 2011). Since elaborating on the diversity of all prokaryotic cell cycles will deprive the current work of detail, in this text we exclusively focus on the cell cycle patterns in eukaryotic organisms. Moreover, unless specified otherwise, all statements made here refer to eukaryotes in general. For a comprehensive description of the cell cycle and its control mechanisms in prokaryotes the reader is advised to refer to the works of (Abner et al. 2014; Lutkenhaus 2010; Samson and Bell 2011).

In the general eukaryotic binary fission cell cycle model, as described by Howard and Pelc, one mother cell gives rise to two identical daughter cells. In its classical organization, the process can be organized as a sequence of events that are separated into four distinct phases (Figure 1-1). During the Gap 1 (G1) phase, cells grow. They accumulate energy reserves and synthesize proteins required for DNA replication, which will then allow them to enter the next phase (Harashima et al. 2013). In late G1 phase is determined whether cell cycle completed by cell division will occur. This event is described as „Start” in *S. cerevisiae*, „restriction point” in mammalian cells and „commitment point” (CP) in algal cells (Bišová and Zachleder 2014; Harashima et al. 2013; Zachleder and van den Ende 1992). Throughout the rest of the text this decision point will be referred to as „commitment point” or „CP” for short. At this stage cells make the decision to either process through the CP or to enter a dormant phase called G0.

This decision can be influenced by extracellular signals that cells receive or depend on the soundness of the intracellular signaling pathways that detect these signals (Barbash and Diehl 2008). Once a cell has passed the CP it enters preparation for the Synthesis (S) phase during which DNA replication takes place. After that, the cell enters a second phase of growth called Gap 2 (G2). The last stage of the binary fission cell cycle is Mitosis (M), where chromosomes condense, the mitotic spindle is formed and sister chromatids are separated. In most cases the M-phase is followed by cell division which ends with newly formed daughter cells (Forsburg and Nurse 1991; Harashima et al. 2013).

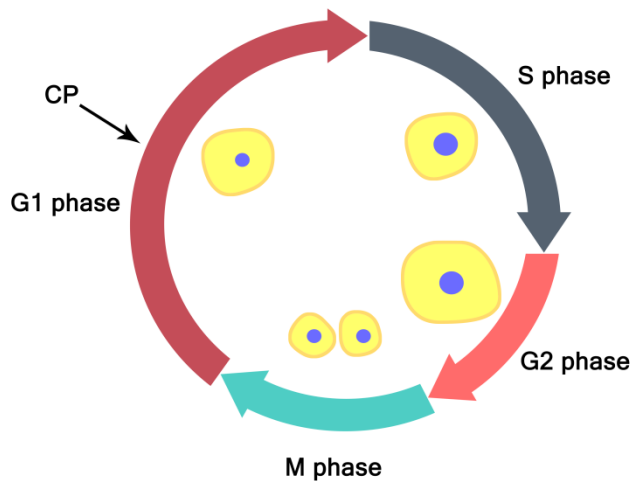


Figure 1-1: The binary fission cell cycle model. During the G1 phase the cell grows and increases mRNA and protein production. During the S phase DNA synthesis takes place. By entering the G2 phase the cell continues to grow and prepares for cell division. Following is the M phase where mitosis takes place.

Unlike most cells some green algae can divide through a division pattern in which one mother cell can give rise to more than two daughter cells (Bišová and Zachleder 2014; Umen 2018). In this so called „multiple fission division pattern”, the mother cell will divide into 2^n daughter cells, where the factor n can generally vary between 1 and 15 (Figure 1-2). In this context binary fission can be seen as a specific case of the multiple fission

cell cycle where cells divide into 2^1 daughter cells. Both cell cycle patterns can be interchangeable in some species and depend entirely on growth rate. Cells grown under unfavorable environmental conditions (light and/or temperature) will divide only into two, while cells grown under favorable conditions will divide into 4, 8, 16 and so on daughter cells (Bišová and Zachleder 2014).

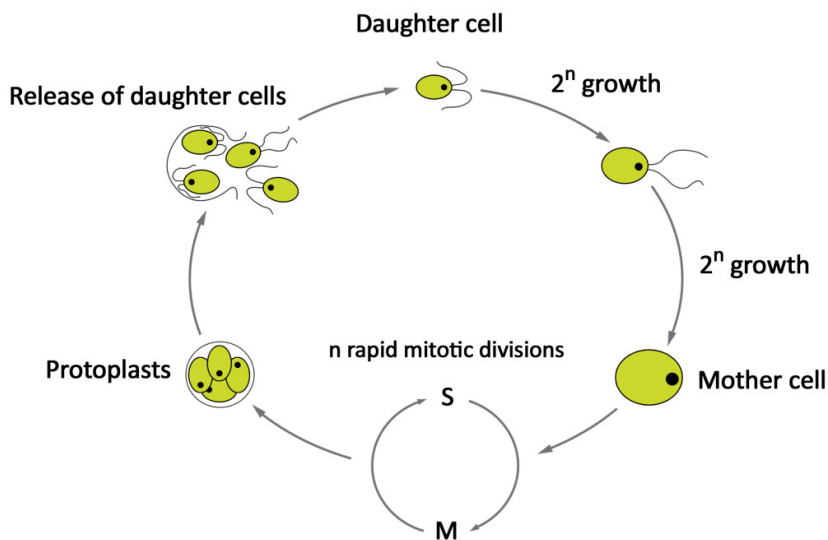


Figure 1-2: Schematic representation of the multiple fission cell cycle in the green *Chlamydomonas reinhardtii*. Under non-limiting conditions, a daughter cell grows and accumulates energy reserves. After reaching a commitment point, the cell keeps on growing, provided that the conditions continue to be favorable. After that the mother cell enters a sequence of rapid mitotic divisions yielding 2^n number of daughter protoplasts which are enclosed in the mother cell wall. In the final stage of the cell cycle the newly formed daughter cells dissolve the mother cell wall enclosure and release from it.

Synchronous algal cultures have been a popular tool in cell cycle studies for more than six decades. Coincidentally, the first such experiments were carried out by Tamiya and colleagues in Japan, almost at the same time when Howard and Pelc postulated their four stages of the binary fission cell cycle model (Tamiya et al. 1953). Although chlorococcal algae from the

genus *Chlorella* were the first to be cultivated in synchronous cultures, other species like *Desmodesmus* (formerly *Scenedesmus*) *quadricauda* and *Chlamydomonas* sp. soon also gained popularity and became prominent cell cycle models in their own right (Lorenzen 1968; Pirson and Lorenzen 1966; Šetlík et al. 1972; Lien and Knutsen 1979).

A notable part of early cell cycle research, utilizing *Desmodesmus quadricauda* as a model organism, was pioneered by Ivan Šetlík and his colleagues at the Department of Photoautotrophic Microorganisms in Třeboň in Czechoslovakia (currently the Czech Republic) (Šetlík et al. 1972; Šetlík et al. 1970; Zachleder and Šetlík 1968). During these early times, the green alga *Desmodesmus quadricauda* proved to be especially convenient because daughter cells arising from a single mother cell remain connected together in a structure called „coenobium”. This physiological feature of *Desmodesmus* sp. offered a fast and straightforward method for the estimation of commitment points acquired during the cell cycle (Zachleder and Šetlík 1968).

One of the main reasons for the use of algae as a cell cycle model was the fact that a high level of synchronization could be easily achieved by exposing the algal cells to alternating periods of light and dark. Such a synchronization procedure was considered to be natural and in many cases yielded populations where 90 to 95 % of the cells were in the same physiological state. However, this high synchronization can be attained only by chlorococcal and volvocal algae that divide by multiple fission (Tamiya 1959).

Another advantage of algae dividing by multiple fission is the flexibility of their cell cycle, which makes it easy to obtain differing cell cycle patterns simply by varying growth conditions or by applying inhibitors (Bišová et al. 2000). However, due to the overlapping phases of the cell cycle, the multiple fission cell cycle model is much more complex than the classical model and is known to be governed by complex regulatory mechanisms (Zachleder and Šetlík 1990).

1.3 The cell cycle regulatory apparatus

The eukaryotic cell cycle consists of a number of precisely controlled events that direct cell growth and differentiation. The first insight into regulation of the eukaryotic cell cycle was gained by the discovery of a group of CDKs that promote transitions through its different phases. These early works established that alternating the activity of CDKs was a key to proper cell cycle progression (Malumbres and Barbacid 2009; Morgan 1997). It was found that CDK activity was up regulated by the expression of proteins called cyclins that formed a complex with CDKs and was down regulated by binding to CDK inhibitory units. It was also discovered that the activity of CDKs could be regulated through phosphorylation as well as by interaction with CDK inhibitors (Harashima et al. 2013; Harashima et al. 2007).

1.3.1 CDKs

The first experiments that uncovered the regulatory mechanisms that govern the cell cycle were done in budding yeast. However, with the later establishment of fission yeast as a model organism for studying the cell cycle, researchers gained the advantage of having two complementary, but evolutionary very distinct genetic systems (Culotti and Hartwell 1971; Forsburg 2001; Hartwell et al. 1970; Nurse 1975; Nurse and Thuriaux 1977). The first experiments established the existence of two genes, *CDC28* in the budding yeast *S. cerevisiae* and *cdc2* in the fission yeast *S. pombe*. Both genes were responsible for the encoding of protein kinases in the two yeast species (Hindley and Phear 1984; Reed et al. 1985). Initially, *CDC28* was thought to be solely responsible for the regulation of the „start“ control point (Hartwell et al. 1974). However, later experiments with *cdc28* mutants led to the conclusion that the product of this gene also initiates a sequence of dependent events that drive the mitotic cell cycle forward in *S. cerevisiae* (Surana et al. 1991). It also became evident that *CDC28* was required for the initiation of two independent pathways during G1:

cytokinesis and DNA replication. In contrast to *CDC28*, the *cdc2* seemed to be crucial for mitosis and was found to affect cell size during G2 (Nurse and Thuriaux 1980). Although at the time of their discovery it appeared that the two genes differed in terms of function and timing of activity during the cell cycle, ensuing studies demonstrated that they are in fact homologs (Beach et al. 1982; Hindley and Phear 1984; Nurse 1985). Later it was established that the product of these two genes, which today is commonly referred to as Cyclin Dependent Kinase 1 or CDK1, is responsible for controlling the whole cell cycle in both yeast species (Morgan 1997). Furthermore, it was shown that homologs of these two genes encoding protein kinases have been preserved during the evolutionary process and have the same function throughout most of the eukaryotic kingdom (John et al. 1989; Lee and Nurse 1987; Riabowol et al. 1989)

In contrast to the two yeast species, which have a single CDK, regulation of the cell cycle in other organisms, such as animals and plants, is directed by small families of multiple CDKs, each with distinct functions. In mammals, CDK1 is responsible for the control of mitosis, while CDK2 controls entry into the S phase. Additionally, mammals also have CDK4 and CDK6, which are responsible for the initiation of the cell cycle in response to mitogenic stimuli, but have different cyclin binding signatures and are only distantly related to *CDC28* and *cdc2* (Harashima et al. 2013; Malumbres et al. 2004). It was found that mammalian cells lacking CDK2 (Steinberg 2003), CDK4 and CDK6 (Malumbres et al. 2004) can survive and proliferate, and CDK1 alone is sufficient to drive the cell cycle (Santamaria et al. 2007). Thus, it appears that although, in the course of evolution, mammals have evolved a variety of different CDKs, CDK1 still remains as the major driver of the cell cycle.

Similarly to yeasts and mammals, plants also contain a *Cdc28/Cdc2* related protein kinase called CDKA1, belonging to a group of so called A-type of kinases (Gutierrez 2005). Plants also contain a plant-specific subset of kinases, B-type CDKs that do not complement the functions of *CDC28* and *cdc2* in yeast (Inagaki and Umeda 2011). The B-type kinases themselves are further divided into two subfamilies - CDKB1 and CDKB2

and are characterized by different cyclin binding signatures (Harashima et al. 2013) and by different gene expression patterns during the cell cycle. CDKB1 is expressed from late S phase until M phase and CDKB2 only from G2 to M phase (Inagaki and Umeda 2011). In contrast to yeasts and mammals, CDKA1 in plants appears not to be essential for cell cycle progression, indicating divergent functional differentiation of the Cdc28/Cdc2 protein kinases in the course of the eukaryote evolution (Nowack et al. 2012). The function of CDKB is less-well characterized. CDKB1 controls G2/M transition (Porceddu et al. 2001), endoreduplication (Boudolf et al. 2004) and homologous recombination (Weimer et al. 2016) while CDKB2 is required for the meristematic function (Andersen et al. 2008).

Regulation of the cell cycle in algae has mostly been studied in the taxon Chlorophyta, where it is similar to that in plants. In fact, green algae were the first organisms of the plant lineage in which a homolog of CDK in yeast was identified (John et al. 1989). CDK activity assays conducted in *Chlamydomonas reinhardtii* revealed a correlation between maximum kinase activities with commitment points and nuclear division, suggesting the existence of different CDK complexes with separate activities (Zachleder et al. 1997). In recent years, the complete sequencing of the genome of *C. reinhardtii* helped to reveal the existence of homologs of all major CDKs present in higher plants. This includes not only A and B-type CDKs, but also CDKs specific only to *C. reinhardtii* (Bišová et al. 2005; Merchant et al. 2007). Importantly, in contrast to higher plants, most of the cell cycle regulators are present as single copy genes, which simplifies functional studies. Isolation of mutants in both CDKA and CDKB homologs in *C. reinhardtii* established their function in the complex multiple fission cell cycle (Atkins and Cross 2018; Cross and Umen 2015; Tulin and Cross 2014; Tulin and Cross 2015). By doing mutational screening of *C. reinhardtii* temperature sensitive mutants F. Cross and his colleagues discovered that although CDKA was not essential for mitosis it was required for appropriate timing of entry into the cell cycle (Atkins and Cross 2018; Tulin and Cross 2014). At the same time CDKA is required for cytokinesis initiation (Tulin

and Cross 2014). In contrast to CDKA, CDKB was found to be required for entry into mitosis (Atkins and Cross 2018; Tulin and Cross 2014). There exists a negative feedback loop where CDKA initiates cell division and activates the transcription of CDKB. The functional CDKB-cyclin B complex is then required for the mitotic spindle formation and for the repression of the activity of CDKA (Atkins and Cross 2018).

In contrast to green algae, with well-established model organisms such as *C. reinhardtii*, relatively little is known about regulation of the cell cycle in other groups of algae. However, with recent advances in genomic sequencing techniques, more genomes from different algal groups have become available. Studies of the emerging model red alga *Cyanidioschyzon merolae* suggest that its cell cycle regulators are similar to those in land plants and green algae. So far, both CDKA as well as the plant specific CDKB have been identified. In *C. merolae* CDKA and CDKB play similar roles to their counterparts in plants and green algae: CDKA controls entry into DNA replication, while CDKB is responsible for the regulation of mitosis (Kobayashi et al. 2009; Sumiya et al. 2016). The fact that *C. merolae*'s genome encodes for a complete set of cell cycle genes as well as CDKB genes suggests that the B-type CDKs were already present in the last common ancestor of red and green algae.

1.3.2 Cyclins

Cyclins, a diverse family of proteins, interact directly with the CDKs and together they form CDK-cyclin complex, where CDK is the active and cyclin the regulatory subunit. The CDK-cyclin complexes controls progression through the cell cycle of eukaryotic cells by phosphorylating a large number of target substrates (Errico et al. 2010; Koivomagi and Loog 2011; Swaffer et al. 2016).

The cyclins are expressed in specific phases of the cell cycle and can pair with different CDKs, thus regulating different stages of the cell cycle (Fuerst et al. 1996). CDKs can also pair with different cyclins meaning that different CDK-cyclin pairs can be formed. Moreover, the cyclins are specifically degraded at certain points of the cell cycle, particularly at the

mitotic anaphase (Jaspersen et al. 1998; Murray et al. 1989), which introduces another level of regulation and allows re-setting of the cell cycle (Novak et al. 1998; Novak et al. 2010).

Similarly to CDKs, cyclins within the eukaryotic kingdom also show remarkable levels of conservation. However, there are also some distinct examples of divergence, especially when it comes to plants and algae. In mammals, there are four major groups of cyclins, consisting of proteins that are produced during S phase (A-type cyclins), M phase (B-type cyclins) and G1 phase (D and E-type cyclins) (Meyerson and Harlow 1994; Murray 2004; Spoorri and Gabrielli 2013). Phylogenetic analysis has shown that similarly to animals plants have conserved the A and B types of cyclins (Wang et al. 2004). Plants also contain D-type cyclins, however their functionality appears to have been diversified when compared to animal D-type cyclins which fulfill their function strictly during the G1 phase (Harashima et al. 2013).

In *Arabidopsis thaliana* there are around 50 genes that encode cyclin related proteins, from which 32 are likely to be involved in regulating the cell cycle. Of those genes, 10 encode A-type, 11 encode B-type, 10 encode D-type and 1 encodes a H-type cyclin involved in activation of other CDK-cyclin complexes (Menges et al. 2005). In comparison, *C. reinhardtii* contains only 7 known cell cycle related cyclins: 1 A-type cyclin 1 B-type cyclin, 4 D-type cyclins and a novel cyclin designated CYCAB1. This *Chlamydomonas* specific cyclin has close homologs from the cyclin A and cyclin B groups, but cannot be placed definitely in neither of them (Bišová et al. 2005; Cross and Umen 2015). According to gene expression analysis of *C. reinhardtii* cyclins, the A and B types appear to act as mitotic cyclins while the hybrid CYCAB1 likely acts as an early activator of cell division and/or S phase. Similarly to plants, each of the D-type cyclins has its own distinct expression profile likely pointing toward separate functions in different stages of the cell cycle (Zones et al. 2015).

1.4 The role of macromolecules

As we have already seen, the cell cycle of eukaryotic organisms consists of a number of accurately controlled events governed by conserved regulators. Since at each division one mother cell gives rise to at least two daughter cells, clearly the mother cells needs to grow prior to division ensuring that the cell size after division will not drop below the limit required for survival. This suggests that there are mechanisms coordinating growth and reproductive (cell cycle) sequences, although the two could in principle operate independently. This led to the proposition of a conceptually simple cell-size checkpoint hypothesis. The hypothesis suggests that eukaryotic cells must possess a mechanism for determining cell size and the existence of a checkpoint that establishes a minimum cell size for progression through the cell cycle. This means that cells that are small can catch up to larger cells by growing and delaying cell cycle progression until they reach the minimum cell size required for satisfying the cell size checkpoint. In contrast, large cells will reach the checkpoint earlier and will progress through the cell cycle more rapidly (Umen 2005). This will ensure that the cells size in a population of cells will not drop below the minimum required for survival. In spite of the conceptual simplicity of the cell-size checkpoint hypothesis, the molecular machinery that must undoubtedly exist in order to facilitate such behavior has been difficult to unravel. Throughout the years, there have been numerous propositions for models that attempt to explain the link between cell growth and progression of the cell cycle. They can be divided into three main categories: geometric, protein concentration and metabolic models.

1.4.1 Geometric models

Geometric models attempt to explain the connection between cell size and cell cycle progression in terms of cell length, diameter or surface to volume ratio sensing mechanisms. Two studies conducted in fission yeast and published in *Nature* in 2009 demonstrated that a gradient of a polarity

factor protein appears to act as a sensing mechanism of cell length and can determine the onset of Cdc2 activation and hence mitosis. This mechanism involves changes in the spatial cellular distribution of two proteins, Pom1 and Cdr2, as the cell grows lengthwise. Pom1 inhibits Cdr2 while Cdr2 is responsible for the promotion of the transition between G2 and M phases. According to the model, in fission yeast, Cdr2 is localized in the mid cell region, whereas the concentration of Pom1 is highest at the cell tips and declines towards the middle of the cell. In short cells, Pom1 efficiently inhibits Cdr2. However, as the cell grows, the Pom1 concentration in the middle of the cell decreases such that Cdr2 becomes activated at a certain critical cell size and triggers the onset of mitosis (Martin and Berthelot-Grosjean 2009; Moseley et al. 2009; Vilela et al. 2010)

Although this gradient of polarity, in principle, can be used to explain the relationship between attaining critical cell size and entry into mitosis in fission yeast, it seems unlikely that this is the whole story. This was illustrated in experiments with a CDK mutant bypassing the Pom1-Cdr2 regulatory system. In these cases cell size homeostasis was still maintained, albeit with a broader size distribution. This indicates the existence of other unknown mechanisms that are responsible for the measurement of cell size and the integration of this information into the cell cycle control apparatus (Coudreuse and Nurse 2010).

1.4.2 Protein concentration models

In general, growth of cells can be defined as the accumulation of cytoplasmic mass that is caused by the accumulation of macromolecules. In this regard, protein concentration models attempt to explain the attainment of critical cell size through the existence of a so called „sizer”, which represents a specific compound that accumulates during growth of the cell until a certain concentration is reached, which then leads to entry into mitosis (Umen 2005). The nature of this putative sizer compound is yet to be identified, although some candidate genes are known.

One such sizer protein was identified in *C. reinhardtii* thanks to isolation of a mutation in *MAT3* gene, which encodes a homolog of the

retinoblastoma protein. The *mat3-4* mutant produces tiny daughter cells. Furthermore, it shows defects in two size-dependent cell cycle controls, 1) the critical cell size for attaining CP is smaller, 2) the mother cell size is misinterpreted leading to super-numerous mitotic division (Umen and Goodenough 2001). Further genetic screen placed *MAT3* downstream of another gene, *CDKG1*, a novel type of cyclin-dependent kinase that directly phosphorylates Mat3 protein (Li et al. 2016). The CDKG1 protein seems to be a *bona fide* sizer with cell size dependent accumulation in nucleus and progressive dilution and degradation with each round of nuclear/cell division. In line with its proposed sizer role, the *cdkg1-2* mutant has slightly bigger daughter cells while the over-expressing line has smaller daughter cells. Similar, even though less pronounced was also the difference in critical cell size at attaining CP (Li et al. 2016). It would be interesting to identify other members of this size sensing pathway and possibly to see if and how it might interact with the cell growth beyond the cell size dependent accumulation of CDKG1.

1.4.3 Metabolic models

Historically, there have also been attempts to link critical cell size with an increase in general metabolic activity and the bulk accumulation of different macromolecules such as total RNA and protein, since both of them are a manifestation of growth. In green algae, the concentrations of both macromolecules appears to increase during the light periods of the cell cycle and usually stabilizes during the dark period (Bišová and Zachleder 2014) but similar behaviors are also true in other organisms (Cipollina et al. 2007; Di Talia et al. 2007; Turner et al. 2012). However, each of the metabolites varies under some conditions, implying that none of them is the sole critical size determinant (John 1984). Therefore, it seems feasible that there is not a single determinant, but rather a combination of different metabolic signals.

The processes of DNA replication, nuclear and cellular division are extremely energy demanding, thus sufficient storage for energy must be available to the cell before it enters cell division (Siddiqui and Stillman

2007). In plant and algal cells, that energy is usually stored in the form of starch, lipids and polyphosphates (Bental et al. 1991; Sulpice et al. 2009). The first two of the compounds serve as a carbon (and energy) supply, the last are mostly an energy store. Combined, they make the cells independent of external supplies of both energy and carbon.

Starch is the primary energy storage macromolecule in plant and algal cells, and as such, is the main source of energy for growth during periods of low light and at night (Izumi et al. 2013). Moreover, microalgal species like *Desmodesmus* sp., *Dunaliella* sp., *Chlamydomonas* sp. and *Chlorella* sp. are known to accumulate levels of starch exceeding 50 % of their dry matter (Miranda et al. 2012). Such over-accumulation of starch or lipids in algae is often connected to nutrient limitations, which lead to a block in cell division (Ballin et al. 1988; Brányiková et al. 2011; Li et al. 2013; Šetlík et al. 1988; Zachleder et al. 1988). Similarly to plants, starch in algae accumulates in the form of starch granules contained within the chloroplast (Figure 1-3) (Kobayashi et al. 1974). The starch content in *Chlamydomonas* sp. has a diurnal oscillation and is highest during the night (Ral et al. 2006). Starch accumulation is light/photosynthesis dependent and its degradation is cell cycle dependent being very rapid during nuclear/cell division (Spudich and Sager 1980; Vítová et al. 2011; Wanka 1968; Wanka 1975), even in the presence of light.

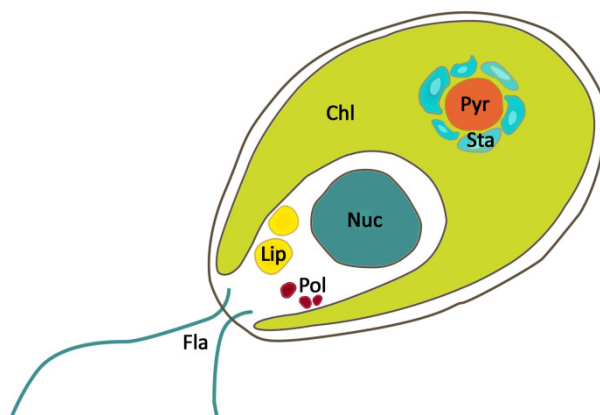


Figure 1-3: Schematic representation of a *Chlamydomonas reinhardtii* cell. **Chl:** chloroplast, **Nuc:** nucleus, **Pyr:** pyrenoid, **Fla:** flagella, **Sta:** starch granules, **Lip:** lipid bodies, **Pol:** polyphosphate grains.

In algae, polyphosphates are contained within single membrane-bound compartments, which are considered to be counterparts of the seed vacuoles in plants (Yagisawa et al. 2009). They increase during cell growth and some of them are specifically used for DNA synthesis in dark (Miyachi et al. 1964). The connection between energy requirements and progression of the cell cycle are not specific to algae. In budding yeast, catabolism of two major energy reserves, lipids and carbohydrates, are connected to the cell cycle through regulation of key metabolic enzymes by CDKs (Ewald et al. 2016; Futcher 2009; Jennifer et al. 2016; Kurat et al. 2009; Zhao et al. 2016).

In the following sections we will depart from the fundamental nature of the cell cycle regulation and we will examine in closer detail some of the applied aspects of the above mentioned energy storage compounds as well as other economically important microalgae derived metabolites.

1.5 Microalgal biotechnology

The cell cycle progression in algae depends largely on growth and the accumulation of energy storage compounds such as starch, lipids, and polyphosphates. These and other high-value secondary metabolites have recently become the focal point of the growing field of microalgal biotechnology.

The first steps of microalgal biotechnology were made in the first half of the last century when microalgae started to be viewed as a solution to the problem with malnourishment in some regions of the world. The main reason for that was their high efficiency of utilization of sunlight and their ability to accumulate biomass much faster than terrestrial plants (Spoehr 1953). In addition to that, many microalgal species have much higher protein content, and thus higher nutritional value, than most agricultural plants (Spoehr 1953). Although microalgae are no longer viewed as the main food source of the future, microalgal biotechnology has seen an immense development in the past several decades, with a number of algae derived products being produced on commercial scale (Figure 1-4).

Although comparatively small, the market share of microalgae derived products is growing and in 2004 the global market for microalgal biomass was estimated to be 5000 tons of dry weight with an yearly turnover of 1250 million USD (Milledge, 2011; Pulz and Gross, 2004).

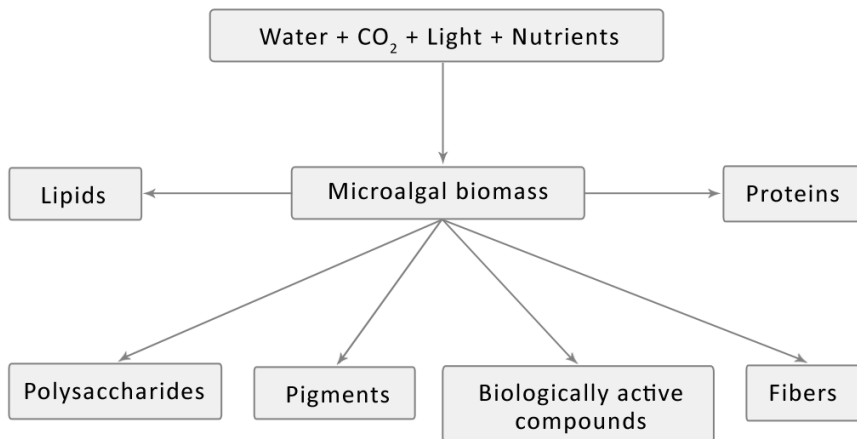


Figure 1-4: Overview of some of the current and prospective substances, which can be produced through microalgal biotechnology.

The first chemical compound synthesized by microalgae on commercial scale was the red-orange pigment β -carotene, which was first extracted from *Dunaliella salina* in 1986 (Spolaore et al. 2006). Currently, β -carotene from microalgae is used mainly as food coloring agent but it also has a number of other applications including animal feed, cosmetics and is also used in health food products as an antioxidant (Del Campo et al. 2007). Astaxanthin derived mostly from *Haematococcus pluvialis* is another type of carotenoid, which is being produced on industrial scale (Guerin et al. 2003). It is a major natural pigmentation source in aquaculture and is responsible for the coloration in economically important fish species like trout, salmon and red sea brim. Moreover, astaxanthin finds application in the nutraceutical, cosmetic and human health industries. The price of astaxanthin on the world market as of 2004 was 2500 USD per kilogram,

and it had an annual world market share of 200 million USD (Del Campo et al. 2007).

Algae are also able to produce secondary metabolites, which have different biological functions. The discovery of externally excreted compounds in *Chlorella vulgaris*, which inhibit bacterial growth was done as early as 1940 by Pratt and Fong (Pratt and Fong 1940). In more recent years however, algae have also gained attention as producers of antiviral and anticancer substances. One prominent example here is the red alga *Porphyridium* sp. which produces a polysaccharide that can slow down or completely inhibit infections of mammalian cells with *Varicella zoster* and *Herpes simplex* viruses (Huleihel et al. 2001).

Synthesis of lipids is another major area of interest in modern algal biotechnology. Poly unsaturated fatty acids (PUFAs) are an important dietary supplement not only for fish species in aquaculture, but also for human and mammalian health and nutrition (Piepho et al. 2011). Commercial production of essential PUFAs in microalgae is currently done by the Dutch company Royal DSM through fermentation of heterotrophic microalgae (Blackburn and Lee-Chang 2018). While there is still no photosynthetic large-scale production of essential PUFAs, future advances in microalgal cultivation technology are likely to make their economical production feasible in the near future.

In recent years, microalgae have gained significant attention as prospective source of polysaccharides like glycogen and starch for the biofuels industry. Both of these polysaccharides have high energy content and serve as energy storage for the cell during unfavorable environmental conditions. Glycogen is found mainly in cyanobacteria while starch is accumulated in eukaryotic algae (Ral et al. 2004). Production of glycogen in laboratory-scale has been demonstrated in the cyanobacterium *Arthrospira* sp. (Aikawa et al. 2012; De Philippis et al. 1992). As previously mentioned, microalgal species like *Scenedesmus* sp., *Dunaliella* sp., *Chlamydomonas* sp. and *Chlorella* sp. are known to be able to produce high amounts of starch and have therefore attracted a lot of attention as a potential feedstock for bioethanol production (Miranda et al. 2012).

Microalgae based bioethanol production has recently become a popular business model that has been adopted by a large number of start-up companies. However, currently none of these companies have been able to profitably produce microalgal bioethanol on industrial scale. As an example of the austerities in the microalgae based biofuels industry here can be given the case of the promising US based start-up Algenol Biotech LLC (Algenol). The company planned to start commercial production of ethanol from microalgae by 2015. In a press release Algenol claimed to be able to reach a yearly production of 34 000 liters of bioethanol per acre at price of around 0.20 EUR per liter (Lane 2013). If achieved this would have provided Algenol with fair amount of competitive advantage when compared to conventional ethanol that at times can reach prices as low as 0.25 EUR per liter (Irwin 2019). However, by October 2015 Algenol did not meet its bioethanol production goals and the employees of the company had to see their founder and CEO announce his sudden resignation and surprising shift of the company's focus away from biofuels (Lane 2015).

Despite the versatility and variety of products that can be produced by microalgae, currently only high value microalgal compounds such as carotenoids and essential PUFAs are manufactured commercially. The main reasons for that are technical challenges of microalgae cultivation technology, which result in high costs of biomass production as well as low product yields. Productivity enhancement of microalgal strains, combined with the development of added value chains is therefore required for improving the commercial potential of microalgae (Wijffels and Barbosa, 2010).

1.6 Production of energy storage compounds in microalgae

In recent years interest in renewable biofuels has provoked an intensive global research effort directed at increasing the production of energy storage compounds in microalgae. Within the scope of this thesis the term "production of energy storage compounds" can be defined as the deliberate diversion of the photosynthetic carbon flow towards the

synthesis of high energy storage compounds in order to produce algal biomass with enhanced starch and/or lipid content. In general, there are two principal approaches for increased production of energy storage compounds in microalgae: through manipulation of environmental factors and through genetic manipulations.

1.6.1 Manipulation of environmental factors

Exposure to environmental stresses such as nutrients, salinity and physical stress factors (i. e. light, pH and temperature) can affect biosynthetic pathways in microalgae and can be used to promote the synthesis of carbohydrates and lipids. However, stressful conditions can also have a detrimental effect on microalgal growth and ultimately reduce the yield of the target molecules. Hence, a more complex approach that explores the stress tolerance mechanisms in microalgae and includes process optimization and strain development is needed in order to achieve efficient bioproduction. For more detailed reviews see (Aratboni et al. 2019; Chen et al. 2017).

From a historical perspective, Spoehr and Milner, 1949 were the first to recognize that environmental conditions influence the chemical composition of microalgae. In their work, they investigated the influence of multiple environmental factors that included temperature, light intensity, CO₂ supply and medium composition on the biomass accumulation and chemical composition of *Chlorella* sp. As a result, they were able to determine that concentrations of fixed nitrogen in the growth medium have direct influence on the lipid accumulation within the algal cells. Their experiments showed that lipid synthesis in *Chlorella* sp. can be triggered through a combination of nutrient stress and high light intensity.

More recent works have successfully demonstrated that nutrient depletion combined with high light intensity can be successfully applied for the production of both lipids and starch in microalgae (Li et al. 2013; Fernandes et al. 2013; Takeshita et. al. 2018; Chen et al. 2017; Mathiot et al. 2019). It has also been established that the synthesis of storage lipids in

microalgae is coupled together with the starch metabolism and hindering the synthesis of starch as energy storage compound could improve lipid synthesis (Mizuno et al. 2013; Siau et al. 2011). According to the results of Fernandes et al., (Fernandes et al. 2013) when exposed to nutrient stress (10 or 5-fold diluted medium) *Parachlorella kessleri* accumulates starch (as primary energy storage) in the start of cultivation while nutrients are still present in the medium. However, as nutrient concentrations are depleted the energy storage is shifted to the accumulation of neutral lipids (as secondary energy storage) in the form of cytoplasmic lipid bodies (Li et al. 2013). Although nutrient depletion has proven to be an effective method for enhancing the production of energy storage compounds in microalgae this is usually achieved in relatively long time periods and at relatively low biomass concentrations. These factors limit the overall productivity of the nutrient depletion method. Hence, an alternative approach is needed that will allow for the fast accumulation of energy storage compounds at high cell densities.

Although less studied, the exposure to temperature stress has also been demonstrated to affect the accumulation of energy storage compounds. In some microalgal species low temperatures can promote the synthesis of certain types of lipids as a way for acclimation to low temperature (An et al. 2013; Jiang and Gao 2004). On the other hand, treatments with high temperature seem to have a higher potential for biotechnological applications. Similarly to the nutrient depletion approach, exposure of microalgae to high enough temperature (also known as restrictive or supra optimal temperature) may induce the accumulation of energy storage compounds. Also similarly to the nutrient depletion approach, high temperature exposure was shown to affect the reproductive processes of the cells leading to inhibition of cell division. However, the supra optimal temperature does not seem to affect the synthetic processes of the cells allowing for the accumulation of very large quantities of starch or lipids in short periods of time (Semenenko et al. 1967; Semenenko and Zvereva 1972; Šetlík et al. 1975). The fact that such temperature treatment approach leads to the rapid synthesis of energy

storage compounds may contribute to increased productivity in a potential biotechnological application.

1.6.2 Genetic manipulation

Usually, different microalgae species or strains are used for different biotechnological applications. For instance, fast growing species such as *C. vulgaris* are often used for bulk production of microalgal biomass, whereas others such as *H. pluvialis*, albeit having slower growth rates, are used for directed synthesis of specific high-value compounds. However, in order to increase the overall productivity and hence the economic viability of a production process high growth rates should be combined with accelerated accumulation of the compound of interest. For detailed reviews see (Hlavová et al. 2015; Radakovits et al. 2010).

Induction of random mutations by mutagens is a well known approach for increasing genetic variability in plants and has also been recently applied to microalgae (Ramazanov and Ramazanov 2006; Tripathi et al. 2001). Chemical and physical mutagens are widely used, mostly because they are easily applied in different doses and their mutagenic properties are well known. Chemical mutagens such as ethyl methane sulfonate (EMS) and methylnitronitrosoguanidine (MNNG) were used in the first mutagenic screenings aimed at improving microalgae for biotechnology applications (Chaturvedi and Fujita 2006; Ong et al. 2010). Physical mutagenesis has also been used to improve productivity of economically important land crops and more recently in microalgae (Hayashi et al. 2007; Kazama et al. 2008; Ota et al. 2013; Takeshita et al. 2018). Approaches here can range from simple exposure to UV radiation which induces point mutations and deletions in the genome to elaborate bombardment of cells with heavy ion beams that may result in chromosome breaks and exchanges. Random mutagenesis has been successfully applied for the creation of a number of biotechnologically relevant strains including starchless mutants of *C. reinhardtii* and *Scenedesmus obliquus*. In those mutants inactivation of the metabolic pathways responsible for starch

synthesis led to the diverting of the carbon influx toward the synthesis of neutral lipids that can be used to produce biodiesel (de Jaeger et al. 2014; Li et al. 2010).

Instead of induction of random mutations by chemical or physical agents a random insertion of foreign DNA fragment into the genome can be performed. In the plant field the most widely used insertional mutagenesis is based on a transfer DNA (T-DNA) fragment of the bacterium *Agrobacterium tumefaciens*. The T-DNA is inserted randomly into the genome and can be used to knock out the function of any non-essential genes producing in such manner knock out mutants. Since the DNA fragment can be readily tagged with a selective marker the affected genes can be easily located. This makes insertional mutagenesis especially suitable for the study of specific genes. However, performing such studies requires an established protocol of DNA transformation in a specific organism. So far this technique has been applied to only a handful of microalgae species the most prominent of which is *C. reinhardtii* (Hlavová et al. 2015).

Instead of inducing mutations in random genes and then screening for mutants with desired phenotype an alternative approach can be taken. Modern reverse genetics aims at altering the levels of expression of specific genes of interest that might lead to a desired phenotype. However, this approach, in contrast to the mutagenesis methods, can be applied only to organisms for which at least basic molecular tools are available. Currently there is only a limited amount of algal species that can benefit from the reverse genetics approach. Most prominent of which are *C. reinhardtii*, *C. merolae*, *Osterococcus tauri*, and *Nannochloropsis* sp. (Derelle et al. 2006; Harris 2001; Matsuzaki et al. 2004; Vieler et al. 2012).

The approach of genetic manipulations offers a whole plethora of possibilities for improving algae for biotechnology applications, however there are also some major limitations. While the generation of large numbers of mutants can be a relatively straight forward process, one of the major bottlenecks of the mutagenesis method lies within the selection of the appropriate mutants which have the preferred traits. The selection

process can be time consuming and it often involves the screening of thousands of mutants. Furthermore, the obtained mutant strains should be handled with caution since they are often prone to reversion to the wild type which results in loss of the preferred phenotype. This is especially true for mutants with point mutations but is also possible in mutants obtained through insertional mutagenesis or reverse genetics (Hlavová et al. 2015). Furthermore, reverse genetic approaches as well as, in some cases, mutagenesis can be applied to only a handful of species. In addition to that, performing genetic manipulations in general is an expensive undertaking that requires highly skilled labor force. In this regard, simply manipulating the growth conditions is a far simpler and cheaper approach to optimizing microalgae for biotechnology applications.

1.7 Raman spectroscopy

The ability to distinguish and analytically quantify macromolecules such as nucleic acids, energy storage compounds and proteins is of immense importance to both fundamental cell cycle and applied biotechnology research. Until recently conventional light and fluorescence microscopy combined with various staining techniques such as Lugol's solution staining for starch or Nile red staining for neutral lipids were used for the visualization of such macromolecules (Figure 1-5). Similarly, conventional biochemical and chromatographic methods for quantitative analysis of macromolecules have remained popular mainly because of their easy accessibility and relative cost effectiveness. Those methods however, also have a number of disadvantages. The effectiveness of traditional staining techniques often varies with different cell types and frequently involves different sample pre-treatment procedures (Gomes et al. 2013). Furthermore, major drawbacks of traditional quantification methods is that they often require large sample volume, involve labor intensive sample preparation and usually cannot be performed in applications which require *in situ* analysis of living cells (Viles and Silverman 1949; Zachleder 1984).

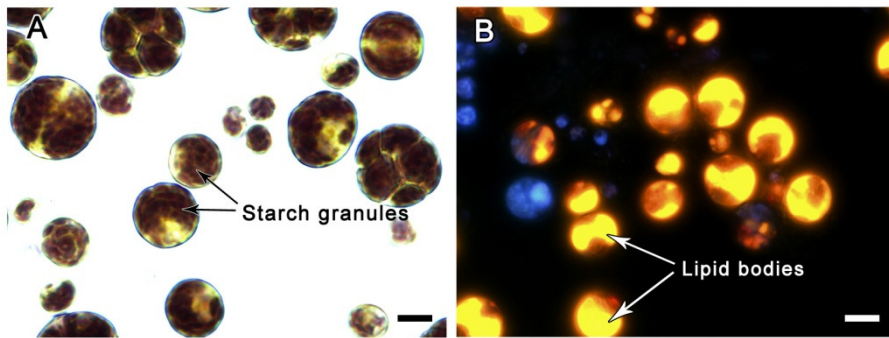


Figure 1-5: Microphotographs of energy storage compounds in the green microalga *Parachlorella kessleri*. **A:** Light microscopy image of starch granules (Lugol's solution staining) found within the chloroplasts. **B:** Fluorescence microscopy image of neutral lipids (Nile red staining) found within cytoplasmic lipid bodies. Size of the scale bar: 2µm.

The employment of advanced Raman spectroscopy for both qualitative and quantitative analysis of intracellular macromolecules could provide a solution to the above listed drawbacks of conventional methods. First discovered in 1928 the principle of Raman spectroscopy is based on inelastic scattering of photons by matter (Krishnan and Raman 1928). In its general form, Raman spectroscopy involves the illumination of a sample with monochromatic light which is usually emitted by a laser. The laser light then interacts with molecular vibrations of the molecules within the sample, resulting in a change of the reflected energy of the laser. This shift in energy results from the different vibrational modes within the system and varies with the molecular composition of the sample. In this way, a unique map of the sample is achieved where different macromolecules are represented by their respective Raman spectral signatures. In the same time this also allows for quantitative analysis of the sample which can be achieved by measuring the intensity of the scattered radiation (Bumrah and Sharma, 2016). Modern advanced Raman spectroscopy is characterized by extreme sensitivity and is able to analyze samples in the picograms size range. Moreover, this techniques is non invasive and can be used to analyze live tissues or isolated living cells (Smith et al. 2016).

Combined with confocal microscopy, Raman spectroscopy can provide detailed two or even three-dimensional images through measurement of several subsequent sample layers. In this way, this non-disruptive method can allow for the creation of 3D biochemical maps of the macromolecule composition of single cells (Majzner et al. 2012). In microalgae, Raman spectroscopy has already been applied as a tool for rapid *in situ* qualitative and quantitative analysis of lipids. Not only that, but it can be also used as high throughput screening method in mutagenic assays (Sharma et al. 2015). Another example of the versatility of Raman spectroscopy is the identification of microalgal species by utilizing the Raman spectral signatures of certain biomolecules. This approach can be especially useful when it comes to differentiating between toxic and non-toxic strains (Wu et al. 1998). The above described applications of Raman spectroscopy indicate that it can be an extremely powerful and versatile tool in areas which require non-destructive handling of samples on the single cell level.

1.8 References

- An M, Mou S, Zhang X, Ye N, Zheng Z, Cao S, Xu D, Fan X, Wang Y, Miao J (2013) Temperature regulates fatty acid desaturases at a transcriptional level and modulates the fatty acid profile in the Antarctic microalga *Chlamydomonas* sp. ICE-L. *Bioresour Technol* 134:151-157 doi:10.1016/j.biortech.2013.01.142
- Abner K, Aaviksaar T, Adamberg K, Vilu R (2014) Single-cell model of prokaryotic cell cycle. *Jour of Theor Biol* 341:78-87 doi:10.1016/j.jtbi.2013.09.035
- Aikawa S, Izumi Y, Matsuda F, Hasunuma T, Chang J S, Kondo A (2012) Synergistic enhancement of glycogen production in *Arthrospira platensis* by optimization of light intensity and nitrate supply. *Bioresour Technol* 108:211-215 doi: 10.1016/j.biortech.2012.01.004
- Andersen SU, Buechel S, Zhao Z, Ljung K, Novak O, Busch W, Schuster C, Lohmann JU (2008) Requirement of B2-type cyclin-dependent kinases for meristem integrity in *Arabidopsis thaliana*. *Plant Cell* 20:88-100 doi:10.1105/tpc.107.054676
- Aratboni AH, Rafiei N, Garcia-Granados R, Alemzadeh A, Morones-Ramírez RJ (2019) Biomass and lipid induction strategies in microalgae for

- biofuel production and other applications. *Microb Cell Fact* 18:1-17
doi:10.1186/s12934-019-1228-4
- Atkins KC, Cross F (2018) Inter-regulation of CDKA/CDK1 and the plant-specific cyclin-dependent kinase CDKB in control of the *Chlamydomonas* cell cycle. *Plant Cell* 30:429–446
doi:10.1105/tpc.17.00759
- Ballin G, Doucha J, Zachleder V, Šetlík I (1988) Macromolecular syntheses and the course of cell cycle events in the chlorococcal alga *Scenedesmus quadricauda* under nutrient starvation: Effect of nitrogen starvation. *Biol Plantarum* 30:81-91
- Barbash O, Diehl JA (2008) Chapter 13 - Regulation of the Cell Cycle. In: Mendelsohn J, Howley MP, Israel MA, Gray JW, Thompson CB (eds) *The Molecular Basis Of Cancer*. 3 edn. Elsevier B. V., Amsterdam, pp 177-188. doi:10.1016/B978-141603703-3.10013-5
- Beach D, Durkacz B, Nurse P (1982) Functionally homologous cell cycle control genes in budding and fission yeast. *Nature* 300:706-709
- Bental M, Pick U, Avron M, Degani H (1991) Polyphosphate metabolism in the alga *Dunaliella salina* studied by ³¹P-NMR. *Biochim Biophys Acta* 1092:21-28
- Bišová K, Krylov DM, Umen JG (2005) Genome-wide annotation and expression profiling of cell cycle regulatory genes in *Chlamydomonas reinhardtii*. *Plant Physiol* 137:1-17
- Bišová K, Vítová M, Zachleder V (2000) The activity of total histone H1 kinases is related to growth and commitment points while the p13(suc1)-bound kinase activity relates to mitoses in the alga *Scenedesmus quadricauda*. *Plant Physiol Biochem* 38:755-764
- Bišová K, Zachleder V (2014) Cell-cycle regulation in green algae dividing by multiple fission. *J Exp Bot* 65:17 doi:10.1093/jxb/ert466
- Blackburn IS, Lee-Chang JK (2018) *Blue Biotechnology: Production and Use of Marine Molecules vol 1*. John Wiley & Sons, Inc., Hoboken
- Boudolf V, Barroco R, Engler JdA, Verkest A, Beeckman T, Naudts M, Inze D, De Veylder L (2004) B1-Type Cyclin-Dependent Kinases Are Essential for the Formation of Stomatal Complexes in *Arabidopsis thaliana*. *Plant Cell* 16:945-955
- Bramhill D (1997) Bacterial cell division. *Annu Rev Cell Dev Biol* 13:395-424
- Brányiková I, Maršálková B, Doucha J, Brányik T, Bišová K, Zachleder V, Vítová M (2011) Microalgae-novel highly efficient starch producers. *Biotechnol Bioeng* 108:766-776 doi:10.1002/bit.23016
- Brawley SH et al. (2017) Insights into the red algae and eukaryotic evolution from the genome of *Porphyra umbilicalis*

- (Bangiophyceae, Rhodophyta). P Natl Acad Sci USA 114:E6361-E6370 doi:10.1073/pnas.1703088114
- Bruce D (2001) The Nobel Prize for Physiology or Medicine 2001. Genome Biol 2:1-3 doi:10.1186/gb-spotlight-20011008-02
- Bumbrah GS, Sharma RM (2016) Raman spectroscopy – Basic principle, instrumentation and selected applications for the characterization of drugs of abuse. Egypt J Forensic Sci 6 (3):209-215 doi:10.1016/j.ejfs.2015.06.001
- Chaturvedi R, Fujita Y (2006) Isolation of enhanced eicosapentaenoic acid producing mutants of *Nannochloropsis oculata* ST-6 using ethyl methane sulfonate induced mutagenesis techniques and their characterization at mRNA transcript level. Phycol Res 54:208-219
- Chen B, Wan C, Mehmood AM, Chang JS, Bai F, Zhao X (2017) Manipulating environmental stresses and stress tolerance of microalgae for enhanced production of lipids and value-added products - A review. Bioresour Technol 244:1198-1206 doi:10.1016/j.biortech.2017.05.170
- Cipollina C, Vai M, Porro D, Hatzis C (2007) Towards understanding of the complex structure of growing yeast populations. J Biotechnol 128:393-402 doi:10.1016/j.jbiotec.2006.10.012
- Čížková M et al. (2008) CDKA and CDKB kinases from *Chlamydomonas reinhardtii* are able to complement *cdc28* temperature-sensitive mutants of *Saccharomyces cerevisiae*. Protoplasma 232:183-191 doi:10.1007/s00709-008-0285-z
- Corellou F, Camasses A, Ligat L, Peaucellier G, Bouget FY (2005) Atypical regulation of a green lineage-specific B-type cyclin-dependent kinase. Plant Physio 138:1627-1636
- Coudreuse D, Nurse P (2010) Driving the cell cycle with a minimal CDK control network. Nature 468:1074-U1474 doi:10.1038/nature09543
- Cross F, Umen J (2015) The *Chlamydomonas* cell cycle. Plant J 82:370-392 doi:10.1111/tpj.12795
- Culotti J, Hartwell LH (1971) Genetic control of the cell division cycle in yeast. II. Seven genes controlling nuclear division. Exp Cell Res 67:389-401
- Curtis HG (1983) Biology, 4 edn. New York, NY: Worth.
- Cvrckova F (2018) A Brief History of Eukaryotic Cell Cycle Research. In: Sahi VP, Baluska F (eds) Concepts in Cell Biology - History and Evolution. Plant Cell Monographs, vol 23. Springer International Publishing AG, New York, pp 67-93

- Dahl M et al. (1995) The D-type *Alfalfa* cyclin gene *Cycms4* complements G(1) cyclin-deficient yeast and is induced in the G(1) phase of the cell-cycle. *Plant Cell* 7:1847-1857
- de Jaeger L, Verbeek RE, Draaisma RB, Martens DE, Springer J, Eggink G, Wijffels RH (2014) Superior triacylglycerol (TAG) accumulation in starchless mutants of *Scenedesmus obliquus*: (I) mutant generation and characterization. *Biotechnol Biofuels* 7(69): doi:10.1186/1754-6834-7-69
- De Philippis R, Sili C, Vincenzini M. (1992) Glycogen and poly-P-hydroxybutyrate synthesis in *Spirulina maxima*. *J General Microbiol* 138: 1623-1628
- Del Campo JA, Garcia-Gonzalez M, Guerrero MG (2007) Outdoor cultivation of microalgae for carotenoid production: current state and perspectives. *Appl Microbiol Biot* 74 (6):1163-1174
- Derelle E, Ferraz C, Rombauts S, Rouze P, Worden AZ, Robbens S, Partensky F, Degroeve S, Echeynie S, Cooke R, Saeys Y, Wuyts J, Jabbari K, Bowler C, Panaud O, Piegu B, Ball SG, Ral J-P, Bouget F-Y, Piganeau G, De Baets B, Picard A, Delseny M, Demaille J, Van de Peer Y, Moreau H (2006) Genome analysis of the smallest free-living eukaryote *Ostreococcus tauri* unveils many unique features. *P Natl Acad Sci USA* 103:11647-11652
- Devault A et al. (1992) Cyclin A potentiates maturation-promoting factor activation in the early *Xenopus* embryo via inhibition of the tyrosine kinase that phosphorylates cdc2. *J Cell Biol* 118:1109-1120
- Di Talia S, Skotheim JM, Bean JM, Siggia ED, Cross FR (2007) The effects of molecular noise and size control on variability in the budding yeast cell cycle. *Nature* 448:947-951 doi:10.1038/nature06072
- Diril MK et al. (2012) Cyclin-dependent kinase 1 (Cdk1) is essential for cell division and suppression of DNA re-replication but not for liver regeneration. *Proc Natl Acad Sci USA* 109:3826-3831 doi:DOI 10.1073/pnas.1115201109
- Elledge SJ (1992) Hot Papers - Cell Biology - 'A New Human p34 Protein Kinase, CDK2, Identified by Complementation of a cdc28 Mutation in *Saccharomyces-Cerevisiae* Is a Homolog of *Xenopus* Eg1' by Elledge,S.J., Spottswood,M.R. *Scientist*, 6:18
- Errico A, Deshmukh K, Tanaka Y, Pozniakovsky A, Hunt T (2010) Identification of substrates for cyclin dependent kinases. *Adv Enzyme Regul* 50:375-399 doi:10.1016/j.advenzreg.2009.12.001
- Evans T, Rosenthal ET, Youngbom J, Distel D, Hunt T (1983) Cyclin: a protein specified by maternal mRNA in sea urchin eggs that is destroyed at each cleavage division. *Cell* 33:389-396

- Ewald JC, Kuehne A, Zamboni N, Skotheim JM (2016) The yeast cyclin-dependent kinase routes carbon fluxes to fuel cell cycle progression. *Mol Cell* 62:532-545 doi:10.1016/j.molcel.2016.02.017
- Fernandes B, Teixeira J, Dragone G, Vicente AA, Kawano S, Bišová K, Příbyl P, Zachleder V, Vítová M (2013) Relationship between starch and lipid accumulation induced by nutrient depletion and replenishment in the microalga *Parachlorella kessleri*. *Bioresour Technol* 144: 268-274 doi:10.1016/j.biortech.2013.06.096
- Ferreira P, Hemerly AS, Villarroel R, Van Montagu M, Inze D (1991) The Arabidopsis Functional Homolog of the p34cdc2 Protein Kinase. *Plant Cell* 3:531-540
- Forsburg SL (2001) The art and design of genetic screens: Yeast. *Nature Reviews Genetics* 2:659-668
- Forsburg SL, Nurse P (1991) Cell cycle regulation in the yeasts *Saccharomyces cerevisiae* and *Schizosaccharomyces pombe*. *Annu Rev Cell Biol* 7:227-256
- Francis D, Sorrell DA (2001) The interface between the cell cycle and plant growth regulators: a mini review. *Plant Growth Regul* 33:1-12
- Frontini M et al. (2012) The CDK Subunit CKS2 counteracts CKS1 to control cyclin A/CDK2 activity in maintaining replicative fidelity and neurodevelopment. *Developmental cell* 23:356-370
- Freeman AK, Dapic V, Monteiro AN (2010) Negative regulation of CHK2 activity by protein phosphatase 2A is modulated by DNA damage. *Cell Cycle* 9:736-747
- Fuerst RA, Soni R, Murray JA, Lindsey K (1996) Modulation of cyclin transcript levels in cultured cells of *Arabidopsis thaliana*. *Plant Physiol* 112:1023-1033
- Futcher B (2009) Tg14 lipase: a big fat target for cell-cycle entry. *Mol Cell* 33:143-144 doi:10.1016/j.molcel.2009.01.003
- Gomes FM, Ramos IB, Wendt C, Girard-Dias W, De Souza W, Machado EA, Miranda K (2013) New insights into the in situ microscopic visualization and quantification of inorganic polyphosphate stores by 4',6-diamidino-2-phenylindole (Freeman et al.)-staining. *Eur J Histochem* 57 (4):227-235. doi: 10.4081/ejh.2013.e34
- Guerin M, Huntley M, Olaizola M (2003) *Haematococcus* astaxanthin: applications for human health and nutrition. *Trends Biotech* 21 (5):210-216
- Gutierrez C (2005) Coupling cell proliferation and development in plants. *Nat Cell Biol* 7(6):535-541
- Hajdu S, I. (2002) Introduction of the cell theory. *Ann Clin Lab Sci* 32:98-100

- Harashima H, Dissmeyer N, Schnittger A (2013) Cell cycle control across the eukaryotic kingdom. *Trends Cell Biol* doi:10.1016/j.tcb.2013.03.002
- Harashima H, Shinmyo A, Sekine M (2007) Phosphorylation of threonine 161 in plant cyclin-dependent kinase A is required for cell division by activation of its associated kinase. *Plant J* 52:435-448
- Hayashi Y, Takehisa Y, Kazama Y, Ichida H, Ryuto H, Fukunishi N, Abe T (2007) Effects of ion beam radiation on mutation induction in rice. *Cyclotrons and their applications* 18: 237-239
- Harris EH (2001) *Chlamydomonas* as a model organism. *Annual Review of Plant Physiology and Plant Molecular Biology* 52:363-406
- Hartwell LH, Culotti J, Reid B (1970) Genetic control of the cell-division cycle in yeast: I. Detection of mutants. *P Natl Acad Sci USA* 66:352-359 doi:10.1073/pnas.66.2.352
- Hartwell LH, Culotti J, Pringle JR, Reid BJ (1974) Genetic control of the cell division cycle in yeast. *Science* 183:46-51
- Hartwell LH, Weinert TA (1989) Checkpoints – controls that ensure the order of cell-cycle events. *Science* 246:629-634
- Hartwell LH (1991) Twenty-five years of cell cycle genetics. *Genetics* 129:975-980
- Hemerly A, Engler JdA, Bergounioux C, Van Montagu M, Engler G, Inze D, Ferreira P (1995) Dominant negative mutants of the Cdc2 kinase uncouple cell division from iterative plant development. *Embo J* 14:3925-3936
- Hindley J, Phear GA (1984) Sequence of the cell division gene CDC2 from *Schizosaccharomyces pombe*: patterns of splicing and homology to protein kinases. *Gene* 31:129-134
- Hlavová M, Turoczy Z, Bišová K (2015) Improving microalgae for biotechnology - From genetics to synthetic biology. *Biotechnol Adv* 33:1194-1203 doi:10.1016/j.biotechadv.2015.01.009
- Howard A, Pelc SR (1953) Synthesis of deoxyribonucleic acid in normal and irradiated cells and its relation to chromosome breakage. *Heredity (Lond) [Suppl]* 6:261-273
- Hu G, Fan Y, Zhang L, Yuan C, Wang J, Li W, Hu Q, Li F (2013) Enhanced Lipid Productivity and Photosynthesis Efficiency in a *Desmodesmus* sp. Mutant Induced by Heavy Carbon Ions. *PLoS ONE*, 8 (4): doi: 10.1371/journal.pone.0060700.
- Huleihel M, Ishanu V, Tal J, Arad S (2001) Antiviral effect of red microalgal polysaccharides on *Herpes simplex* and *Varicella zoster* viruses. *J Appl Phycol* 13:127-134
- Hunt T, Nasmyth K, Novak B (2011) The Cell Cycle. *Philos Trans R Soc Lond B Biol Sci* 366:3494-3497 doi:10.1098/rstb.2011.0274

- Huysman MJJ, Tanaka A, Bowler C, Vyverman W, De Veylder L (2015) Functional characterization of the diatom cyclin-dependent kinase A2 as a mitotic regulator reveals plant-like properties in a non-green lineage. *BMC Plant Biol* 15:11 doi:10.1186/s12870-015-0469-6
- Inagaki S, Umeda M (2011) Cell-cycle control and plant development. In: *Int Rev Cell Mol Biol*, vol 291. 2011/10/25 edn. Academic Press, pp 227-261 doi:B978-0-12-386035-4.00007-0
- Irwin S (2019) Why are ethanol prices so low? *Farmdoc daily* (9): 23, Department of Agricultural and Consumer Electronics, University of Illinois at Urbana-Champaign. Online article: <https://farmdocdaily.illinois.edu/2019/02/why-are-ethanol-prices-so-low.html> Retrieved on 18.02.2019
- Izumi M, Hidema J, Makino A, Ishida H (2013) Autophagy contributes to nighttime energy availability for growth in *Arabidopsis*. *Plant Physiol* 161:1682-1693 doi:10.1104/pp.113.215632
- Jaspersen SL, Charles JF, Tinker-Kulberg RL, Morgan DO (1998) A late mitotic regulatory network controlling cyclin destruction in *Saccharomyces cerevisiae*. *Mol Biol Cell* 9:2803-2817
- Jennifer CE, Andreas K, Nicola Z, Jan MS (2016) The yeast cyclin-dependent kinase routes carbon fluxes to fuel cell cycle progression. *Mol Cell* 62:532-545 doi:10.1016/j.molcel.2016.02.017
- Jiang HM, Gao KS (2004) Effects of lowering temperature during culture on the production of polyunsaturated fatty acids in the marine diatom *Phaeodactylum tricornutum* (Bacillariophyceae). *J Phycol* 40:651-654 doi:DOI 10.1111/j.1529-8817.2004.03112.x
- John PC, Sek FJ, Lee MG (1989) A homolog of the cell cycle control protein p34^{cdc2} participates in the division cycle of *Chlamydomonas*, and a similar protein is detectable in higher plants and remote taxa. *Plant Cell* 1:1185-1193
- John PCL (1984) Control of the cell division cycle in *Chlamydomonas*. *Microbiol Sci* 1:96-101
- Johnston GC, Singer RA (1978) RNA synthesis and control of cell division in yeast *S. cerevisiae*. *Cell* 14:951-958
- Kazama Y, Saito H, Miyagai M, Takehisa H, Ichida H, Miyazawa Y, Mishiba K, Kanaya T, Suzuki K, Bae C, Miyoshi K, Mii M, Abe T (2008) Effect of heavy ion-beam irradiation on plant growth and mutation induction in *Nicotiana tabacum*. *Plant Biotech* 25:105-111
- Kobayashi T, Tanabe I, Obayashi A (1974) On the properties of the starch granules from unicellular green algae. *Agr Biol Chem*, 38:941-946
- Kobayashi Y, Kanesaki Y, Tanaka A, Kuroiwa H, Kuroiwa T, Tanaka K (2009) Tetrapyrrole signal as a cell-cycle coordinator from organelle to

- nuclear DNA replication in plant cells. P Natl Acad Sci USA 106:803-807 doi:10.1073/pnas.0804270105
- Koivomagi M, Loog M (2011) Cdk1: A kinase with changing substrate specificity. Cell Cycle 10:3625-3626
- Krishnan KS, Raman CV (1928) A new type of secondary radiation. Nature 121 (3048):501-502. doi: 10.1038/121501c0
- Kurat CF, Wolinski H, Petschnigg J, Kaluarachchi S, Andrews B, Natter K, Kohlwein SD (2009) Cdk1/Cdc28-dependent activation of the major triacylglycerol lipase Tgl4 in yeast links lipolysis to cell-cycle progression. Mol Cell 33:53-63 doi:10.1016/j.molcel.2008.12.019
- Kyle DJ (2001) The large-scale production and use of a single-cell oil highly enriched in docosahexaenoic acid. ACS Symposium Series 788:92-107 doi:10.1021/bk-2001-0788.ch008
- Lane J (2013) Algenol hits 9K gallons/acre mark for algae-to-ethanol process. Online article: <http://www.biofuelsdigest.com/bdigest/2013/03/11/algenol-hits-9k-gallonsacre-mark-for-algae-to-ethanol-process/> Retrieved on 18.02.2020
- Lane J (2015) Algenol CEO exits; staff cut by 25%, investors re-up for two years, new direction tipped. Online article: <http://www.biofuelsdigest.com/bdigest/2015/10/25/algenol-ceo-exits-staff-cut-by-25-investors-re-up-for-two-years-new-direction-tipped/> Retrieved on 18.02.2020
- Lee MG, Nurse P (1987) Complementation used to clone a human homologue of the fission yeast cell cycle control gene cdc2. Nature 327:31-35
- Lee SK, Chou H, Ham TS, Lee TS, Keasling JD (2008) Metabolic engineering of microorganisms for biofuels production: from bugs to synthetic biology to fuels. Curr Opin Biotech 19(6):556-563 doi:10.1016/j.copbio.2008.10.014
- Levi C, Gibbs M (1984) Starch degradation in synchronously grown *Chlamydomonas reinhardtii* and characterization of the amylase. Plant Physiol 74:459-463
- Li X, Přebyl P, Bišová K, Kawano S, Cepák V, Zachleder V, Čížková M, Brányiková I, Vítová M (2013) The microalga *Parachlorella kessleri* – a novel highly-efficient lipid producer. Biotechnol Bioeng 110:97-107
- Li Y, Han D, Hu G, Dauvillee D, Sommerfeld M, Ball S, Hu Q (2010) *Chlamydomonas* starchless mutant defective in ADP-glucose pyrophosphorylase hyper-accumulates triacylglycerol. Metabol Engineer 12(4):387-391 doi: 10.1016/j.ymben.2010.02.002

- Li YB, Liu DY, Lopez-Paz C, Olson B, Umen JG (2016) A new class of cyclin dependent kinase in *Chlamydomonas* is required for coupling cell size to cell division. *eLife* 5:28 doi:10.7554/eLife.10767
- Lien T, Knutsen G (1979) Synchronous growth of *Chlamydomonas reinhardtii* (Chlorophyceae): a review of optimal conditions. *J Phycol* 15:191-200
- Lorenzen H (1968) Aspects of synchronous culturing of *Chlorella*. *Phykos* 7:50-57
- Lutkenhaus J (2010) Growth and development: prokaryotes. *Curr Opin Microbiol* 13:727-729
- Majzner K, Kaczor A, Kachamakova-Trojanowska N, Fedorowicz A, Chlopicki S, Baranska M (2012) 3D confocal Raman imaging of endothelial cells and vascular wall: Perspectives in analytical spectroscopy of biomedical research. *Analyst* 138:603-610. doi: 138. 10.1039/c2an36222h
- Malumbres M, Barbacid M (2009) Cell cycle, CDKs and cancer: a changing paradigm. *Nat Rev Cancer* 9:153-166
- Malumbres M, Sotillo R, Santamaría D, Galán J, Cerezo A, Ortega S, Dubus P, Barbacid M. (2004) Mammalian cells cycle without the D-type Cyclin-dependent kinases Cdk4 and Cdk6. *Cell* 118:493-504
- Martin SG, Berthelot-Grosjean M (2009) Polar gradients of the DYRK-family kinase Pom1 couple cell length with the cell cycle. *Nature* 459:852-856 doi:10.1038/nature08054
- Mathiot C, Ponge P, Gallard B, Sassi J, Delrue F, Le Moigne N (2019) Microalgae starch-based bioplastics: Screening of ten strains and plasticization of unfractionated microalgae by extrusion. *Carbohydr Polym* 208:142-151
- Matsuzaki M et al. (2004) Genome sequence of the ultrasmall unicellular red alga *Cyanidioschyzon merolae* 10D. *Nature* 428:653-657
- Meijer L, Arion D, Golsteyn R, Pines J, Brizuela L, Hunt T, Beach D (1989) Cyclin is a component of the sea urchin egg M-phase specific histone H1 kinase. *EMBO J* 8:2275-2282
- Menges M, de Jager SM, Gruissem W, Murray JAH (2005) Global analysis of the core cell cycle regulators of *Arabidopsis* identifies novel genes, reveals multiple and highly specific profiles of expression and provides a coherent model for plant cell cycle control. *Plant J* 41:546-566 doi:10.1111/j.1365-313X.2004.02319.x
- Merchant SS et al. (2007) The *Chlamydomonas* genome reveals the evolution of key animal and plant functions. *Science* 318:245-250 doi:10.1126/science.1144744

- Merrick KA, Larochelle S, Zhang C, Allen JJ, Shokat KM, Fisher RP (2008) Distinct activation pathways confer cyclin-binding specificity on Cdk1 and Cdk2 in human cells. *Mol Cell* 32:662-672
- Meyerson M, Harlow E (1994) Identification of G1 kinase activity for cdk6, a novel cyclin D partner. *Mol Cell Biol* 14:2077-2086
- Milledge JJ (2011) Commercial applications of microalgae other than as biofuels: a brief review. *Rev Environ Sci Biotech* 10:31-41
- Miyachi S, Kanai R, Mihara S, Miyachi S, Aoki S (1964) Metabolic roles of inorganic polyphosphates in *Chlorella* cells. *Biochim Biophys Acta* 93:625-634
- Mizuno Y, Sato A, Watanabe K, Hirata A, Takeshita T, Ota S, Sato N, Zachleder V, Tsuzuki M, Kawano S (2013) Sequential accumulation of starch and lipid induced by sulfur deficiency in *Chlorella* and *Parachlorella* species. *Bioresource Technol* 129:150-155
- Miranda JR, Passarinho PC, Gouveia L (2012) Bioethanol production from *Scenedesmus obliquus* sugars: the influence of photobioreactors and culture conditions on biomass production. *Appl Microbiol Biotechnol* 96:555-564
- Morgan DO (1997) Cyclin-dependent kinases: engines, clocks, and microprocessors. *Annu Rev Cell Develop Biol* 13:261-291
- Moriyama T, Terasawa K, Sekine K, Toyoshima M, Koike M, Fujiwara M, Sato N (2010) Characterization of cell-cycle-driven and light-driven gene expression in a synchronous culture system in the unicellular rhodophyte *Cyanidioschyzon merolae*. *Microbiology-(UK)* 156:1730-1737 doi:10.1099/mic.0.037754-0
- Moseley JB, Mayeux A, Paoletti A, Nurse P (2009) A spatial gradient coordinates cell size and mitotic entry in fission yeast. *Nature* 459:857-860 doi:10.1038/Nature08074
- Murray AW (2004) Recycling the cell cycle: Cyclins Revisited. *Cell* 116:221-234
- Murray AW, Solomon MJ, Kirschner MW (1989) The role of cyclin synthesis and degradation in the control of maturation promoting factor activity. *Nature* 339:280-286
- Norbury C, Nurse P (1991) Cyclins and cell cycle control. *Curr Biol* 1:23-24
- Norbury C, Nurse P (1989) Control of the higher eukaryote cell cycle by p34^{cdc2} homologues. *Biochim Biophys Acta* 989:85-95
- Novak B, Csikasz-Nagy A, Gyorffy B, Nasmyth K, Tyson JJ (1998) Model scenarios for evolution of the eukaryotic cell cycle. *Philos Trans R Soc Lond B Biol Sci* 353:2063-2076
- Novak B, Vinod PK, Freire P, Kapuy O (2010) Systems-level feedback in cell-cycle control. *Biochem Soc Trans* 38:1242-1246 doi:10.1042/BST0381242

- Nowack Moritz K et al. (2012) Genetic Framework of Cyclin-Dependent Kinase Function in *Arabidopsis*. *Dev Cell* 22:1030-1040
- Nurse P (1975) Genetic control of cell size at division in yeast. *Nature* 256:547-551
- Nurse P (1985) Cell cycle control genes in yeast. *Trends Genet* 1:51-55 doi:10.1016/0168-9525(85)90023-X
- Nurse P, Thuriaux P (1977) Controls over the timing of DNA replication during the cell cycle of fission yeast. *Exp Cell Res* 107:365-375
- Nurse P, Thuriaux P (1980) Regulatory genes controlling mitosis in the fission yeast *Schizosaccharomyces pombe*. *Genetics* 96:627-637
- Nurse P (2000) A long twentieth century of the cell cycle and beyond. *Cell* 100:71-78
- Ong S-C, Kao C-Y, Chiu S-Y, Tsai M-T, Lin C-S (2010) Characterization of the thermal-tolerant mutants of *Chlorella* sp. with high growth rate and application in outdoor photobioreactor cultivation. *Bioresour Technol* 101:2880-2883
- Ota S, Matsuda T, Takeshita T, Yamazaki T, Kazama Y, Abe T, Kawano S (2013) Phenotypic spectrum of *Parachlorella kessleri* (Chlorophyta) mutants produced by heavy-ion irradiation. *Bioresour Technol* 149:432-438
- Pan KZ, Saunders TE, Flor-Parra I, Howard M, Chang F (2014) Cortical regulation of cell size by a sizer *cdr2p*. *Elife* 3:e02040 doi:10.7554/eLife.02040
- Paweletz N (2001) Walther Flemming: Pioneer of mitosis research. *Nature Rev Mol Cell Biol* 2:72-75 doi:10.1038/35048077
- Piepho M, Arts MT, Wacker A (2011) Species-specific variation in fatty acid concentrations of four phytoplankton species: does phosphorus supply influence the effect of light intensity or temperature. *J Phycol* 47:1-10
- Pirson A, Lorenzen H (1966) Synchronized dividing algae. *Plant Physiol* 17:439-458
- Poon RYC, Yamashita K, Adamczewski JP, Hunt T, Shuttleworth J (1993) The *cdc2*-related protein p40MO15 is the catalytic subunit of a protein kinase that can activate p33^{cdc2} and p34^{cdc2}. *EMBO J* 12:3123-3132
- Porceddu A, Stals H, Reichheldt JP, Segers G, De Veylder L, Barroco RD, Casteels P, Van Montagu M, Inze D, Mironov V (2001) A plant-specific cyclin-dependent kinase is involved in the control of G(2)/M progression in plants. *J Biol Chem* 276:36354-36360
- Pratt R, Fong J (1940) Further evidence that *Chlorella* cells form a growth-inhibiting substance. *Am J Bot* 27 (6):431-436

- Pringle JR, Hartwell LH (eds) (1981) The *Saccharomyces cerevisiae* cell cycle vol 11A. The Molecular Biology of the Yeast *Saccharomyces*: Life Cycle and Inheritance. Cold Spring Harbor Laboratory, Cold Spring Harbor, New York
- Pulz O, Gross W (2004) Valuable products from biotechnology of microalgae. *Appl Microbiol Biotech* 65:635-648
- Radakovits R, Jinkerson RE, Darzins A, Posewitz MC (2010) Genetic engineering of algae for enhanced biofuel production. *Eukaryot Cell* 9:486-501 doi:10.1128/EC.00364-09
- Ral JP, Derelle E, Ferraz C, Wattebled F, Farinas B, Corellou F, Buleon A, Slomianny MC, Delvalle D, d'Hulst C, Rombauts S, Moreau H, Ball S (2004) Starch division and partitioning. A mechanism for granule propagation and maintenance in the picophytoplanktonic green alga *Ostreococcus tauri*. *Plant Physiol* 136(2):3333-3340
- Ral JP, Colleoni C, Wattebled F, Dauvillée D, Nempont C, Deschamps P, Li Z, Morell MK, Chibbar R, Purton S, d'Hulst C, Ball SG (2006) Circadian clock regulation of starch metabolism establishes GBSSI as a major contributor to amylopectin synthesis in *Chlamydomonas reinhardtii*. *Plant Physiol* 142:305-317 doi:10.1104/pp.106.081885
- Ramazanov A, Ramazanov Z (2006) Isolation and characterization of a starchless mutant of *Chlorella pyrenoidosa* STL-PI with a high growth rate, and high protein and polyunsaturated fatty acid content. *Phycol Res* 54(4):255–259
- Reed SI, Hadwiger JA, Lörincz AT (1985) Protein kinase activity associated with the product of the yeast cell division cycle gene CDC28. *Proc Natl Acad Sci USA* 82:4055-4059
- Renaudin JP et al. (1996) Plant cyclins: A unified nomenclature for plant A-, B- and D- type cyclins based on sequence organization. *Plant Mol Biol* 32:1003-1018
- Riabowol K, Draetta G, Brizuela L, Vandre D, Beach D (1989) The cdc2 kinase is a nuclear protein that is essential for mitosis in mammalian cells. *Cell* 57:393-401
- Sablowski R, Dornelas MC (2014) Interplay between cell growth and cell cycle in plants. *Journal of Exp Bot* 65:2703-2714 doi:10.1093/jxb/ert354
- Samson RY, Bell SD (2011) Cell cycles and cell division in the archaea. *Curr Opin Microbiol* 14:350-356 doi:10.1016/j.mib.2011.04.005
- Santamaria D, Barrière C, Cerqueira A, Hunt S, Tardy C, Newton K, Cáceres JF, Dubus P, Malumbres M, Barbacid M. (2007) Cdk1 is sufficient to drive the mammalian cell cycle. *Nature* 448:811-815
- Semenenko VE, Vladimirova MG, Orleanskaja OB (1967) K fiziologičeskij karakteristike *Chlorella* sp. K pri vysokych temperaturach. I.

- Razobscajuscie dejstvée extremalnoj temperatury kletocnyh funkcii Chlorelly. *Fiziol Rast* 14:612-625
- Semenenko VE, Zvereva MG (1972) Sravnitelnoe izucenije perestrojki v napravlenosti fotosinteza u dvuch stammov Chlorelly pri razobsceniji kletocnyh funkcij extremalnoj temperaturaj. *Fiziol Rast* 19:229-238
- Šetlík I, Vendlová J, Zachleder V (1970) The sequence of events leading to cellular division of *Scenedesmus quadricauda*. *Annu Rep Algolog Lab Trebon for 1969*:59-87
- Šetlík I, Berková E, Doucha J, Kubín S, Vendlová J, Zachleder V (1972) The coupling of synthetic and reproduction processes in *Scenedesmus quadricauda*. *Archives of Hydrobiology/Supplement 41, Algological Studies 7*:172-213
- Šetlík I, Zachleder V, Doucha J, Berková E, Bartoš J (1975) The nature of temperature block in the sequence of reproductive processes in *Algological Studies 14*:70-104
- Šetlík I, Ballin G, Doucha J, Zachleder V (1988) Macromolecular syntheses and the course of cell cycle events in the chlorococcal alga *Scenedesmus quadricauda* under nutrient starvation: Effect of sulphur starvation. *Biol Plantarum 30*:161-169
- Sharma SK, Nelson DR, Abdrabu R, Khraiwesh B, Jijakli K, Arnoux M, O'Connor MJ, Bahmani T, Cai H, Khapli S, Jagannathan R, Salehi-Ashtiani K. (2015) An integrative Raman microscopy-based workflow for rapid in situ analysis of microalgal lipid bodies. *Biotechnol Biofuels 8*:164 doi: 10.1186/s13068-015-0349-1
- Siaut M, Cuiné S, Cagnon C, Fessler B, Nguyen HM, Carrier P, Beyly A, Beisson F, Triantaphylidès C, Li-Beisson Y, Peltier G (2011) Oil accumulation in the model green alga *Chlamydomonas reinhardtii*: characterization, variability between common laboratory strains and relationship with starch reserves. *BMC Biotechnol 11*: 7 doi: 10.1186/1472-6750-11-7.
- Siddiqui, Stillman B (2007) The biochemistry of initiating eukaryotic DNA replication. *J Biol Chem 282*:32370–32383
- Silver G, A. (1987) Virchow, the heroic model in medicine: health policy by accolade. *Am J Public Health 77*:82-88
- Simanis V, Nurse P (1986) The cell cycle control gene *cdc2+* of fission yeast encodes a protein kinase potentially regulated by phosphorylation. *Cell 45*:261-268
- Shitsukawa N, Ikari C, Shimada S, Kitagawa S, Sakamoto K, Saito H, Ryuto H, Fukunishi N, Abe T, Takumi S, Nasuda S, Murai K (2007) The einkorn wheat (*Triticum monococcum*) mutant maintained

- vegetative phase, is caused by a deletion in the *VRN1* gene. *Genes Genet Syst* 82:167-170
- Smith R, Wright KL, Ashton L (2016) Raman spectroscopy: an evolving technique for live cell studies. *Analyst* 141:3590-3600. doi: 10.1039/c6an00152a
- Soni DV, Sramkoski RM, Lam M, Stefan T, Jacobberger W (2008) Cyclin B1 is rate limiting but not essential for mitotic entry and progression in mammalian somatic cells. *Cell Cycle* 7:1285-1300
- Spoehr H, Milner H (1949) The chemical composition of *Chlorella*; effect of environmental conditions. *Plant Physiol* 24 (1): 120-149
- Spoehr H (1953) The need for a new source of food. In Burlew JS (ed.) *Algal culture: from laboratory to pilot plant*, Carnegie Institution of Washington Publication, Washington, D. C.
- Spoerri L, Gabrielli B (2013) Similar, not the same: diverse roles and regulation of cyclin Es. *Cell Cycle* 12:715 doi:23909
- Spolaore P, Joannis-Cassan C, Duran E, Isambert A (2006) Commercial applications of microalgae. *J Biosci Bioeng* 101:87–96
- Spudich JL, Sager R (1980) Regulation of the *Chlamydomonas* cell-cycle by light and dark. *J Cell Biol* 85:136-146
- Steinberg D (2003) A cell-cycle couple loses its luster. *The Scientist* 17:26-27
- Sulpice R et al. (2009) Starch as a major integrator in the regulation of plant growth. *Proc Nat Acad Sci of USA* 106:10348-10353 doi:10.1073/pnas.0903478106
- Sumiya N, Fujiwara T, Era A, Miyagishimaa S (2016) Chloroplast division checkpoint in eukaryotic algae. *Proc Natl Acad Sci U S A* 113:E7629-E7638 doi:10.1073/pnas.1612872113
- Surana U, Robitsch H, Price C, Schuster T, Nasmyth K (1991) The role of CDC28 and cyclins during mitosis in the budding yeast *Saccharomyces cerevisiae*. *Cell* 65:145-161
- Swaffer MP, Jones AW, Flynn HR, Snijders AP, Nurse P (2016) CDK substrate phosphorylation and ordering the cell cycle. *Cell* 167:1750-+ doi:10.1016/j.cell.2016.11.034
- Tachibana K, Hara M, Hattori Y, Kishimoto T (2008) Cyclin B-Cdk1 controls pronuclear union in interphase. *Curr Bio* 18:1308-1313
- Takaki T, Echalié A, Brown NR, Hunt T, Endicott JA, Noble MEM (2009) The structure of CDK4/cyclin D3 has implications for models of CDK activation. *PNAS* 106:4171-4176
- Takeshita T, Ivanov IN, Oshima K, Ishii K, Kawamoto H, Ota S, Yamazaki T, Hirata A, Kazama Y, Abe T, Hattori M, Bišová K, Zachleder V, Kawano S (2018) Comparison of lipid productivity of *Parachlorella kessleri* heavy-ion beam irradiation mutant PK4 in laboratory and

- 150-L mass bioreactor, identification and characterization of its genetic variation. *Algal Res* 35:416-426 doi:10.1016/j.algal.2018.09.005
- Tamiya H (1959) Process of growth of *Chlorella* studied by the technique of synchronous culture. In: Kachroo P (ed) Proceedings of the Symposium on Algology. Indian Council of Agricultural Research, New Delhi, pp 128-137
- Tamiya H, Iwamura T, Shibata K, Hase E, Nihei T (1953) Correlation between photosynthesis and light-independent metabolism in growth of *Chlorella*. *Biochimica et Biophysica Acta* 12:23-40
- Tripathi U, Venkateswaran G, Sarada R, Ravishankar GA (2001) *Haematococcus pluvialis* for improved production of astaxanthin by mutagenesis. *W J Microbiol Biotechnol* 17:143-148
- Tulin F, Cross FR (2014) A microbial avenue to cell cycle control in the plant superkingdom. *Plant Cell* 26:4019-4038 doi:10.1105/tpc.114.129312
- Tulin F, Cross FR (2015) Cyclin-dependent kinase regulation of diurnal transcription in *Chlamydomonas*. *Plant Cell* 27:2727-2742 doi:10.1105/tpc.15.00400
- Turner JJ, Ewald JC, Skotheim JM (2012) Cell size control in yeast. *Curr Biol* 22:R350-R359 doi:10.1016/j.cub.2012.02.041
- Umen JG (2005) The elusive sizer. *Curr Op Cell Bio* 17:435-441
- Umen JG, Goodenough UW (2001) Control of cell division by a retinoblastoma protein homolog in *Chlamydomonas*. *Genes Dev* 15:1652-1661
- Umen JG (2018) Sizing up the cell cycle: systems and quantitative approaches in *Chlamydomonas*. *Curr Opin Plant Biol* 46:96-103 doi:10.1016/j.pbi.2018.08.003
- Vieler A et al. (2012) Genome, Functional Gene Annotation, and Nuclear Transformation of the Heterokont Oleaginous Alga *Nannochloropsis oceanica* CCMP1779. *PLoS Genet* 8:e1003064
- Vilela M, Morgan JJ, Lindahl PA (2010) Mathematical model of a cell size checkpoint. *Plos Comput Biol* 6:11 doi:e1001036
- Viles FJ, Silverman L (1949) Determination of starch and cellulose with anthrone. *Anal Chem* 21 (Gräslund et al.):950-953. doi: 10.1021/ac60032a019
- Vítová M, Bišová K, Umyšová D, Hlavová M, Kawano S, Zachleder V, Čížková M (2011) *Chlamydomonas reinhardtii*: duration of its cell cycle and phases at growth rates affected by light intensity. *Planta* 233:75-86 doi:10.1007/s00425-010-1282-y

- Vítová M, Zachleder V (2005) Points of commitment to reproductive events as a tool for analysis of the cell cycle in synchronous cultures of algae. *Folia Microbiol* 50:141-149
- Wang G, Kong H, Sun Y, Zhang X, Zhang W, Altman N, dePamphilis CW, Ma H (2004) Genome-wide analysis of the cyclin family in Arabidopsis and comparative phylogenetic analysis of plant cyclin-like proteins. *Plant Physiol* 135:1084-1099
- Wanka F (1968) Ultrastructural changes during normal and colchicine-inhibited cell division of *Chlorella*. *Protoplasma* 66:105-130
- Wanka F (1975) Possible role of the pyrenoid in the reproductional phase of the cell cycle of *Chlorella*. *Colloq Intern CNRS*, 240:132-136
- Watson JD, Crick FH (1953) Molecular structure of nucleic acids; a structure for deoxyribose nucleic acid. *Nature* 171:737-738
- Weimer AK, Biedermann S, Harashima H, Roodbarkelari F, Takahashi N, Foreman J, Guan Y, Pochon G, Heese M, Van Damme D, Sugimoto K, Koncz C, Doerner P, Umeda M, Schnittger A. (2016) The plant-specific CDKB1-CYCB1 complex mediates homologous recombination repair in Arabidopsis. *EMBO J.* 35(19):2068-2086 doi: 10.15252/embj.201593083
- Wijffels RH, Barbosa MJ (2010) An outlook on microalgal biofuels. *Science* 329:796-799
- Wu Q, Nelson WH, Hargraves P, Zhang J, Brown CW, Seelenbinder JA (1998) Differentiation of algae clones on the basis of resonance Raman spectra excited by visible light. *Anal Chem* 70:1782-1787 doi:10.1021/ac971098b
- Yagisawa F et al. (2009) Identification of novel proteins in isolated polyphosphate vacuoles in the primitive red alga *Cyanidioschyzon merolae*. *Plant J* 60:882-893
- Zachleder V, Šetlík I (1968) Induction of nuclear division in *Scenedesmus quadricauda*. *Annu Rep Algolog Lab Trebon for 1968*:44-65
- Zachleder V (1984) Optimization of nucleic acids assay in green and blue-green algae. Extraction procedures and the light-activated reaction for DNA. *Algol Stud* 36 (1):313-328. doi: 10.1127/algol_stud/67/1984/313
- Zachleder V, Ballin G, Doucha J, Šetlík I (1988) Macromolecular syntheses and the course of cell cycle events in the chlorococcal alga *Scenedesmus quadricauda* under nutrient starvation: Effect of phosphorus starvation. *Biol Plantarum* 30:92-99
- Zachleder V, Šetlík I (1990) Timing of events in overlapping cell reproductive sequences and their mutual interactions in the alga *Scenedesmus quadricauda*. *J Cell Sci* 97:631-638

- Zachleder V, van den Ende H (1992) Cell cycle events in the green alga *Chlamydomonas eugametos* and their control by environmental factors. *J Cell Sci* 102:469-474
- Zachleder V, Schläfli O, Boschetti A (1997) Growth-controlled oscillation in activity of histone H1 kinase during the cell cycle of *Chlamydomonas reinhardtii* (Chlorophyta). *J Phycol* 33:673-681
- Zhao G, Chen YP, Carey L, Fitcher B (2016) Cyclin-dependent kinase coordinates carbohydrate metabolism and cell cycle in *S. cerevisiae*. *Mol Cell* 62:546-557 doi:10.1016/j.molcel.2016.04.026
- Zones JM, Blaby IK, Merchant SS, Umen JG (2015) High-Resolution Profiling of a Synchronized Diurnal Transcriptome from *Chlamydomonas reinhardtii* Reveals Continuous Cell and Metabolic Differentiation. *Plant Cell* 27:2743-2769 doi:10.1105/tpc.15.00498

Coordination of growth and cell cycle progression in green algae

Chapter II

Goals and hypotheses

Ivan N. Ivanov



The question of the coordination between growth and cell cycle progression is fundamental to our understanding of the living world and is one of the last standing enigmas in biology. Not only that, but since growth (i.e. accumulation of metabolites) and cell cycle progression are closely connected, a deeper understanding of their mutual link can have significant implications for algal biotechnology. In order to address our present lack of understanding in those areas the current doctoral thesis adopted the following research objectives:

Goal 1: *To identify how growth processes affect the cell cycle progression and particularly the attainment of commitment point in green algae.*

Goal 2: *To gain deeper understanding of the function of the cell cycle in green algae and to investigate the influence of the combination of environmental factors and metabolic signals on its progression.*

Goal 3: *To establish whether our thus far acquired knowledge of the intrinsic workings of the cell cycle in green algae can be translated into an approach for the industrial production of economically important metabolites such as starch.*

Goal 4: *To develop and establish a reliable method, based on Raman spectroscopy, for the observation and the quantification of intracellular macromolecules.*

When it comes to the language of the scientific method, the aforementioned goals can be rendered in a specific, verifiable combination of a working hypothesis and a null hypothesis. Because of the large scope and rather high complexity of the goals at hand not one but rather several different combinations of a working and a null hypothesis ought to be formulated. In the hereafter described combinations the working hypothesis represents a semantic statement that we presume is true based

on our current state of knowledge on the topic and/or previously obtained empirical data that supports the hypothesis in question. In contrast, the null hypothesis represents the default position, namely that there are no grounds of believing that the working hypothesis is true. These combinations of working and null hypothesis can be formulated as follow:

Working hypothesis 1: Cell cycle progression in *D. quadricauda* is in direct correlation with cell growth and the attainment of critical cell size (Chapter 4).

Null hypothesis 1: Cell cycle progression in *D. quadricauda* is not in direct correlation with cell growth and the attainment of critical cell size (Chapter 4).

Working hypothesis 2: Supraoptimal temperature inhibits the cell cycle in *C. reinhardtii* causing cell cycle arrest and over accumulation of starch (Chapters 5 and 6).

Null hypothesis 2: Supraoptimal temperature does not inhibit the cell cycle in *C. reinhardtii* and does not cause cell cycle arrest or over accumulation of starch (Chapters 5 and 6).

Working hypothesis 3: Production of starch through supraoptimal temperature in *C. reinhardtii* is possible in pilot scale (Chapter 6).

Null hypothesis 3: Production of starch through supraoptimal temperature in *C. reinhardtii* is not possible in pilot scale (Chapter 6).

Working hypothesis 4: Starch and other macromolecules in *D. quadricauda* can be successfully observed and quantified using confocal Raman microscopy (Chapter 7)

Null hypothesis 4: Confocal Raman microscopy cannot be used for the observation and quantification of starch and other macromolecules in *D. quadricauda* (Chapter 7).

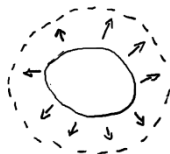
In order to achieve the previously listed goals, in the next chapter we examine the current knowledge of the coordination between growth and cell cycle progression in green algae and other model organisms in greater detail. Furthermore, chapters 4 to 7 are the focal point of the experimental work of this thesis. There we take upon the task of investigating whether the working or the null hypothesis is in accordance with the experimental evidence.

Coordination of growth and cell cycle progression in green algae

Chapter III

Growth and the cell cycle in green algae dividing by multiple fission

Ivan N. Ivanov, Milada Vítová, Kateřina Bišová





Growth and the cell cycle in green algae dividing by multiple fission

Ivan Nedyalkov Ivanov^{1,2} · Milada Vítová¹ · Kateřina Bišová¹

Received: 31 January 2019 / Accepted: 15 July 2019

© Institute of Microbiology, Academy of Sciences of the Czech Republic, v.v.i. 2019

Abstract

Most cells divide into two daughter cells; however, some green algae can have different division patterns in which a single mother cell can sometimes give rise to up to thousands of daughter cells. Although such cell cycle patterns can be very complex, they are governed by the same general concepts as the most common binary fission. Moreover, cell cycle progression appears to be connected with size, since cells need to ensure that their size after division will not drop below the limit required for survival. Although the exact mechanism that lets cells measure cell size remains largely unknown, there have been several prominent hypotheses that try to explain it.

Cell cycle organization

The life of a cell is demarcated by two cell divisions. In one division, the cell is born and in the second division, it divides into daughter cells and de facto disappears. This is referred to as a cell cycle and has fascinated cell biologist for more than a century. The nuclear division, mitosis, was observed early and led to the division of the cell cycle into two periods, nuclear and cellular divisions, and the interphase between the two divisions. This simple view was elaborated on in the experiments of Alma Howard and Stephen Pelc (Howard and Pelc 1953) leading to the current view of cell cycle organization. Howard and Pelc's experiments provided evidence of timely separation of DNA synthesis and mitosis leading to a cell cycle model composed of four phases: G1, S, G2, and M. G1 is generally considered a major growth phase. G1 phase is then followed by DNA synthesis, S phase, where DNA replication takes place. After DNA replication is completed, the cell enters the G2 phase during which it prepares for nuclear division and also grows, although this growth phase is usually not so pronounced. Finally, the cell enters M phase,

splitting the chromosomes duplicated during S phase, then dividing the cell nuclei and whole cells. The cell enters G1 phase again and the cycle is repeated. Although this cell cycle organization appears quite simple, it should be kept in mind that the distinction described above is mostly semantic and as such does not necessarily reflect the reality within the cells where many processes tend to overlap from one phase to the next. Moreover, the most critical parts of the cell cycle are those when seemingly “nothing” happens but in fact the most critical decision processes are in play. Finally, any division, as part of the cell cycle, is clearly dependent on preceding growth that duplicates the structure to be divided. Thus, each cell cycle is closely intertwined with cell growth, although, as of yet, no clear connecting mechanism has been described. All of these questions are discussed below with an emphasis on the cell cycle and growth in green algae dividing by multiple fission, but in places, we also discuss interesting examples of other model systems. We refer the reader to original articles and to recent reviews that provide a comprehensive view of the topic.

Dedicated to the memory of Prof. Ivan Šetlík.

✉ Kateřina Bišová
bisova@alga.cz

¹ Institute of Microbiology, Centre Algatech, Laboratory of Cell Cycles of Algae, Opatovický mlýn, Czech Academy of Sciences, 379 81 Třeboň, Czech Republic

² Faculty of Science, University of South Bohemia, Branišovská 1760, 370 05 České Budějovice, Czech Republic

Green algae dividing by multiple fission

Unlike most cells in nature, some green algae can divide through a division pattern in which one mother cell can give rise to more than two daughter cells, denoted as multiple fission; for review, see Bišová and Zachleder (2014) and Zachleder et al. (2016). Such green algae, including species from genera *sensu lato Scenedesmus*, *Chlorella*, and *Chlamydomonas*, have been favourite model systems,

particularly for their fast growth and ease of cultivation. For more than six decades, some of them have been used for analysis of the cell cycle, starting with the first synchronization of *Chlorella* cultures by the group of Tamiya (Tamiya et al. 1953). Later on, other species such as *Desmodesmus* (formerly *Scenedesmus*) *quadricauda*, *Chlamydomonas* sp. gained popularity and became prominent cell cycle models in their own right (Lien and Knutsen 1972, 1979; Lorenzen 1968; Pirson and Lorenzen 1966; Šetlík et al. 1972).

A notable part of early cell cycle research utilizing *Desmodesmus quadricauda* as a model organism was pioneered by Ivan Šetlík and his colleagues at the Department of Photoautotrophic Microorganisms in Třeboň in Czechoslovakia (now the Czech Republic) (Šetlík et al. 1972, 1975; Zachleder et al. 1975). During these early times, the green alga *D. quadricauda* proved to be especially convenient because daughter cells arising from a single mother cell remain connected in a structure called a coenobium. This physiological feature of *D. quadricauda* offered a fast and straightforward method for the reverse analysis of cell cycle processes experienced by the cell (Šetlík et al. 1972) (for more details see below).

One of the main advantages of algae as a cell cycle model organism stems from the ease of reaching a high level of synchronization. The synchronization procedure is based on the naturally present feature of green algae that grow autotrophically during the day and undergo DNA replication/s and nuclear and cellular divisions during the night. Thus, alternating periods of light/dark provide a natural means for synchronization of algal cultures. Such a synchronization procedure is not only natural but also very fast, reliable, and yields populations where 90 to 95% of the cells were in the same physiological state (Bišová and Zachleder 2014). Another advantage of algae dividing by multiple fission is the flexibility of their cell cycle, which makes it easy to obtain differing patterns of the cell cycle simply by varying growth conditions or by applying inhibitors (Bišová et al. 2000). However, the multiple fission cell cycle model is much more complex than the classical model of binary fission (for details see below) and is governed by complex regulatory mechanisms (Zachleder and Šetlík 1990).

Cell multiplication is composed of growth and structure reproduction steps

Cell division is the final part of the cell cycle but clearly in order to divide without sacrificing its viability the cell had to grow previously, so there are materials and structures to be divided. The life of a cell from its birth up to its division into daughter cells could be thus modelled as comprising growth, in the simplest case scenario equal to G1 phase, and the reproductive sequence consisting of DNA replication, nuclear and cellular divisions (Mitchison 1971). From now on, we

will use the terms growth sequence and reproductive sequence to refer to these two processes and to avoid confusion. The processes of growth and cell reproduction are fundamentally different and could in principle run independently without any functional interconnection. It is important to understand and keep in mind the distinction, as in reality, growth and reproductive sequences overlap extensively. In addition, it is useful to understand the cell cycle not as a cycle but rather as a sequence of events, the growth sequence and the reproductive sequence (Cooper 1979, 1984; Šetlík and Zachleder 1984). The sequences could be performed over more than one cycle between two cell divisions. This helped our understanding of the regulation of the bacterial cell cycle but, to a certain extent, it is also true for eukaryotes, particularly green algae dividing by multiple fission (see below).

In green algae dividing by multiple fission, the growth sequence is (during autotrophic growth) dependent on light while the reproductive sequence is light-independent. This is not only useful for culture synchronization, as discussed above, but also has striking consequences for studies of the cell cycle, since it allows the separation of growth and reproductive sequences by inserting a period of dark. This unique property is absent from other unicellular models used to study cell cycle regulation or growth and cell cycle coordination, such as budding and fission yeast. This property was also an elegant tool used to analyse how growth and reproductive sequences overlap. In budding yeast, a pioneering genetic screen of Hartwell, Pringle, and their co-workers (Pringle and Hartwell 1981) lead to the definition of Start as the earliest gene-controlled event in G1 and, more importantly, as the point when cells become committed to the mitotic cell cycle (Nurse 1985). By analogy, a similar regulatory point was genetically identified in fission yeast (Nurse and Bissett 1981). In algae, cultures sequentially transferred in the dark or treated with photosynthesis inhibitors would, with time spent on light, suddenly become committed to nuclear and cell divisions and divide even in the dark, i.e. in the absence of further energy. This was referred to by different authors as a ‘point-of-no-return’ (Moberg et al. 1968), ‘induction of division’ (Šetlík et al. 1972), ‘transition point’ (Spudich and Sager 1980), or ‘commitment point’ (John 1984, 1987) and it is a functional equivalent of Start in yeast (John 1984). Throughout the manuscript, we refer to this decision point as CP.

As the experiment with light-dark treatment suggested, a certain degree of growth was required prior to attaining CP. Indeed, critical cell size is a prerequisite for reaching a commitment to divide, not only in algae (John 1984, 1987), but also in fission yeast (Fantes and Nurse 1977; Fantes and Nurse 1978; Nurse 1975). Growth has several attributes including but not limited to an increase in RNA, protein, energy reserves, and an increase in cell size (cell volume and surface) but it remains unclear which of them or their combinations are decisive in attaining CP.

Growth and reproductive sequences are regulated differently

The CP has fascinated algal cell biologists for decades, yet it remains enigmatic and its regulation is not fully understood. The intersection of growth and reproductive sequences at attainment of CP has such pronounced effects on cell physiology that similarly to division of the cell cycle into mitosis and interphase, the cell cycle of algae can be divided into pre-CP and post-CP periods. This is because the cell, when committed to division, is fundamentally different from the incompetent un-committed cell prior to CP. The pre-CP period consists solely of the growth sequence. In contrast, the post-CP period may, in the dark, consist of only the reproductive sequence but, generally, consists of one to several reproductive sequence/s as well as one to several growth sequence/s. The post-CP period on light is roughly equivalent to the post-Start period in fission or budding yeast, where both growth and reproductive sequences run concurrently. In contrast, the post-CP period in the dark is unique to green algae and it is a powerful tool for assessing the regulation of the two periods, as well as coordination between growth and reproductive sequences in general.

The growth and cell cycle progression in green algae dividing by multiple fission is controlled by two key factors, light and temperature (Bišová and Zachleder 2014). Light functions as both a source of energy for cell growth and as a signal molecule affecting its behaviour. Here, we will limit ourselves to the effect of different light intensities as the best-established topic. Temperature affects general metabolism of the cell so that it is roughly accelerated twofold with each 10 °C increase in temperature, within the physiological range of the species (John 1984; Vítová et al. 2011a). The effect of both treatments on synchronized cultures of algae was studied, for the first time, by Morimura on *Chlorella ellipsoidea* as early as 1959 (Morimura 1959). Morimura used two different set-ups. In each of them, he set one of the factors, light or temperature, to optimal and non-limiting values so as not to affect cell cycle progression. The other factor varied. A variation in light intensity from very low to high (but not stressing) levels led to improved growth, bigger mother cells, and more daughter cells released, suggesting a trophic effect of light. Morimura's experiments were later repeated on other algal species such as *D. quadricauda* (Šetlík et al. 1988; Zachleder 1995), *Chlamydomonas eugametos*, and *Chlamydomonas reinhardtii* (John 1984; Vítová et al. 2011a, b; Zachleder and Šetlík 1990; Zachleder and van den Ende 1992) with very similar outcomes. This led to the conclusion that light intensity is a key component affecting growth rate under constant temperature, and with increasing light intensity, the growth rate is increased. Importantly, the CP was always attained at the same, critical cell size. Furthermore, the length of the pre-CP period was proportional to light intensity

(and growth rate). The lower the light intensity, the longer the pre-CP period, supporting involvement of a sizer. In contrast, the post-CP period, switched on by attainment of the CP, remained mostly unaffected by light intensity and appeared to be determined by a timer. The length of the post-CP period is determined mostly by the reproductive sequence, which must be completed prior to cell division. Thus, we believe it is not necessary to postulate a timer since the duration of the reproductive sequence, i.e. DNA replication and nuclear and cellular divisions, is already constant at a given temperature. This suggests that pre-CP and post-CP periods are regulated differently. The pre-CP period is set by growth rate and regulated by a sizer, while the post-CP period appears to be timer-regulated. Such a combination of timer and sizer on regulation of the cell cycle was described both in algae and in other organisms (Donnan and John 1983; Fantes and Nurse 1977; John 1984; Masui and Wang 1998; Spudich and Sager 1980; Sveiczler et al. 1996; Šetlík et al. 1972; Wang et al. 2000; Zachleder et al. 2002; Zachleder and Šetlík 1990). Interestingly, although ubiquitously present, the combination of sizer and timer for governing pre-CP and post-CP periods also seems to be important for the multiple fission cell cycle.

Experiments on the effects of different temperatures on growth and cell cycle progression were less often carried out, probably due to the more complicated experimental design. In Morimura's temperature experiments, increasing temperature increased growth rates due to a general effect of temperature on the entire metabolism and it also affected the duration of the cell cycle (Morimura 1959). The effect of temperature on growth and cell cycle progression was distinct from the effect of light intensity. Firstly, the critical cell size differed at different temperatures and secondly, the duration of the post-CP period varied due to changes of general metabolic rates. This suggested that both the sizer and timer change at different temperatures. From the two, the change in timer is to be expected due to different metabolic rates, while the change in critical cell size is rather surprising. The results of Morimura were confirmed on other green algae with the same outcomes (Donnan et al. 1985; Donnan and John 1983; John 1984; Vítová et al. 2011a, b; Zachleder et al. 2019).

Cells can divide in different cell cycle patterns

In order to multiply and proliferate, both prokaryotic and eukaryotic cells have to go through a series of precisely controlled events that are commonly described as the cell cycle. While recent advances in prokaryotic genome sequencing have revealed some surprising similarities with eukaryotes in terms of cell cycle mechanics, some prokaryotes, such as many archaeal species, have cell cycle patterns that are fundamentally different from those in eukaryotes (Bramhill 1997; Samson and Bell 2011). Intriguingly, they also share strikingly

similar concepts with cell cycle organization of some green algae (and other eukaryotes), as mentioned above, and is discussed below in more detail. The focus of this review is on eukaryotic green algae, but for a comprehensive description of the cell cycle and its control mechanisms in prokaryotes, the reader is referred to Abner et al. (2014), Lutkenhaus (2010), Robert (2015), Samson and Bell (2011), and Willis and Huang (2017).

C1 cycle (binary division)

Above we described a classical cell cycle scheme as described by Howard and Pelc, where one mother cell gives rise to two, more or less identical, daughter cells. Such a cell cycle scheme consists of a single growth sequence and a single reproductive sequence, hence C1 (Fig. 1). A daughter cell will grow until it reaches critical cell size whereupon it will attain CP. Attaining of CP will allow for one round of DNA replication and nuclear

and cellular divisions to occur. Such cell cycle organization is common for the majority of organisms. It is well characterized and described in detail elsewhere (Morgan 2006) so here we will not go into a detailed description. Green algae dividing by multiple fission also utilize this cell cycle organization, but only at very slow growth rates (Bišová and Zachleder 2014; Zachleder et al. 2016).

Cn cycle (multiple fission)

Division by multiple fission, here denoted as the Cn cycle, is widely spread within chlorophycean algae, while it is missing in their naked relatives (Floyd 1978; Kirk 1998). The binary (C1) and multiple fission (Cn) patterns of the cell cycle can be interchangeable in some species, depending on growth rate. Cells grown under unfavourable environmental (light and/or temperature) conditions will divide only into two, while cells grown under favourable conditions will divide into 4, 8, 16,

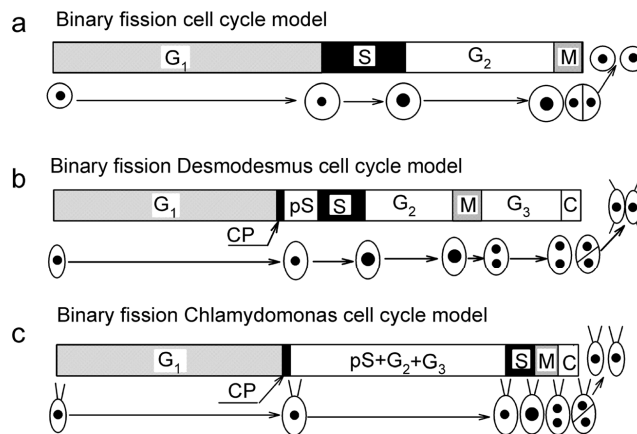


Fig. 1 Diagrams showing different types of cell cycle phases, including the classical cell cycle model and those found in *Desmodemus* and *Chlamydomonas*, which divide into two daughter cells. **a**: Classical type cell cycle after (Howard and Pelc 1953), **b**: Desmodemus-type cell cycle after Zachleder and van den Ende (1992). Individual bars show the sequence of cell cycle phases and events during which, growth and reproductive processes take place. Only one reproductive sequence leading to the duplication of cell structures occurs during the cycle of cells dividing into two daughter cells (panels a, b, c). Thus, all of the schemes correspond to a C1 type of cell cycle (number of daughter cells is 2¹). Schematic pictures of the cells indicate their size during the cell cycle and the black circles inside illustrate the size and number of nuclei. Large black spots indicate a doubling of DNA. The lines at the terminal cells of *Desmodemus* coenobia represent spines typical for the species *D. quadricauda*. The lines at the top of the *Chlamydomonas* cells represent flagella, which are retracted by the cells before DNA replication begins. **G1**: the phase during which the threshold size of the cell is attained. It can be called a **pre-commitment period** because it is terminated when the commitment point is reached. **CP**: the stage in the

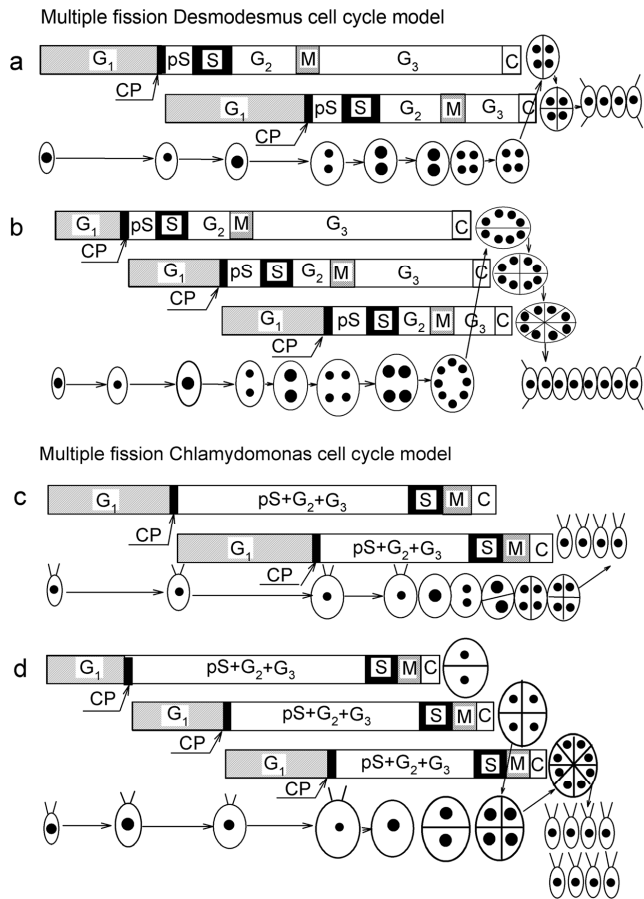
cycle at which the cell becomes committed to triggering and terminating the sequence of processes leading to the duplication of reproductive structures (**post-commitment period**), which consists of **pS**: the pre-replication phase between the commitment point and the beginning of DNA replication. The processes required for the initiation of DNA replication are assumed to happen during this phase. **S**: the phase during which DNA replication takes place. **G2**: the phase between the termination of DNA replication and the start of mitosis. Processes leading to the initiation of mitosis are assumed to take place during this phase. **M**: the phase during which nuclear division occurs. **G3**: the phase between nuclear division and cell division. The processes leading to cellular division are assumed to take place during this phase. **C**: the phase during which cell cleavage and daughter cell formation occurs. In *Chlamydomonas*, apparent G₂ and G₃ phases are missing; it can, however, be assumed that all the required processes happen during the prolonged gap phase, which is thus denoted pS+G₂+G₃ (adapted by permission from Springer: “The cell cycle of microalgae” by Zachleder et al. (2016), In: Borowitzka MA, Beardell J, Raven JA, eds. *The physiology of microalgae*. Cham: Springer International Publishing Switzerland, 3–46, Copyright 2016)

and so on daughter cells (Bišová and Zachleder 2014; Zachleder et al. 2016). This is dictated by the dependence of growth sequence, as a sizer-regulated process, on reaching critical cell size at a pace dictated by growth rate. In contrast, the reproductive sequence depends on the completion of all required processes, being timer-controlled. This is further accentuated by the growth sequence being light-dependent, while the reproductive sequence is light-independent. The combination of the two properties allows the cells to maximize their exploitation of light energy for photosynthesis without interruption from cell division. It also permits higher growth rates to be achieved compared with species dividing by binary fission (Rading et al. 2011).

The Cn cycle starts off the same as the C1 cell cycle by entering a growth sequence. Once the critical cell size is reached, the cells will attain CP and start the reproductive

sequence, which would eventually lead to division into two daughter cells. Here, begins the distinction from the C1 cycle. If the cell is still in the light and is able to grow, it will, immediately after attaining CP, start another growth phase, which could eventually lead to attaining another CP and starting a new reproductive sequence, thus producing four daughter cells from a single mother cell. At a sufficiently high growth rate (high light intensity), this could repeat itself one or several more times (Fig. 2). The number of reproductive sequences, n , that could be initiated, is given by species-specific limitations as well as growth rates; e.g., *D. quadricauda* can only start three reproductive sequences that would be completed by cell division into eight daughter cells (2^3) (Šetlík and Zachleder 1984). In contrast, *Chlamydomonas reinhardtii* can start up to four reproductive sequences under optimal conditions, leading to division into 16 daughter cells (Lien and

Fig. 2 Diagrams showing different types of cell cycle phases found in *Desmodesmus* and *Chlamydomonas* dividing by multiple fission (cell cycle type Cn). **a, b**: *Desmodesmus*-type cell cycle after Šetlík and Zachleder (1984), and **c, d**: *Chlamydomonas*-type cell cycle after Zachleder and van den Ende (1992). For description of figure characteristics, see Fig. 1. Two (a, c) or three (b, d) consecutive growth sequences and partially overlapping reproductive sequences occur within a single cycle in cells dividing into four daughter cells (a, b) or eight daughter cells (b, d) (adapted by permission from Springer: "The cell cycle of microalgae" by Zachleder et al. (2016), In: Borowitzka MA, Beardell J, Raven JA, eds. *The physiology of microalgae*. Cham: Springer International Publishing Switzerland, 3–46, Copyright 2016)



Knutsen 1972, 1979; Vitová et al. 2011b) and mutant cells can start even more overlapping sequences (Umen and Goodenough 2001). Thus, within the multiple fission (Cn) cell cycle, there are several consecutive growth sequences and several overlapping reproductive sequences. In this way, the cells exploit maximum available energy at high light intensity by producing a maximum number of daughter cells. At the same time, the constant duration of the post-CP period ensures that at slow growth rates, the reproductive sequence is always completed on time and does not further depend on reaching a critical cell size for the next reproductive sequence. For more details on execution and types of Cn cycle, please see Bišová and Zachleder (2014).

A consequence of this type of cycle is that cells can grow beyond critical cell size for one reproductive sequence but are unable to reach critical cell size for attaining a further CP and starting the next reproductive sequence. Such cells will be bigger at birth and would require less growth to reach critical cell size and attain CP in the next cell cycle. This property is not unique to multiple fission cell cycles. In fact, it is a common part of binary fission (C1 cycle) in cells grown at high growth rates. The only difference is that in multiple fission cell cycles, such an overlap between cell cycles can be more pronounced. This is nicely demonstrated in fast-growing *D. quadricauda* cells, especially when illuminated during cell division (Zachleder et al. 2002). Such cells will continue to increase their size until they can reach critical cell size for attaining the fourth CP for division into 16 daughter cells. This will start the reproductive sequence. However, this will not lead to division into 16 daughter cells and it will not affect the timing of the already running reproductive sequences. There are two possible causes: either the reproductive sequence was started too late to be connected with the previous ones or it is simply because this species is unable to divide into more than 8 daughter cells. Instead, this will lead to DNA replication and possibly nuclear division immediately in the newborn daughter cells, even in the dark. Thus, there is an overlap between two successive cell cycles. The ubiquitous presence of such events in the multiple fission cell cycle leads us to accept the concept of a reproductive sequence as was proposed by Cooper (Cooper 1979, 1984) instead of a cell cycle. Such an overlap between successive cell cycles is quite common among bacteria but was thought not to exist in eukaryotes (Bišová and Zachleder 2014). Clearly, there is no barrier preventing the overlap of cell cycles even in eukaryotes, under specific conditions.

In the discussion above, we implied that reaching a critical cell size will lead to attainment of CP and to the start of the reproductive sequence. However, results with *D. quadricauda*, as discussed above, suggest that to perceive CP as a single point in algae would be an oversimplification. This is not surprising since in yeast, Start is not a single point within a cell cycle but rather a period regulated by several

genes (Forsburg and Nurse 1991; Nurse 1985; Pringle and Hartwell 1981). This could be further demonstrated on a different example. During growth in light, the cell increases its cell size but it also synthesises RNA and protein. Such synthesis runs in steps where the steps of RNA accumulation precede the steps of protein accumulation. Interestingly, it seems that reaching the RNA step is a prerequisite for DNA replication but not for nuclear division. Reaching the step of protein accumulation is related to completion of nuclear division (Zachleder and Šetlík 1988). Thus, CP is a sequence of processes rather than a single point within the cell cycle and reaching different critical values will lead to switching on of different components of the reproductive sequence.

Cell size—how is it measured?

As we have already seen, the eukaryotic organisms seem to retain a mechanism able to coordinate growth and reproductive sequences although the two could in principle run independently. This is particularly true for a critical cell size required for attaining CP and starting reproductive sequence, which ensures that the cell size after division will not drop below the limit required for survival. This led to the proposition of a conceptually simple cell size checkpoint hypothesis. The hypothesis suggests that eukaryotic cells possess a mechanism for determining cell size and the existence of a checkpoint that establishes a minimum cell size for progression through the cell cycle. This means that cells that are small can catch up to larger cells by growing and delaying cell cycle progression until they reach the minimum cell size required for satisfying the cell size checkpoint. In contrast, large cells will reach the checkpoint earlier and will progress through the cell cycle more rapidly (Umen 2005). This will ensure that the cell size in a population of cells will not drop below the minimum required for survival. In spite of the conceptual simplicity of the cell size checkpoint hypothesis, the molecular machinery that must undoubtedly exist in order to facilitate such behaviour has been surprisingly difficult to unravel. Throughout the years, there have been numerous propositions for models that attempt to explain the link between cell growth and progression of the cell cycle (for a short overview on the known types of sizer, please see Haupt and Minc (2018)). Generally, the models can be divided into three main categories: geometric, protein concentration, and metabolic models.

Geometric models

Geometric models attempt to explain the connection between cell size and cell cycle progression in terms of cell length, diameter, or surface to volume ratio-sensing mechanisms. Two studies conducted in fission yeast and published in *Nature* in 2009 demonstrated that a gradient of a polarity

factor protein appears to act as a sensing mechanism of cell length and can determine the onset of activation key cell cycle regulator, cyclin-dependence kinase, and CDK, leading to mitosis. This mechanism involves changes in the spatial cellular distribution of two proteins, Pom1 and Cdr2, as the cell grows lengthwise. Pom1 inhibits Cdr2, while Cdr2 is responsible for the promotion of the transition between G2 and M phases. According to the model, in fission yeast, Cdr2 is localized in the mid cell region, whereas the concentration of Pom1 is highest at the cell tips and declines towards the middle of the cell. In short cells, Pom1 efficiently inhibits Cdr2. However, as the cell grows, the Pom1 concentration in the middle of the cell decreases such that Cdr2 becomes activated at a certain critical cell size and triggers the onset of mitosis (Martin and Berthelot-Grosjean 2009; Moseley et al. 2009; Vilela et al. 2010)

Although this gradient of polarity, in principle, can be used to explain the relationship between attaining critical cell size and entry into mitosis in fission yeast, it seems unlikely that this is the whole story. This was illustrated in experiments with a CDK mutant bypassing the Pom1-Cdr2 regulatory system. In these cases, cell size homeostasis was still maintained, albeit with a broader size distribution. This indicates the existence of other unknown mechanisms that are responsible for the measurement of cell size and the integration of this information into the cell cycle control (Coudreuse and Nurse 2010). A feasible explanation is also an alternative model where a cell measures its surface area by reviewing the amount of membrane-bound Cdr2 (Deng et al. 2014; Pan et al. 2014).

Protein concentration models

In general, growth of cells can be defined as the accumulation of cytoplasmic mass that is caused by the accumulation of macromolecules. Protein concentration models attempt to explain the attainment of critical cell size through the existence of a sizer, which is a compound that accumulates during growth of the cell until a certain concentration is reached, which then leads to entry into mitosis (Umen 2005). One such sizer protein was identified in *C. reinhardtii* thanks to isolation of a mutation in *MAT3* gene, which encodes a homologue of retinoblastoma protein. The *mat3-4* mutant produces tiny daughter cells. Furthermore, it shows defects in two size-dependent cell cycle controls: (1) the critical cell size for attaining CP is smaller and (2) the mother cell size is misinterpreted leading to super-numerous mitotic division (Umen and Goodenough 2001). Further, genetic screen placed *MAT3* downstream of another gene, *CDKG1*, a novel type of cyclin-dependent kinase that directly phosphorylates Mat3 protein (Li et al. 2016). CDKG1 protein seems to be a bona fide sizer with cell size-dependent accumulation in nucleus and progressive dilution and degradation with each round of

nuclear/cell division. In line with its proposed sizer role, *cdkg1-2* mutant has slightly bigger daughter cells, while the over-expressing line has smaller daughter cells. Similar, even though less pronounced was also the difference in critical cell size at attaining CP (Li et al. 2016). It would be interesting to identify other members of this size sensing pathway and possibly to see if and how it might interact with the cell growth beyond the cell size-dependent accumulation of CDKG1.

Metabolic models

The most basic manifestation of growth is the accumulation of macromolecules, which leads to an increase in cell volume and size. Historically, there have been attempts to link critical cell size with an increase in metabolic activity and the accumulation of different macromolecules such as total RNA and protein, since both of them are a manifestation of growth. In green algae, the concentrations of both macromolecules appear to increase during the light periods of the cell cycle and usually stabilize during the dark period (absence of growth) (for more details on RNA and protein accumulation in relation to cell cycle see Zachleder et al. (2016)). Similar behaviours are also true in other organisms (Cipollina et al. 2007; Di Talia et al. 2007; Turner et al. 2012). However, each of the metabolites varies under some conditions, implying that none of them is the sole critical size determinant (John 1984). Therefore it seems feasible that there is not a single determinant, but rather a combination of different metabolic signals.

Furthermore, the processes of DNA replication and nuclear and cellular divisions are extremely energy demanding; thus, sufficient storage for energy must be available to the cell before it enters cell division (Siddiqui and Stillman 2007). In plant and algal cells, that energy is usually stored in the form of starch, lipids, and polyphosphates (Bental et al. 1991; Sulpice et al. 2009). Two of the compounds serve as a carbon supply, the last are both phosphate and energy store. Combined, they make the cells independent of external supplies of both energy and carbon.

Starch is the primary energy storage macromolecule in plant and algal cells, and as such, is the main source of energy for growth during periods of low light and at night (Izumi et al. 2013). Moreover, microalgal species like *Desmodesmus* sp., *Dunaliella* sp., *Chlamydomonas* sp., and *Chlorella* sp. are known to accumulate levels of starch exceeding 50% of their dry weight (Miranda et al. 2012). Such over-accumulation of starch or lipids in algae is often connected to nutrient limitations, which lead to a block in cell division (Ballin et al. 1988; Brányiková et al. 2011; Li et al. 2013; Šetlík et al. 1988; Zachleder et al. 1988). Similarly to plants, starch in algae accumulates in the form of starch granules contained within the chloroplast (Kobayashi et al. 1974). The starch content in *Chlamydomonas* sp. has a diurnal oscillation and is highest during the night (Ral et al. 2006). Starch accumulation is light/

photosynthesis-dependent and its degradation is cell cycle-dependent being very rapid during nuclear/cell division (Spudich and Sager 1980; Vítová et al. 2011b; Wanka 1968, 1975; Zachleder et al. 2019), even in the presence of light. Polyphosphates are in algae contained within single membrane-bound compartments, which are considered to be counterparts of the seed vacuoles in plants (Yagisawa et al. 2009). They increase during cell growth and some of them are specifically used for DNA synthesis in the dark (Miyachi et al. 1964). The connection between energy requirements and progression of the cell cycle is not specific to algae. In budding yeast, catabolism of two major energy reserves, lipids and carbohydrates, is connected to the cell cycle through regulation of key metabolic enzymes by the cell cycle regulators, cyclin-dependent kinases (Ewald et al. 2016; Futcher 2009; Kurat et al. 2009; Zhao et al. 2016).

All the results discussed above indicate a direct connection between cell size and the cell cycle although the mechanism is not entirely known. The hypothesis of cell size (or any of its other determinants) being the sole factor determining progression of the cell cycle has been questioned by the recent experiments of Zachleder and co-workers (Zachleder et al. 2019) where cells of the green alga *D. quadricauda* were cultivated either at 20 °C or 30 °C. The results revealed that temperature profoundly influenced cell size and cell cycle duration, with the cells grown at 20 °C having a larger cell size and taking almost twice as long to complete their cell cycle compared with cells at 30 °C, which were much smaller and had a shorter cell cycle. The most intriguing were the results of shift experiments, where cells grown at either 20 °C or 30 °C were transferred to darkness to prevent further growth, and then cultivated at the same or the other temperature. Cells transferred to the lower temperature produced fewer nuclei and daughter cells, and some of them were unable to complete division. Correspondingly, cells placed in the dark at the higher temperature divided faster into more daughter cells than the controls. These differences correlated with shifts in the preceding CDK activity but they did not correlate with cell size. This is in clear contradiction of the sizer hypothesis, which postulates that cell size determines the extent of cell cycle progression and suggests that in *D. quadricauda*, progression of the cell cycle is not cell size-dependent. Instead, the growth and reproductive sequence run independently and only appear to coordinate, particularly under stable temperature.

Concluding remarks

Eukaryotic organisms can proliferate through a variety of division patterns; the most common of which is division through binary fission. Some chlorococcal and volvocal algae, however, divide through a pattern called multiple fission, in which some of the phases of the cell cycle overlap. This type of cell division has probably evolved in algae characterized by fast

growth rates and was a response to alternating periods of light and dark. Dividing to more than two daughter cells means that a mother cell can increase its volume more than twice during a favourable period of abundant light (Bišová and Zachleder 2014; Zachleder et al. 2016).

Cell cycle progression in algae depends largely on growth and the accumulation of storage compounds such as starch, lipids, and polyphosphates. It also appears that passing of the commitment point and entry into mitotic division depends on the accumulation of the so-called sizer compounds; the nature of which currently remains largely unknown. However, the strict dependence of cell cycle progression on cell size or accumulation of any metabolite has been challenged by recent experiments in the green alga *D. quadricauda* (Zachleder et al. 2019).

There have been tremendous advances in cell cycle research over the past 60 years; the most significant of which was probably discovering the regulation of the cell cycle by complexes of cyclin-dependent kinases with cyclins, which led to the Nobel Prize award to L. Hartwell, T. Hunt, and P. Nurse in 2001. Although these discoveries have brought a much needed insight into the internal organization of cell cycle control, there is still much to be discovered about the interaction between growth and cell division.

Funding information The work was supported by the Grant Agency of the Czech Republic (grant no. 19-12607S) and by the National Programme of Sustainability I (project no. LO1416).

References

- Abner K, Aavikkaar T, Adamberg K, Vilu R (2014) Single-cell model of prokaryotic cell cycle. *J Theor Biol* 341:78–87
- Ballin G, Doucha J, Zachleder V, Šetlík I (1988) Macromolecular syntheses and the course of cell cycle events in the chlorococcal alga *Scenedesmus quadricauda* under nutrient starvation: effect of nitrogen starvation. *Biol Plant* 30:81–91
- Bental M, Pick U, Avron M, Degani H (1991) Polyphosphate metabolism in the alga *Dunaliella salina* studied by ³¹P-NMR. *Biochim Biophys Acta* 1092:21–28
- Bišová K, Zachleder V (2014) Cell-cycle regulation in green algae dividing by multiple fission. *J Exp Bot* 65:2585–2602
- Bišová K, Vítová M, Zachleder V (2000) The activity of total histone H1 kinases is related to growth and commitment points while the p13(suc1)-bound kinase activity relates to mitoses in the alga *Scenedesmus quadricauda*. *Plant Physiol Biochem* 38:755–764
- Bramhill D (1997) Bacterial cell division. *Annu Rev Cell Dev Biol* 13:395–424
- Brányiková I, Maršáliková B, Doucha J, Brányik T, Bišová K, Zachleder V, Vítová M (2011) Microalgae-novel highly efficient starch producers. *Biotechnol Bioeng* 108:766–776
- Cipollina C, Vai M, Porro D, Hatzis C (2007) Towards understanding of the complex structure of growing yeast populations. *J Biotechnol* 128:393–402
- Cooper S (1979) A unifying model for the G1 period in prokaryotes and eukaryotes. *Nature* 280:17–19
- Cooper S (1984) The continuum model as a unified description of the division cycle of eukaryotes and prokaryotes. In: Nurse P, Streiblová E (eds) *The microbial cell cycle*. Boca Raton, CRC Press, pp 7–18

- Coudreuse D, Nurse P (2010) Driving the cell cycle with a minimal CDK control network. *Nature* 468:1074–1079
- Deng L, Baldissard S, Kettenbach AN, Gerber SA, Moseley JB (2014) Dueling kinases regulate cell size at division through the SAD kinase Cdr2. *Curr Biol* 24:428–433
- Di Talia S, Skotheim JM, Bean JM, Siggia ED, Cross FR (2007) The effects of molecular noise and size control on variability in the budding yeast cell cycle. *Nature* 448:947–951
- Donnan L, John PCL (1983) Cell cycle control by timer and sizer in *Chlamydomonas*. *Nature* 304:630–633
- Donnan L, Carvill EP, Gilliland TJ, John PCL (1985) The cell-cycles of *Chlamydomonas* and *Chlorella*. *New Phytol* 99:1–40
- Ewald JC, Kuehne A, Zamboni N, Skotheim JM (2016) The yeast cyclin-dependent kinase routes carbon fluxes to fuel cell cycle progression. *Mol Cell* 62:532–545
- Fantes P, Nurse P (1977) Control of cell size at division in fission yeast by a growth-modulated size control over nuclear division. *Exp Cell Res* 107:377–386
- Fantes PA, Nurse P (1978) Control of the timing of cell division in fission yeast. Cell size mutants reveal a second control pathway. *Exp Cell Res* 115:317–329
- Floyd GL (1978) Mitosis and cytokinesis in *Asteromonas gracilis*, a wall-less green monad. *J Phycol* 14:440–445
- Forsburg SL, Nurse P (1991) Cell cycle regulation in the yeasts *Saccharomyces cerevisiae* and *Schizosaccharomyces pombe*. *Annu Rev Cell Biol* 7:227–256
- Futcher B (2009) Tg14 lipase: a big fat target for cell-cycle entry. *Mol Cell* 33:143–144
- Haupt A, Minc N (2018) How cells sense their own shape - mechanisms to probe cell geometry and their implications in cellular organization and function. *J Cell Sci* 131:1–10
- Howard A, Pele SR (1953) Synthesis of deoxyribonucleic acid in normal and irradiated cells and its relation to chromosome breakage. *Heredity (Lond)* 6:261–273
- Izumi M, Hidema J, Makino A, Ishida H (2013) Autophagy contributes to nighttime energy availability for growth in *Arabidopsis*. *Plant Physiol* 161:1682–1693
- John PCL (1984) Control of the cell division cycle in *Chlamydomonas*. *Microbiol Sci* 1:96–101
- John PCL (1987) Control points in the *Chlamydomonas* cell cycle. In: Wiesnar W, Robinson DG, Starr RC (eds) *Algal development molecular and cellular aspects*. Springer-Verlag, Berlin, pp 9–16
- Kirk DL (1998) *Volvox*: molecular genetic origins of multicellularity and cellular differentiation. Cambridge University Press, Cambridge
- Kobayashi T, Tanabe I, Obayashi A (1974) On the properties of the starch granules from unicellular green algae. *Agric Biol Chem* 38:941–946
- Kurat CF, Wolinski H, Petschnigg J, Kaluarachchi S, Andrews B, Natter K, Kohlwein SD (2009) Cdk1/Cdc28-dependent activation of the major triacylglycerol lipase Tg14 in yeast links lipolysis to cell-cycle progression. *Mol Cell* 33:53–63
- Li X, Příbyl P, Bišová K, Kawano S, Cepák V, Zachleder V, Čížková M, Brányiková I, Vitová M (2013) The microalga *Parachlorella kessleri*—a novel highly efficient lipid producer. *Biotechnol Bioeng* 110:97–107
- Li Y, Liu D, Lopez-Paz C, Olson BJ, Umen JG (2016) A new class of cyclin dependent kinase in *Chlamydomonas* is required for coupling cell size to cell division. *eLife* 5:e10767
- Lien T, Knutsen G (1972) Synchronous cultures of *Chlamydomonas reinhardtii* synthesis of repressed and derepressed phosphatase during the life cycle. *Biochim Biophys Acta* 287:154–163
- Lien T, Knutsen G (1979) Synchronous growth of *Chlamydomonas reinhardtii* (Chlorophyceae): a review of optimal conditions. *J Phycol* 15:191–200
- Lorenzen H (1968) Aspects of synchronous culturing of *Chlorella*. *Phykos* 7:50–57
- Lutkenhaus J (2010) Growth and development: prokaryotes. *Curr Opin Microbiol* 13:727–729
- Martin SG, Berthelot-Grosjean M (2009) Polar gradients of the DYRK-family kinase Pom1 couple cell length with the cell cycle. *Nature* 459:852–856
- Masui Y, Wang P (1998) Cell cycle transition in early embryonic development of *Xenopus laevis*. *Biol Cell* 90:537–548
- Miranda JR, Passarinho PC, Gouveia L (2012) Bioethanol production from *Scenedesmus obliquus* sugars: the influence of photobioreactors and culture conditions on biomass production. *Appl Microbiol Biotechnol* 96:555–564
- Mitchison JM (1971) *The biology of the cell cycle*. Cambridge University Press, Cambridge
- Miyachi S, Kanai R, Mihara S, Miyachi S, Aoki S (1964) Metabolic roles of inorganic polyphosphates in *Chlorella* cells. *Biochim Biophys Acta* 93:625–634
- Moberg S, Knutsen G, Goksoyr J (1968) The point of no return concept in cell division. The effects of some metabolic inhibitors on synchronized *Chlorella pyrenoidosa*. *Physiol Plant* 21:390–400
- Morgan DO (2006) *Cell cycle: principles of control*. New Science Press, London
- Morimura Y (1959) Synchronous culture of *Chlorella*. I. Kinetic analysis of the life cycle of *Chlorella ellipsoidea* as affected by changes of temperature and light intensity. *Plant Cell Physiol* 1:49–62
- Moseley JB, Mayeux A, Paoletti A, Nurse P (2009) A spatial gradient coordinates cell size and mitotic entry in fission yeast. *Nature* 459:857–U858
- Nurse P (1975) Genetic control of cell size at division in yeast. *Nature* 256:547–551
- Nurse P (1985) Cell cycle control genes in yeast. *Trends Genet* 1:51–55
- Nurse P, Bissett Y (1981) Gene required in G1 for commitment to cell cycle and in G2 control of mitosis in fission yeast. *Nature* 292:558–560
- Pan KZ, Saunders TE, Flor-Parra I, Howard M, Chang F (2014) Cortical regulation of cell size by a sizer cdr2p. *eLife* 3:e02040
- Pirson A, Lorenzen H (1966) Synchronized dividing algae. *Plant Physiol* 17:439–458
- Pringle JR, Hartwell LH (eds) (1981) *The Saccharomyces cerevisiae cell cycle*. Cold Spring Harbor Laboratory, Cold Spring Harbor
- Rading MM, Engel TA, Lipowsky R, Valleriani A (2011) Stationary size distributions of growing cells with binary and multiple cell division. *J Stat Phys* 145:1–22
- Ral JP, Colleoni C, Wattedbled F, Dauville D, Nempont C, Deschamps P, Li Z, Morell MK, Chibbar R, Purton S et al (2006) Circadian clock regulation of starch metabolism establishes GBSSI as a major contributor to amylopectin synthesis in *Chlamydomonas reinhardtii*. *Plant Physiol* 142:305–317
- Robert L (2015) Size sensors in bacteria, cell cycle control, and size control. *Front Microbiol* 6:515
- Samson RY, Bell SD (2011) Cell cycles and cell division in the archaea. *Curr Opin Microbiol* 14:350–356
- Šetlík I, Zachleder V (1984) The multiple fission cell reproductive patterns in algae. In: Nurse P, Streiblová E (eds) *The microbial cell cycle*. Boca Raton, CRC Press Inc., pp 253–279
- Šetlík I, Berková E, Doucha J, Kubín S, Vendlová J, Zachleder V (1972) The coupling of synthetic and reproduction processes in *Scenedesmus quadricauda*. *Arch Hydrobiol* 41:172–213
- Šetlík I, Zachleder V, Doucha J, Berková E, Bartoš J (1975) The nature of temperature block in the sequence of reproductive processes in *Chlorella vulgaris* BEJERINCK. *Arch Hydrobiol* 14:70–104
- Šetlík I, Ballin G, Doucha J, Zachleder V (1988) Macromolecular syntheses and the course of cell cycle events in the chlorococcal alga *Scenedesmus quadricauda* under nutrient starvation: effect of sulphur starvation. *Biol Plant* 30:161–169
- Siddiqui, Stillman B (2007) The biochemistry of initiating eukaryotic DNA replication. *J Biol Chem* 282:32370–32383

- Spudich JL, Sager R (1980) Regulation of the *Chlamydomonas* cell cycle by light and dark. *J Cell Biol* 85:136–145
- Sulpice R, Pyl ET, Ishihara H, Trenkamp S, Steinfath M, Witucka-Wall H, Gibon Y, Usadel B, Poree F, Piques MC, von Korff M, Steinhauser MC, Keurentjes JJB, Guenther M, Hoehne M, Selbig J, Fernie AR, Altmann T, Stitt M (2009) Starch as a major integrator in the regulation of plant growth. *Proc Natl Acad Sci U S A* 106:10348–10353
- Sveiczar A, Novak B, Mitchison J (1996) The size control of fission yeast revisited. *J Cell Sci* 109:2947–2957
- Tamiya H, Iwamura T, Shibata K, Hase E, Nihei T (1953) Correlation between photosynthesis and light-independent metabolism in growth of *Chlorella*. *Biochim Biophys Acta* 12:23–40
- Turner JJ, Ewald JC, Skotheim JM (2012) Cell size control in yeast. *Curr Biol* 22:R350–R359
- Umen JG (2005) The elusive sizer. *Curr Opin Cell Biol* 17:435–441
- Umen JG, Goodenough UW (2001) Control of cell division by a retinoblastoma protein homolog in *Chlamydomonas*. *Genes Dev* 15:1652–1661
- Vilela M, Morgan JJ, Lindahl PA (2010) Mathematical model of a cell size checkpoint. *PLoS Comput Biol* 6:11
- Vitová M, Bišová K, Hlavová M, Kawano S, Zachleder V, Čížková M (2011a) *Chlamydomonas reinhardtii*: duration of its cell cycle and phases at growth rates affected by temperature. *Planta* 234:599–608
- Vitová M, Bišová K, Umysová D, Hlavová M, Kawano S, Zachleder V, Čížková M (2011b) *Chlamydomonas reinhardtii*: duration of its cell cycle and phases at growth rates affected by light intensity. *Planta* 233:75–86
- Wang P, Hayden S, Masui Y (2000) Transition of the blastomere cell cycle from cell size-independent to size-dependent control at the midblastula stage in *Xenopus laevis*. *J Exp Zool* 287:128–144
- Wanka F (1968) Ultrastructural changes during normal and colchicine-inhibited cell division of *Chlorella*. *Protoplasma* 66:105–130
- Wanka F (1975) Possible role of the pyrenoid in the reproductive phase of the cell cycle of *Chlorella*. *Colloq Intern CNRS* 240:132–136
- Willis L, Huang KC (2017) Sizing up the bacterial cell cycle. *Nat Rev Microbiol* 15:606–620
- Yagisawa F, Nishida K, Yoshida M, Ohnuma M, Shimada T, Fujiwara T, Yoshida Y, Musumi O, Kuroiwa H, Kuroiwa T (2009) Identification of novel proteins in isolated polyphosphate vacuoles in the primitive red alga *Cyanidioschyzon merolae*. *Plant J* 60:882–893
- Zachleder V (1995) Regulation of growth processes during the cell cycle of the chlorococcal alga *Scenedesmus quadricauda* under a DNA replication block. *J Phycol* 30:941–947
- Zachleder V, Šetlík I (1988) Distinct controls of DNA-replication and of nuclear division in the cell-cycles of the chlorococcal alga *Scenedesmus quadricauda*. *J Cell Sci* 91:531–539
- Zachleder V, Šetlík I (1990) Timing of events in overlapping cell reproductive sequences and their mutual interactions in the alga *Scenedesmus quadricauda*. *J Cell Sci* 97:631–638
- Zachleder V, van den Ende H (1992) Cell-cycle events in the green alga *Chlamydomonas eugametos* and their control by environmental factors. *J Cell Sci* 102:469–474
- Zachleder V, Doucha J, Berková E, Šetlík I (1975) The effect of synchronizing dark period on populations of *Scenedesmus quadricauda*. *Biol Plant* 17:416–433
- Zachleder V, Ballin G, Doucha J, Šetlík I (1988) Macromolecular syntheses and the course of cell cycle events in the chlorococcal alga *Scenedesmus quadricauda* under nutrient starvation: effect of phosphorus starvation. *Biol Plant* 30:92–99
- Zachleder V, Bišová K, Vitová M, Kubín Š, Hendrychová J (2002) Variety of cell cycle patterns in the alga *Scenedesmus quadricauda* (Chlorophyta) as revealed by application of illumination regimes and inhibitors. *Eur J Phycol* 37:361–371
- Zachleder V, Bišová K, Vitová M (2016) The cell cycle of microalgae. In: Borowitzka MA, Beardall J, Raven JA (eds) *The physiology of microalgae*. Dordrecht, Springer, pp 3–46
- Zachleder V, Ivanov I, Vitová M, Bišová K (2019) Effects of cyclin-dependent kinase activity on the coordination of growth and the cell cycle in green algae at different temperatures. *J Exp Bot* 70:845–858
- Zhao G, Chen Y, Carey L, Futcher B (2016) Cyclin-dependent kinase coordinates carbohydrate metabolism and cell cycle in *S. cerevisiae*. *Mol Cell* 62:546–557

Publisher's note Springer Nature remains neutral with regard to jurisdictional claims in published maps and institutional affiliations.

Chapter IV

Effects of cyclin-dependent kinase activity on the coordination of growth and the cell cycle in green algae at different temperatures

Vilem Zachleder, Ivan N. Ivanov, Milada Vítová, Kateřina Bišová





RESEARCH PAPER

Effects of cyclin-dependent kinase activity on the coordination of growth and the cell cycle in green algae at different temperatures

Vilém Zachleder^{1,†}, Ivan Ivanov^{1,2,†}, Milada Vítová¹, and Kateřina Bišová^{1,*}

¹ Laboratory of Cell Cycles of Algae, Centre Algatech, Institute of Microbiology, Czech Academy of Sciences, Opatovický mlýn, 379 81 Třeboň, Czech Republic

² Faculty of Science, University of South Bohemia, Branišovská 1760, 370 05 České Budějovice, Czech Republic

[†] These authors contributed equally to this work.

* Correspondence: bisova@alga.cz

Received 8 May 2018; Editorial decision 22 October 2018; Accepted 2 November 2018

Editor: James Murray, Cardiff University, UK

Abstract

The progression of the cell cycle in green algae dividing by multiple fission is, under otherwise unlimited conditions, affected by the growth rate, set by a combination of light intensity and temperature. In this study, we compared the cell cycle characteristics of *Desmodesmus quadricauda* at 20 °C or 30 °C and upon shifts between these two temperatures. The duration of the cell cycle in cells grown under continuous illumination at 20 °C was more than double that at 30 °C, suggesting that it was set directly by the growth rate. Similarly, the amounts of DNA, RNA, and bulk protein content per cell at 20 °C were approximately double those of cells grown at the higher temperature. For the shift experiments, cells grown at either 20 °C or 30 °C were transferred to darkness to prevent further growth, and then cultivated at the same or the other temperature. Upon transfer to the lower temperature, fewer nuclei and daughter cells were produced, and not all cells were able to finish the cell cycle by division, remaining multinuclear. Correspondingly, cells placed in the dark at the higher temperature divided faster into more daughter cells than the control cells. These differences correlated with shifts in the preceding cyclin-dependent kinase activity, suggesting that cell cycle progression was not related to growth rate or cell biomass but correlated with cyclin-dependent kinase activity.

Keywords: Cyclin-dependent kinase activity, *Desmodesmus quadricauda*, DNA replication, light/dark intervals, nuclear and cellular division, protein, RNA, starch accumulation, temperature.

Introduction

Growth and cell cycle progression are interconnected: progression of the cell cycle occurs only once the initial growth phase is complete and the cell has increased in size and accumulated sufficient key macromolecules, such as RNA and protein, and/or energy reserves. It is not clear which of these or other factors are sensed by the cell as determinants of reaching the growth threshold, although reaching the threshold before cell division is

essential for cell survival, otherwise cell size would decrease with each division, leading to cell death. This understanding led to the proposal of the existence of a sizer mechanism interconnecting growth and cell cycle progression, allowing progression into the cell cycle only when the growth threshold has been met.

Some chlorococcal and volvocal algae divide by multiple fission, that is, 2ⁿ daughter cells are released at the end of the

Abbreviations: CDK, cyclin dependent kinase; CP, commitment point; μ , growth rate in terms of number of doublings per hour.

© The Author(s) 2018. Published by Oxford University Press on behalf of the Society for Experimental Biology.
All rights reserved. For permissions, please email: journals.permissions@oup.com

cell cycle, where n is the number of doublings. This is caused by the occurrence of one or more (n) overlapping sequences of reproductive events, such as DNA replication (S phase), G₂ phase, nuclear division (M phase), G₃ phase, and cytokinesis (C), within one cell cycle. Each of these reproductive sequences is preceded by a growth phase leading mostly to an approximate doubling of cell mass, bulk RNA, and bulk protein per cell (for a review, see Bišová and Zachleder, 2014; Zachleder *et al.*, 2016). The dependence of the cell cycle on growth correlates with the attainment of a cell cycle commitment point (CP), which is functionally equivalent to START in yeasts (Reed, 1980) and the restriction point in mammalian cells (Pardee, 1974). Attainment of a CP marks the beginning of each reproductive sequence and separates it from the preceding growth phase. The cell cycle of the green alga *Desmodesmus quadricauda* (formerly *Scenedesmus quadricauda*) consists of 1, 2, or 3 reproductive sequences, according to the growth conditions (Zachleder and Šetlík, 1990), each starting at CP and leading to the duplication of DNA, mitosis, and cytokinesis (Fig. 1). Individual reproductive sequences during the multiple fission cell cycle overlap and are terminated by a common cell division.

In algae that divide by multiple fission, the number of reproductive sequences and the extent to which they overlap increases with the growth rate. For autotrophically grown cultures, the main factors affecting growth rate are light intensity

(John, 1984; Zachleder and Šetlík, 1990; Vítová *et al.*, 2011b) and temperature (Šetlík *et al.*, 1975; Donnan *et al.*, 1985; Vítová *et al.*, 2011a). Increasing light intensity will speed up photosynthesis, growth processes, and the accumulation of bulk RNA and protein (Vítová and Zachleder, 2005), leading to the attainment of more CPs and an increase in the number of reproductive sequences occurring within one cell cycle. The cell size at CP—the critical cell size for division—remains the same, independent of the light intensity (John, 1984; Zachleder and Šetlík, 1990). Increasing temperature within the normal physiological range will have a similar effect, leading to increased growth and faster attainment of CP (Zachleder and van den Ende, 1992; Vítová *et al.*, 2011a). However, there is one crucial difference between the two factors. Changes in temperature will affect not just growth and the number of CPs attained but also the duration of the sequences of reproductive events, an effect that is independent of light intensity.

Cell cycle progression is governed by the activity of cyclin-dependent kinases (CDKs) in all eukaryotes, including green algae. CDK activity promotes the attainment of CP and mitosis (John *et al.*, 1989; Zachleder *et al.*, 1997; Bisova *et al.*, 2000, 2005). In the plant kingdom, cell cycle progression is regulated by two related CDKs, CDKA and plant-specific CDKB. CDKA is responsible for regulating the transitions from G₁ to S phase and from G₂ to M phase. CDKB is responsible specifically for regulating S phase and M phase (Francis, 2007). In

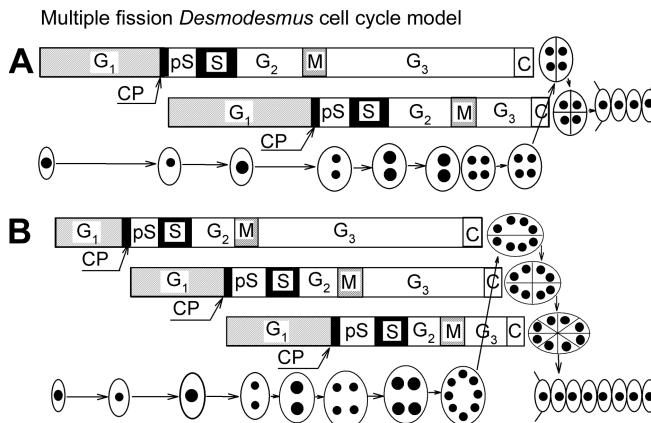


Fig. 1. Diagrams showing the multiple-fission cell cycle in the green alga *Desmodesmus quadricauda*. Two or three partially overlapping sequences of growth and reproductive events occur within a single cycle in cells dividing into four daughter cells (A) or eight daughter cells (B). Individual bars show the sequence of cell cycle phases. Schematic pictures of the cells represent their size during the cell cycle, and the black circles inside them illustrate the size and number of nuclei. Large black circles indicate a doubling of DNA. The diagonal lines extending from the terminal cells of *D. quadricauda* coenobia represent spines, typical for this species. G₁, the phase during which the threshold size of the cell is attained. It can be termed a pre-commitment period because it is terminated when the commitment point is reached. CP, the commitment point. This is the stage in the cell cycle at which the cell becomes committed to triggering and terminating the sequence of reproductive events (e.g. DNA replication, nuclear and cellular divisions). pS, the pre-replication phase between the CP and the beginning of DNA replication. The processes required for the initiation of DNA replication are assumed to happen during this phase. S, the phase during which DNA replication takes place. G₂, the phase between the termination of DNA replication and the start of mitosis. Processes leading to the initiation of mitosis are assumed to take place during this phase. M, the phase during which nuclear division occurs. G₃, the phase between nuclear division and cell division. The processes leading to cell division are assumed to take place during this phase. C, the phase during which cell cleavage and formation of daughter cells occurs. (Modified after Zachleder *et al.*, 1997, Growth-controlled oscillation in activity of histone H1 kinase during the cell cycle of *Chlamydomonas reinhardtii* (Chlorophyta). *Journal of Phycology* 33, 673–681, with permission; and adapted by permission from Springer: The cell cycle of microalgae by Zachleder *et al.*, 2016, In: Borowitzka MA, Beardell J, Raven JA, eds. The physiology of microalgae. Cham: Springer International Publishing Switzerland, 3–46, Copyright 2016).

Chlamydomonas reinhardtii, another green alga that divides by multiple fission, CDKA promotes entry into the cell cycle, the attainment of CP, and initiation of the first DNA replication. CDKB is an essential CDK responsible for spindle formation and nuclear division, and subsequent rounds of DNA replication (Tulin and Cross, 2014; Atkins and Cross, 2018).

The role of light (light intensity, the illumination regimen, and light composition) in regulating the algal cell cycle is well established. The effect of temperature has been less studied because of the more complicated experimental design that is required, and investigations into the effect of changing temperature on cell cycle progression are lacking. Here, we studied the effect of temperature shifts on cell cycle progression in *D. quadricauda*. To separate the effects of temperature on growth processes and the cell cycle, we prevented further growth upon a shift in temperature by applying a dark treatment, which did not affect the cell cycle events that were already committed. This setup allowed us to independently compare the effects of temperature on growth (the synthesis of RNA, protein, and starch) and the cell cycle (DNA replication and nuclear and cellular divisions). We sought to determine whether relationships set up at one temperature would be retained after a temperature change, for example, whether there is a direct correlation between growth and cell cycle progression, as implied by the sizer hypothesis.

Materials and methods

Organism and culture methods

The chlorococcal alga *Desmodesmus quadricauda* (Turp.) Bréb., strain Greifswald/15, was obtained from the Culture Collection of Autotrophic Microorganisms kept at the Institute of Botany, Třeboň, Czech Republic. The cultures were maintained on mineral 1/2 SS medium as described elsewhere (Hlavová et al., 2016).

Synchronization procedure and cultivation conditions

To obtain synchronous populations of daughter cells, optimal growth conditions were used: incident light intensity $420 \mu\text{mol photons m}^{-2} \text{s}^{-1}$ of photosynthetically active radiation (400–720 nm), temperature 30 °C, and aeration with 2% added CO₂ (v/v). The use of a low concentration of cells ($1 \times 10^6 \text{ cells ml}^{-1}$) prevented a substantial decrease in the mean light intensity ($264 \mu\text{mol photons m}^{-2} \text{s}^{-1}$) due to a shadowing effect from growing cells. Synchronization was carried out by using 15/9 h alternating light/dark periods (Hlavová et al., 2016).

Suspensions of synchronous cells were cultivated in rectangular plate-parallel vessels ($44 \times 24.5 \times 2.3 \text{ cm}$, volume 2200 ml) or glass cylinders (inner diameter 3 cm, volume 300 ml) illuminated from one side by a panel of dimmable incandescent lamps (OSRAM DULUX L55W/950 Daylight) with incident irradiance at the surface of the culture vessel $\sim 420 \mu\text{mol photons m}^{-2} \text{s}^{-1}$. Culture vessels were immersed in water baths kept at a constant temperature of either 20 °C or 30 °C. The cultures were aerated with a mixture of air and carbon dioxide (2% v/v) at a flow rate of 15 l h^{-1} (for the tubes) or 60 l h^{-1} (for the plate-parallel vessels). Cells were counted using a Bürker counting chamber.

For the experiments, only cultures with at least 98% of eight-celled coenobia were used. Each experiment was repeated at least five times. Individual processes of the cell cycle were performed in the same time window, with the midpoints varying by a maximum of 1 h in the control cultures. In the samples placed in darkness, the progression of nuclear and cellular division depended on the actual state of the particular culture. Each of the experiments represented a time series of culture behavior

in the light and dark, so the processes could be readily followed even if they were slightly delayed or advanced in the actual culture. The general rules governing culture behavior were the same and did not affect the experimental outcome.

Assessment of commitment, nuclear division, and cell division

To determine whether and how many cells attained CP and the number of CPs, cells were sampled at hourly intervals and incubated in the dark at the defined experimental temperature. Cells that had passed their CP for cell division formed daughter coenobia; the number of daughter cells per coenobium indicated the number of CPs passed by the mother cell (Vítová and Zachleder, 2005). The proportion of mother cells that formed four- and/or eight-celled daughter coenobia was determined by examination with a light microscope. The number of nuclei per cell was calculated after staining with 4,6'-diamidino-2-phenylindol (DAPI) according to Zachleder and Cepák (1987). Commitment, nuclear division, and cell division curves were obtained by plotting the cumulative percentages as a function of sampling time.

Temperature coefficient

The optimal temperature for *D. quadricauda* is 30 °C (Šetlík et al., 1972) and 20 °C is within the physiological range for the alga. The temperature coefficient (Q_{10}) was calculated as the ratio of the growth rate in terms of number of doublings per hour (μ) or as the ratio of the duration of cell cycles or their phases (in h) for a given 10 °C change in temperature.

Microscopy

Observations by transmitted light and fluorescence microscopy were made using an Olympus BX51 microscope equipped with a charge-coupled device camera (F-ViewII). A U-MWIBA2 filter block (excitation/emission: 460–490/510–550 nm) was used for DAPI fluorescence.

Determination of total DNA, RNA, and protein

Total nucleic acids were extracted according to Lukavský et al. (1973). The DNA assay was carried out as described by Zachleder (1984). The sediment remaining after nucleic acid extraction was quantified for protein according to the procedure described by Lowry et al. (1951).

Determination of starch

A modification of the method of McCready et al. (1950) was used, as described previously (Brányiková et al., 2011).

Inhibition of cyclin-dependent kinase activity

Roscovitine, a specific inhibitor of CDK (Planchais et al., 1997), was added to synchronized cultures transferred into darkness at 30 °C after 8 hours of growth at 30 °C in light. Roscovitine was prepared from a 20 mM stock solution dissolved in DMSO to a final concentration of 50, 100, 200, or 400 μM .

Kinase assay

For each assay, the same number of cells from the same volume of culture was used; the cultures were not diluted during experiments. Cell pellets containing 2×10^7 cells were harvested during the cell cycle, washed with SCE buffer [100 mM sodium citrate, 2.7 mM sodium EDTA, adjusted to pH 7 with citric acid], snap frozen in liquid nitrogen, and stored at $-70 \text{ }^\circ\text{C}$. Protein lysates were prepared as described by Bisova et al. (2005). The cleared lysates were directly used for the assay or were affinity purified with CrCKS1 beads as described by Bisova et al. (2005), with the modification of a 2 h incubation at 4 °C as described by Hlavová et al. (2011). Histone H1 kinase activity was assayed as described by Langan et al. (1989) in a final volume of 10 μl with either 7 μl of cleared

whole-cell lysate or the CrCKS1 bead-purified fraction, corresponding to 20 μl of whole-cell lysate. The reactions were started by adding the master mix to a final composition of 20 mM HEPES, pH 7.5, 15 mM MgCl_2 , 5 mM EGTA, 1 mM DTT, 0.1 mM ATP, 0.2% (w/v) histone (Sigma H5505), and 0.370 MBq [γ - ^{32}P] ATP. For the kinase inhibitor experiments, roscovitine was added directly to the master mix from a 20 mM stock in DMSO to a final concentration of 200 μM (Bisova *et al.*, 2005). All reactions were incubated for 30 min at room temperature and then stopped by adding 5 μl of 5 \times SDS sample buffer [250 mM Tris-HCl, pH 6.8, 50% (v/v) glycerol, 10% (w/v) SDS, 100 mM DTT, 0.5% (w/v) bromophenol blue], incubated for 2 min at 98 $^\circ\text{C}$, and immediately cooled. Proteins were separated by SDS-PAGE in 15% gels (Laemmli, 1970). Phosphorylated histone bands were visualized by autoradiography and analyzed using a phosphorimager (Storm 860, Molecular Dynamics). The extent of phosphorylation was quantified using Image Studio Lite software (LI-COR Biosciences). To compare between samples and experiments, the sum of pixel intensity within the same area was normalized to the background pixel intensity to yield pixel intensity values of the signal. These were further normalized to the pixel intensity of histone bands in the gels stained with Coomassie Brilliant Blue. Resulting values are presented as the sum of pixel intensity and are comparable across experiments. Each experiment was repeated at least three times and representative experimental results are shown.

Results

In continuous light, growth is slower at 20 $^\circ\text{C}$ but cell cycle progression is similar at 20 $^\circ\text{C}$ and 30 $^\circ\text{C}$

Before the experiment, cultures were grown for three consecutive cell cycles at 30 $^\circ\text{C}$ or 20 $^\circ\text{C}$ under a light/dark illumination regime and then left to grow in continuous light. At both temperatures, three consecutive CPs were attained by all cells (Fig. 2). Once committed, cells consecutively performed three nuclear divisions, becoming progressively binuclear, tetranuclear, and finally octanuclear (Fig. 2). Their cell cycle was terminated by the formation of eight-celled (octuplet) daughter coenobia (Fig. 2).

All pre-commitment and post-commitment phases, as well as the whole cell cycle (as measured at midpoints of corresponding curves; Fig. 2), were markedly longer at the lower temperature (Fig. 2B). The temperature coefficients (Q_{10}), calculated as the ratios of (i) growth rates (μ), (ii) the duration of

pre- and post-commitment phases, and (iii) the duration of the whole cell cycle at the two temperatures, ranged from 1.5 to 4 (Table 1).

The Q_{10} values of the growth-related processes (RNA and protein accumulation) fluctuated around 2, suggesting that these processes were temperature controlled (Table 2). The Q_{10} of DNA replication varied from 1.56 to 2 (Table 2).

Daughter cells from cultures grown for several cell cycles at 20 $^\circ\text{C}$ (Fig. 3) contained two-fold higher levels of RNA, protein, and DNA at the beginning of the cell cycle than those grown at 30 $^\circ\text{C}$ (Fig. 3A, B, D, Table 2). Consequently, the relative content of these macromolecules at the end of the cell cycle was higher than in cells grown at 30 $^\circ\text{C}$, and resulted in the release of larger daughter cells, although the number of daughter cells remained at eight. Cells grown at 20 $^\circ\text{C}$ contained two-fold higher amounts of DNA per nucleus (compare Figs 2B and 3D) and thus entered the cell cycle with duplicated genomic DNA.

The proportion of cells progressing through the cycle decreases upon a shift to a lower temperature

Cultures grown at 30 $^\circ\text{C}$ in the light were transferred after 4, 6, 8, and 14 hours to darkness and kept at the same temperature (Fig. 4A–D) or at 20 $^\circ\text{C}$ (Fig. 4E–H). Prolongation of light exposure at 30 $^\circ\text{C}$ caused a gradual increase in the fraction of the population that attained the first, second, and third CPs. In the dark at 30 $^\circ\text{C}$, each attainment of CP was, in the corresponding fraction of the population, followed by the first, second, and third nuclear divisions (Fig. 4A–D) and then the release of the corresponding proportion of four- or eight-celled daughter coenobia.

Cells of the same culture transferred to the dark at 20 $^\circ\text{C}$ showed nuclear division later and in a lower proportion of cells than those committed in the light at 30 $^\circ\text{C}$ (compare Fig. 4A–D and E–H). The most remarkable effect of the transfer to a lower temperature in the dark was that tetranuclear cells were unable to finish their cell cycles by cellular division. Consequently, no four-celled daughter coenobia were formed

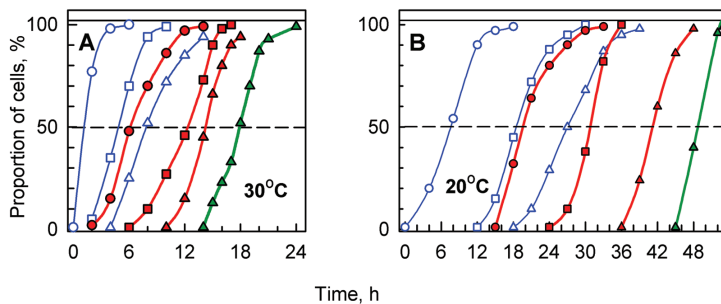


Fig. 2. Synchronized cultures of the green alga *Desmodesmus quadricauda* grown under continuous light. The synchronized cultures were grown at the same mean light intensity of 420 $\mu\text{mol photons m}^{-2} \text{s}^{-1}$ and at 30 $^\circ\text{C}$ (A) or 20 $^\circ\text{C}$ (B). Blue lines: percentage of cells that attained the commitment point for the first (open circles), second (open squares), and third (open triangles) sequence of reproductive events. Red lines: percentage of cells that passed the first (closed circles), second (closed squares), and third (closed triangles) nuclear divisions. Green lines: percentage of cells that released eight daughter cells.

Table 1. Growth rate, duration of the cell cycle and its phases, number of daughter cells, and temperature coefficients in synchronized populations of the alga *Desmodesmus quadricauda* grown at temperatures of 30 °C and 20 °C

	μ	Pre-CP1	Pre-CP2	Pre-CP3	Post-CP1	Post-CP2	Post-CP3	CC	DC
20 °C	0.064	8	11	8	12	12	15	47	8
30 °C	0.166	2	4	3	6	8	8	18	8
Q_{10}	2.6	4	2.8	2.7	2	1.5	1.8	2.6	

μ , Growth rate in term of doublings per hour; CC, duration (h) of the cell cycle; pre-CP1, pre-CP2, pre-CP3, post-CP1, post-CP2, post-CP3, phases of the cell cycle (duration in h); DC, number of daughter cells; Q_{10} , temperature coefficient.

Table 2. DNA, RNA, and protein content, and temperature coefficients at the start and end of the cell cycle and at the commitment points in synchronized populations of the alga *Desmodesmus quadricauda* grown at 20 °C and 30 °C

	Start	End	CP1	CP2	CP3
RNA (pg cell⁻¹)					
20 °C	8	55	15	30	45
30 °C	4	22	8	15	23
Q_{10}	2	2.5	1.88	2	1.96
Protein (pg cell⁻¹)					
20 °C	50	400	70	150	300
30 °C	25	175	30	60	140
Q_{10}	2	2.28	2.33	2.5	2.14
DNA (pg cell⁻¹)					
20 °C	0.4	3.5	0.8	1.5	2.5
30 °C	0.2	1.6	0.4	0.8	1.6
Q_{10}	2	1.56	2	1.88	1.56

CP1, CP2, CP3, First, second, and third commitment points (at midpoints of commitment curves; Q_{10} , temperature coefficient for a given 10 °C change in temperature as the ratio of compound content in pg cell⁻¹ for the two temperatures.

in the dark, and only cells whose nuclei divided into eight completed their cell cycle by division into eight-celled daughter coenobia (Fig. 4E–G; see also Fig. 5B).

The proportion of cells progressing through the cycle increases upon a shift to a higher temperature

Cultures grown at 20 °C in the light were transferred after 15, 21, 27, or 39 h of growth to darkness and kept at the same temperature (Fig. 5A–D) or at 30 °C (Fig. 5E–H). Growth processes at 20 °C were slower than at 30 °C (Table 2), which led to a slower and more temporally spread attainment of CPs (compare the time distances between the curves of attaining individual CPs and their steepness in Figs 4 and 5). Similarly, the rate of nuclear division was slower both in the light and dark, due to the cells' slower metabolism at the lower temperature (compare the time distances between the curves of individual nuclear divisions in Figs 4 and 5).

After transfer to the dark at 21 h, similar to the situation for transfers from 30 °C to 20 °C, only some of the cells that underwent nuclear division into four nuclei also divided into four-celled daughter cell coenobia (Fig. 5B).

For cultures grown in light for 27 and 39 h (Fig. 5C, D), the number of cells able to undergo nuclear division increased, reaching 100% of the cell population (Fig. 5D). In contrast to the cultures transferred to darkness after shorter light intervals,

all cells that were committed to division of their nuclei into four or eight completed their cell cycles, dividing into four- or eight-celled daughter coenobia (Fig. 5C, D).

When the cells grown in light at 20 °C were transferred to darkness at 30 °C, there was a significant increase in the rate and proportion of nuclear and cellular divisions within the population relative to cultures transferred to darkness at 20 °C (compare Fig. 5A–C and 5E–G). The cells underwent more nuclear and cellular divisions than were committed to in the light at 20 °C, and this took place over a shorter time interval. All cells that completed at least two nuclear divisions into four nuclei completed their cell cycles by cell division (compare Fig. 5A–D and 5E–H or Figs 7 and 8). The cells transferred into the dark at 30 °C after 39 h in the light showed nuclear division into eight nuclei and released eight-celled daughter coenobia, similar to cells transferred into the dark at 20 °C (Fig. 5H). However, 30% of the newly born daughter cells underwent a nuclear division, becoming binuclear (Fig. 5H). This nuclear division was part of the next cell cycle. No such additional nuclear division occurred in the cells kept in the dark at 20 °C (Fig. 5D).

Rates of macromolecular synthesis vary with temperature

In separate experiments, the synthesis of macromolecules related to cell growth (total RNA and protein), the accumulation of energy reserves (starch), and cell reproduction (DNA replication) were followed at 30 °C in cells grown in the light and then transferred after 9 or 13 h to darkness, where they were kept at 30 °C or 20 °C (Fig. 6A–D). In another set of experiments, cultures grown at 20 °C were transferred to the dark after 10 or 20 h and kept at 20 °C or 30 °C (Fig. 6E–H).

RNA and protein accumulated during the continuous light period until values corresponding to the number of daughter cells formed at the end of the cell cycle were attained (Table 2). For cultures grown at 30 °C or 20 °C in the light, there was no significant difference in the accumulation of RNA (Fig. 6A, E) or protein (Fig. 6B, F), or the degradation of starch (Fig. 6C, G) when transferred to either 20 °C or 30 °C in the dark. Starch degradation started immediately after transfer to the dark regardless of the temperature at which cells had been maintained in the light, but was slightly faster in cells transferred to 30 °C than 20 °C (Fig. 6C, G).

DNA replication was faster in the dark at 30 °C than 20 °C (Fig. 6D, H). The final DNA content in cultures transferred to the dark later in the cell cycle was comparable between the two treatments (Fig. 6D). In contrast, in cultures transferred to the dark earlier in the cell cycle, the final DNA content per cell

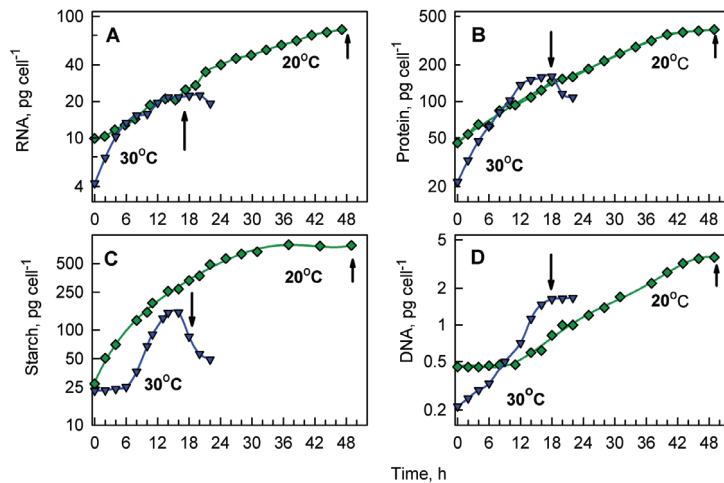


Fig. 3. Changes in the contents of RNA (A), protein (B), starch (C), and DNA (D) in synchronized populations of the alga *Desmodesmus quadricauda* grown at different temperatures. The cultures were grown in continuous light with a mean light intensity of $420 \mu\text{mol photons m}^{-2} \text{s}^{-1}$ at either 30 °C (triangles) or 20 °C (diamonds). Arrows indicate the time midpoints of cellular division.

was about 1.5 times higher at 30 °C than at 20 °C (Fig 6D). Faster and more pronounced DNA replication was a prerequisite and correlated with the faster and more numerous nuclear divisions observed in cultures transferred to 30 °C in the dark (Figs 4, 5, 7, 8).

Cell cycle progression correlates with CDK activity

Differences in cell cycle progression upon transfer from one temperature to the other could not be explained by changes in any macromolecule measured, suggesting that the levels of these macromolecules were not critical. We therefore determined whether the onset of activity of the main cell cycle regulator, CDK, was correlated with total RNA or bulk proteins as determinants of critical cell biomass, or with cell cycle processes being performed. We analyzed two types of kinase activities present in whole-cell lysates, activity relating to the attainment of CP and to nuclear division, and activity purified by affinity to CrCKS1 protein, relating to nuclear division (Bišová *et al.*, 2000). Comparison of the two activities revealed that, in most cases, they overlapped, so that CKS1-bound kinase activity was ‘hidden’ within the whole-cell lysate activity, although it was about 10-fold lower (compare Supplementary Fig. S1 at JXB online with Figs 7 and 8). The only difference was a more prominent peak of CKS1-bound activity preceding cellular division(s) (Supplementary Fig. S1), which was very low or absent in the whole-cell lysates. In both the whole-cell lysate and CKS1-bound fraction, kinase activities were inhibited by roscovitine (Supplementary Fig. S2), a specific inhibitor of CDK (Planchais *et al.*, 1997), confirming that they represent CDK-like activities.

The activities of whole-cell lysates were assayed in aliquots of synchronized populations grown in light at 30 °C (Fig. 7) or 20 °C (Fig. 8), and subsequently transferred to darkness at

either the same temperature or to the lower or higher temperature (i.e. 20 °C or 30 °C, respectively). The activities of CDK before and after transfer into darkness were compared with changes in nuclear and cellular division(s). Individual synchronized cultures differed slightly (see Materials and methods), which led to slight variations in the timing of CDK activity between individual experiments, but the correlations described below were maintained.

The rate of change and level of CDK activity decreases upon a shift to darkness at a lower temperature

For cultures grown at 30 °C, subpopulations of synchronized cultures were transferred into darkness at 30 °C or 20 °C after 4, 6, 8, 10, or 14 h of illumination (Fig. 7).

As described above, with prolonged light exposure at 30 °C, the number of committed cells as well as the number of attained CPs increased, followed by an increase in the proportion of cells undergoing nuclear division (Fig. 7A–E). In all experimental variants, nuclear divisions were tightly coupled with and related to variations in CDK activity (Fig. 7; Supplementary Fig. S3). In the dark at 30 °C, individual nuclear divisions followed each other within a short time interval (Fig. 7B, C), concomitant with a sharp peak of CDK activity. These peaks related to the start of individual nuclear divisions and overlapped in time (Fig. 7B, C, D).

In the cultures grown in 30 °C and then transferred to darkness at 20 °C, the numbers of cells undergoing nuclear division into two, four, or eight nuclei during the dark period were lower than those committed in the light at 30 °C and then undergoing nuclear division in the dark at 30 °C (Fig. 7F–J). The level of CDK activity after transfer from 30 °C in the light to 20 °C in darkness (Fig. 8F–I) was lower, and the peaks were broader than those measured in cells maintained in darkness at 30 °C. This was in line with the slower rate and lower proportion of

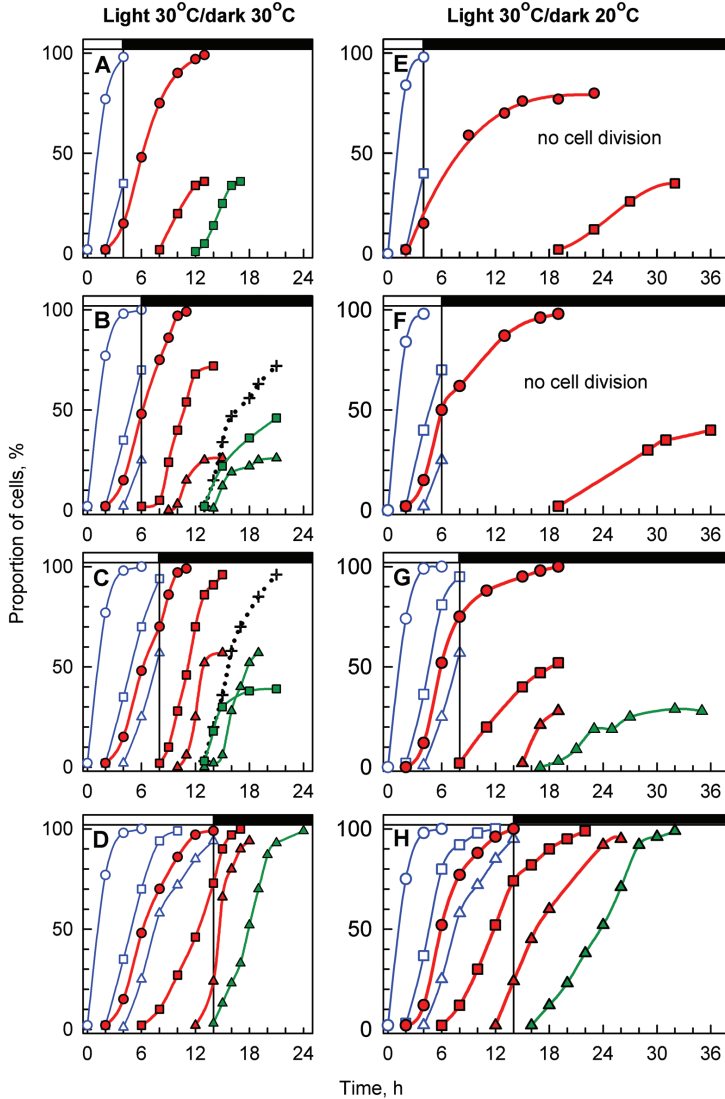


Fig. 4. Time courses of individual commitment points, nuclear divisions, and cellular divisions in synchronized populations of *Desmodesmus quadricauda* grown in light at 30 °C and then placed into the dark after 4, 6, 8, or 14 h and kept at 30 °C (A–D) or 20 °C (E–H). Blue lines: percentage of cells that attained the commitment point for the first (open circles), second (open squares), and third (open triangles) sequence of reproductive events. Red lines: percentage of cells that passed the first (closed circles), second (closed squares), and third (closed triangles) nuclear divisions. Green lines: percentage of cells that completed the second (closed squares) and third (closed triangles) cellular divisions and released four or eight daughter cells. Dotted black lines: percentage of all cells that produced daughter cells (crosses). Periods of dark are marked with black bars at the top of each graph.

nuclear divisions in populations at 20 °C (compare Fig. 8A–D and 8F–J; see also Figs 4, 5, 7, 8). As at 30 °C, the peaks of CDK activity were concomitant with nuclear divisions. Thus, at both 30 °C and 20 °C, the timing of the increase in CDK activity correlated with the timing and proportion of nuclear

divisions in the populations, even though there were significant differences between the cultures placed into darkness at the two temperatures. To visualize the correlation better, we used cumulative time-course values of kinase activities and compared them with the cumulative number of nuclei per cell over time

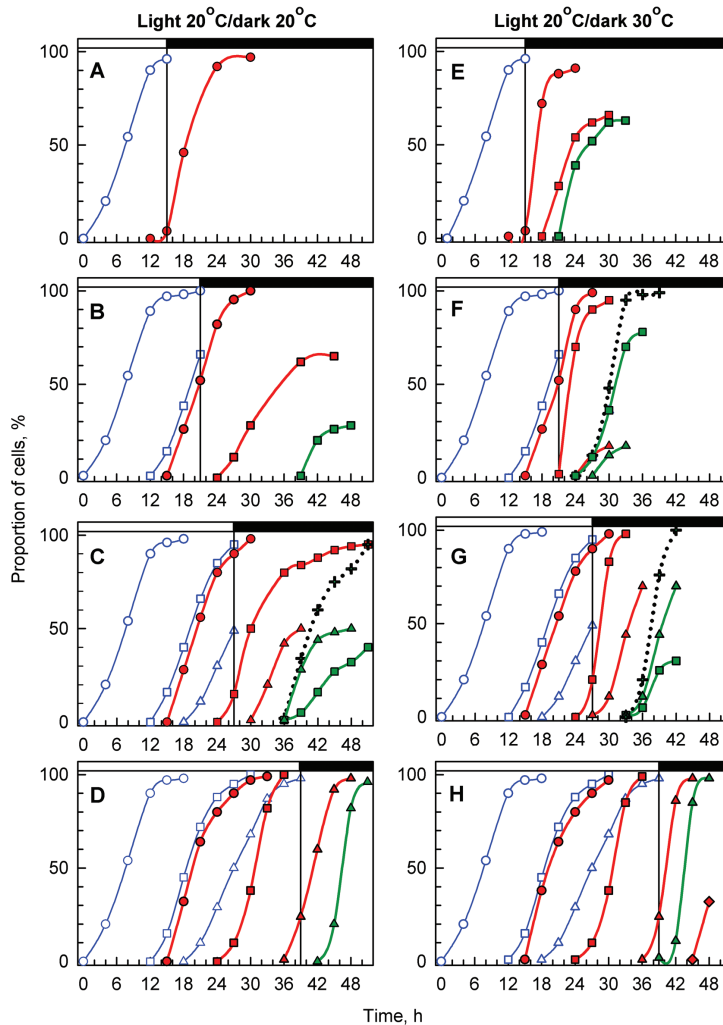


Fig. 5. Time courses of individual commitment points, nuclear divisions, and cellular divisions in synchronized populations of *Desmodesmus quadricauda* grown in light at 20 °C and then placed into the dark after 15, 21, 27, or 39 h and kept at 20 °C (A–D) or 30 °C (E–H). Blue lines: percentage of cells that attained the commitment point for the first (open circles), second (open squares), and third (open triangles) sequence of reproductive events. Red lines: percentage of cells that passed the first (closed circles), second (closed squares), and third (closed triangles) nuclear divisions; daughter cells that underwent additional nuclear division are indicated with diamonds. Green lines: percentage of cells that completed the second (closed squares) and third (closed triangles) cellular divisions and released four or eight daughter cells. Dotted black lines: percentage of all cells that produced daughter cells (crosses). Periods of dark are marked with black bars at the top of each graph.

(Supplementary Fig. S3). This type of plot clearly showed that CDK activity preceded nuclear division, which was proportional to the levels of CDK activity (Supplementary Fig. S3).

The rate of change and level of CDK activity increases upon a shift to darkness at a higher temperature

Due to the slower cell metabolism at 20 °C, the cell cycle was more than twice as long as at 30 °C (Fig. 2). Because of this, to

transfer cells grown at 20 °C in light to the dark at a similar cell cycle time, the light period had to be prolonged. Cultures grown at 20 °C were transferred into the dark (at 30 °C or 20 °C) after 15, 21, 27, or 39 h (Fig. 8). The first division of nuclei occurred later in the culture grown at 20 °C than at 30 °C (20 h versus 9 h) and the following nuclear divisions were further apart at 20 °C (12 h versus 4 h) (compare Figs 7E and 8E).

As for the cells grown at 30 °C, the activity of CDK increased before nuclear division (Fig. 8; Supplementary Fig. S3), and

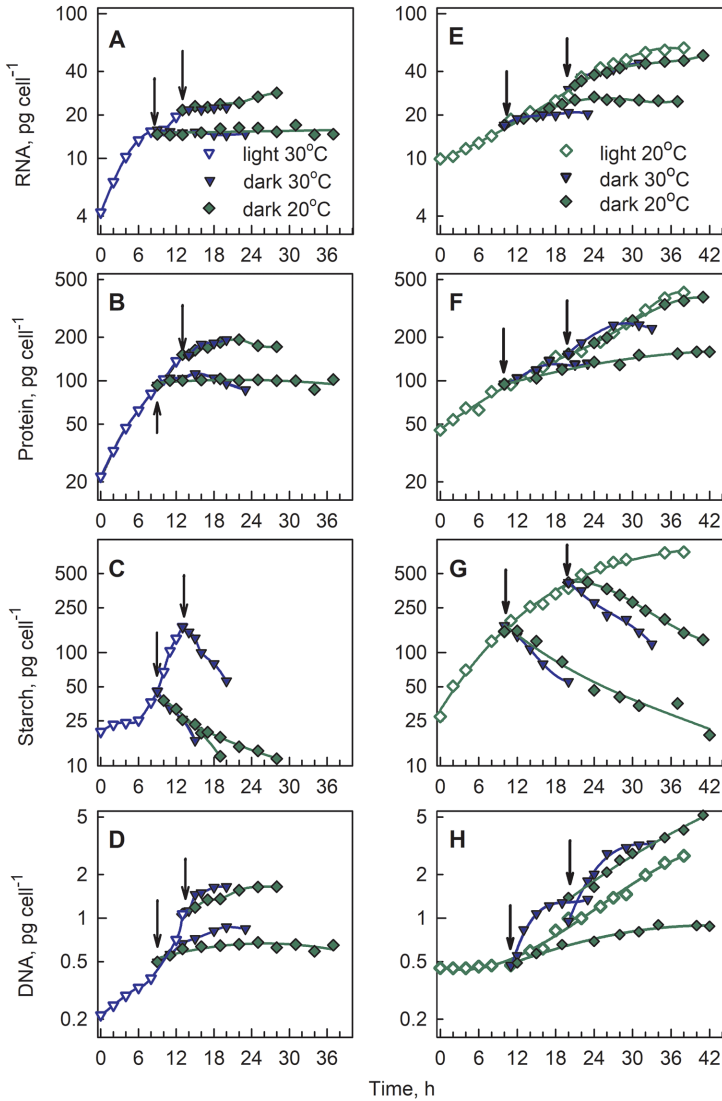


Fig. 6. Changes in the content of RNA (A, E), protein (B, F), starch (C, G), and DNA (D, H) during the cell cycle in synchronized populations of *Desmodesmus quadricauda*. The cultures were grown at 30 °C (A–D) or 20 °C (E–H). (A–D) Macromolecular synthesis in cells permanently illuminated at 30 °C (blue line, open triangles) or placed in darkness after 9 or 13 h (arrows) and kept at 30 °C (blue line, closed triangles) or 20 °C (green line, closed diamonds). (E–H) Macromolecular synthesis in cells permanently illuminated at 20 °C (green line, open diamonds) or placed in darkness after 10 or 20 h (arrows) and kept at 20 °C (green line, closed diamonds) or 30 °C (blue line, closed triangles).

the level and timing of CDK activity correlated with the number of cells undergoing nuclear division and the number of nuclear divisions in individual cells (Fig. 8). In cells cultivated in the light at 20 °C, CDK activity was delayed compared with those at 30 °C, and its peaks were more separated in time, corresponding with individual nuclear divisions (Fig. 8A). With

prolongation of the light period to 21 h or more, the activities of CDK preceding the first and second nuclear divisions started to overlap, resulting in a broader distribution of CDK activity with two peaks (Fig. 8B–E). In contrast to cultures grown in the light at 30 °C, division into eight nuclei in cultures grown at 20 °C was in all cases preceded by a peak of

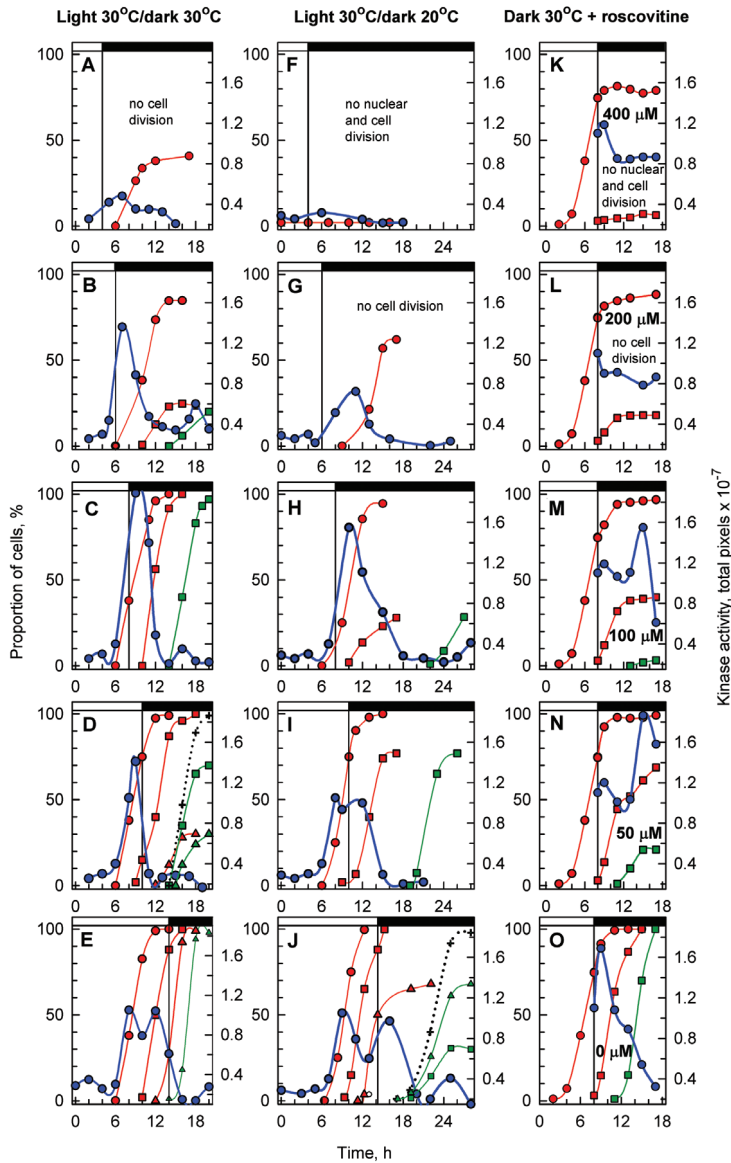


Fig. 7. Activity of CDK in whole-cell lysates and the courses of nuclear and cellular divisions in synchronized populations of *Desmodium quadricauda* grown in light at 30 °C and then placed into darkness after 4, 6, 8, 10, or 14 h, and kept at 30 °C (A–E) or 20 °C (F–J). The specific inhibitor of CDK activity roscovitine at different concentrations (50–400 μM) (K–N) or DMSO as a control (O) were applied to cultures transferred to darkness at 30 °C after 8 h of light. Periods of dark are marked with black bars at the top of each graph. Blue lines: activity of CDK. Red lines: percentage of cells that passed the first (closed circles), second (closed squares), and third (closed triangles) nuclear divisions. Green lines: percentage of cells that completed the second (closed squares) and third (closed triangles) cellular divisions and released four or eight daughter cells. Dotted black lines: percentage of all cells that produced daughter cells (crosses).

CDK activity that was well separated in time from preceding peaks (compare Figs 7 and 8).

Transfer of cells grown at 20 °C into darkness at 30 °C caused extensive changes in the timing of cell cycle processes,

which were correlated with changes in CDK activity. As a rule, nuclear divisions occurred shortly after transfer to 30 °C, at a higher rate and in more cells than in cells kept 20 °C (compare Fig. 8A–D and 8F–I). CDK activity reached a sharp peak

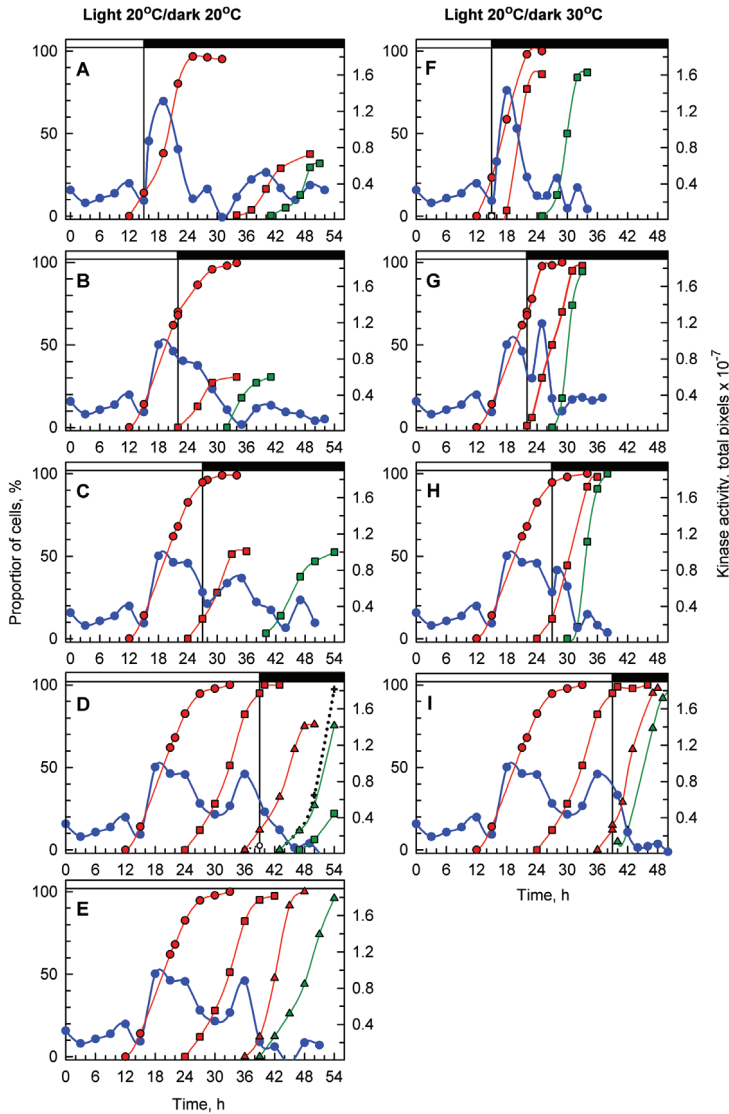


Fig. 8. Activity of CDK in whole-cell lysates and the courses of nuclear and cellular division in synchronized populations of *Desmodesmus quadricauda* grown in light at 20 °C and then placed into darkness after 15, 22, 27, or 39 h and kept at 20 °C (A–D) or 30 °C (F–I). One culture was grown at 20 °C in continuous light (E). Blue lines: activity of CDK. Red lines: percentage of cells that passed the first (closed circles), second (closed squares), and third (closed triangles) nuclear divisions. Green lines: percentage of cells that completed the second (closed squares) and third (closed triangles) cellular divisions and released four or eight daughter cells. Dotted black lines: percentage of all cells that produced daughter cells (crosses). Periods of dark are marked with black bars at the top of each graph.

within 1 or 2 h after transfer to darkness at 30 °C (Fig. 8G, H) while such sharp peaks were absent in cultures transferred to darkness at 20 °C (compare Fig. 8B, C, G and H). Kinase activity maxima were higher at 30 °C than at 20 °C, and the peaks were sharper, in line with faster completion of nuclear

division. The lower kinase activities at 20 °C correlated with the slower completion of nuclear and/or cell divisions and the lower proportion of cells in the population undergoing nuclear and/or cell division. For another illustration of the correlation, see Supplementary Fig. S3.

To determine whether there were temperature-dependent differences in total kinase activity, we compared the cumulative CDK activity at the two temperatures with the accumulated number of nuclei per cell (Supplementary Fig. S3). The results clearly demonstrate that although the rates of change of CDK activity were slower at 20 °C, total CDK activity correlated only with the number of completed nuclear and/or cellular divisions within the population, and not with temperature (Supplementary Fig. S3). In all cases, CDK activity correlated with nuclear divisions, confirming a tight connection between CDK activity and cell cycle progression.

Inhibition of CDK activity by roscovitine simulates its decrease through transfer to lower temperature

To assess whether the correlation between CDK activity and changes in cell cycle progression was causative or not, we transferred subcultures of synchronized cultures grown in light at 30 °C for 8 h into darkness with increasing concentrations of the CDK inhibitor roscovitine (Fig. 7K–O). In control cultures without roscovitine, all the cells underwent nuclear division into four nuclei and completed cell division into four-celled coenobia (Fig. 7O, compare also with Fig. 7C). Increasing concentrations of roscovitine progressively inhibited nuclear and cellular division as well as kinase activities in whole-cell lysates (Fig. 7K–N). With the highest concentration of roscovitine (400 μM), CDK activity was completely blocked, which was reflected by a complete block of nuclear division and cell division (Fig. 7K). The effect of the inhibitor mimicked the effect of shorter light exposure (compare Fig. 7M with 7B and 7C). This proved a causal relationship between changes in CDK activity at different temperatures and cell cycle progression, as was suggested by the correlations illustrated in Figs 7 and 8 and Supplementary Fig. S3.

Discussion

In green algae dividing by multiple fission, the critical cell size at which the cells attain CP remains constant at different growth rates set by different light intensities. The rate of attaining the critical cell size and the number of CPs vary, but the duration of the reproductive sequences is set by the metabolic rate and remains constant (Vítová *et al.*, 2011b). This is true not only in algae but also in yeasts (Beach *et al.*, 1982), mammalian cells (Pardee, 1989), and plant cells (Jones *et al.*, 2017). In contrast, temperature affects both growth-related processes before CP attainment and the duration of the sequence of reproductive events, even at the same light intensity (Fig. 2). This stems from a temperature effect on general metabolism and fits with established knowledge about temperature responses in other algae (Zachleder *et al.*, 2002; Vítová and Zachleder, 2005).

Results of experiments performed at 20 °C and 30 °C suggested that threshold levels of the macromolecules assumed to be involved in establishing a constant critical size (RNA, protein, and starch) were doubled at 20 °C compared with 30 °C. The question was whether this threshold requirement for entry into CP would be retained after transfer between two different but physiological temperatures (either from 20 °C to 30 °C or

from 30 °C to 20 °C) when the cells are placed into darkness to block any direct involvement of light on growth. Should there be a direct relationship between critical cell size (and/or its determinants) and attainment of CP, we expected that progression of the cell cycle would continue after transfer, similar to the control culture maintained at the original temperature, although with different kinetics dictated by different metabolic rates at the two temperatures. In contrast, if critical cell size and CP attainment were not simply correlated, then upon transfer the progression of the cell cycle should differ from that of the control at the original temperature. The results of the transfer experiments rather unexpectedly proved the second of these options. The role of temperature in the timing of cell cycle events thus goes beyond its effect on growth rate, in contrast to changing the light intensity at a constant temperature, which has a simple trophic effect (Zachleder and Šetlík, 1990).

Upon transfer to the dark, at either 30 °C or 20 °C, the accumulation of RNA and proteins ceased, and their levels stayed constant (Fig. 6A, B, E, F). Starch was extensively degraded in the dark at rates that were faster at 30 °C, but the final levels of starch were similar at both temperatures (Fig. 6C, G). In general, all growth processes that depend directly on a carbon and energy supply stopped or substantially slowed upon transfer to the dark. In contrast, processes essential for cell survival and reproduction, particularly DNA replication and nuclear division, are not directly dependent on energy from photosynthesis; even in the light they depend on starch (and other) reserves, and thus they can be performed in the dark (Wanka, 1968, 1975). Although general protein synthesis slows or ceases in the dark, this does not affect gene expression and protein synthesis related to cell cycle events, which still run in the dark. If protein synthesis is completely inhibited by the addition of cycloheximide, DNA replication and nuclear division are completely suppressed (Zachleder *et al.*, 2002).

The accumulation of DNA was comparable for cultures grown at 30 °C and then moved to the dark at either 30 °C or 20 °C (Fig. 6D). In contrast, there was a striking difference in DNA accumulation in cultures grown at 20 °C and then placed into darkness at either 30 °C or 20 °C. In the cultures placed into darkness at 30 °C, DNA accumulation started earlier, was faster, and could have reached higher values (Fig. 6H). This result suggested that there might be different effects of a temperature shift on the progression of the cell cycle. Generally, cell cycle progression was accelerated in cultures transferred from the light at 20 °C to darkness at 30 °C. The cells behaved as if they attained more CPs; they underwent more nuclear divisions and completed more cell divisions. Some of these cells completed cell divisions even under conditions where no cell division was detectable in the control cultures kept at 20 °C (Figs 5, 7, 8). The opposite behavior was observed in cultures grown in the light at 30 °C and transferred to the dark at 20 °C. Cells in these cultures were unable to complete nuclear or cell divisions committed at 30 °C (Fig. 4). The increased rate of individual cell cycle processes at 30 °C and the slower rate at 20 °C were expected and were most probably caused simply by different metabolic rates at the two temperatures, as reflected by the temperature coefficient, Q_{10} (Table 1). In contrast, the fact that cells seemingly attained more or fewer

CPs than implied by their critical cell biomass at the culture temperature suggested that the cells are at different stages in the cycle, independent of cell size. This also implies that neither critical cell size (biomass) nor any other macromolecule we analyzed is a determinant of CP. Thus, the two processes—that is, growth up to critical cell biomass and attainment of CP—are simply correlated under stable growth conditions but are not causally related.

CDK activity changed distinctly with temperature shifts, preceding both temporally (Figs 7, 8; Supplementary Fig. S3) and functionally (Fig. 7K–O) nuclear and to some extent cellular divisions in the cultures and determining the progression of division. The completion of each nuclear division correlated with cells reaching certain threshold total CDK activity levels, which were similar at 30 °C and 20 °C (Figs 7, 8; Supplementary Fig. S3), although reaching the threshold activity was delayed at 20 °C. Furthermore, the application of increasing concentrations of roscovitine, a specific CDK inhibitor (Planchais *et al.*, 1997), altered the extent of cell cycle progression, confirming that alternating CDK activity levels control cell cycle progression. In some organisms, CDK activity seems to be related to cell size. In plants, a model incorporating an increase in active CDK with cell size fits the behavior of dividing cells in the apical meristem (Jones *et al.*, 2017). In *C. reinhardtii*, the abundance, and possibly the activity, of a specific CDK, CDKG1, regulates the number of mother cell divisions and thus the daughter cell size (Li *et al.*, 2016). In other organisms, alternating CDK activity can be a regulatory variable on its own. In the simple system of fission yeast encoding a single cell cycle-regulating CDK, the progression of the cell cycle can be simplified so that a single monomolecular module of CDK linked with cyclin is able to drive the cell cycle in a manner similar to wild-type cells (Coudreuse and Nurse, 2010). This is achieved simply by alternating two CDK activity thresholds at entry to the S and M phases, and functions even in the absence of most forms of canonical regulation. It is not clear whether such a simple model is operating in *D. quadricauda*, where, as in other plants, cell cycle progression is regulated by two CDKs, CDKA and CDKB, which have different roles in cell cycle regulation (Tulin and Cross, 2014; Atkins and Cross, 2018). Although we could detect a threshold CDK activity related to nuclear division (Supplementary Fig. S3), it is not clear if this represents CDKA and/or CDKB. Moreover, we were unable to detect a threshold CDK level related to DNA replication. In plant meristems, altering either CDKA or CDKB complex kinase activity will affect the cell size and duration of the individual cell cycle phases but not the total length of the cell cycle (Jones *et al.*, 2017). It would be interesting to see how this relates to cell cycle progression in *D. quadricauda* that is not directly connected to attaining a critical cell size. Unfortunately, given the lack of genetic tools, we were unable to separate the CDKA and CDKB kinase activities, as antibodies to CDKA and CDKB recognized and immunoprecipitated both proteins (Hlavová *et al.*, 2011). Moreover, CDK activity in whole-cell lysates generally overlapped with the kinase activity specifically bound to CKS1 beads (Supplementary Fig. S1), suggesting that

the CKS1-bound protein fraction also contains both CDKA and CDKB. In some cases, CKS1-bound kinase activity differed from that in whole-cell lysates (Supplementary Fig. S1), hinting at the possibility that one of the complexes is preferentially affinity purified. This was true particularly for the CKS1-bound activity peak at cellular division (compare Figs 7, 8, and Supplementary Fig. S1). In *C. reinhardtii*, CDKB is an essential CDK responsible for spindle formation and nuclear division and subsequent DNA replication, once CDKA-dependent initiation has occurred (Tulin and Cross, 2014; Atkins and Cross, 2018). We assume that cell division-related kinase activity might be the action of CDKB. Clearly, mutants in CDKA and/or CDKB would be very useful in analyzing the roles of the two kinases in regulating cell cycle progression in *D. quadricauda*, the relationship to temperature shifts, and the nature of threshold CDK activities.

In the temperature shift experiments, the critical cell size (and/or the amount of different macromolecules), or the state of the cell more generally, seems to be ‘reinterpreted’ based on the current cultivation temperature. This reinterpretation was manifested as changes in CDK activity followed by changes in the number of nuclear divisions (and other cell cycle-related processes) per cell, and/or their proportion within the population. The activity of the CDK complex is regulated on multiple levels: (i) transcription of CDK or the cyclin subunit, (ii) post-translational modification, (iii) protein–protein interaction, and (iv) subunit degradation (Francis, 2007; Inagaki and Umeda, 2011; Van Leene *et al.*, 2011). Changes in kinase activity occurred within 1–2 h of a temperature shift (Fig. 8G, H), suggesting that they might have occurred at the level of changes in post-translational modification and/or protein–protein interactions of existing CDK complexes. Alternatively, they could be caused simply by temperature sensitivity of the CDK complexes themselves. The protein levels of both CDKA and CDKB are quite steady during the cell cycle of *D. quadricauda* (Hlavová *et al.*, 2011). Similarly, the level of the CDK inhibitor Wee1 kinase was steady. Moreover, the levels of Wee1 kinase do not seem to interfere with CDK activity (Hlavová *et al.*, 2011). Thus, it is feasible that the activity of CDK is affected by changes in protein–protein interactions. Candidates for such regulators are CDK inhibitors that have not so far been identified in green algae owing to their high sequence divergence (Bisova *et al.*, 2005).

Supplementary data

Supplementary data are available at *JXB* online.

Fig. S1. The activity of CDK in the CKS1-bound fraction and the courses of nuclear and cellular division in synchronized populations of *Desmodesmus quadricauda*.

Fig. S2. Inhibition of CDK activity by roscovitine in whole-cell lysate and in the CKS1-bound fraction.

Fig. S3. Cumulative time-course values of kinase activities in whole-cell lysates, cumulated number of nuclei, and completed cell divisions in synchronized populations of *Desmodesmus quadricauda*.

Acknowledgements

The authors are grateful to Professor Paul Nurse (The Francis Crick Institute, London) for inspirational talks and discussions. The authors greatly appreciate the help of Mrs Anna Kubínová with algal cultures, data analysis, and compiling. This work was supported by the Grant Agency of the Czech Republic (grant no. 15-09231S) and by the National Programme of Sustainability I (project no. LO1416).

References

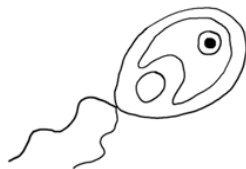
- Atkins KC, Cross FR. 2018. Interregulation of CDKA/CDK1 and the plant-specific cyclin-dependent kinase CDKB in control of the *Chlamydomonas* cell cycle. *The Plant Cell* **30**, 429–446.
- Beach D, Durkacz B, Nurse P. 1982. Functionally homologous cell cycle control genes in budding and fission yeast. *Nature* **300**, 706–709.
- Bišová K, Krylov DM, Umen JG. 2005. Genome-wide annotation and expression profiling of cell cycle regulatory genes in *Chlamydomonas reinhardtii*. *Plant Physiology* **137**, 475–491.
- Bišová K, Vítová M, Zachleder V. 2000. The activity of total histone H1 kinases is related to growth and commitment points while the p13^{sup1}-bound kinase activity relates to mitoses in the alga *Scenedesmus quadricauda*. *Plant Physiology and Biochemistry* **38**, 755–764.
- Bišová K, Zachleder V. 2014. Cell-cycle regulation in green algae dividing by multiple fission. *Journal of Experimental Botany* **65**, 2585–2602.
- Brányiková I, Maršálková B, Doucha J, Brányik T, Bišová K, Zachleder V, Vítová M. 2011. Microalgae—novel highly efficient starch producers. *Biotechnology and Bioengineering* **108**, 766–776.
- Coudreuse D, Nurse P. 2010. Driving the cell cycle with a minimal CDK control network. *Nature* **468**, 1074–1079.
- Donnan L, Carvill EP, Gilliland T J, John PCL. 1985. The cell-cycles of *Chlamydomonas* and *Chlorella*. *New Phytologist* **99**, 1–40.
- Francis D. 2007. The plant cell cycle – 15 years on. *New Phytologist* **174**, 261–278.
- Hlavová M, Čížková M, Vítová M, Bišová K, Zachleder V. 2011. DNA damage during G₂ phase does not affect cell cycle progression of the green alga *Scenedesmus quadricauda*. *PLoS ONE* **6**, 1–13.
- Hlavová M, Vítová M, Bišová K. 2016. Synchronization of green algae by light and dark regimes for cell cycle and cell division studies. In: Caillaud M-C, ed. *Plant cell division: methods and protocols*. New York: Springer Science, 3–16.
- Inagaki S, Umeda M. 2011. Cell-cycle control and plant development. *International Review of Cell and Molecular Biology* **291**, 227–261.
- John PC. 1984. Control of the cell division cycle in *Chlamydomonas*. *Microbiological Sciences* **1**, 96–101.
- John PC, Sek FJ, Lee MG. 1989. A homolog of the cell cycle control protein p34cdc2 participates in the division cycle of *Chlamydomonas*, and a similar protein is detectable in higher plants and remote taxa. *The Plant Cell* **1**, 1185–1193.
- Jones RA, Forero-Vargas M, Withers SP, Smith RS, Traas J, Dewitte W, Murray JAH. 2017. Cell-size dependent progression of the cell cycle creates homeostasis and flexibility of plant cell size. *Nature Communications* **8**, 15060.
- Laemmli UK. 1970. Cleavage of structural proteins during the assembly of the head of bacteriophage T4. *Nature* **227**, 680–685.
- Langan TA, Gautier J, Lohka M, Hollingsworth R, Moreno S, Nurse P, Maller J, Sclafani RA. 1989. Mammalian growth-associated H1 histone kinase: a homolog of *cdc2+*/*CDC28* protein kinases controlling mitotic entry in yeast and frog cells. *Molecular and Cellular Biology* **9**, 3860–3868.
- Li Y, Liu D, López-Paz C, Olson BJ, Umen JG. 2016. A new class of cyclin dependent kinase in *Chlamydomonas* is required for coupling cell size to cell division. *Elife* **5**, e10767.
- Lowry OH, Rosebrough NJ, Farr AL, Randall RJ. 1951. Protein measurement with the Folin phenol reagent. *The Journal of Biological Chemistry* **193**, 265–275.
- Lukavský J, Tetík K, Vendlová J. 1973. Extraction of nucleic acid from the alga *Scenedesmus quadricauda*. *Archives of Hydrobiology* **9**(Suppl 41), 416–426.
- McCready RM, Guggolz J, Silveira V, Owens HS. 1950. Determination of starch and amylose in vegetables. *Analytical Chemistry* **22**, 1156–1158.
- Pardee AB. 1974. A restriction point for control of normal animal cell proliferation. *Proceeding of the National Academy of Sciences, USA* **71**, 1286–1290.
- Pardee AB. 1989. G1 events and regulation of cell proliferation. *Science* **246**, 603–608.
- Planchais S, Glab N, Tréhin C, Perennes C, Bureau JM, Meijer L, Bergounioux C. 1997. Roscovitine, a novel cyclin-dependent kinase inhibitor, characterizes restriction point and G2/M transition in tobacco BY-2 cell suspension. *The Plant Journal* **12**, 191–202.
- Reed SI. 1980. The selection of *S. cerevisiae* mutants defective in the start event of cell division. *Genetics* **95**, 561–577.
- Šetlík I, Berková E, Doucha J, Kubín S, Vendlová J, Zachleder V. 1972. The coupling of synthetic and reproduction processes in *Scenedesmus quadricauda*. *Archives of Hydrobiology* **7**(Suppl 41), 172–213.
- Šetlík I, Zachleder V, Doucha J, Berková E, Bartoš J. 1975. The nature of the temperature block in the sequence of reproductive processes in *Chlorella vulgaris* BEIJERINCK. *Archives of Hydrobiology* **14**(Suppl 49), 70–104.
- Tulin F, Cross FR. 2014. A microbial avenue to cell cycle control in the plant superkingdom. *The Plant Cell* **26**, 4019–4038.
- Van Leene J, Boruc J, De Jaeger G, Russinova E, De Veylder L. 2011. A kaleidoscopic view of the Arabidopsis core cell cycle interactome. *Trends in Plant Science* **16**, 141–150.
- Vítová M, Bišová K, Hlavová M, Kawano S, Zachleder V, Čížková M. 2011. *Chlamydomonas reinhardtii*: duration of its cell cycle and phases at growth rates affected by temperature. *Planta* **234**, 599–608.
- Vítová M, Bišová K, Umysová D, Hlavová M, Kawano S, Zachleder V, Čížková M. 2011. *Chlamydomonas reinhardtii*: duration of its cell cycle and phases at growth rates affected by light intensity. *Planta* **233**, 75–86.
- Vítová M, Zachleder V. 2005. Points of commitment to reproductive events as a tool for analysis of the cell cycle in synchronous cultures of algae. *Folia Microbiologica* **50**, 141–149.
- Wanka F. 1968. Ultrastructural changes during normal and colchicine-inhibited cell division of *Chlorella*. *Protoplasma* **66**, 105–130.
- Wanka F. 1975. Possible role of the pyrenoid in the reproductive phase of the cell cycle of *Chlorella*. *Colloquium Internationale CNRS* **240**, 132–136.
- Zachleder V. 1984. Optimization of nucleic acids assay in green and blue-green algae: extraction procedures and the light-activated reaction for DNA. *Archives of Hydrobiology* **36**(Suppl 67.3), 313–328.
- Zachleder V, Bišová K, Vítová M. 2016. The cell cycle of microalgae. In: Borowitzka MA, Beardell J, Raven JA, eds. *The physiology of microalgae*. Cham: Springer International Publishing Switzerland, 3–46.
- Zachleder V, Bišová K, Vítová M, Kubín Š, Hendrychová J. 2002. Variety of cell cycle patterns in the alga *Scenedesmus quadricauda* (Chlorophyta) as revealed by application of illumination regimes and inhibitors. *European Journal of Phycology* **37**, 361–371.
- Zachleder V, Cepák V. 1987. Visualization of DNA containing structures by fluorochrome DAPI in those algal cells which are not freely permeable to the dye. *Archives of Hydrobiology* **47**(Suppl 78.2), 157–168.
- Zachleder V, Schläfli O, Boschetti A. 1997. Growth-controlled oscillation in activity of histone H1 kinase during the cell cycle of *Chlamydomonas reinhardtii* (Chlorophyta). *Journal of Phycology* **33**, 673–681.
- Zachleder V, Šetlík I. 1990. Timing of events in overlapping cell reproductive sequences and their mutual interactions in the alga *Scenedesmus quadricauda*. *Journal of Cell Science* **97**, 631–638.
- Zachleder V, van den Ende H. 1992. Cell-cycle events in the green alga *Chlamydomonas eugametos* and their control by environmental factors. *Journal of Cell Science* **102**, 469–474.

Coordination of growth and cell cycle progression in green algae

Chapter V

Cell cycle arrest by supraoptimal
temperature in the alga
Chlamydomonas reinhardtii

Vilem Zachleder, Ivan N. Ivanov, Milada Vítová, Kateřina Bišová



Article

Cell Cycle Arrest by Supraoptimal Temperature in the Alga *Chlamydomonas reinhardtii*

 Vilém Zachleder^{1,†}, Ivan Ivanov^{1,2,†}, Milada Vítová¹  and Kateřina Bišová^{1,*} 

¹ Laboratory of Cell Cycles of Algae, Centre Algotech, Institute of Microbiology of the Czech Academy of Sciences, 37981 Třeboň, Czech Republic; zachleder@alga.cz (V.Z.); ivanov@alga.cz (I.I.); vitova@alga.cz (M.V.)

² Faculty of Science, University of South Bohemia, Branišovská 1700, 37005 České Budějovice, Czech Republic

* Correspondence: bisova@alga.cz; Tel.: +420-384-340-485

† These authors contributed equally to this work.

Received: 26 August 2019; Accepted: 8 October 2019; Published: 11 October 2019



Abstract: Temperature is one of the key factors affecting growth and division of algal cells. High temperature inhibits the cell cycle in *Chlamydomonas reinhardtii*. At 39 °C, nuclear and cellular divisions in synchronized cultures were blocked completely, while DNA replication was partly affected. In contrast, growth (cell volume, dry matter, total protein, and RNA) remained unaffected, and starch accumulated at very high levels. The cell cycle arrest could be removed by transfer to 30 °C, but a full recovery occurred only in cultures cultivated up to 14 h at 39 °C. Thereafter, individual cell cycle processes began to be affected in sequence; daughter cell release, cell division, and DNA replication. Cell cycle arrest was accompanied by high mitotic cyclin-dependent kinase activity that decreased after completion of nuclear and cellular division following transfer to 30 °C. Cell cycle arrest was, therefore, not caused by a lack of cyclin-dependent kinase activity but rather a blockage in downstream processes.

Keywords: cell cycle arrest; cell size; *Chlamydomonas reinhardtii*; cyclin-dependent kinase; DNA replication; synchronized cultures; supraoptimal temperature; starch accumulation

1. Introduction

Light and temperature are two key factors that affect growth and development of plants, including green algae. For each organism, there are three temperature ranges with distinct effects on cell physiology. Firstly, the optimum growth temperature is where growth rate reaches a maximum. Secondly, the range below and above the optimum is where growth and cell division are possible, yet at lower rates. The final range is temperatures too low or too high to allow for cell division, cell growth, or cell survival. Within the physiological range surrounding the optimum, a 10 °C increase in temperature will increase metabolic rate two-fold. Increasing temperature will thus speed up growth as well as shorten individual phases of the cell cycle and its total duration, as shown in different algae such as *Chlorella ellipsoidea* [1], *Chlamydomonas reinhardtii* [2], *Chlamydomonas eugametos* [3], and *Desmodesmus quadricauda* [4]. Individual metabolic processes are differentially sensitive to temperature, which contributes to distinct cell responses within a temperature range. Cell division and duration of the cell cycle seem to be more sensitive to temperature than growth. Cultures of *C. reinhardtii* grown at increasing temperatures will, at first, increase growth rates and shorten the cell cycle, as predicted by the two-fold increase in metabolic rate [2]. With a further temperature increase between 28 and 37 °C, duration of the cell cycle will be prolonged, while the growth rates will remain comparable. Since a temperature increase of 10 °C should double the growth rate, maintaining similar growth rates between the two temperatures implies that the growth rate effectively decreases in contrast to predictions. Thus, although the cells are not yet visibly stressed, such temperatures are physiologically

supraoptimal. Would a further increase in temperature lead to cell division arrest? When optimizing growth conditions for synchronized cultures of *C. reinhardtii*, Lien and Knutsen noted that at 1 °C above the optimal growth temperature, some cells started to exhibit inhibited cell division [5]. But such effects might be so subtle that they can only be detected in synchronized cultures when the entire culture is of a similar age. In distantly related alga, *Chlorella vulgaris*, an increase in temperature of 6–7 °C above the growth optima arrested nuclear and cellular divisions, but not DNA replication, and the effect on growth was negligible [6]. Cell cycle arrest thus seems to be one of the first physiological processes affected by even small increases in temperature above the optimum, but the nature of the arrest remains unknown. It is unclear if the arrest is caused by an effect on cell cycle regulatory protein activities (such as cyclin-dependent kinases) or by an effect on downstream cell cycle events.

C. reinhardtii is a model species that divides by multiple fission. Its cell cycle can be modeled as a series of overlapping reproductive sequences, each of them consisting of cell cycle entry at commitment point (CP) that switches on DNA replication (S phase), nuclear division (M phase), and cell division (C) (Figure 1) [5,7–10]. During growth in G₁ phase, cells attain their first CP, which would lead to completion of a single reproductive sequence (i.e., division into two daughter cells). At sufficiently fast growth rates, they may also attain consecutive CPs (*n*), each of which will eventually lead to completion of one reproductive sequence [11,12], independent of further energy supply (i.e., even in the dark). The mother cell can, therefore, divide into 2, 4, 8, or 16 (2^{*n*}) cells [5].

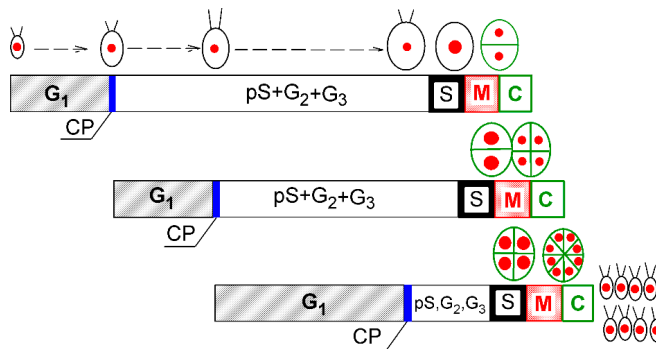


Figure 1. Schematic diagram of growth and the cell cycle in a single cell of *Chlamydomonas reinhardtii*. The schematic pictures reflect increasing cell size. The red full circles inside the cells illustrate the size and number of nuclei. Larger red circles indicate a doubling of DNA. Green ellipsoids and lines represent protoplast division. Diagram shows a model of cell cycle progression in *C. reinhardtii* dividing by multiple fission into 8 daughter cells. Three bars indicate three overlapping growth and reproductive sequences terminated by division into 2, 4, and 8 daughter cells, respectively. Precommitment period (G₁): the period until threshold critical cell size for commitment to divide (CP) is reached and CP is attained. Postcommitment period consists of pS—the prereplication phase between the CP attainment and the beginning of DNA replication. The processes required for initiation of DNA replication are assumed to happen during this phase. S: DNA replication takes place. G₂: the phase between the termination of DNA replication and the start of mitosis (M). Processes leading to the initiation of mitosis are assumed to take place during this phase. G₃: the phase separating mitosis from cellular division, which is clearly visible in some algae dividing by multiple fission. The processes leading to cellular division are assumed to take place during this phase. C: the phase during which cell cleavage (protoplast fission) and daughter cell formation occurs. For *C. reinhardtii*, it is typical that all “gap” phases are combined into one prolonged phase. The distances between individual cell cycle phases correspond to the cell cycle progression in a real culture (Figure 2). Modified after Zachleder et al. [13], Bišová and Zachleder [14], and Zachleder et al. [15].

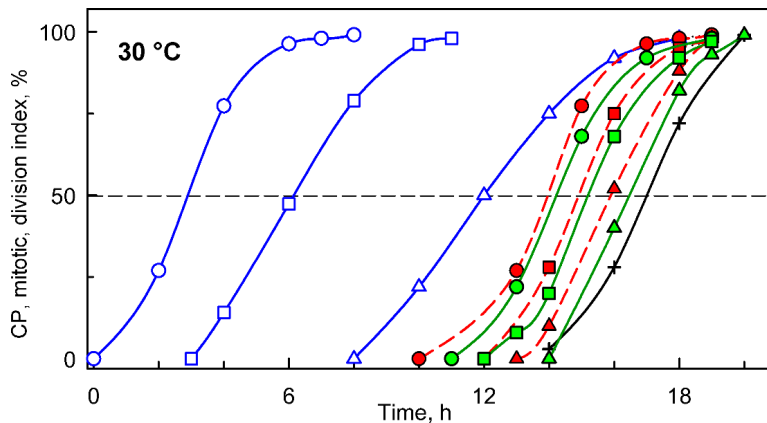


Figure 2. Graphical representation of the cell cycle progression in synchronized cultures of the *Chlamydomonas reinhardtii* grown at 30 °C at an incident light intensity of $500 \mu\text{mol m}^{-2} \text{s}^{-1}$. Time courses of individual commitment point/s, nuclear division/s, protoplast fission/s, and daughter cell release in synchronized cultures of *C. reinhardtii*. Blue curves (CP indices): cumulative percentage of cells, in a given population (100%), that attained the commitment point (CP) for the first (circles), second (squares), and third (triangles) reproductive sequence. Red curves (mitotic indices): cumulative percentage of cells, in a given population (100%), that divided their nuclei into 2 (circles), 4 (squares), and 8 (triangles). Green curves (division/protoplast fission indices): cumulative percentage of cells, in a given population (100%), that divided their protoplasts into 2 (circles), 4 (squares), and 8 (triangles). Black curve, crosses: cumulative percentage of cells that released daughter cells. Black dashed line at 50% depicts midpoint of each event in a population of cells.

In single algal cells (and in synchronized cultures that mimic them), growth is manifested by an increase in cell size, RNA, protein, and starch (and other energy components) per cell, which leads to the accumulation of dry matter and an increase in absorbance (A_{750}) of the culture. Growth is a prerequisite for cell division, as the attainment of each CP depends on reaching a critical cell size [10,16], which involves a doubling of cell size, cell mass, RNA, and protein per cell [2,11,12,15,17]. Growth is, therefore, tightly connected with the cell cycle so the number of reproductive sequences and released daughter cells are dictated by cell size [10,16]. Moreover, although there might be growth in the absence of cell division, division in the absence of growth leads to decreasing cell size and is, thus, limited to specific cases. Temperature affects growth as well as the entire cellular metabolism. Thus, it affects the duration of the growth phase prior to attainment of CP, the precommitment period, as well as the postcommitment period, where, under most conditions, growth runs concurrently with reproductive sequences [2–4]. This is in contrast to light that only affects growth and the duration of the precommitment period, but the postcommitment period remains constant [3,17]. Thus, the effect of temperature on the cell cycle is quite complex, even within the physiological range.

In plants, including algae, the cell cycle is regulated by two types of cyclin-dependent kinases (CDKs), CDKA and plant-specific CDKB. *C. reinhardtii* CDKA [18] and CDKB homologues are encoded by single genes [19] and have nonoverlapping functions [20]. CDKA promotes entry into cell division at CP and is also required to initiate the first DNA replication [20]. CDKB is the specific mitotic kinase that is required for spindle formation, nuclear division, and subsequent rounds of S phase, but not for cytokinesis [20]. Only CDKB is essential, whilst the null mutant of CDKA prolongs growth and delays cell division [21].

In the present paper, we describe the effect of supraoptimal temperature on cell cycle arrest and recovery in synchronized cultures of *C. reinhardtii*. We show that a supraoptimal temperature inhibited cell reproduction and the expenditure of starch, while normal growth continued, leading to

the formation of giant cells with elevated levels of starch. Cell cycle arrest comprised a block in nuclear and cellular division, while DNA replication was less affected. Arrest was accompanied by high mitotic kinase activities that declined following nuclear and cellular division/s. Cell cycle arrest was, therefore, not caused by a lack of cyclin-dependent kinase activity but rather a blockage in downstream processes.

2. Materials and Methods

2.1. Organism and Culture

The unicellular alga *Chlamydomonas reinhardtii* wild-type 21gr (CC-1690) was obtained from the Chlamydomonas Resource Center at the University of Minnesota (St. Paul, MN, USA). The cultures were grown on high salt medium (HS) as described by Sueoka [22] with a doubled concentration of Ca^{2+} ions and a tenfold increase in Mg^{2+} ions. Trace elements (1 mL per 1 L of medium) as described by Zachleder and Šetlík [23] were used instead of Hutner's trace elements. For routine subculturing, the cultures were streaked every three weeks onto modified high salt medium solidified by agar and grown at an incident light intensity of $100 \mu\text{mol m}^{-2} \text{s}^{-1}$ of photosynthetically active radiation.

2.2. Synchronization Procedure

For synchronization, 300 mL of liquid HS medium was inoculated directly from plates, and the cultures were placed in glass cylinders (inner diameter 30 mm, height 500 mm) at 30°C and "aerated" with a mixture of air and CO_2 (2%, v/v) at a flow rate of 15 L h^{-1} . The cylinders were illuminated from one side by a panel of dimmable fluorescent lamps (OSRAM DULUX L55W/950 Daylight, Milano, Italy) with light intensity adjusted to an incident light intensity of $500 \mu\text{mol m}^{-2} \text{s}^{-1}$ of photosynthetically active radiation at the surface of the cylinders. Synchronization was carried out by 13/11 h alternating light/dark (L/D) periods, as was described previously [24].

Suspensions of synchronous cells were diluted to a maximum concentration between 1.5×10^6 and 2×10^6 cells mL^{-1} and cultivated in rectangular plate-parallel vessels ($440 \times 245 \times 23$ mm, volume 2200 mL) at the same incident light conditions as used for synchronization. The flow rate of the aeration mix was 60 L h^{-1} . Culture vessels were immersed in water baths kept at constant temperatures of either 30 or 39°C . Each experiment was carried out in triplicate. Individual processes of the cell cycle were performed at the same time with midpoints varying by a maximum of one hour. Assessments of CP attainment, cell division, cell size, and cell number were carried out as described by Hlavová et al. [24]. Dry matter was determined according to Brányiková et al. [25].

2.3. Determination of Total DNA, RNA, Protein, and Starch

Total nucleic acid was extracted and analyzed according to Wanka [26], as modified by Lukavský et al. [27]. For DNA content, the light-activated reaction of diphenylamine with hydrolyzed DNA was used, as described by Decallonne and Weyns [28] with modifications of Zachleder [29]. The sediment remaining after nucleic acid extraction was used for protein determination after Lowry et al. [30]. Starch content was determined by the anthrone method [31] as modified by Brányiková et al. [25]. Two technical replicates were used for each analysis. Variations between duplicates did not exceed 5% of the mean.

2.4. Activity of Cyclin-Dependent Kinases

Protein lysates were prepared as described by Hlavová et al. [32]. They were directly assayed or affinity-purified by CrCKS1 beads as described by Bisova et al. [19] with modifications as described by Hlavová et al. [32]. Histone H1 kinase activity was assayed as previously described [33] in a final volume of $10 \mu\text{L}$ with either $7 \mu\text{L}$ of clear whole cell lysate or the CrCKS1 beads fraction corresponding to $20 \mu\text{L}$ of whole cell lysate. The reactions were initiated by adding the master mix to a final composition of 20 mM HEPES, pH 7.5, 15 mM MgCl_2 , 5 mM EGTA, 1 mM DTT, 0.1 mM ATP, 0.2% (w/v) histone

(Sigma H5505) and 0.370 MBq [γ ^{32}P] ATP. All the chemicals were purchased from Sigma-Aldrich (Prague, Czech Republic).

Proteins were separated on 15% SDS-PAGE gels [34]. Phosphorylated histone bands were visualized by autoradiography, analyzed using a Phosphoimager (Storm 860, Molecular Dynamics, GE Healthcare, Prague, Czech Republic), and quantified using Image Studio Lite software (LI-COR Biosciences, v. 5.2, Lincoln, NE, USA) as described by Zachleder et al. [4].

3. Results

3.1. Cell Cycle Progression Differs between 30 °C and 39 °C, but Growth Remains Unaffected

When a synchronized culture was grown at 30 °C, it sequentially attained three CPs, with midpoints at approximately 3, 6, and 12 h after the onset of light (Figure 2, blue circles, squares and triangles, respectively). Each of the CPs switched on one reproductive sequence, leading to three rounds of nuclear division (Figure 2, red circles, squares and triangles, respectively) in a clustered pattern with midpoints within a short time interval of three hours between 13 and 16 h. Each of the nuclear divisions was immediately followed by protoplast fission (Figure 2, green circles, squares and triangles respectively), so no multinuclear intermediates occurred in the cells. The divided protoplasts remained attached within the mother cell wall until the freely moving flagellated daughter cells were formed and released with a midpoint at 17 h (for a schematic illustration, see Figure 1).

Entry into the cell cycle was preceded by growth to a critical cell size. Microscopically, cells grown at 30 °C started as flagellated daughter cells (Figure 3A) that increased in size (Figure 3B) until they underwent cell division and gave rise to the next generation of daughter cells (Figure 3C), which could then undergo a similar sequence, provided that the growth conditions did not change. To study the effect of temperature on the cell cycle, we determined the lowest supraoptimal temperature that caused cell cycle arrest but did not affect growth. The heat stress temperature (42 °C) was not appropriate because this not only caused cell cycle arrest but also affected growth and cellular metabolism [35]. For *Chlamydomonas*, the optimal growth temperature was 35 °C, and at temperatures above 36 °C, protoplast fission and daughter cell release were inhibited [5]. Temperatures between 36 and 42 °C were, therefore, tested for their potential to cause cell cycle arrest. The lowest effective temperature was 39 °C, when protoplast division and daughter cell release were inhibited in 95%–100% of the population. In contrast, at 39 °C, comparing cell size and RNA (Figures 3 and 4), cells grew similarly to controls. This was true until cells at 30 °C started to divide. Thereafter, the cells at 39 °C continued to grow for at least another 10 h, to more than double the size (1409.7 ± 50.7) of cells grown at 30 °C (640.3 ± 43.7) (Figure 3). These large cells then became pale due to decreased chlorophyll content and ceased growth (Figure 3F,G), but they retained a high content of starch (Figure 3G,H). The cells grown at 39 °C did not divide for the entire duration of the experiment (Figure 3G), corresponding to a duration of almost two control cell cycles.

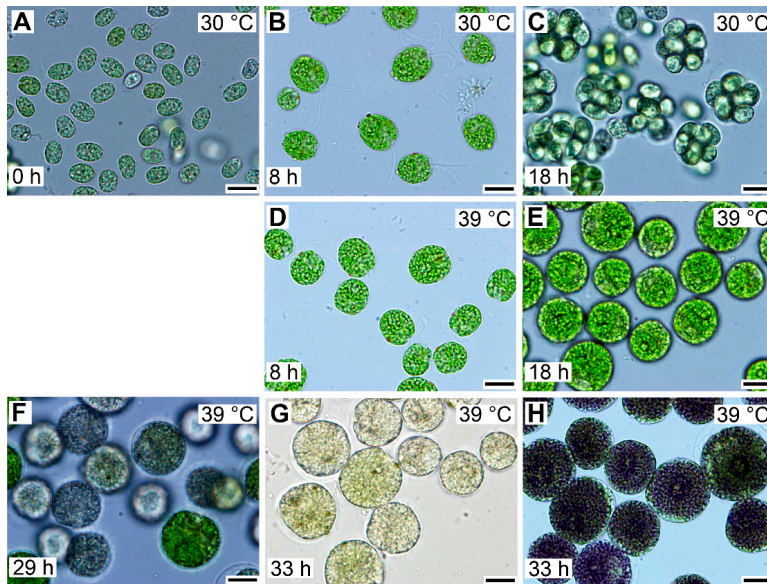


Figure 3. Photomicrographs of cells in synchronized cultures of *Chlamydomonas reinhardtii* grown in incident light $500 \mu\text{mol m}^{-2} \text{s}^{-1}$ at 30 °C (A–C) or 39 °C (D–H). The cultivation temperature and the cell age in hours are indicated in the pictures. The control cells, grown at 30 °C, divided at 18 h and thereafter entered a new cell cycle sequence similar to the one depicted in panels A–C. In contrast, the cells grown at 39 °C did not divide even after prolonged cultivation. They attained a maximum size after about 29 h of growth and started to lose chlorophyll (F). After 33 h, the majority of the cells lost chlorophyll and accumulated enormous amounts of starch in the form of grains (G), which can be visualized by staining with Lugol solution (H). Cultures at both 30 and 39 °C started from the same initial culture, so the cells depicted in panel A for 30 °C reflect also the cells present at 0 h at 39 °C. Bar = 10 μm .

The total RNA content (Figure 4A) doubled several times in cells grown at 30 °C, reached a maximum just before cellular division, and then decreased once the cells had divided (Figure 4A). DNA replication, as the first reproductive event, started by the 9th to 10th hour of the cell cycle and was completed by the 14th hour. During this time, DNA multiplied about 8-fold, corresponding to the production of 8 daughters per mother cell, and decreased again with cell division (Figure 4B). Cells grown at 39 °C accumulated RNA with similar kinetics to those of the control culture at 30 °C. They continued to grow and increased total RNA even at the time corresponding to division in the control cells, reaching about a 1.6-fold higher content of RNA compared to the maximum attained at 30 °C (Figure 4A). No division occurred at 39 °C. DNA replication at 39 °C started with about a 6 h delay, but it only increased about 3- to 4-fold compared to initial values and was, thus, more than 2-fold lower than the maximum seen in control cultures grown at 30 °C (Figure 4B).

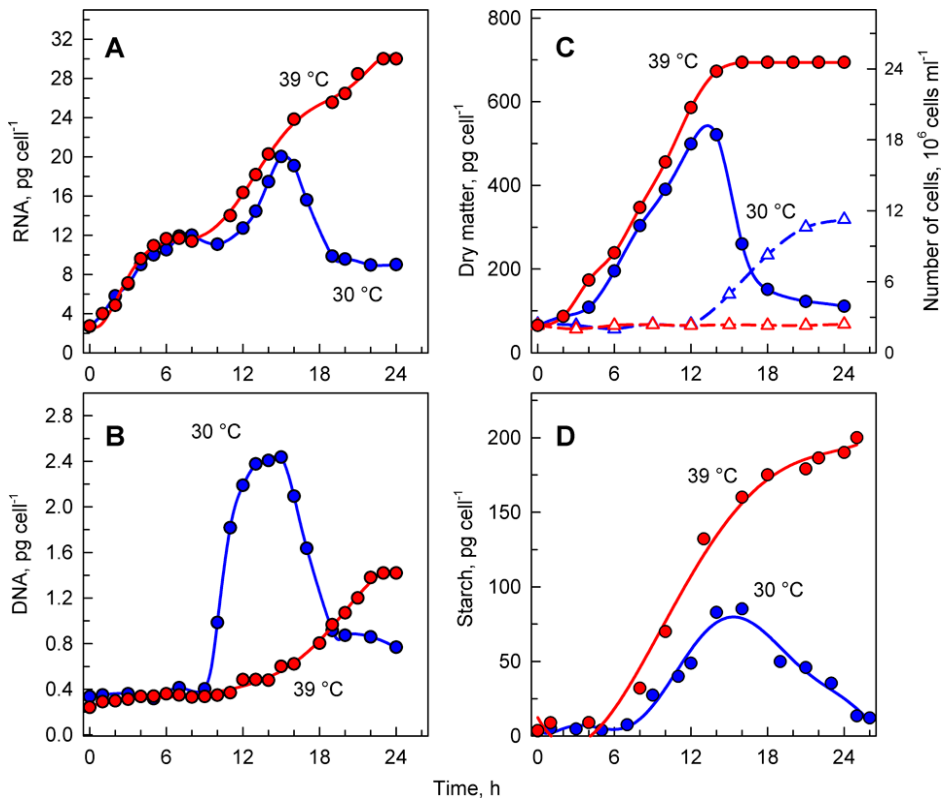


Figure 4. The course of RNA synthesis (A), DNA replications (B), changes in the number of cells and concentration of dry matter (C), and total starch (D) in the synchronized culture of *Chlamydomonas reinhardtii* grown under continuous illumination of incident light intensity $500 \mu\text{mol m}^{-2} \text{s}^{-1}$ at 30 °C (blue lines and symbols) or 39 °C (red lines and symbols).

3.2. Starch Reserves Accumulate and are Not Consumed at 39 °C

Growth at 30 and 39 °C was comparable with changes in total RNA content (Figure 4A) as well as for increases in dry matter (Figure 4C). The two cultures had virtually the same kinetics of dry matter increase up to the time when cellular divisions started in the control cultures (Figure 4C). In the control cultures, cell division led to a drop in dry matter per cell (Figure 4C), whilst the culture at 39 °C continued to increase dry matter for at least two more hours.

Microscopic analysis indicated that cells grown at 39 °C accumulated starch (Figure 3G,H). In *C. reinhardtii*, starch is used as a primary storage molecule and serves as the energy supply for cell reproduction as well as dark metabolism. In the culture grown at 30 °C, starch steadily increased up to about 10-times the initial value. About the time when the cells divided, the starch content plateaued and then decreased, probably because it was used as a source of energy and carbon for cell reproduction (Figure 4D, blue circles). The culture grown at 39 °C accumulated starch much faster than at 30 °C (Figure 4D, red circles). The final total starch content per cell at 39 °C was more than 2-fold higher than that of the maximum reached at 30 °C (Figure 4D). The rate of accumulation of starch at 39 °C (Figure 4D) was much higher than that of other growth processes (total RNA, dry matter) at the same temperature (Figure 4A,C).

3.3. Cells Transferred from 39 °C to 30 °C Recover from Cell Cycle Arrest

The effects of the supraoptimal temperature, 39 °C, seemed to be at least two-fold. Firstly, it induced cell cycle arrest, and secondly, in the absence of cell division, it caused a rapid accumulation of starch at rates exceeding synthesis of other metabolites. However, is the effect reversible? Cultures grown at 39 °C were transferred to the dark at 30 °C, where growth was inhibited due to the absence of an energy source, but the cell cycle continued. Control cultures grown at 30 °C attained 3 consecutive CPs, leading to initiation of the reproductive sequence for division into 2, 4, and 8 daughter cells (Figure 5A, blue lines), and thereafter divided into 8 daughter cells with a midpoint at the 17th hour (Figure 2).

Synchronized cells cultivated at 39 °C grew similarly to their 30 °C controls (Figures 3 and 4), but nuclear division and protoplast fission were inhibited, and daughter cells were not formed (Figure 3) even when put into darkness at 39 °C. This demonstrated that cell cycle arrest was dependent solely on temperature and not on a combination of light and temperature stress. Because of the absence of cell division in dark at 39 °C, to assess attaining of CP, cells growing at 39 °C were transferred to darkness at 30 °C (Figure 5A, red curves). At this temperature, the cells completed nuclear and cellular divisions and produced daughter cells, suggesting that during the relatively undisturbed growth at 39 °C, CPs were, indeed, attained, but the corresponding reproductive processes were blocked. The attainment of CPs at 39 °C was similar to that at 30 °C, with the first CP being delayed by about two hours at 39 °C, and the proportion of the population attaining the third CP for division into eight daughter cells was about 25% lower than controls (Figure 5A). After 16 or more hours of cultivation at 39 °C, the cells were no longer capable of complete recovery from the effect of high temperature, and the number of committed cells started to decrease (Figure 5A). The relationship between growth and CP attainment was maintained, as the proportion of dividing daughter cells produced in the dark increased with the prolongation of growth at 39 °C. Consequently, the number of daughter cells formed in the population that was transferred to darkness at 30 °C increased (Figure 5B–G) until the inhibitory effect of prolonged cultivation at 39 °C was manifested from the 16th hour (Figure 5H). Daughter cell release occurred at about the same time in cultures darkened at the 6th, 8th, 10th, and 12th hours (Figure 5C–F). It was slightly delayed in transfers after the 4th and 14th hours (Figure 5B,G) and delayed most in cultures transferred after the 16th hour. The delay in daughter cell release in cultures transferred at the 14th and 16th hour was most probably dictated by the fact that the entire reproductive sequence, including mitosis, protoplast fission, and daughter cell release, could have proceeded only after transfer to 30 °C.

A more detailed analysis of the dark 30 °C recovery from growth at 39 °C confirmed that growth ceased once the cells were put into darkness. This is clear from changes in total RNA and protein as well as the amount of dry matter that remained constant after the dark transfer or was slightly reduced, probably due to using some reserves for dark metabolism (Figure 6A–C). Based on changes in mean cell volume, cells transferred to darkness at 30 °C, after 4 and 8 h at 39 °C, started to release daughter cells with a slight delay compared to control cells grown at 30 °C (Figure 6D); this was also confirmed by the increase in cell number (Figure 6F). Daughter cell release was delayed by 4–6 h in cultures transferred at 12 and 14 h (Figure 6D,F). Cells transferred after 16 h were not only slightly delayed in daughter cell release, as shown by changes in mean cell volume (Figure 6D), but the number of daughter cells released (2.6-fold increase) was lower than the number expected from direct counting of cell divisions (3.8-fold increase; compare Figures 5H and 6F). This was caused by some of the divided daughter cells not hatching and staying connected in clumps.

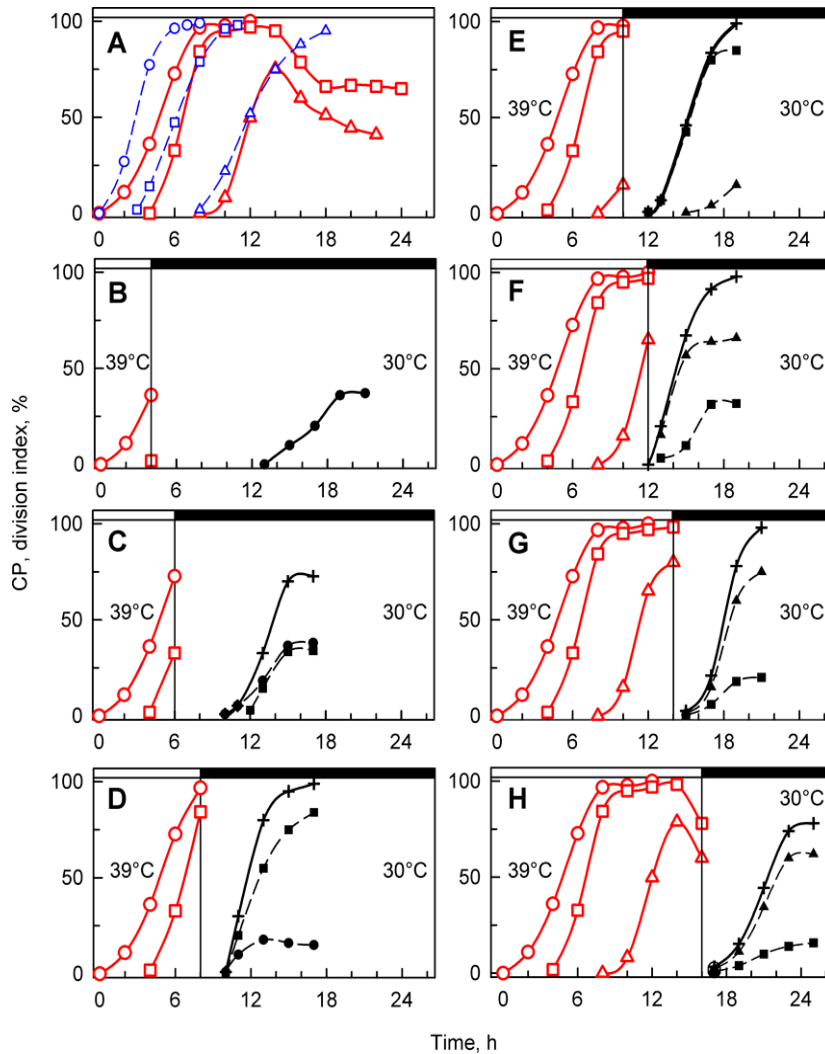


Figure 5. Time courses of individual CPs and cellular divisions in synchronized populations of *Chlamydomonas reinhardtii*. Panel A, the cells were grown in light at 30 °C (blue lines) or 39 °C (red lines); panels B–H, the cells were grown at 39 °C and then placed in the dark after 4, 6, 8, 10, 12, 14, and 16 h, respectively, and kept at 30 °C. No cell divisions occurred at 39 °C (A). Blue lines (CP indices): cumulative percentage of cells in a given population (100%) grown at 30 °C that attained commitment points (CPs) for the first (circles), second (squares), and third (triangles) reproductive sequences. Red lines (CP indices): the cells were grown at 39 °C and transferred bihourly to the dark at 30 °C. The cumulative percentage of 2, 4, and 8 daughter cells released in the dark in a given population (100%) is plotted as the attainment of the commitment points for the first (circles), second (squares), and third (triangles) reproductive sequences. Black dashed lines (division indices): cumulative percentage of cells that completed the first (full circles), second (full squares), and third (full triangles) cellular divisions and released 2, 4, or 8 daughter cells in a given population (100%). Black full lines, crosses: cumulative percentage of all cells in a given population (100%) that released daughter cells at 30 °C in dark. Times of transfer into darkness at 30 °C are indicated by vertical lines and by dark boxes above the graphs.

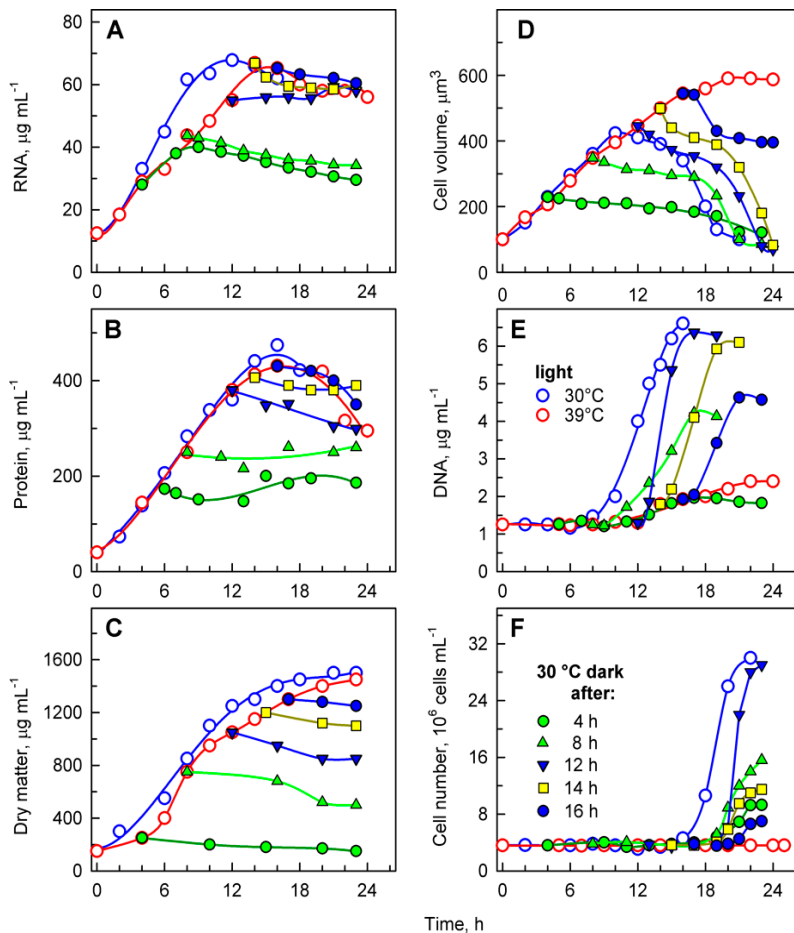


Figure 6. Changes in total RNA (A), total protein (B), dry matter (C), mean cell volume (D), DNA (E), and number of cells (F) in synchronized populations of *Chlamydomonas reinhardtii* grown at 30 °C (blue open circles), 39 °C (red open circles), and transferred from 39 °C into the dark at 30 °C at the 4th hour (green solid circles), 8th hour (green solid triangles), 12th hour (blue solid converted triangles), 14th hour (yellow solid squares), and 16th hour (blue solid circles), respectively.

DNA replication increased with the length of incubation in light at 39 °C, from 4 to 14 h (Figure 6F), but started to decrease from 16 h (Figure 6F). The timing of DNA replication reflected the timing of cell division (compare Figures 5 and 6E), as is typical for *C. reinhardtii*. DNA replication was delayed by about 2 h in cultures transferred after 8 and 12 h (Figure 6E). The delay increased to 6 h for cultures transferred after 14 h, and to 8 h for cultures transferred after 16 h (Figure 6E). The delay suggests that DNA replication was inhibited by the supraoptimal temperature treatment and could fully recover only after transfer to 30 °C. The number of daughter cells released also increased with the length of incubation in light at 39 °C, from 4 to 12 h (Figure 6F), and decreased thereafter (Figure 6F). These data (Figure 6E,F) confirmed results from direct microscopy counts of the number of daughter cells per mother cell (Figure 5) and further strengthened the idea of an inhibitory effect of prolonged incubation at supraoptimal temperatures. The extent of the effect was manifested in descending order, from daughter cell release, number of daughter cells formed per mother cell, and extent of DNA replication,

so that DNA replication was the last affected, and daughter cell release was the first to be altered by the supraoptimal temperature.

3.4. CDK Activity Changes Upon a Shift to Darkness at 30 °C

A supraoptimal temperature was shown to block the cell cycle, particularly nuclear and cellular divisions, while DNA replication proceeded, albeit later and to a lesser extent. Some of the cell cycle regulatory machinery must, therefore, be active to switch on DNA replication. However, it is not clear whether the limiting factor blocking the cell cycle is related to the activity of key cell cycle regulators, cyclin-dependent kinases (CDKs), or whether activity was not affected and the cell cycle was blocked further downstream. In *C. reinhardtii* there are two cell cycle regulatory CDKs, CDKA and CDKB [19,20]. Temperature-sensitive mutants of both were isolated [20], and their cell cycle regulatory functions were analyzed in detail [21,36]. Unfortunately, because of the temperature-sensitivity of the mutants, they could not be used in our experiments. Instead, we adopted a more general analysis of CDK activity in two types of protein mixtures containing different proportions of CDK complexes. Firstly, we analyzed CDK activity in whole cell lysates. Such unpurified extracts contained all the CDK complexes present at the same time in the cells; activity was related to attaining CP as well as to the completion of nuclear and cellular divisions [37]. Specific mitotic CDK complexes were purified through their affinity to bind to CrCKS1 protein. Activity bound to CrCKS1 protein beads corresponded almost exclusively to the completion of nuclear and cellular divisions [19] and encompassed activities of both CDKA and CDKB complexes [20]. Thus, although both types of protein extracts contained CDKA as well as CDKB complexes, the proportions of the two complexes in the mixture, as well as their activities, might differ because of the isolation procedure.

Activities in whole cell lysates were followed in aliquots of synchronized populations grown in light at 30 or 39 °C, and subsequently transferred from 39 °C to darkness at 30 °C (Figure 7). At 30 °C, CDK activity peaked at two distinct time points (Figure 7A). A smaller, less pronounced peak correlated with the attainment of CPs (Figure 5A), and the larger, more pronounced peak correlated with the onset of DNA replication and preceded nuclear and cellular divisions (Figure 7A). Similar peaks were also observed at 39 °C. Their occurrence and duration were affected by temperature. The CP-related peak started at the same time as the control, but its duration was prolonged, in agreement with a slower attainment of CP at 39 °C (Figure 7B). The second, more pronounced peak was delayed at 39 °C; it preceded the onset of DNA replication and decreased thereafter (Figure 7B). Since no nuclear and cellular divisions occurred at 39 °C, the peak of whole cell lysate CDK activity seemed to be specifically related to DNA replication. Interestingly, the maxima of the two peaks were comparable at both 30 and 39 °C, although the extent of DNA replication differed between the two cultures (Figure 7A,B).

Transfer from light at 39 °C to darkness at 30 °C did not affect the timing of the CP-related peak, but in most cases, it resulted in a shift of timing and extent of CDK activity of the second peaks related to DNA replication, and possibly nuclear and cellular division. For transfer after cultivation for 4 h in light at 39 °C, the second peak occurred at a comparable time point as at 39 °C and preceded the onset of DNA replication. This was comparable to the peak in 39 °C grown cells with similar levels of DNA replication (Figure 7C). For cultures transferred to darkness at 30 °C after 8 h at 39 °C, the second peak of CDK activity occurred 3 h earlier (Figure 7D) and again preceded the onset of DNA replication, followed by nuclear and cellular divisions. The peak was more pronounced either because more DNA was replicated or because of the simultaneous occurrence of nuclear and cellular divisions. After transfer at 12 h, the increase in CDK activity started similarly to the 39 °C control, but reached the peak five hours later, and the CDK activity was double that of the peak at 39 °C (Figure 7E). The increase corresponded with the onset of DNA replication as well as nuclear and cellular divisions that occurred between 12 and 18 h. Once cell division was complete, CDK activity decreased. Transfer after 16 h at 39 °C occurred after the DNA replication-related peak was attained at 39 °C, and following the transfer, CDK activity increased again and attained another peak 2–3 h later. This peak corresponded to the completion of further DNA replication as well as nuclear and cellular divisions.

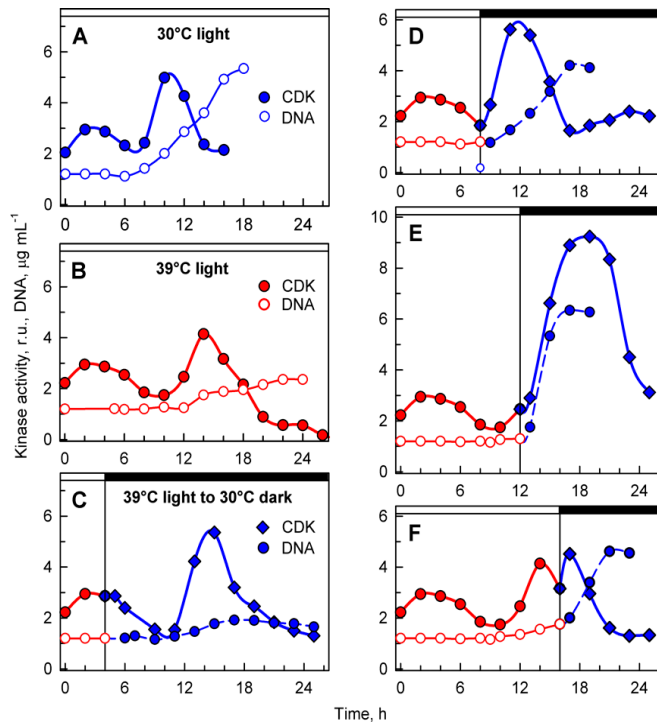


Figure 7. Activity of cyclin-dependent kinase (CDK) in whole-cell lysates prepared from synchronized cultures of *Chlamydomonas reinhardtii* cultivated under different light and temperature conditions. Panels **A, B**, the cells were grown in continuous light at 30 °C (**A**) or 39 °C (**B**); panels **C–F**, the cells were grown at 39 °C and then placed into the dark after 4, 8, 12, and 16 h and kept at 30 °C. Solid blue lines, full circles, kinase activity in cultures grown in continuous light at 30 °C; solid red lines, full circles, kinase activity in cultures grown in continuous light at 39 °C; solid blue lines, diamonds, kinase activity in cultures transferred from light at 39 °C to darkness at 30 °C. Solid blue lines, empty circles, DNA content in cells grown at 30 °C; solid red lines, empty circles, DNA content in cells grown at 39 °C; dashed blue lines, full circles, DNA content in cells transferred from 39 to 30 °C. Times of transfer into darkness are indicated by vertical lines and by dark boxes above the graphs.

To complement the analyses of whole cell lysate kinase activities, CDK activity bound to CrCKS1 beads was also assessed in the same set of experiments (Figure 8). At 30 °C, the CrCKS1 bead-bound CDK activity increased at the 10th hour and stayed elevated until the 18th hour, when it then decreased (Figure 8A). This peak corresponded with the onset of DNA replication (Figure 4B, blue curve), was maintained over three rounds of DNA replication and nuclear and cell divisions (Figure 2), and fell after they were completed. At 39 °C, the increase in CDK activity started about two hours earlier, reached similar levels as at 30 °C, and never decreased (Figure 8B), possibly because of the absence of nuclear and cellular divisions. In the culture transferred from 39 °C to darkness at 30 °C after 4 h in light, the increase in kinase activity occurred earlier compared to its mother culture at 39 °C, but the final activities were comparable. The increase in CDK activity preceded, by about 5 h, the onset of cell division in a small proportion of culture, and the activity started to decrease slightly once cell division was complete (Figure 8C). For cultures transferred to darkness at 30 °C after 8 or 10 h at 39 °C, CDK activity exceeded that of the original culture at 39 °C within 3 h of transfer, reached a peak at the completion of cell division, and decreased thereafter (Figure 8D,E). The culture grown at 30 °C for 14 or more hours completed cell divisions and released daughter cells (Figures 2, 5A and 8A). Nuclear and

cell divisions were blocked at 39 °C, but when cultures grown at 39 °C were transferred into darkness at 30 °C, divisions occurred almost immediately. Within one hour of transfer, fifty percent or more of cells completed the first nuclear and cellular divisions (Figure 8F,G). Nuclear and cellular divisions were accompanied by decreased kinase activities (Figure 8F,G).

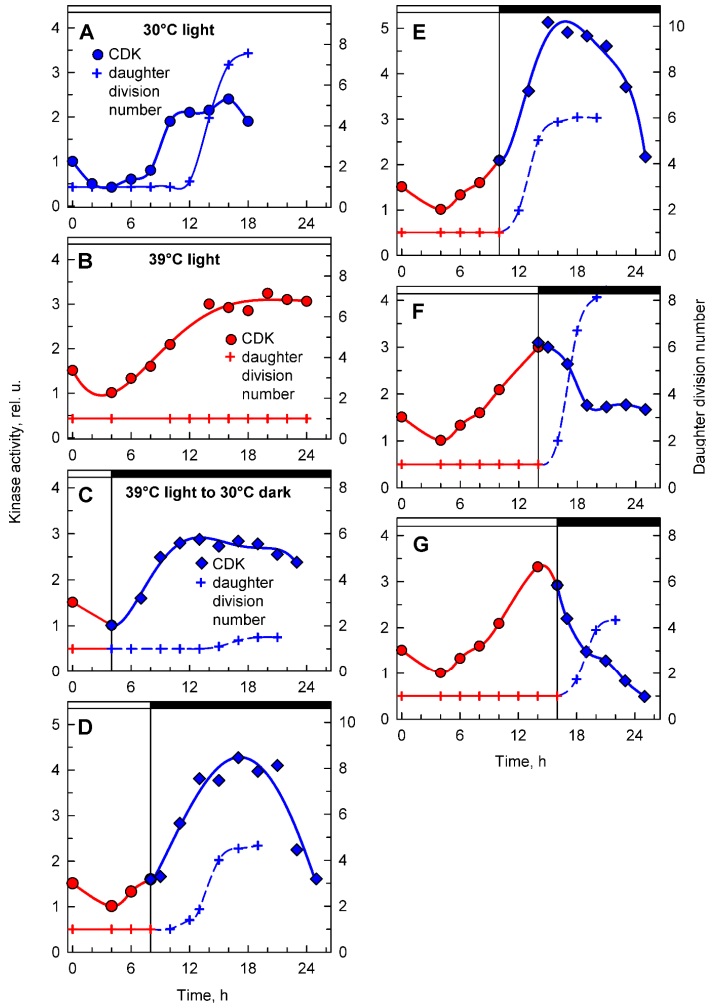


Figure 8. Activity of CDK in CrCKS1-bound fractions prepared from synchronized cultures of *Chlamydomonas reinhardtii* cultivated under different conditions of light and temperature. Panels A, B, the cells were grown in continuous light at 30 °C (A) or 39 °C (B); panels C–G, the cells were grown at 39 °C and then placed into darkness after 4, 8, 10, 14, and 16 h and kept at 30 °C. Blue lines, circles, kinase activity in cultures grown in continuous light at 30 °C; red lines, circles, kinase activity in cultures grown in continuous light at 39 °C; blue lines, diamonds, kinase activity in cultures transferred from light at 39 °C into darkness at 30 °C. Blue solid line, crosses, daughter division number—number of daughter cells released per mother cell at 30 °C; red solid line, crosses, daughter division number at 39 °C; blue dashed line, crosses, daughter division number after transfer from 39 °C to 30 °C. Times of transfer into dark are indicated by vertical lines and by dark boxes above the graphs.

4. Discussion

Cultivation temperature affects the entire metabolism of cells, including their ability to complete the cell cycle. The sensitivities of different metabolic processes are not the same, as shown by the temperature optima for growth and photosynthesis, which can differ by as much as 10 °C [38]. Similarly, the upper temperature limits for growth, photosynthesis, and respiration can differ [38]. The ability of cells to divide seems to be the most temperature-sensitive process, as cell division is blocked even when growth is barely affected. Indeed, cell division of *C. reinhardtii* was blocked by cultivation at 39 °C, but growth was comparable between 30 and 39 °C (Figures 3–6). Cells cultivated at 39 °C exhibited two main effects: (1) cell cycle arrest (Figures 3, 5 and 6) and (2) accumulation of starch (Figure 4); these are probably interconnected. Within the physiological range, a temperature increase of 10 °C generally leads to a speeding up of metabolism by about two-fold. This is also true for the duration of the cell cycle in *C. reinhardtii* [2] or in *C. eugametos* [3]. The fact that growth was not enhanced in the present experiments, as would have been expected within the physiological temperature range, suggested that the higher temperature had some inhibitory effects that lessened the growth rate, which was only slightly higher than at 30 °C (i.e., to about half of the predicted one). A similar decrease in growth rate, accompanied by successive prolongation of the cell cycle, as well as its individual steps, was shown in cultures of *C. reinhardtii* [2] and *C. eugametos* [3] cultivated at temperatures above the optimum. It is, thus, to be expected that a further increase in temperature up to 39 °C, as used in recent experiments, would cause a complete arrest of nuclear and cellular division. It has been established that yet another increase in temperature to a heat shock temperature of 42 °C has numerous effects on *C. reinhardtii*; it not only arrested the cell cycle but also caused significant inhibition of growth processes. There was only about a 1.6-fold increase in total protein within 24 h of heat shock treatment at 42 °C [35], compared to about a 10-fold increase in total protein within the same period at 39 °C (Figure 6B). In contrast, 39 °C treatment had only a limited specific effect; it negatively affected the cell cycle and positively affected starch accumulation. Cell growth at 39 °C was not affected for about 18 h and continued during the period of DNA replication and nuclear and cellular divisions in cultures grown at 30 °C. This led to the accumulation of giant nondividing cells rich in starch. Among the growth parameters, starch was outstanding as the only one showing a striking difference between cultures grown at 30 and 39 °C (Figure 4). In the control cultures, cells increased their starch content more than 10-fold (up to 80 pg cell⁻¹, Figure 4), but a majority of this was used during cell division, even though the cells were grown in continuous light (Figure 4). This confirms that cell reproduction is an extreme energy-demanding process, in which large amounts of energy are required for DNA replication and nuclear and cellular divisions, as was previously shown [17,39]. Correspondingly, the blockage of cell division at 39 °C and prevention of starch expenditure led to the accumulation of high levels of starch. At 39 °C, this was further accentuated by faster starch production at high temperatures and high light (Figure 4). Over-accumulation of starch by a block in cell division has been a recurring theme, as it has been shown for *Chlorella vulgaris* starved of nitrogen, sulfur, and phosphate [25]; nitrogen- or phosphorus-starved *Desmodesmus quadricauda* [40,41]; as well as in nitrogen- and sulfur-starved *C. reinhardtii* [42,43]. Starch accumulation was also induced when nuclear DNA replication was inhibited [44] as well as by high temperature [45]. In contrast, the heat shock treatment of *C. reinhardtii* led to only a 46% increase in starch content over the 24 h period, and energy reserves were mostly accumulated in the form of lipids [35]. In algae capable of producing both starch and lipids, starch overproduction is the first response to stress, and with prolongation, it is replaced with lipid production [46,47] possibly to store more energy in a more compact form for stress recovery [48].

The cell cycle arrest at 39 °C was maintained even in darkness but was removed once the cells were shifted to 30 °C (Figure 5). With prolonged incubation at 39 °C, the ability of cells to fully recover from the block was decreased. The first affected process was daughter cell splitting; the second, the extent of cell division and the number of daughter cells formed; and the third, the extent of DNA replication (Figures 5 and 6). A similar order of sensitivity, with cell division being the most sensitive process, was also shown for cell cycle arrest following exposure to different concentrations of cadmium

in *Desmodesmus quadricauda*, a green alga that does not split daughter cells [49]. Likewise, the formation of palmelloids (i.e., unsplit daughter cells) was characteristic for the salt stress response [50]. Thus, the response to high temperature seems to follow general rules or mechanisms involved in stress responses. The incomplete recovery from cultivation at 39 °C is in conflict with the presumably complete recovery from heat shock at 42 °C [35,51]. This might seem surprising because the heat shock conditions of 42 °C were more severe than cultivation at 39 °C. However, the heat shock experiments were carried out with asynchronous cultures, where only about 20% of the cells in the population were dividing at 25 °C, which is the cultivation temperature used in the experiments [35]. Subtle changes seen in the synchronized cultures grown at 39 °C would therefore be impossible to detect.

The cell cycle arrest at 39 °C was the most striking effect of supraoptimal temperature. Its occurrence under heat shock conditions of 42 °C was hypothesized to be caused by reduced CDK activity [35], but it has never been tested; thus, the mechanism has remained enigmatic. In principle, there are two possible mechanisms: (1) cell cycle arrest due to low CDK activity and/or (2) a cell cycle block downstream of CDK activity. Of all the reproductive processes, DNA replication was the least sensitive to high-temperature treatment (Figures 4 and 6). Similarly, DNA replication was not affected by high-temperature treatment of *Chlorella vulgaris*, and, instead, the block was just prior to nuclear division [6]. In fact, in *Chlorella vulgaris*, several rounds of DNA replication were performed, as the final DNA content was 16-fold higher than initial values [6]. In *C. reinhardtii*, DNA replication increased between two- and four-fold (Figures 4 and 6), so DNA replication was not only delayed in timing but occurred to a lesser extent even at a supraoptimal temperature. Kinase activity in whole-cell extracts preceded DNA replication, decreased once DNA replication ceased, and, thus, apart from timing, did not differ between 30 and 39 °C (Figure 7). In a simplified system of fission yeast, it was shown that low levels of CDK activity allows DNA replication to occur, whilst higher levels are required for nuclear division [52]. This would fit the hypothesis of reduced CDK activity, allowing DNA replication to occur but being unable to switch on nuclear division. Notwithstanding the fact that the *C. reinhardtii* cell cycle is regulated by a more complex network of two CDKs, this hypothesis does not fit the data on mitotic kinase activities (Figure 8). Instead, mitotic kinase activities were comparable between 30 and 39 °C. The main difference between the two treatments was stabilization of a high mitotic CDK activity that only decreased after nuclear and cellular divisions (Figure 8). This supports the idea that the cell cycle block occurred downstream of CDK. The mitotic CDK behavior seems to phenocopy that of CDKA kinase in the anaphase-promoting complex (APC) mutant, *cdc27-6*, with persistent slightly higher kinase activity compared with control cells [21]. This implies involvement of APC in the supraoptimal temperature-induced cell cycle arrest. APC, the main E3 ubiquitin ligase to control mitotic progression and exit in all eukaryotes [53], has been shown to inhibit both CDKA and CDKB in *C. reinhardtii* [21]. In opisthokonts, APC is activated by mitotic kinases but kept inactive by spindle assembly checkpoint until all chromosomes are properly assembled [54]. Tubulin polymerization is known to be temperature sensitive [55]. Thus, it could be assumed that microtubule and, hence, spindle stability would be affected by supraoptimal temperature, leading to activation of the spindle assembly checkpoint, inhibition of APC, and maintenance of mitotic kinase activity. In the present experiments, the completion of cell division lagged behind the increase in mitotic kinase activity. The delay was successively shortened with the time the culture spent at 39 °C (Figure 8, compare A and D to E, F, G). This suggests that many of the processes required for completion of mitotic and cellular division may run even at 39 °C, and the cell cycle arrest is located very shortly before the onset of CDK inactivation. This further supports the idea of microtubule stability and possibility of the spindle checkpoint being involved in the arrest.

Author Contributions: Conceptualization, K.B. and V.Z.; methodology, I.I.; validation, K.B., M.V., and V.Z.; formal analysis, I.I.; investigation, I.I., M.V., V.Z., and K.B.; resources, K.B.; data curation, I.I., V.Z., and K.B.; writing—original draft preparation, V.Z., K.B., and I.I.; writing—review and editing, I.I., M.V., V.Z., and K.B.; visualization, V.Z., M.V., and K.B.; supervision, K.B.; project administration, K.B.; funding acquisition, K.B.

Funding: This research was funded by Grantová Agentura České Republiky, grant number 15-09231S, and by the National Programme of Sustainability I, project no. LO1416.

Acknowledgments: We are obliged to K. Ondrejmišková and J. Sýkorová for excellent technical support. We thank J. D. Brooker for critical reading and language editing of the text.

Conflicts of Interest: The authors declare no conflicts of interest. The funders had no role in the design of the study; in the collection, analyses, or interpretation of data; in the writing of the manuscript, or in the decision to publish the results.

References

- Morimura, Y. Synchronous culture of *Chlorella*. I. Kinetic analysis of the life cycle of *Chlorella ellipsoidea* as affected by changes of temperature and light intensity. *Plant Cell Physiol.* **1959**, *1*, 49–62.
- Vitová, M.; Bišová, K.; Hlavová, M.; Kawano, S.; Zachleder, V.; Čížková, M. *Chlamydomonas reinhardtii*: Duration of its cell cycle and phases at growth rates affected by temperature. *Planta* **2011**, *234*, 599–608. [[CrossRef](#)] [[PubMed](#)]
- Zachleder, V.; van den Ende, H. Cell cycle events in the green alga *Chlamydomonas eugametos* and their control by environmental factors. *J. Cell Sci.* **1992**, *102*, 469–474.
- Zachleder, V.; Ivanov, I.; Vitová, M.; Bišová, K. Effects of cyclin-dependent kinase activity on the coordination of growth and the cell cycle in green algae at different temperatures. *J. Exp. Bot.* **2019**, *70*, 845–858. [[CrossRef](#)] [[PubMed](#)]
- Lien, T.; Knutsen, G. Synchronous growth of *Chlamydomonas reinhardtii* (Chlorophyceae): A review of optimal conditions. *J. Phycol.* **1979**, *15*, 191–200. [[CrossRef](#)]
- Šetlík, I.; Zachleder, V.; Doucha, J.; Berková, E.; Bartoš, J. The nature of temperature block in the sequence of reproductive processes in *Chlorella vulgaris* BEIJERINCK. *Arch. Hydrobiol. Suppl. 49 Algal. Stud.* **1975**, *14*, 70–104.
- Coleman, A.W. The nuclear-cell cycle in *Chlamydomonas* (Chlorophyceae). *J. Phycol.* **1982**, *18*, 192–195. [[CrossRef](#)]
- Craigie, R.A.; Cavalier-Smith, T. Cell volume and the control of the *Chlamydomonas* cell cycle. *J. Cell Sci.* **1982**, *54*, 173–191.
- Lien, T.; Knutsen, G. Synchronized cultures of a cell wall-less mutant of *Chlamydomonas reinhardtii*. *Arch. Microbiol.* **1976**, *108*, 189–194. [[CrossRef](#)]
- Donnan, L.; John, P.C.L. Cell cycle control by timer and sizer in *Chlamydomonas*. *Nature* **1983**, *304*, 630–633. [[CrossRef](#)]
- John, P.C.L. Control of the cell division cycle in *Chlamydomonas*. *Microbiol. Sci.* **1984**, *1*, 96–101. [[PubMed](#)]
- John, P.C.L. Control points in the *Chlamydomonas* cell cycle. In *Algal Development*; Wiesnar, W., Robinson, D.G., Starr, R.C., Eds.; Springer: Berlin, Germany, 1987; pp. 9–16.
- Zachleder, V.; Schläfli, O.; Boschetti, A. Growth-controlled oscillation in activity of histone H1 kinase during the cell cycle of *Chlamydomonas reinhardtii* (Chlorophyta). *J. Phycol.* **1997**, *33*, 673–681. [[CrossRef](#)]
- Bišová, K.; Zachleder, V. Cell-cycle regulation in green algae dividing by multiple fission. *J. Exp. Bot.* **2014**, *65*, 2585–2602. [[CrossRef](#)] [[PubMed](#)]
- Zachleder, V.; Bišová, K.; Vitová, M. The cell cycle of microalgae. In *The Physiology of Microalgae*; Borowitzka, M.A., Beardall, J., Raven, J.A., Eds.; Springer: Dordrecht, The Netherlands, 2016; Volume 6, pp. 3–46.
- Donnan, L.; John, P.C.L. Timer and sizer controls in the cell cycles of *Chlamydomonas* and *Chlorella*. In *The Microbial Cell Cycle*; Nurse, P., Streiblová, E., Eds.; CRC Press: Boca Raton, FL, USA, 1984; pp. 231–251.
- Vitová, M.; Bišová, K.; Umysová, D.; Hlavová, M.; Kawano, S.; Zachleder, V.; Čížková, M. *Chlamydomonas reinhardtii*: Duration of its cell cycle and phases at growth rates affected by light intensity. *Planta* **2011**, *233*, 75–86. [[CrossRef](#)] [[PubMed](#)]
- John, P.C.; Sek, F.J.; Lee, M.G. A homolog of the cell cycle control protein p34^{cdc2} participates in the division cycle of *Chlamydomonas*, and a similar protein is detectable in higher plants and remote taxa. *Plant Cell* **1989**, *1*, 1185–1193.
- Bisova, K.; Krylov, D.M.; Umen, J.G. Genome-wide annotation and expression profiling of cell cycle regulatory genes in *Chlamydomonas reinhardtii*. *Plant Physiol.* **2005**, *137*, 1–17. [[CrossRef](#)]

20. Tulin, F.; Cross, F.R. A microbial avenue to cell cycle control in the plant superkingdom. *Plant Cell* **2014**, *26*, 4019–4038. [[CrossRef](#)]
21. Atkins, K.C.; Cross, F. Inter-regulation of CDKA/CDK1 and the plant-specific cyclin-dependent kinase CDKB in control of the *Chlamydomonas* cell cycle. *Plant Cell* **2018**, *30*, 429–446. [[CrossRef](#)]
22. Sueoka, N. Mitotic replication of deoxyribonucleic acid in *Chlamydomonas reinhardtii*. *Proc. Natl. Acad. Sci. USA* **1960**, *46*, 83–91. [[CrossRef](#)]
23. Zachleder, V.; Šetlík, I. Effect of irradiance on the course of RNA synthesis in the cell cycle of *Scenedesmus quadricauda*. *Biol. Plant.* **1982**, *24*, 341–353. [[CrossRef](#)]
24. Hlavová, M.; Vítová, M.; Bišová, K. Synchronization of green algae by light and dark regimes for cell cycle and cell division studies. In *Plant Cell Division*; Caillaud, M.-C., Ed.; Springer Science: New York, NY, USA, 2016; pp. 3–16.
25. Brányiková, I.; Maršálková, B.; Doucha, J.; Brányik, T.; Bišová, K.; Zachleder, V.; Vítová, M. Microalgae-novel highly efficient starch producers. *Biotechnol. Bioeng.* **2011**, *108*, 766–776. [[CrossRef](#)] [[PubMed](#)]
26. Wanka, F. Über den Einfluss des Lichts auf die Nucleinsäuresynthese bei Synchronkulturen von *Chlorella pyrenoidosa*. *Ber. Dtsch. Bot. Ges.* **1962**, *75*, 457–464.
27. Lukavský, J.; Tetík, K.; Vendlová, J. Extraction of nucleic acid from the alga *Scenedesmus quadricauda*. *Arch. Hydrobiol. Suppl. 41 Algal. Stud.* **1973**, *9*, 416–426.
28. Decallonne, J.R.; Weyns, C.J. A shortened procedure of the diphenylamine reaction for measurement of deoxyribonucleic acid by using light activation. *Anal. Biochem.* **1976**, *74*, 448–456. [[CrossRef](#)]
29. Zachleder, V. Optimization of nucleic acids assay in green and blue-green algae: Extraction procedures and the light-activated reaction for DNA. *Arch. Hydrobiol. Suppl. 67 Algal. Stud.* **1984**, *36*, 313–328. [[CrossRef](#)]
30. Lowry, O.H.; Rosenbrough, N.S.; Farr, A.L.; Randall, R.J. Protein measurement with the folin-phenol reagent. *J. Biol. Chem.* **1951**, *193*, 265–275.
31. McCready, R.M.; Guggolz, J.; Silveira, V.; Owens, H.S. Determination of starch and amylose in vegetables. *Anal. Chem.* **1950**, *22*, 1156–1158. [[CrossRef](#)]
32. Hlavová, M.; Čížková, M.; Vítová, M.; Bišová, K.; Zachleder, V. DNA damage during G2 phase does not affect cell cycle progression of the green alga *Scenedesmus quadricauda*. *PLoS ONE* **2011**, *6*, e19626. [[CrossRef](#)]
33. Langan, T.A.; Gautier, J.; Lohka, M.; Hollingsworth, R.; Moreno, S.; Nurse, P.; Maller, J.; Sclafani, R.A. Mammalian growth-associated H1 histone kinase: A homologue of cdc2+/CDC28 protein kinases controlling mitotic entry in yeast and frog cells. *Mol. Cell. Biol.* **1989**, *9*, 3860–3868. [[CrossRef](#)]
34. Laemmli, U.K. Cleavage of structural proteins during the assembly of the head of bacteriophage T4. *Nature* **1970**, *227*, 680–685. [[CrossRef](#)]
35. Hemme, D.; Veyel, D.; Muhlhaus, T.; Sommer, F.; Juppner, J.; Unger, A.K.; Sandmann, M.; Fehrlé, I.; Schonfelder, S.; Steup, M.; et al. Systems-wide analysis of acclimation responses to long-term heat stress and recovery in the photosynthetic model organism *Chlamydomonas reinhardtii*. *Plant Cell* **2014**, *26*, 4270–4297. [[CrossRef](#)]
36. Tulin, F.; Cross, F.R. Cyclin-dependent kinase regulation of diurnal transcription in *Chlamydomonas*. *Plant Cell* **2015**, *27*, 2727–2742. [[CrossRef](#)] [[PubMed](#)]
37. Zachleder, V. The course of reproductive events in the chloroplast cycle of the chlorococcal alga *Scenedesmus quadricauda* as revealed by using inhibitors of DNA replication. *Plant Cell Physiol.* **1997**, *38*, 56.
38. Sorokin, C. Tabular comparative data for the low-and high-temperature strains of *Chlorella*. *Nature* **1959**, *184*, 613–614. [[CrossRef](#)] [[PubMed](#)]
39. Wanka, F. Ultrastructural changes during normal and colchicine-inhibited cell division of *Chlorella*. *Protoplasma* **1968**, *66*, 105–130. [[CrossRef](#)] [[PubMed](#)]
40. Ballin, G.; Doucha, J.; Zachleder, V.; Šetlík, I. Macromolecular syntheses and the course of cell cycle events in the chlorococcal alga *Scenedesmus quadricauda* under nutrient starvation: Effect of nitrogen starvation. *Biol. Plant.* **1988**, *30*, 81–91. [[CrossRef](#)]
41. Zachleder, V.; Ballin, G.; Doucha, J.; Šetlík, I. Macromolecular syntheses and the course of cell cycle events in the chlorococcal alga *Scenedesmus quadricauda* under nutrient starvation: Effect of phosphorus starvation. *Biol. Plant.* **1988**, *30*, 92–99. [[CrossRef](#)]

42. Siant, M.; Cuine, S.; Cagnon, C.; Fessler, B.; Nguyen, M.; Carrier, P.; Beyly, A.; Beisson, F.; Triantaphylides, C.; Li-Beisson, Y.; et al. Oil accumulation in the model green alga *Chlamydomonas reinhardtii*: Characterization, variability between common laboratory strains and relationship with starch reserves. *BMC Biotechnol.* **2011**, *11*, 7. [[CrossRef](#)]
43. Philipps, G.; Happe, T.; Hemschemeier, A. Nitrogen deprivation results in photosynthetic hydrogen production in *Chlamydomonas reinhardtii*. *Planta* **2012**, *235*, 729–745. [[CrossRef](#)]
44. Zachleder, V. The effect of hydroxyurea and fluorodeoxyuridine on cell cycle events in the chlorococcal alga *Scenedesmus quadricauda* (Chlorophyta). *J. Phycol.* **1994**, *30*, 274–279. [[CrossRef](#)]
45. Semenenko, V.E.; Vladimirova, M.G.; Orleanskaya, O.B. Physiological characteristics of *Chlorella* sp. K under conditions of high extremal temperatures I. Uncoupling effect of extreme temperatures on the cellular functions of *Chlorella*. *Plant Physiol.* **1967**, *14*, 612–625.
46. Fernandes, B.; Teixeira, J.; Dragone, G.; Vicente, A.A.; Kawano, S.; Bišová, K.; Příbyl, P.; Zachleder, V.; Vítová, M. Relationship between starch and lipid accumulation induced by nutrient depletion and replenishment in the microalga *Parachlorella kessleri*. *Bioresour. Technol.* **2013**, *144*, 268–274. [[CrossRef](#)] [[PubMed](#)]
47. Mizuno, Y.; Sato, A.; Watanabe, K.; Hirata, A.; Takeshita, T.; Ota, S.; Sato, N.; Zachleder, V.; Tsuzuki, M.; Kawano, S. Sequential accumulation of starch and lipid induced by sulfur deficiency in *Chlorella* and *Parachlorella* species. *Bioresour. Technol.* **2013**, *129*, 150–155. [[CrossRef](#)] [[PubMed](#)]
48. Roessler, P.G. Environmental control of glycerolipid metabolism in microalgae: Commercial implications and future research directions. *J. Phycol.* **1990**, *26*, 393–399. [[CrossRef](#)]
49. Bišová, K.; Hendrychová, J.; Cepák, V.; Zachleder, V. Cell growth and division processes are differentially sensitive to cadmium in *Scenedesmus quadricauda*. *Folia Microbiol.* **2003**, *48*, 805–816. [[CrossRef](#)]
50. Khona, D.K.; Shirolikar, S.; Gawde, K.K.; Hom, E.; Deodhar, M.A.; D'Souza, J.S. Characterization of salt stress-induced palmelloids in the green alga, *Chlamydomonas reinhardtii*. *Algal Res.* **2016**, *16*, 434–448. [[CrossRef](#)]
51. Mühlhaus, T.; Weiss, J.; Hemme, D.; Sommer, F.; Schroda, M. Quantitative shotgun proteomics using a uniform 15N-labelled standard to monitor proteome dynamics in time course experiments reveals new insights into the heat stress response of *Chlamydomonas reinhardtii*. *Mol. Cell. Biol.* **2011**, *10*.
52. Coudreuse, D.; Nurse, P. Driving the cell cycle with a minimal CDK control network. *Nature* **2010**, *468*, 1074–1079. [[CrossRef](#)]
53. Marocco, K.; Bergdoll, M.; Achard, P.; Criqui, M.C.; Genschik, P. Selective proteolysis sets the tempo of the cell cycle. *Curr. Opin. Plant Biol.* **2010**, *13*, 631–639. [[CrossRef](#)]
54. Castro, A.; Bernis, C.; Vigneron, S.; Labbé, J.-C.; Lorca, T. The anaphase-promoting complex: A key factor in the regulation of cell cycle. *Oncogene* **2005**, *24*, 314–325. [[CrossRef](#)]
55. Lodish, H.; Berk, A.; Zipursky, S.L.; Matsudaira, P.; Baltimore, D.; Darnell, J. *Mol. Cell. Biol.*; W. H. Freeman & Co.: New York, NY, USA, 2000.

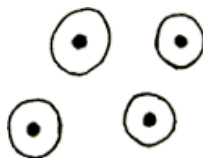


© 2019 by the authors. Licensee MDPI, Basel, Switzerland. This article is an open access article distributed under the terms and conditions of the Creative Commons Attribution (CC BY) license (<http://creativecommons.org/licenses/by/4.0/>).

Chapter VI

Starch production in
Chlamydomonas reinhardtii
through supraoptimal temperature
treatment cultivated in a pilot-scale
photobioreactor

Ivan N. Ivanov, Milada Vítová, Vilém Zachleder, Maria J. Barbosa,
Kateřina Bišová



Abstract

Increase in temperature can have profound effects on the cell cycle and cell division in green algae while growth and synthesis of energy storage compound are less influenced. In *Chlamydomonas reinhardtii* laboratory experiments have shown that exposure to supraoptimal temperature (39 °C) causes a complete block of nuclear and cellular division accompanied by increased accumulation of starch. In this work we explore the potential of supraoptimal temperature as a method for starch production in *C. reinhardtii* in pilot-scale photobioreactors. The method was successfully applied and resulted in a considerable, near 3-fold, enhancement of starch content in *C. reinhardtii* at low biomass densities. Moreover, maximum starch content at the supraoptimal temperature was reached within 1-2 days and within 5 days in the control culture at optimal temperature. Therefore supraoptimal temperature treatment provides rapid starch accumulation and it poses a viable alternative to other starch inducing methods such as nutrient depletion. However, technical challenges such as bioreactor design and improvements in light availability within the culture still need to be dealt with.

4.1 Introduction

Together with light and nutrient availability temperature is one of the major abiotic factors affecting growth in microalgae (Fernandes et al. 2013; Vítová et al. 2011a; Vítová et al. 2011b). Temperature has been found to affect individual metabolic processes in various ways. Cell division and the duration of the cell cycle are particularly susceptible to changes in temperature while other parts of the cell metabolism such as growth and other related synthetic processes appear to be less influenced by such differences (Zachleder et al. 2018; Zachleder et al. 2019).

In green algae dividing by multiple fission a gradual increase of temperature results in a physiological response according to which at first cells increase their growth rate and shorten their cell cycle. Upon further

increase in temperature, an optimal point is reached at which growth rate is at its maximum and cell cycle duration is at its minimum. However, after exceeding this optimal temperature the duration of the cell cycle is gradually prolonged while growth rates remain unaffected (Vítová et al. 2011a). Eventually, after reaching a certain temperature (hereafter referred to as supraoptimal) the cell cycle is completely blocked while growth metabolism remains seemingly further unaffected (Vítová et al. 2011a; Zachleder et al. 2019). This effect of supraoptimal temperature was first observed in the 60 and 70 years of the last century during small-scale laboratory experiments conducted with *Chlorella* sp. (Semenenko et al. 1969; Semenenko et al. 1967; Šetlík et al. 1975; Zachleder et al. 2019). It was determined that the specific supraoptimal temperature that causes cell cycle arrest varies between species of microalgae and must be controlled within a very narrow range. Otherwise the cells won't achieve cell cycle arrest (temperature lower than supraoptimal) or will have their metabolism strongly affected which might lead to a cell death (temperature higher than supraoptimal) (Zachleder et al. 2019).

An inherent property of cell division is that it is an energy demanding process consuming majority of the cell energy reserves. A simple block of cell division leads to accumulation of starch and/or lipids in microalgal cultures grown in nitrogen (and other nutrient) starvation or limitation conditions (Brányiková et al. 2011; Lacour et al. 2012). A combination of cell cycle arrest and unaltered growth metabolism, as is the case of supraoptimal temperature treatment, leads to the build-up of surplus energy reserves (Šetlík et al. 1975; Zachleder et al. 2019). For starch producing green algae, the accumulation of starch under supraoptimal temperature can be extensive and it can reach levels considerably higher than those in cells cultivated under optimal growth temperature and hence it can be utilized as a method for increased starch productivity.

Chlamydomonas reinhardtii has served as a well-established model organism for a number of years (Ferrante et al. 2008; Merchant et al. 2007; Vlček et al. 2008). This green alga benefits from a wide array of readily available molecular tools for genetic engineering and strain optimisation

(Griesbeck et al. 2006; Scaife et al. 2015). However, in spite of these benefits the adoption of *C. reinhardtii* as biotechnology platform has been mostly limited. Only recently, attempts were made at increasing the starch content of *C. reinhardtii* by utilising techniques such as nutrient deprivation and temperature stress (Mathiot et al. 2019; Zachleder et al. 2019). Although nutrient deprivation is an effective technique which can increase the starch content of *C. reinhardtii* to almost 49% (w/w) the build-up is rather slow and it can take weeks until the maximum concentration is reached which slows down overall productivity (Mathiot et al. 2019). In contrast, temperature stress, and more notably supraoptimal temperature treatment, can provide a rapid method for starch accumulation within short periods of time. Such fast accumulation of starch was observed in laboratory-scale experiments where synchronized cultures of *C. reinhardtii* were cultivated both at an optimal growth temperature (30 °C) and at the supraoptimal temperature (39 °C). The results revealed that initially the cells at 30 °C accumulated starch as they grew in size. However, their starch content decreased with the onset of cell division. The cells at 39 °C grew in size similarly to those at 30 °C, but contrary to them they didn't divide. Instead, they continued to grow and after 24 hours the final total starch content of the cells at 39°C was more than twice higher than the highest reached at 30°C. Such observations indicate that supraoptimal temperature treatment of *C. reinhardtii* cultures can lead to rapid build-ups of starch (Zachleder et al. 2019). Although promising, these results were obtained only in controlled laboratory conditions which utilized synchronized cultures with relatively low biomass densities that were exposed to abundant light intensities. Hence, the applicability of the supraoptimal temperature method for industrial production of starch is still largely unknown.

In the present study we examine the potential for starch production through supraoptimal temperature in *C. reinhardtii*, a method which has already been proven to provide a rapid 2-fold increase in starch yields under laboratory conditions (Zachleder et al. 2019) and we attempt to adapt it to pilot-scale. In doing so we investigate whether and how biomass

density affects starch productivity, the possibility of culture recovery and reuse after the supraoptimal temperature treatment as well as the potential practical challenges and limitations of the method. To our knowledge the here described experiments are the first attempt to outline the deployment of supraoptimal temperature technology for the production of starch in microalgae on pilot-scale.

4.2 Materials and methods

4.2.1 Microorganism and culturing conditions

The algal strain used in experiments, the unicellular alga *Chlamydomonas reinhardtii* wild type 21gr (CC-1690) was obtained from the Chlamydomonas Resource Center at University of Minnesota (St. Paul, MN, USA). For routine subculturing, the strains were streaked onto culture plates containing standard high salt (HS) medium (Sueoka 1960) solidified by agar every three weeks.

For the purpose of the experiments a starting culture was cultivated in a bench-top flat-panel airlift photobioreactor (Algaemist, Technical Development Studio, Wageningen University, the Netherlands) in the following manner: 400 mL of liquid HS medium was inoculated directly from the culture plates and was cultivated at 30 °C and under constant incident light intensity 500 $\mu\text{mol photons m}^{-2} \text{s}^{-1}$ PhAR provided by LED lamps (BXRA W1200, Bridgelux, USA). The cultures were aerated with a mixture of air and CO₂ (2%, v/v) at a flow rate of 15 L h⁻¹ in order to provide a carbon source and mixing of the cell suspension.

4.2.2 Culture medium for the pilot-scale cultivation

All of the here described experiments were performed under photoautotrophic conditions. The culture medium used for the pilot-scale experiments was based on the HS medium, but was modified in order to facilitate high biomass yields with the NH₄Cl concentration being increased

5 fold. This resulted in a growth medium with the following final composition: 250 g/L NH_4Cl , 2 g/L $\text{CaCl}_2 \cdot 2\text{H}_2\text{O}$, 20 g/L $\text{MgSO}_4 \cdot 7\text{H}_2\text{O}$, 1.84 g/L $\text{C}_{10}\text{H}_{12}\text{FeN}_2\text{NaO}_8$, 0.05 g/L $\text{Na}_2\text{MoO}_4 \cdot 2\text{H}_2\text{O}$, 3.09 g/L H_3BO_3 , 1.18 g/L $\text{MnSO}_4 \cdot 7\text{H}_2\text{O}$, 1.40 g/L $\text{CoSO}_4 \cdot 7\text{H}_2\text{O}$, 1.24 g/L $\text{CuSO}_4 \cdot 5\text{H}_2\text{O}$, 1.43 g/L $\text{ZnSO}_4 \cdot 7\text{H}_2\text{O}$, 72 g/L KH_2PO_4 , 134 g/L K_2HPO_4 . For preparation of the medium 100x concentrated stock solutions of macroelements and microelements were used. All components excluding phosphates were diluted in distilled H_2O and autoclaved for 20 min at 121 °C. After cooling, the sterile phosphates were added. The medium used for cultivation in the pilot-scale flat-panel photobioreactor was not sterilized and tap water was used for the dilution of the stock solutions. In the course of the experiments, pH was monitored daily and was maintained at 7.0 ± 0.1 by the addition of 2M NaOH. Foam formation in the reactor vessels was controlled with the help of 10x diluted antifoam silicone Snapsil RE 20 containing 30% active compound (Product code: 84538.290, VWR International, LLC, USA).

4.2.3 Pilot-scale flat-panel photobioreactor

A flat-panel Algae-Germ photobioreactor with two cultivation vessels each with a total volume of 25 L (20 L of culture volume) (Figure 4-1) was used in all of the here described experiments. The photobioreactor was situated at 51°59'45.6"N, 5°39'25.7"E in Wageningen, the Netherlands and was placed within a green-house with the panels facing 240° SW. Each of the cultivation vessels had the following dimensions: length: 70 cm, height: 72 cm, width (optical path: 5 cm). Cooling and heating of the microalgal culture suspension was provided by two refrigerating/heating circulators (Julabo GmbH, Germany) that circulated water through temperature control coils which were submerged in the culture suspension. A simple aeration system helped with the constant introduction of a mixture of air and CO_2 (2%, v/v) and provided mixing of the culture suspension. Both cultivation vessels were constantly illuminated by a panel of luminescent lamps (Master TL-D 58W/840, PHILIPS, Netherlands) which delivered 50

$\mu\text{mol photons m}^{-2} \text{ s}^{-1}$ of PhAR (measured at the vessel surface). However, the majority of PhAR delivered to the cultures was through exposure to natural sunlight.

4.2.4 Experimental approach

All of the experiments were performed in the time-span between July 17th and September 17th 2018 (Table 4-1). Each experiment consisted of two phases. During the biomass accumulation phase one cultivation vessel was filled with 20 L of HS medium and was inoculated with 0.8 L of starting inoculum with cell concentration of approximately $3.5 \times 10^7 \text{ cells/mL}^{-1}$. The resulting culture with initial cell concentration of approximately $1.4 \times 10^6 \text{ cells/mL}^{-1}$ was then cultivated at 30 °C for 4 to 6 days. The supraoptimal temperature phase started upon reaching a biomass concentration exceeding 1.0 g L^{-1} . At this point the culture was diluted with HS medium and was separated into two cultivation vessels which were then transferred to 30 °C or 39 °C.

Table 4-1: Overview of the experiments performed including date and duration. Temperature and initial biomass concentration after the dilution of the culture from the biomass accumulation phase are shown. All experiments were performed in the summer of 2018.

Experiment date	Total duration [days]	Temperature treatment [°C]	Dry matter at the beginning of experiment [g L^{-1}]
17.07-31.07	14	39	0.2
		39	0.8
13.08-23.08	10	39	0.1
		39	0.2
23.08-03.09	11	39	0.1
		39	0.8
03.09-17.09	12	30	0.1
		39	0.1

4.2.5 Light Measurements

The photon flux density (I_{ph} , $\mu\text{mol photons m}^{-2}\text{s}^{-1}$) was measured with a LI-COR 190-SA 2π PhAR (400-700 nm) quantum sensor (LiCor, USA). Continuous light data logging was made with a sensor from the same model and manufacturer mounted outdoors and facing the sky parallel to the ground.

To obtain a measure of light energy absorbed by the cell suspension grown at different concentrations of cells the mean light intensity (I) was calculated according to the law of Lambert-Beer: $I = (I_i - I_t) / \ln(I_i / I_t)$ where I_i is the incident light intensity at the surface of the culture vessel and I_t is the transmitted light intensity measured at the rear side of the culture vessel. The mean light ($\mu\text{mol cell}^{-1}$) was calculated by dividing the mean light intensity during 24 hours (obtained by means of continuous light data logging) by the number of cells for that period.

4.2.6 Cell size and cell number measurements

1 mL culture suspension aliquots were taken, fixed with 10 μL of Lugol solution (1 g I, 5 g KI, 100 mL H_2O) and stored at 4 °C. Cell diameter was measured on microphotographs taken with an Olympus Camedia C-5050 Zoom digital camera. The microphotographs were then analyzed using ImageJ image processing and analysis software (U. S. National Institute of Health, USA). The cell diameter was re-calculated to volume by a basic formula assuming spherical cell shape. Cell number was determined by means of a Bürker counting chamber (Meopta, Czech Republic).

4.2.7 Dry matter measurements

Aliquots of 50 mL culture suspension were taken and centrifuged (1580R, Labogene Co., Ltd., South Korea) for 10 minutes at 4000 rpm. The supernatant was then removed and the remaining pellet was transferred in a 2 mL test tube that was pre-weighted and dried for 24 hours at 105 °C.

The test tube with the pellet was then placed for 24 hours at 105 °C. After cooling down for 2 hours the test tube with the pellet was weighted on an analytical scale (CP224S-OCE, Sartorius AG, Germany) and the weight of the pellet was determined by subtracting the weight of the previously measured empty test tube.

4.2.8 Starch Analysis

A starch specific enzymatic method was used to accurately estimate biomass starch content. Aliquots of 10 mL of culture suspension were harvested and centrifuged (1580R, Labogene Co., Ltd., South Korea) for 10 minutes at 4000 rpm. The supernatant was then discarded and the resulting pellets were stored at -20 °C. After thawing, the cells in the pellets were disintegrated by adding 300 µL of glass beads (0.7 mm in diameter) and vigorously vortexing (MS3, IKA - Werke GmbH & Co. KG, Germany) for 15 min. Depigmentation of the samples was done by adding 1 mL of 80% (v/v) ethanol to the pellet and incubation in a water bath for 15 min at 68 °C after which the samples were centrifuged (1580R, Labogene Co., Ltd., South Korea) for 2 min at 14 000 rpm and the supernatant was removed. The depigmentation procedure was repeated 3 to 4 times (or until the pellet was completely discolored). After that 1 mL of α -amylase from porcine pancreas (Sigma-Aldrich, USA) solution (0.5 g·L⁻¹ w/v in 0.1 M sodium phosphate buffer (pH 6.9) were added to the samples and were incubated for 1 hour at 37°C. The samples were centrifuged (1580R, Labogene Co., Ltd., South Korea) for 2 min at 14 000 rpm after which the supernatant was used for the quantification of reducing sugars through the DNSA color reaction as described in (Miller 1959). In short, 500 µL of supernatant were mixed with 500 µL dinitrosalicylic acid (DNSA) solution (1% (w/v) DNSA, 30% (w/v) potassium sodium tartrate tetrahydrate, 20% (v/v) 2M sodium hydroxide) and incubated for 5 minutes at 105 °C on a heat block. Following a cooling down period of 10 minutes at room temperature the mixture was diluted five-fold with distilled water after which the absorbance of the samples was measured at 570 nm. The

concentration of starch was estimated through a calibration curve of potato starch (Lach-Ner, Czech Republic) digested with α -amylase.

4.2.9 Microscopic observations and starch staining

Microscopic observations during the course of the experiments were done daily on a Leica Laborlux S microscope. Staining of starch was done using the same iodine solution that was used for the fixation of the cell counting samples in a 1:10 ratio of staining solution volume to sample volume.

4.3 Results

As previously shown, starch accumulation in *C. reinhardtii* can be induced by nutrient depletion (Ball et al. 1990; Mathiot et al. 2019). In order to exclude this possibility we included a biomass accumulation phase at optimal temperature prior to the supraoptimal temperature phase. The purpose of the biomass accumulation phase was to demonstrate that the cultures were not limited by nutrients and to estimate the typical starch content in *C. reinhardtii* cultures during the exponential growth phase under optimal growth temperature. The reader is advised to refer to Table 4-1 for an overview of the time span of the experiments as well as combinations of biomass densities and temperature treatments applied.

4.3.1 The effects of supraoptimal temperature

To assess the effects of supraoptimal temperature on cell growth and division as well as starch accumulation we used a comparison of parallel treatments of 30 °C (control) and 39 °C. At first a *C. reinhardtii* culture was cultivated at 30 °C for 6 days. After reaching a biomass concentration of 1.0 g L⁻¹ the culture was diluted with HS medium to 0.1 g L⁻¹ and split into two cultures which were then cultivated at 30 °C and 39 °C respectively (Figure 4-1).

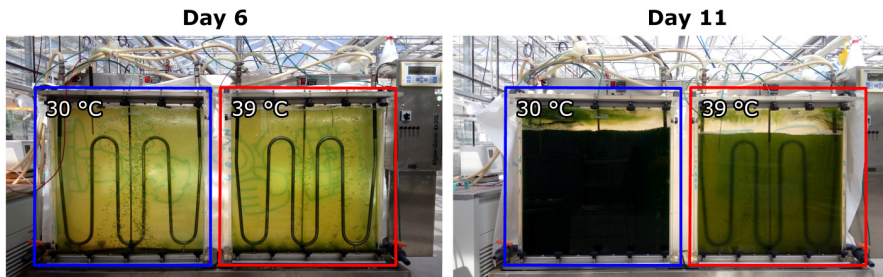


Figure 4-1: Changes of optical densities of *C. reinhardtii* cultures starting at the same optical density (day 6, left photobioreactors) and grown at the same light intensity (left photobioreactors) grown for 5 days at temperature 30 °C and 39 °C (day 11, right photobioreactors). For description of the photobioreactors see materials and Methods 4.2.3.

The control culture cultivated at 30 °C had a similar biomass accumulation pattern to the one before the dilution and returned to the pre-dilution biomass concentration within 6 days (reaching a maximum of nearly 1 g L⁻¹) (Figure 4-2A). In contrast, the biomass accumulation of the culture at 39 °C stopped after 2 days and reached a maximum of only 0.4 g L⁻¹. Starch accumulation in terms of percentage of dry matter (DM) was much more prominent in the culture cultivated at 39 °C reaching 18% of DM as opposed to 8% of DM at 30 °C (Figure 4-2C). In terms of starch in mg mL⁻¹ starch accumulation was faster in the supraoptimal temperature culture reaching a maximum of 0.07 g L⁻¹ in only two days as opposed to 5 days and 0.06 g L⁻¹ in the culture cultivated at 30 °C (Figure 4-2D).

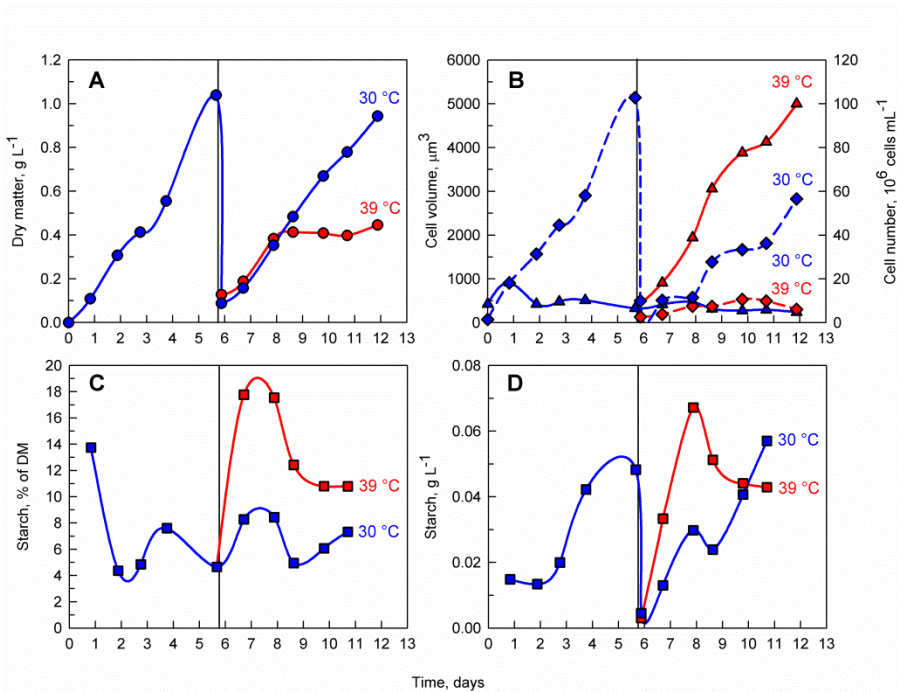


Figure 4-2: Effect of supraoptimal temperature on dry matter accumulation (A), average cell volume (solid line, triangles) and cell number (dashed line, diamonds) (B), % of starch in the microalgal biomass (C) and starch concentration in the culture (D). The straight vertical line at day 6 represents the shift from biomass accumulation phase to supraoptimal temperature phase. Blue lines represent cultivation at 30 °C while red lines represent cultivation at 39 °C. During the biomass accumulation phase a single *C. reinhardtii* culture was cultivated at 30 °C. After 6 days the culture was diluted to a biomass concentration of 0.1 g L^{-1} and divided into two separated cultures. One of the cultures was cultivated at 39 °C (supraoptimal temperature treatment) while the other one was cultivated at 30 °C (control). Panel B represents cell volume as the median cell volume of the cells while cell number is represented as an estimation of the mean amount of cells within a defined volume of culture suspension.

Microscopic observations of the culture cultivated at 30 °C did not reveal any change in the cell division pattern with cells having a median cell volume of $422 \mu\text{m}^3$ and cell division occurring as expected during the course of the experiment with mother cells dividing predominantly into 8 daughter cells (Figure 4-2B and Figure 4-3). In contrast, the cells

transferred to 39 °C largely stopped dividing and the few dividing cells formed mostly 2 or 4 daughter cells. The inhibition of cell division was also reflected in the median cell volume which increased eight fold at 39 °C reaching 3479 μm^3 .

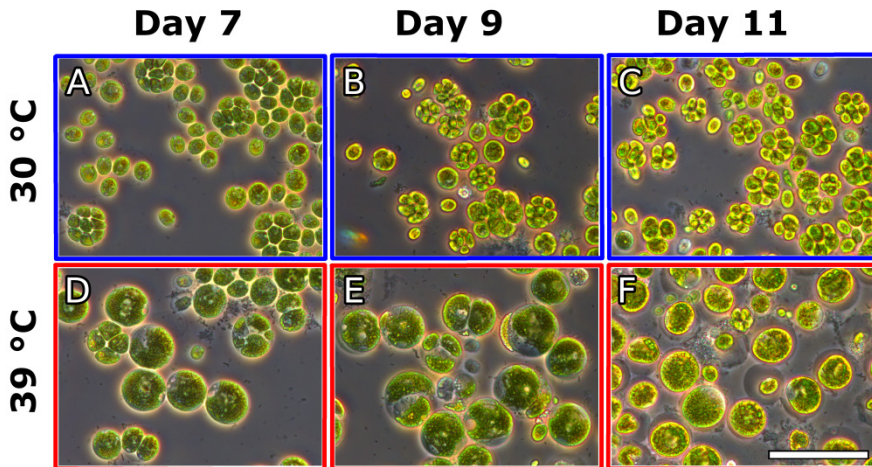


Figure 4-3: Effect of supraoptimal temperature on the cell division pattern and cell size in *C. reinhardtii*. The algal culture was cultivated for 6 days at 30 °C after which it was split, transferred to 30 °C (A-C) and 39 °C (D-F) and monitored for another 5 days. Day 7 corresponds to the first day after the split. Size of bar: 50 μm .

4.3.2 Optimal biomass density for a supraoptimal temperature treatment

Light availability within the culture suspension itself is regarded as a function of biomass density. To study the effect of light availability on starch accumulation under supraoptimal temperature two parallel cultures of different biomass concentrations were compared. In doing so a *C. reinhardtii* culture was cultivated at 30 °C for 6 days. After reaching a biomass concentration of 1.5 g L^{-1} the culture was diluted with complete HS medium to avoid nutrient limitation and split into two cultures with initial biomass concentration of 0.2 g L^{-1} and 0.8 g L^{-1} respectively (Figure 4-4A). Immediately after the dilution both cultures were transferred to 39 °C. Within the first three days of the transfer both cultures increased in biomass and reached a maximum of 0.6 g L^{-1} and 1.0 g L^{-1} respectively.

After this the biomass concentration in the less dense culture remained constant while the biomass in the denser culture started to decline rapidly. The difference in biomass concentration was also reflected in the mean light availability in the cultures, with the cells in the less dense culture being exposed to notably more light than the ones in the denser culture (Figure 4-4B). The relative starch accumulation was remarkably fast and much more prominent in the less dense culture reaching a maximum of 13.2 % of DM within the first day of the transfer to 39 °C (Figure 4-4C). This rapid 3-fold increase from the initial culture represents a striking contrast to the starch values within the denser culture which did not experience any noteworthy rise when compared to the pre-treatment phase. When accounted for the differences in biomass concentrations in both cultures, the absolute starch concentration in the culture cultivated at 39 °C was about 20% higher than the one cultivated at 30 °C. However, the maximum starch concentration reached 39 °C was still similar to the one reached during the biomass accumulation phase (Figure 4-4D).

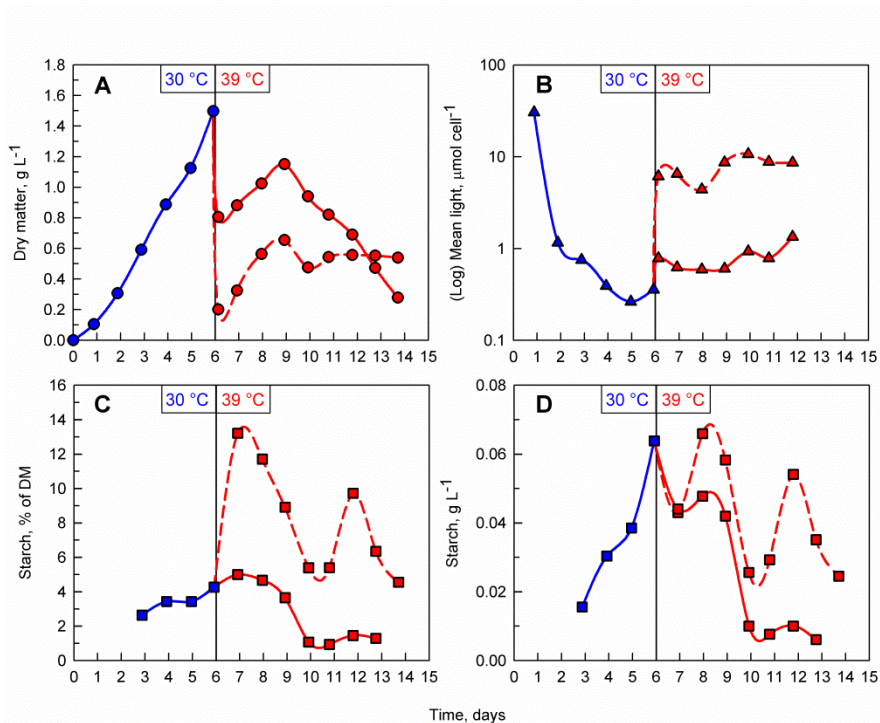


Figure 4-4: Effect of different biomass concentrations at supraoptimal temperature on the course of dry matter (A), mean light availability (B), % of starch in the biomass (C), and starch concentration (D) in the culture. The vertical line at day 6 represents the shift between biomass accumulation phase and supraoptimal temperature phase. Blue lines and markers indicate cultivation at 30 °C and red lines and markers indicate cultivation at 39 °C. During the biomass accumulation phase a single *C. reinhardtii* culture was cultivated at 30 °C. After 6 days the culture was split into two, transferred to 39 °C and was diluted to 0.2 g L⁻¹ (dashed red line) and 0.8 g L⁻¹ (solid red line) respectively.

4.3.3 Transfer back to optimal temperature

As previously demonstrated the supraoptimal temperature treatment allows fast accumulation of starch during which the maximum relative content is reached rapidly within 1 to 2 days. However, due to the nature of the temperature block of cell division, a biomass accumulation phase is required before the treatment can be applied. Thus a possible starch production process on industrial scale will involve a fed-batch culture

which is treated with consecutive alterations of temperature between 30 and 39°C. To investigate whether the cells are viable and their cell cycle block can recover after the supraoptimal temperature phase, we cultivated the *C. reinhardtii* culture at 30 °C for 4 days. After reaching a biomass concentration of 1.2 g L⁻¹ the culture was diluted with fresh HS medium and split into two cultures with initial biomass concentration of 0.1 g L⁻¹ and 0.8 g L⁻¹ respectively (Figure 4-5A). Immediately after the dilution, both cultures were transferred to 39 °C for a period of three days. During the transfer to supraoptimal temperature biomass accumulation in both cultures decreased with the decrease being much more pronounced in the 0.8 g L⁻¹ culture. When the culture was moved back to 30 °C biomass accumulation resumed in the 0.1 g L⁻¹ culture while in the 0.8 g L⁻¹ culture biomass concentrations declined gradually. The difference in initial biomass concentration after the dilution was also reflected in the mean light availability in the cultures, with the cells in the less dense culture being exposed to notably more light than the ones in the dense culture (Figure 4-5B). Starch synthesis was much more pronounced in the 0.1 g L⁻¹ culture with relative starch content increasing 4-fold and reaching nearly 20% of DM within the first day of transfer to supraoptimal temperature (compared to only 8% of DM in the 0.8 g L⁻¹ culture)(Figure 4-5C). Although starch concentrations in terms of % of DM were higher in the 0.1 g L⁻¹ culture when compared the starch concentration in both cultures was nearly identical resulting again by the difference in biomass concentration within the two cultures (Figure 4-5D).

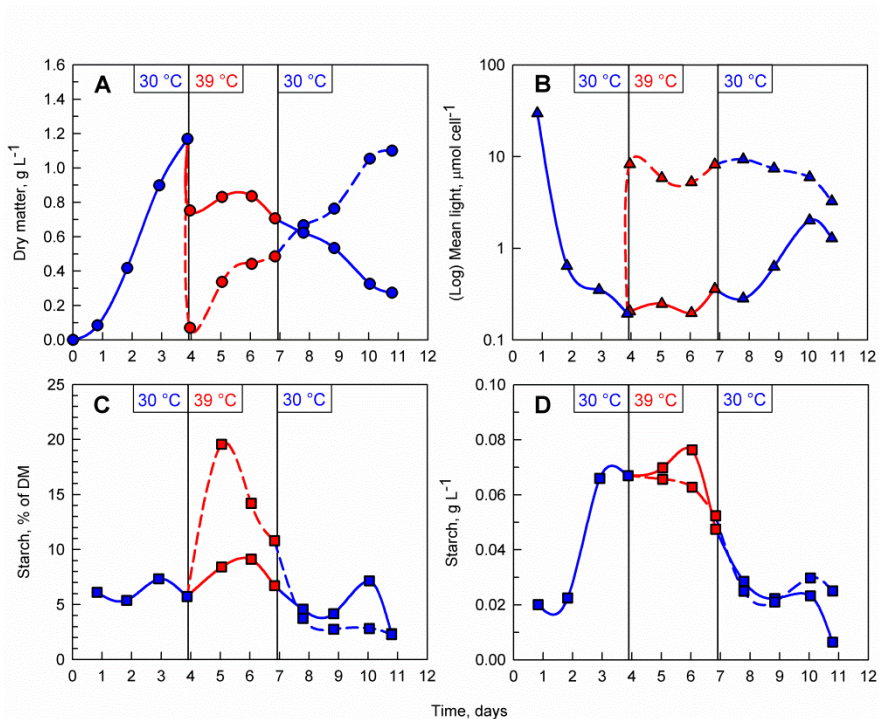


Figure 4-5: Effect of the combination of temperature shifts and different biomass concentrations on the course of dry matter (A), mean light availability (B), % of starch in the biomass (C), and starch concentration in the culture (D). A single *C. reinhardtii* culture was cultivated at 30 °C. After 4 days the culture was split into two, transferred to 39 °C and diluted to 0.1 mg mL⁻¹ (dashed red lines) and 0.8 mg mL⁻¹ (solid red lines) respectively. On day 7 the 0.1 mg mL⁻¹ culture (dashed blue lines) and the 0.8 mg mL⁻¹ culture (solid blue line) were transferred back to 30 °C. Vertical lines at days 4 and 7 indicate those shifts in temperature (from 30 °C to 39 °C at day 4 and back from 39 °C to 30 °C at day 7).

Microscopic observations and analysis of the cell cycle revealed that *C. reinhardtii* cells were dividing as expected during the biomass accumulation phase at 30 °C (Figure 4-6A) and transfer to supraoptimal temperature resulted in block of cell division (Figure 4-6B, C, E, F). The cells in the 0.1 g L⁻¹ culture were larger and rounder as opposed to the cells in the 0.8 g L⁻¹ culture which were smaller (Figure 4-6B and E). Staining with iodine revealed the presence of large amounts of starch granules in the chloroplasts of the cells in both cultures 1 day after the transfer (Figure 4-

6C and F). Upon transfer back to 30 °C the cell cycle progression was restored in the 0.1 g L⁻¹ culture within 1 day (Figure 4-6D) as opposed to the cells in the 0.8 g L⁻¹ which did not recover (Figure 4-6G).

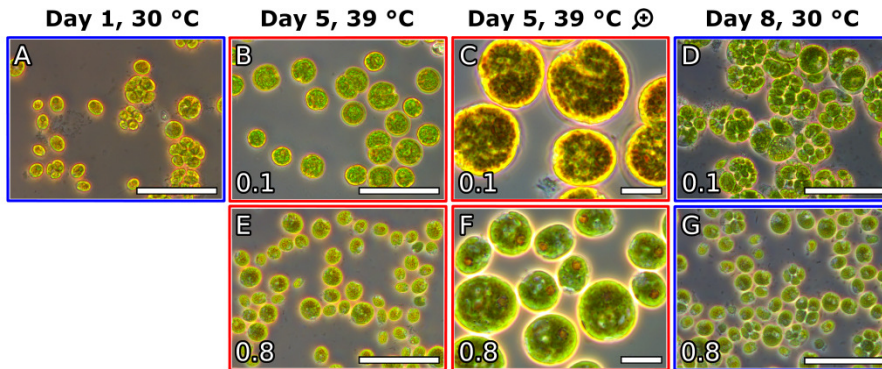


Figure 4-6: Microscopic observations. A: Cells during day one of the biomass accumulation phase at 30 °C. B and E: Cells one day after transfer to 39 °C and dilution to 0.1 g L⁻¹ and 0.8 g L⁻¹ respectively. C and F: magnification and iodine staining of starch granules in the cells from panels B and E respectively. D and G: one day after transfer back to 30 °C of the cells in the 0.1 g L⁻¹ and 0.8 g L⁻¹ culture. Size of bar on panels A, B, D, E, G: 50 μm, panels C and F: 10 μm.

4.4 Discussion

4.4.1 The effects of supraoptimal temperature on starch accumulation in *C. reinhardtii* at the pilot-scale

The transfer of the cultures from optimal to supraoptimal temperature proved to have a notable effect on both the cell cycle progression and the accumulation of energy reserves in the form of starch within the cells of *C. reinhardtii*. Cell division was inhibited and the relative starch accumulation was enhanced more than 2-fold (Figures 4-2C, 4-4C and 4-5C, and Table 4-2). As a result of the lack of cell division and the increased internal starch storage the mean cell volume was also larger in the cells cultivated at the supraoptimal temperature when compared to those in the control at 30 °C. These observations are in agreement with results from supraoptimal

temperature experiments conducted with synchronized cultures of *C. reinhardtii* in laboratory-scale (Zachleder et al. 2019) and resemble the effect of supraoptimal temperature on *Chlorella* sp. (Semenenko et al. 1967).

The increase in starch as energy storage molecule during a period of inhibited cell division supports the inverse relationship between chemical energy storage and energy expenditure which is needed for the normal operation of the cell cycle at optimal growth conditions. Increased starch accumulation in green algae is generally linked to a block of the cell cycle and was observed not only as an effect of supraoptimal temperature treatment but also as a response to other types of stress such as nutrient deprivation (Fernandes et al. 2013; Mathiot et al. 2019; Siaut et al. 2011).

Starch synthesis as response to nitrogen depletion in laboratory-scale experiments with *C. reinhardtii* cultures has been reported to increase starch content to up to $70 \mu\text{g } 10^{-6}$ cells (i.e. 70 pg/cell). However, this type of treatment required 7 days of nitrogen starvation until the maximum starch content was reached (Siaut et al. 2011). In another set of laboratory-scale experiments this time using sulphur depletion as inducer of starch accumulation starch levels reached up to 49% of DM after 20 days (Mathiot et al. 2019). Such results, however, are produced in stable laboratory conditions and their direct extrapolation to industrial-scale yields is often unrealistic. This is mainly due to the associated unstable production and environmental conditions which are difficult to control during a large-scale cultivations and result in decreased productivity. When compared the figures from laboratory experiments, our pilot-scale cultivation of *C. reinhardtii* achieved more modest starch figures of 21% of DM or 16 pg/cell but these were achieved in significantly shorter time periods (only 1 to 2 days). Such a significant decrease in cultivation time might prove of notable importance for the economic viability of industrial scale production of microalgae based starch.

4.4.2 The importance of light availability

A modern biotechnological process requires high productivity and cost efficiency. This can only be achieved through rapid accumulation times and high concentrations of the desired product. In order for microalgal starch production to be economically viable starch yields per volume of culture have to be high. This is only possible through increased starch content per cell at high biomass concentrations. Our experiments indicated that in the case of cultivation in flat-panel photobioreactors an increase in biomass density led to a decrease in mean light availability within the culture (Figures 4-4B and 4-5B). This led to reduction in the starch content and ultimately limited the effectiveness of the supraoptimal temperature treatment (Table 4-2). As a result, although the supraoptimal treatment led to a faster accumulation times, the maximum starch concentration reached during the cultivations at 39 °C did not show any notable increase over the maximum starch concentrations reached at 30 °C.

Furthermore, in our cultivation systems, the combination of high cell density (leading to low light availability) and supraoptimal temperature seems to have a negative effect on *C. reinhardtii* cultures after a certain time period. In both cultivations at starting biomass density of 0.8 mg mL⁻¹ biomass decline was observed after 3 days of exposure to supraoptimal temperature and the cultures did not recover when transferred back to optimal growth temperature. Not only that, but light penetration in the high biomass cultures was further hindered by excessive biofilm formation (Appendix, Figure 4-8).

When synthesis of a substance such as starch is linked to the photosynthetic capacity of the cell and consequently to light availability, the production on a large-scale makes an efficient utilization of light necessary. In this regard, an effective reactor design that ensures proper light distribution within a high biomass density culture is essential. Tubular photo-bioreactors are one such option. They have been shown to offer enhanced light distribution within the culture suspension and *C. reinhardtii* has been successfully cultivated in them to relatively high biomass

densities combined with enhanced starch productivity (Mathiot et al. 2019).

Table 4-2: Comparison of the effect of supraoptimal temperature in combination with various initial biomass concentrations on the maximum relative starch content in dry algal biomass and the time when the maximum starch concentration was attained.

Initial DW [g L ⁻¹]	Temperature [°C]	Max. starch content [% of DM]	Max. starch concentration [g L ⁻¹]	Max. starch concentration accumulation time [days]
0.1	39	21 [*]	0.067 [*]	1.3 [*]
0.2	39	14 ^{**}	0.069 ^{**}	2 ^{**}
0.8	39	7 ^{**}	0.060 ^{**}	2 ^{**}
0.1	30	8	0.057	5

^{*} Shown value is an average of three cultivations

^{**} Shown value is an average of two cultivations

4.4.3 Perspectives

As indicated by the results starch accumulation under supraoptimal temperature is rather fast (Table 4-2) and in our opinion this provides the method with a major advantage over other starch induction strategies such as nutrient depletion. In the context of large scale cultivation of microalgae fast turnaround times are important not only because they allow for higher productivity, but also because they reduce the risk of biological contaminants such as competitive microalgal species or grazers. This makes the supraoptimal temperature method a viable option for increasing starch productivity in microalgae.

Based on recent results it can be assumed that a tentative industrial scale production of starch based on the here outlined supraoptimal temperature method can employ both batch and semi-batch mode of operation. This is made possible by the fact that the culture can be recovered and reused as inoculum after the temperature treatment

(Figures 4-5A and 4-6). The production flow can consist of alternating biomass accumulation (6-7 days) and temperature treatment (1-2 days) phases. Moreover, large and heavy cells that are filled with starch should enable better downstream processing of the biomass. However the economic viability of the process depends highly on improving bioreactor the design and reducing the associated energy and labour costs. Provided that these hurdles have been overcome and assuming year round cultivation, a culture volume of 50 L, biomass concentration of 2 g L⁻¹ and a relative starch content of 50 % of DM in such manner starch productivity per m² can reach up to 2.4 kg of starch per annum.

4.5 Conclusions

The method of supraoptimal temperature treatment was successfully applied in pilot-scale and resulted in a considerable, near 3-fold, enhancement of starch content in *C. reinhardtii* at low biomass densities. Moreover, starch synthesis was faster with the maximum being reached within only 1-2 days when compared to 5 days at optimal temperature. The supraoptimal temperature treatment provides a viable alternative to other starch inducing methods such as nutrient depletion. This is especially true when times required for starch accumulation are taken under account. However, technical challenges such as bioreactor design and improved light availability per cell still need to be dealt with.

4.6 References

- Ball SG, Dirick L, Decq A, Martiat JC, Matagne RF (1990) Physiology of starch storage in the monocellular alga *Chlamydomonas reinhardtii*. *Science* 66:1-9
- Brányiková I, Maršálková B, Doucha J, Brányik T, Bišová K, Zachleder V, Vítová M (2011) Microalgae-novel highly efficient starch producers. *Biotechnol Bioeng* 108:766-776
- Fernandes B, Teixeira J, Dragone G, Vicente AA, Kawano S, Bišová K, Příbyl P, Zachleder V, Vítová M (2013) Relationship between starch and lipid accumulation induced by nutrient depletion and

- replenishment in the microalga *Parachlorella kessleri*. *Bioresour Technol* 144:268-274
- Ferrante P, Catalanotti C, Bonente G, Giuliano G (2008) An Optimized, Chemically Regulated Gene Expression System for *Chlamydomonas*. *PLoS ONE* 3:e3200
- Griesbeck C, Kobl I, Heitzer M. (2006) *Chlamydomonas reinhardtii*: a protein expression system for pharmaceutical and biotechnological proteins. *Mol Biotechnol* 34:213-223
- Lacour T, Sciandra A, Talec A, Mayzaud P, Bernard O (2012) Neutral lipid and carbohydrate productivities as a response to nitrogen status in *Isochrysis* sp. (T-iso; Haptophyceae): starvation vs. limitation. *J Phycol* 48(3):647-656
- Mathiot C, Ponge P, Gallard B, Sassi J, Delrue F, Le Moigne N (2019) Microalgae starch-based bioplastics: Screening of ten strains and plasticization of unfractionated microalgae by extrusion. *Carbohydr Polymer* 208:142-151
- Merchant SS, Prochnik SE, Vallon O, Harris EH, Karpowicz SJ, Witman GB, Terry A, Salamov A, Fritz-Laylin LK, Marechal-Drouard L, et al. (2007) The *Chlamydomonas* genome reveals the evolution of key animal and plant functions. *Science* 318:245-250
- Miller GL (1959) Use of dinitrosalicylic acid reagent for determination of reducing sugar. *Analyt Chem* 31:426-428
- Scaife MA, Nguyen G, Rico J, Lambert D, Helliwell KE, Smith AG (2015) Establishing *Chlamydomonas reinhardtii* as an industrial biotechnology host. *Plant J* 82:532–546
- Semenenko VE, Vladimirova MG, Opleanskaja OB, Raikov NI, Kovanova ES (1969) K fiziologiceskoj karakteristike *Chlorella* sp. K pri vysokych extremalnych temperaturach. II. Izmenenie biosinteza, ultrastruktury i aktivnosti fotosynteticeskogo aparata Chlorelly pri razobscenii kletocnych funkcij extremalnoj temperatury. *Fiziol Rast* 16:210-220
- Semenenko VE, Vladimirova MG, Orleanskaja OB (1967) K fiziologiceskoj karakteristike *Chlorella* sp. K pri vysokych temperaturach. I. Razobscajuscie dejstvee extremalnoj temperatury kletocnye funkcii Chlorelly. *Fiziol Rast* 14:612-625
- Šetlík I, Zachleder V, Doucha J, Berková E, Bartoš J (1975) The nature of temperature block in the sequence of reproductive processes in *Chlorella vulgaris* BEIJERINCK. *Archives of Hydrobiology /Suppl* 49 *Algological Studies* 14:70-104.
- Siaut M, Cuine S, Cagnon C, Fessler B, Nguyen M, Carrier P, Beyly A, Beisson F, Triantaphylides C, Li-Beisson Y, et al. (2011). Oil accumulation in the model green alga *Chlamydomonas reinhardtii*:

- characterization, variability between common laboratory strains and relationship with starch reserves. *BMC Biotechnol* 11:7
- Sueoka N (1960) Mitotic replication of deoxyribonucleic acid in *Chlamydomonas reinhardtii*. *Proc Natl Acad Sci U S A* 46:83-91
- Vítová M, Bišová K, Hlavová M, Kawano S, Zachleder V, Čížková M (2011a) *Chlamydomonas reinhardtii*: duration of its cell cycle and phases at growth rates affected by temperature. *Planta* 234:599-608
- Vítová M, Bišová K, Umysová D, Hlavová M, Kawano S, Zachleder V, Čížková M (2011b) *Chlamydomonas reinhardtii*: duration of its cell cycle and phases at growth rates affected by light intensity. *Planta* 233:75-86
- Vlček D, Ševčovičová A, Sviežená B, Gálová E, Miadoková E (2008) *Chlamydomonas reinhardtii*: a convenient model system for the study of DNA repair in photoautotrophic eukaryotes. *Curr Genet* 53:1-22
- Zachleder V, Ivanov IN, Vitova M, Bisova K (2018) Effects of cyclin-dependent kinase activity on the coordination of growth and the cell cycle in green algae at different temperatures. *J Exp Bot* 70(3):845-858
- Zachleder V, Ivanov IN, Vitova M, Bisova K (2019) Cell Cycle Arrest by Supraoptimal Temperature in the Alga *Chlamydomonas reinhardtii*. *Cells* 8:18

Appendix

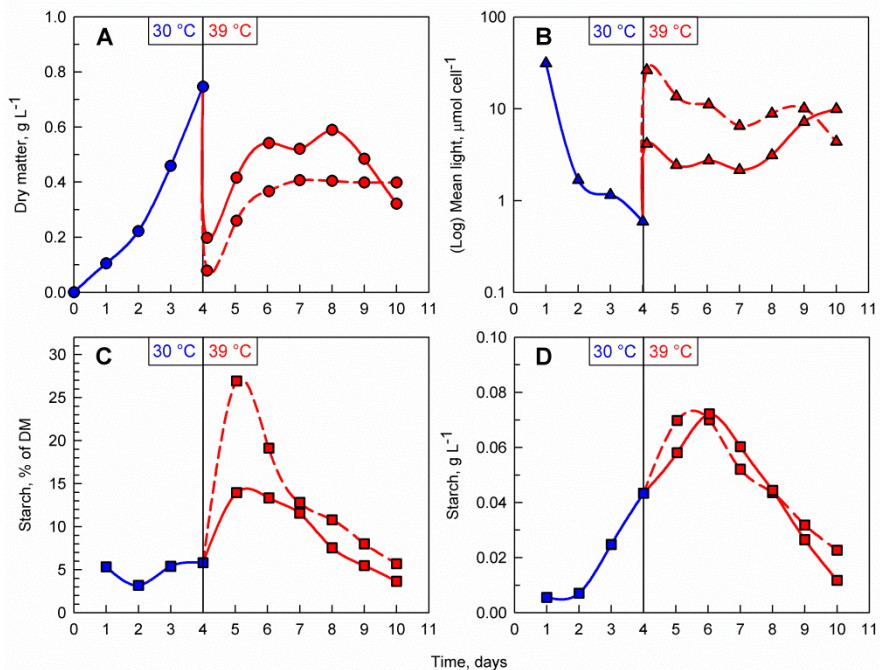


Figure 4-7.: Effect of the combination of supraoptimal temperature and different biomass concentrations (A) on % of starch in the microalgal biomass (B), mean light availability (C) and starch concentration in the culture (D).

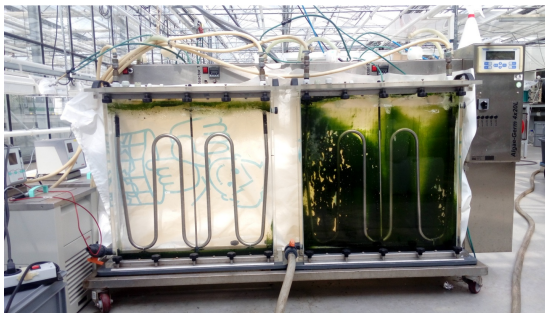


Figure 4-8: Cultivation vessels where *C. reinhardtii* cultures treated with supraoptimal temperature and with different starting densities have been cultured. The photograph was taken moments after the culture suspension from both panels was discarded. Left panel: culture with starting biomass density of 0.1 g L⁻¹. Right panel: excessive bio film formation on the back wall where culture with starting biomass 0.8 g L⁻¹ was cultivated.

Chapter VII

Comparing biochemical and Raman microscopy analyzes of starch, lipids, polyphosphate, and guanine pools during the cell cycle of *Desmodesmus quadricauda*

Šárka Moudříková, Ivan N. Ivanov, Ladislav Nedbal, Vilém Zachleder,
Kateřina Bišová, Peter Mojzeš



Abstract

Photosynthetic energy conversion and the resulting photoautotrophic growth of green algae can only occur in daylight, but DNA replication, nuclear and cellular divisions occur often during night. In such a light/dark regime the algal culture becomes synchronized. In this study, synchronized cultures of a green alga *Desmodesmus quadricauda* were studied for the dynamics of starch, lipid, polyphosphates, and guanine pools during the cell cycle by two independent methodologies: by the conventional biochemical analyzes of cell suspension and by Raman microscopy of single algal cells. Raman microscopy reports not only on the mean concentrations but also on the distribution of pools within cells. Raman microscopy was more sensitive in detecting lipids than the biochemical analysis; both of the methods, as well as the conventional fluorescence microscopy, were comparable in detecting polyphosphates. Discrepancies in detection of starch by Raman microscopy are discussed. The power of Raman microscopy was proved particularly strong in detection of guanine, which was traceable by its unique vibrational signature. Guanine microcrystals occurred specifically at around the time of DNA replication and prior to nuclear division. Interestingly, guanine crystals co-localized with polyphosphates in the vicinity of nuclei around the time of nuclear division.

5.1 Introduction

Green algae dividing by multiple fission such as *Chlorella sp.*, *Chlamydomonas sp.* and chlorococcal alga *Desmodesmus quadricauda* chosen here as the model experimental organism grow very fast and multiply their cells rapidly making them ideal model organisms for algal biotechnology as well as cell biology (Zachleder et al. 2016). During the day time, their cells grow fast without interruption from cell division, which occurs at night. This feature leads to natural synchronization of such algae by diurnally alternating day light. The same light/dark regime can be used in laboratory, yielding highly synchronized cultures composed of uniformly

aged and sized cells at the same life and cell cycle phase. The culture synchronization allows studying suspensions of algal cells that are all in well-defined phase of their life and cell cycles.

The cell cycle, i. e. period between two cell divisions, consist of two parts: growth and reproductive sequence. Each reproductive sequence is composed of DNA replication, nuclear division and cell division. Cells of most organisms divide into two daughter cells and their cell cycle consist of a single growth and reproductive sequence. The cell cycle of *D. quadricauda*, and of some other chlorococcal and volvocal algae, may consist of one or several pairs of growth and reproductive sequences, thus leading to so called multiple fission. Depending on the number of growth and reproductive sequences, single mother cell of *D. quadricauda* can produce two, four or eight daughter cells. The daughter cells originating from one mother cells remain connected by a shared cell wall in a structure called coenobium. The obligate coenobial growth of this species provides convenient means of monitoring, by simple counting cells in particular coenobia, its twofold, fourfold or higher multiple fission pattern. Furthermore, the coenobia of *D. quadricauda* are particularly suitable for long-term microscopic studies, including Raman microscopy, since they can be easily immobilized between the microscope slide and the coverslip with their two largest dimensions parallel to the slide surface, and, consequently, cellular structures of all cells of each coenobium can be found in the same focal plane.

In green algae dividing by multiple fission, the photosynthetic assimilation of carbon dioxide supports growth of most of cell structures during the light phase as well as accumulation of energy and other reserves that are required for and spent or distributed by the cell division in the dark phase. Thus, increasing cell volume, accumulation of bulk RNA and protein content or increasing energy and carbon stores can all serve to quantify growth. In multiple fission, the cell growth is composed of several growth sequences. Each of them is completed by reaching a critical size, in which the cells reach approximately double of their original mass, and double their original RNA, protein, starch and lipid contents. Upon this, the

cells enter into reproductive sequence by attaining commitment point (Šetlík and Zachleder 1984; Zachleder and van den Ende 1992) thus connecting the completion of growth sequence to reproductive one (Donnan and John 1983). Once committed, the reproductive sequence can be completed in darkness without external energy and carbon supply. At the same time, the cells can, depending on growth conditions, enter another growth sequence that would once completed allow for another reproductive sequence to occur before new coenobium is formed. In this way, individual growth sequences consecutively follow each other whilst reproductive sequences run concurrently and overlap within one cell cycle. Under the favorable conditions, the cells of *D. quadricauda* can consecutively replicate DNA in as many as three separate rounds and divide nuclei, becoming bi-, tetra- and octonuclear (Figure 5-1) (Šetlík et al. 1972; Zachleder et al. 1975; Šetlík and Zachleder 1984; Zachleder et al. 2002; Vítová and Zachleder 2005). The number of reproductive sequence/s as well as the extent of their overlap within a single cell cycle, is determined by growth rate, which is governed by environmental conditions so that at higher growth rates more reproductive sequences are started (Šetlík et al. 1972; Šetlík and Zachleder 1984; Zachleder and Šetlík 1988; Zachleder and Šetlík 1990; Zachleder and van den Ende 1992; Tukaj, et al. 1996; Zachleder 1997).

To better understand the dependence of the reproductive sequence entry in the commitment point and its progression on the reserves of energy, carbon and other major biogenic elements and essential biomolecules, it is necessary to quantify those reserves in different cell cycle phases, preferably in their mutual relationship, spatial context and temporal evolution. At the macroscopic level of the cell culture suspension, conventional analytical methods to study the algal biomass can be used (Zachleder and Šetlík 1988; Zachleder et al. 2016). To analyze spatial and temporal distribution of different macromolecules at the level of individual cells, the biomolecules can be stained or fluorescently labeled and visualized by means of optical and fluorescence microscopy (Vítová et al. 2005; Terashima et al. 2014; Xie et al. 2014). However, when applying

standard approaches, each biomolecular compound is usually labeled and monitored individually. Consequently, the information about spatial and temporal relationships between the different substances at the level of individual cells is averaged and lost.

Raman microscopy is a label-free method that combines the advantages of molecular specificity of Raman spectroscopy with a high spatial resolution of optical confocal microscopy (Dieing et al. 2011). Raman microscopy has been widely used in biology in the recent years (Butler et al. 2016), because it is relatively simple to use, with no need to introduce artificial staining or labelling to the sample, and it is able to detect several chemical components of the sample simultaneously, largely non-destructively and with a sub-cellular resolution. In microalgae, an extensive use of Raman microscopy have been long hampered by a strong autofluorescence of their photosynthetic apparatus that reaches intensities by several orders of magnitude higher than the wanted Raman signal. This narrowed the applicability of Raman microscopy for studies of carotenoids that exhibit resonantly enhanced Raman signal (Jehlicka et al. 2014; Koch et al. 2017; Li et al. 2017), or to algal cells with high content of neutral lipids (Samek et al. 2010; Wu et al. 2011; Meksiarun et al. 2015).

To observe conventional Stokes Raman signal of other biomolecules, such as starch, proteins and polyphosphates (polyP), a high power in-focus photobleaching has been commonly used to remove the fluorescence background (Huang et al. 2010; Chiu et al. 2017). However, in-focus photobleaching strongly slows down the acquisition of Raman maps and often results in thermal decomposition and burning of the inspected cells. We have recently demonstrated that a wide-area, low-intensity photobleaching of a whole algal cell (or even multiple cells at once) by a defocused laser beam shortens the time needed for photobleaching to several seconds per cell, and enables one to reliably observe and identify starch, lipid and polyP granules within individual microalgal cells with a sub-cellular spatial resolution (Moudříková et al. 2016). The analytical strength of Raman microscopy has been further demonstrated by

identifying hitherto unknown guanine microcrystals in two species of microalgae (Moudříková et al. 2017).

In the present paper, we analyzed the dynamics of starch, lipid, polyP and guanine pools during the cell cycle of *D. quadricauda* simultaneously by biochemical analyses of the synchronized algal suspension, and by conventional fluorescent microscopy and Raman microspectroscopy of individual algal cells from synchronized algal culture. The power of Raman imaging was demonstrated by identifying guanine microcrystals occurring close to dividing nuclei of *D. quadricauda* cells in synchrony to polyP grains.

5.2 Materials and methods

5.2.1 Experimental organism

The chlorococcal alga *Desmodesmus quadricauda* was obtained from the Culture Collection of Autotrophic Organisms, Institute of Botany (CCALA, Czech Academy of Sciences, Třeboň, Czech Republic). The culture collection also describes the earlier taxonomic classification as *Scenedesmus quadricauda* (Turpin) Brébisson, (strain Greifswald 15), under which the organism was identified in numerous publications. The genus *Desmodesmus* (*Chlorophyta*, *Chlorococcales*, *Scenedesmus*) was later separated from genus *Scenedesmus* (An et al. 1999). A phylogenetic analysis based on plastid genomics has further distinguished *D. quadricauda* from the closely related *Desmodesmus communis* (Buchheim et al. 2012).

5.2.2 Algae cultivation and synchronization of cultures

To prepare synchronized cultures, the microalgae were inoculated either from agar plate or from a liquid culture and cultivated in a glass tube (3 cm diameter) placed in a temperature-controlled water bath at 30 °C (30–32 °C for Raman experiments). Cultivation medium according to Zachleder and Šetlík (Zachleder and Šetlík 1982) was used; this medium is

based on algal composition and provides nutrients for up to 6 g dry matter (DM) of algae per liter. The culture was aerated with air enriched to 2 % CO₂ (flow rate 350 mL·min⁻¹). The glass tubes were exposed to 500 μmol (photons)·m⁻²·s⁻¹ from panel of fluorescent tubes for biochemical experiments and to 150 μmol (photons)·m⁻²·s⁻¹ from a panel of warm-white light-emitting diodes for Raman experiments.

For synchronization, the cultures were observed by light microscopy for two or three cycles to set the correct length of both the light and dark periods under given conditions so that the cells divided mostly into eight daughter cells (connected in eight-celled coenobia). The lengths of light and dark periods were chosen according to the growth parameters of the cells. The time for darkening the cells was when about 10 % of cells started their first protoplast fission. The length of the dark period was chosen to allow all cells of the population to release their daughter cells and then the duration of the light and dark periods was kept constant (15/9 h light/dark cycle), for details on synchronization procedure see (Hlavová et al. 2016). At the day of the experiments, the synchronized daughter cells were diluted to 1-1.5×10⁶ cells·mL⁻¹ to avoid light-limitation and used as inoculums for experimental cultures. For biochemical experiments, the cultures were cultivated in glass plan parallel cultivation cuvettes with light path 2.5 cm and inner volume 2 liters, illuminated by incident light intensity 500 μmol (photons)·m⁻²·s⁻¹ of photosynthetically active radiation provided by a panel of fluorescent tubes. For Raman experiments, the cultures were grown in glass tubes of 3-cm diameter, illuminated by incident light intensity 150 μmol (photons)·m⁻²·s⁻¹ from a panel of warm-white light-emitting diodes. Due to the differences in the culture cultivation, the experimental cultures for biochemical experiments contained exclusively 8-celled coenobia while the cultures for Raman experiments contained both eight- and four-celled coenobia. Only the two innermost cells of eight-celled coenobia were used for Raman mapping. The cultures were sampled hourly for biochemical experiments and as permitted by the analysis for the Raman experiments (for details see below).

5.2.3 4',6-diamidine-2'-phenylindole dihydrochloride (DAPI) staining

Nuclei were stained with fluorochrome 4',6-diamidine-2'-phenylindole dihydrochloride (DAPI) and observed through a fluorescent microscope using the method described by (Zachleder and Cepák 1987) and (Hlavová et al. 2016). Twenty microliters of DAPI solution (5 µg/ml in 0.25 % (w/v) sucrose, 1 mM EDTA, 0.6 mM spermidine, 0.05 % (v/v) mercaptoethanol, 10 mM Tris-HCl, pH 7.6) were added to the frozen cell pellet, vortexed and kept for 20–30 minutes in dark at room temperature. The stained cells were observed using Olympus microscope with 360–370 nm excitation and 420–460 emission filters.

5.2.4 Cell size and number

The cell suspension for Coulter counter measurement was stored frozen (–20 °C). Prior to the measurement, it was let to thaw in room temperature and vortexed thoroughly for several minutes. According to the cell cycle stage, 0.4 or 0.8 mL of cell culture was diluted appropriately with ISOTON II solution to total volume of 10 mL. Two mL of the sample (approximately 10^4 – 10^5 cells per mL in the final solution, in accordance to the Coulter counter instructions) were measured using Multisizer 3 (Beckman Coulter, USA), aperture size was 100 µm. Cell number was also determined in the Bürker counting chamber (Meopta, Czech Republic).

5.2.5 Assessment of commitment points and cell division curves

To determine whether and how many commitment points were passed, the cells were sampled at appropriate time intervals and incubated at 30°C in darkness. At the end of the cell cycle, the percentages of binuclear daughter cells, four- and eight-celled daughter coenobia, and undivided mother cells were estimated by light and/or fluorescence microscopy (Hlavová et al. 2016). The values obtained by the assay of samples were

plotted against the times of sampling. The curves are termed commitment curves. The proportion of mother cells, sporangia and daughter cells were determined by light microscopy in cells fixed in Lugol solution (1 g I, 5 g KI, 100 mL H₂O) at a final concentration of 10 µL of Lugol solution per 1 mL of cell suspension. Cell division and daughter cell release curves were obtained by plotting the cumulative percentages as a function of sampling time.

5.2.6 Polyphosphate visualization

For polyP visualization, the samples were taken at designated time points during the cell cycle. In each sample, 1 mL of cell suspension was spun down for 2 min at 5 000× g, the supernatant was removed and the sample was stored at -20°C until staining. For staining, the method of Ota et al. 2016 was used.

5.2.7 Biochemical analyses

a. Estimation of bulk RNA, DNA and protein

The procedure of Wanka 1962 as modified by Lukavský et al. 1973 was used for the extraction of the total nucleic acids. The samples were centrifuged in 10 mL centrifuge tubes, which also served for storage of the samples. The pellet of algal cells was stored under 1 mL of ethanol at 20°C. The algae were extracted 5 times with 0.2 M perchloric acid in 50 % ethanol for 50 min at 20°C and 3 times with an ethanol-ether mixture (3:1) at 70°C for 10 min. Such pre-extracted samples were stored in ethanol. Total nucleic acids were extracted and hydrolyzed by 0.5 M perchloric acid at 60°C for 5 h. After hydrolysis, concentrated perchloric acid was added to achieve a final concentration of 1 M perchloric acid in the sample. Absorbance of total nucleic acids in the supernatant was read at 260 nm.

The light activated reaction of diphenylamine with hydrolyzed DNA, as described by Decallonne and Weyns 1976 was used with the following

modification (Zachleder 1984). The diphenylamine reagent (4 % diphenylamine in glacial acetic acid, w/v) was mixed with the samples of the total nucleic acid extracts in ratio 1:1 and the mixture in the test tubes was illuminated from two sides with fluorescent lamps (Tesla Z, 40 W). The incident radiation from each side was $20 \text{ W}\cdot\text{m}^{-2}$. After 6 h of illumination at 40°C , the difference between the absorbance at 600 nm and at 700 nm was estimated. The RNA content was calculated as a difference between the total nucleic acid and DNA content.

The sediment remaining after the nucleic acid extraction was used for protein determination. It was hydrolyzed by 1N NaOH for 1 hour at 70°C . The protein concentration in the supernatant after the centrifugation of the hydrolysate (15 minutes, $5300\times g$, room temperature) was estimated by BCA assay (Thermo Fisher) according to manufacturer's instructions. The same procedure was carried out with calibration curve set by different concentrations of bovine serum albumin.

b. Starch assay

Cell pellets containing approximately 2×10^6 cells·mL⁻¹ were harvested during the cell cycle, washed with SCE buffer (100 mM sodium citrate, 2.7 mM EDTA-Na₂, pH 7 (citric acid)), snap frozen in liquid nitrogen and stored at -20°C . After thawing the cells in the pellets were disintegrated by adding 200 μL of distilled water and 300 μL of zirconium beads (0.7 mm in diameter) followed by vigorous vortexing for 15 min at room temperature. Depigmentation of the samples was done by adding 1 mL of 80 % (v/v) ethanol to the pellet and incubating in a water bath for 15 min at 68°C after which the samples were centrifuged for 2 min at $14\,000\times g$ and the supernatant was removed. The depigmentation procedure was repeated 3 to 4 times (or until the pellet was completely discolored). After that, 1 mL of α -amylase from porcine pancreas (Sigma-Aldrich, USA) solution (0.5 mg·mL⁻¹ w/v in 0.1 M sodium phosphate buffer (pH 6.9)) were added to the samples and they were incubated for 1 hour at 37°C . The samples were centrifuged for 2 min at $14\,000\times g$ and the supernatant was used for the

quantification of reducing sugars through the DNSA color reaction as described in (Miller 1959). In short, 500 μL of supernatant were mixed with 500 μL dinitrosalicylic acid (DNSA) solution (1 % (w/v) 3,5- DNSA, 30 % (w/v) potassium sodium tartrate tetrahydrate, 20 % (v/v) 2M sodium hydroxide) and incubated for 5 minutes at 105°C on a heat block. Following a cooling down period of 10 minutes at room temperature, the mixture was diluted five-fold with distilled water, after which the absorbance of the samples was measured at 570 nm. The concentration of starch was estimated through a calibration curve of potato starch (Lach-Ner, Czech Republic) digested with α -amylase.

c. Total phosphate assay

Cell pellets, containing at least 4×10^7 cells, were harvested at designated time points during the cell cycle, washed with distilled water and stored at -20°C. After thawing, 1 mL of distilled water was added to the pellets in addition to 300 μL of zirconium beads (0.7 mm in diameter). The cells were disrupted by vigorous vortexing for 15 min at 4°C. The samples were centrifuged for 2 min at $14\,000 \times g$, after which the supernatant was discarded. The pellets were washed three times with a 5 % (w/v) solution of sodium hypochlorite in order to remove any pigments that might interfere with the spectrophotometric measurements. After the last wash, 200 μL of 0.67 % (w/v) potassium persulfate were added to the pellet. The samples were finally autoclaved at 121 °C for 20 min. After cooling down, 200 μL of sample were pipetted on a 96 micro well plate together with 8 μL of an ammonium molybdate tetrahydrate solution (1.2% (w/v) ammonium molybdate tetrahydrate, 4.8 % (w/v) potassium antimonyl tartarate sequihydrate and 16 % (v/v) sulfuric acid) and 2 μL of 7.2 % (w/v) L-ascorbic acid. The plate was incubated for 20 min in darkness at room temperature, after which the absorbance of the samples was measured at 880 nm in a plate reader (Infinite F200, Tecan Trading AG, Switzerland). For the quantification of total phosphate and polyP, a

calibration curve was constructed using a phosphate standard for ion chromatography (Sigma-Aldrich, Prague, Czech Republic).

d. Polyphosphate assays

The samples for the estimation of polyP were collected, stored, disintegrated and depigmented similarly to the samples for total phosphates. After the depigmentation with 5 % (w/v) solution of sodium hypochlorite, 100 μ L of distilled water were added to the pellet. Following an incubation time of 5 minutes, the samples were centrifuged for 2 minutes at 14 000 \times g and the resulting supernatant was collected. The elution with distilled water was repeated twice in order to ensure the optimal extraction of polyP from the pellet. Precipitation of polyP was done by addition of 1.8 mL of 100 % ethanol to the collected supernatant. The samples were centrifuged for 10 min. at 14 000 \times g after which the supernatant was removed. The resulting pellet was then re-suspended in 500 μ L of distilled water. The hydrolysis of polyP to orthophosphates was achieved by adding of 100 μ L of 0.67 % (w/v) potassium persulfate after which the samples were autoclaved for 20 min at 121 $^{\circ}$ C. After cooling, the samples were treated and analyzed as described in the quantification of total phosphates (Ota et al. 2016).

5.2.8 Raman analyses

a. Sample preparation

To study the content and intracellular distribution of storage biomolecules during the cell cycle by Raman microscopy, fresh living cells have been needed because of problematic photobleaching of autofluorescence of chemically fixed or frozen cells. Samples from the synchronized culture of *D. quadricauda* were taken every 30–60 minutes, as permitted by the duration of the Raman scanning, from the start of the light phase (T = 0:00 h), considered as the beginning of the cell cycle, up to

the end of the cycle ($T = 24:00$ h); the first sample was taken 15 min after the start of the light phase.

For Raman measurement, 0.5 mL of the cell suspension was centrifuged ($2000\times g$ for ca. 15 s), the supernatant was discarded and a part of the pellet was mixed with ca. 20 μL of low-gelling agarose (Sigma Aldrich, 2 % solution, $T = 39$ °C). A few μL of the agar mixture were placed between a quartz slide and a quartz coverslip, these were sealed with Covergrip sealant (Biotium, USA). The sample preparation took about 13 minutes from taking the sample to the start of Raman measurement.

b. Raman measurement

Raman maps were acquired with a confocal Raman microscope WITec alpha300 RSA (WITec, Germany) equipped with an oil-immersion objective UPlanFLN 100 \times , NA 1.30 (Olympus, Japan). The spectra were excited with a 532 nm laser (excitation power of ca. 20 mW at the sample). The lateral and axial resolutions of the Raman microscope (according to standard test of Raman confocality by means of silicon wafer (Everall 2009; Moudříková et al. 2016) were ca. 250 and 900 nm, respectively. Scanning step of 125 nm in both x and y direction (thus below the Rayleigh diffraction limit of the experimental setup) was used, with a 0.1 s acquisition time per pixel. The spectra were measured in the range of 220–3850 cm^{-1} at once. This range covers characteristic (< 1800 cm^{-1}) as well as stretching (> 2800 cm^{-1}) vibrations of biomolecules and water. Prior to Raman mapping, a wide-area photobleaching of the entire algal coenobium by a defocused 532-nm laser beam was applied as described previously to get rid of the strong autofluorescence of chlorophyll (Moudříková et al. 2016). At each sampling point, a two-dimensional Raman map of the two innermost cells of a randomly selected eight-celled coenobium was acquired.

c. Data treatment

Raman maps were treated with Project Four *Plus* (WITec, Germany) and our own scripts for GNU Octave (Eaton et al. 2015) and Matlab (MathWorks, USA) (Palacky et al. 2011). Firstly, signals of cosmic rays were removed using automated and manual functions of Project Four *Plus*. Next, to compensate eventual variations of laser power and efficiency of signal collection, Raman maps of different cells have been normalized to the common intensity scale as follows: the pixels of the map obviously belonging to the surrounding medium have been identified automatically according to the missing band of carbon-hydrogen stretching vibrations. For each Raman map, the average spectrum of the surrounding medium was calculated and the integral intensity of the oxygen-hydrogen stretching band of water (background corrected) was used as the standard intensity for uniform normalization of Raman maps. Next, spectral regions with characteristic Raman bands of respective biomolecules were selected for starch (457–507 cm^{-1} , band maximum at 479 cm^{-1}), lipids (2836–2869 cm^{-1} , band maximum at 2854 cm^{-1}), polyphosphate (1143–1190 cm^{-1} , band maximum at 1159 cm^{-1}), guanine (613–684 cm^{-1} , band maximum at 651 cm^{-1}) and the region of carbon-hydrogen stretching vibrations of all biomolecules containing C-H bonds (2795–3060 cm^{-1} , band maximum at around 2935 cm^{-1}). The non-Raman background was subtracted as a bisector connecting mean intensities at the last 4-10 spectral points delimiting the upper and lower ends of the regions. Spectra with high content of the respective biomolecules and the appropriate wavenumber regions are shown in supplementary Figure 5-S1.

For visualization of distributions of the biomolecules under study in *D. quadricauda* cells, the intensity of the band (after background correction) was calculated by integrating the band's area. The integral intensities in Raman maps are expressed in color scale, for a given biomolecule the same scale was used in all maps. Darkest color shade corresponds to the mean intensity found in the surrounding medium and the lightest one to the

maximum value. The only exception is the intensity of carbon-hydrogen stretching vibrations, where the darkest shade corresponds to zero.

To estimate the content of the respective biomolecules in the cells, the pixels corresponding to both of the two cells on each Raman map were identified using manual functions of Project Four *Plus*. The signal from every 2×2 pixels was merged together to reduce the noise, and the background-corrected bands of biomolecules were integrated. For each Raman map i , mean value m_i and standard error s_i of the integral intensity in the merged pixels of the surrounding medium were calculated. For each pair of cells, the integral intensities were summed for pixels where the signal was greater than $m_i + 7s_i$. Remaining pixels displaying signal below this threshold were excluded from the summation.

5.3 Results

5.3.1 Cell cycle characteristics

Cultures of *D. quadricauda* were synchronized by diurnal, alternating light/dark regime. During the cultivation, the cell cycle progression was analyzed hourly, as well as changes in bulk RNA, protein, DNA, starch, polyP, total phosphates and lipid contents. These standard physiological and biochemical experiments set up a baseline to which the results from Raman microscopy were correlated. At a given light intensity, half of the population attained the first commitment point shortly after being put in light. By the sixth and tenth hour, more than 50 % of the population attained the second and third commitment points, respectively. Attainment of each of the commitment points was followed by DNA replication, nuclear division and cell division. Within the population, the attainments of the second and third commitment points were closely followed by completing nuclear division into two and four nuclei, respectively. The third nuclear division together with the first protoplast division occurred shortly before darkening the cells at 15th hour of the cell

cycle. The cell cycle was concluded after about 22 hours when all mother coenobia released daughter coenobia (Figure 5-1).

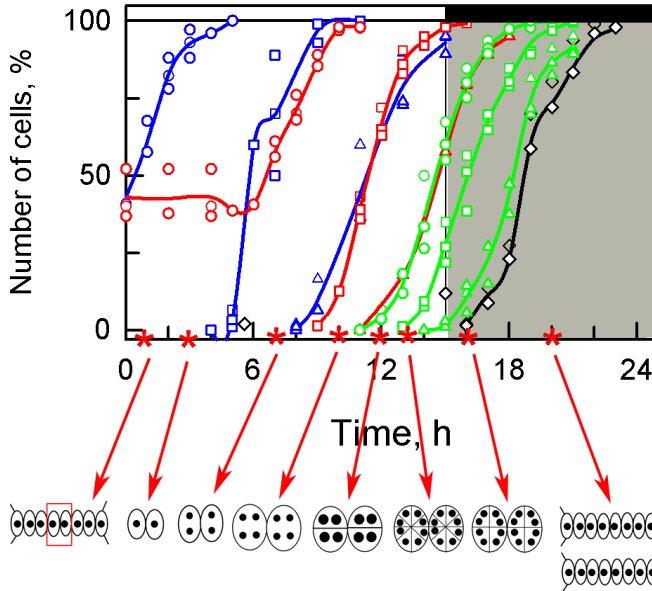


Figure 5-1: Dynamics of growth and the cell cycle in synchronized cultures of *D. quadricauda*.

Upper part: Time courses of individual commitment points, nuclear division, protoplast fission and daughter cell release. Blue lines: cumulative percentage of the cells, which attained the commitment point for the first (circles), second (squares) and third (triangles) reproductive sequence, respectively; red lines: cumulative percentage of the cells, in which the first (circles), second (squares), and third (triangles) nuclear division was terminated; green lines: cumulative percentage of cells, in which the first (circles), second (squares) and third (triangles) cell division was terminated, respectively; black line, empty diamonds: percentage of the cells, which released daughter coenobia. Light (15 hours) and dark periods (9 hours) are marked by stripes above panels and separated by vertical line. The lines represent the means of at least three independent experiments. The raw values are plotted as dots, the line connects the mean values of the experiments. All values calculated per parental cell even after their division (17:00 to 22:00 h).

Bottom part: Schematic representation of the cells at the time-points (denoted by red asterisks) corresponding to the set samples analyzed by Raman microscopy in Figure 5-4 (full set of Raman measurements is available in Supplementary Figure 5-1S). Schematic pictures of the cells indicate changes in their size. The full circles inside illustrate the ploidy and number of nuclei during the cell cycle. Larger circles indicate a doubling of DNA. For more details see text. Modified after Zachleder et al. 1997, Bišová and Zachleder 2014, and Zachleder et al. 2016.

5.3.2 Bulk analysis of cell composition

Biochemical analysis showed that accumulation of RNA (Figure 5-2A) progressed rapidly in the early light period, followed by a lower rate of RNA synthesis in the late light period and in dark. The total protein content increased with a small delay after the RNA accumulation in light and, in the dark period, the protein accumulation stopped and, later in night, the protein amount even slightly decreased (Figure 5-2B). A significant increase in the DNA content was observed only after the seventh hour of the cell cycle, which coincides with the midpoint of the first round of nuclear division. The increase of DNA synthesis then continued until the end of the cell cycle (Figure 5-2C). Starch started to be synthesized immediately after the cultures were exposed to light and continued steadily throughout the light period (Figure 5-2D). The rate of starch accumulation was faster until the tenth hour when the cells attained the third commitment point. It slowed down from then on as the cells underwent the second and third nuclear divisions. In dark, the starch reserves were catabolized to support nuclear and cellular divisions that were taking place in absence of photosynthetic energy conversion.

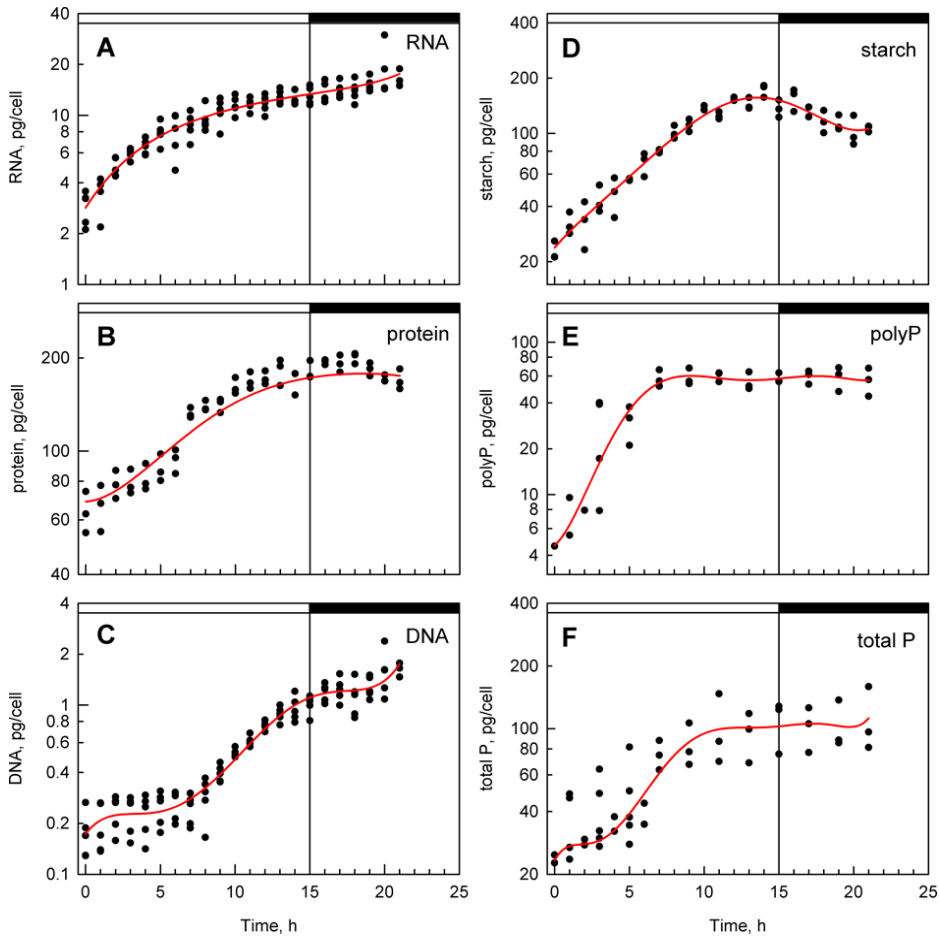


Figure 5-2: Time courses of accumulation of RNA (A), protein (B), DNA (C), starch (D), polyphosphates (polyP) (E) and total phosphates (F) in synchronized cultures of *D. quadricauda*. Light (15 h) and dark periods (7 h) are marked by stripes above panels and separated by vertical line. Values from five different experiments are showed as dots, the smoothed line of the mean of the five experiments is shown as a read line in each panel. Values were calculated per parental cell even if divided (17:00 to 22:00 h).

Total phosphate and polyphosphate (polyP) content increased soon after transfer into light (Figure 5-2E, F). The increase continued until about seventh hour when DNA replication started and the first round of nuclear

division was completed in half of the population. Thereafter, both total and polyP levels plateaued.

PolyP granules can be also detected using conventional fluorescence microscopy after staining with high concentrations of DAPI (Ota et al. 2016). PolyP granules were visible as groups of yellow spots on both sides of the bluish nuclei in the longitudinal direction (Figure 5-3). They were present already in the first hour of the cell cycle. They seemed to multiply both in number and in extent of fluorescence in the next two hours and their localization was, conspicuously, at the outer side of two newly formed nuclei. With time, both their fluorescence and number decreased. By seventh hour of the cell cycle, they were represented by groups of tiny yellow spots close to the outer cell edge in the vicinity of nuclei. From the ninth hour, the spots became even smaller and in most cells they disappeared by the tenth hour. In about ten percent of cells, the polyP granules persisted for one more hour and were localized both to the perinuclear area and to the outer cell edge. Even in these cells, the granules disappeared by the eleventh hour of the cell cycle.

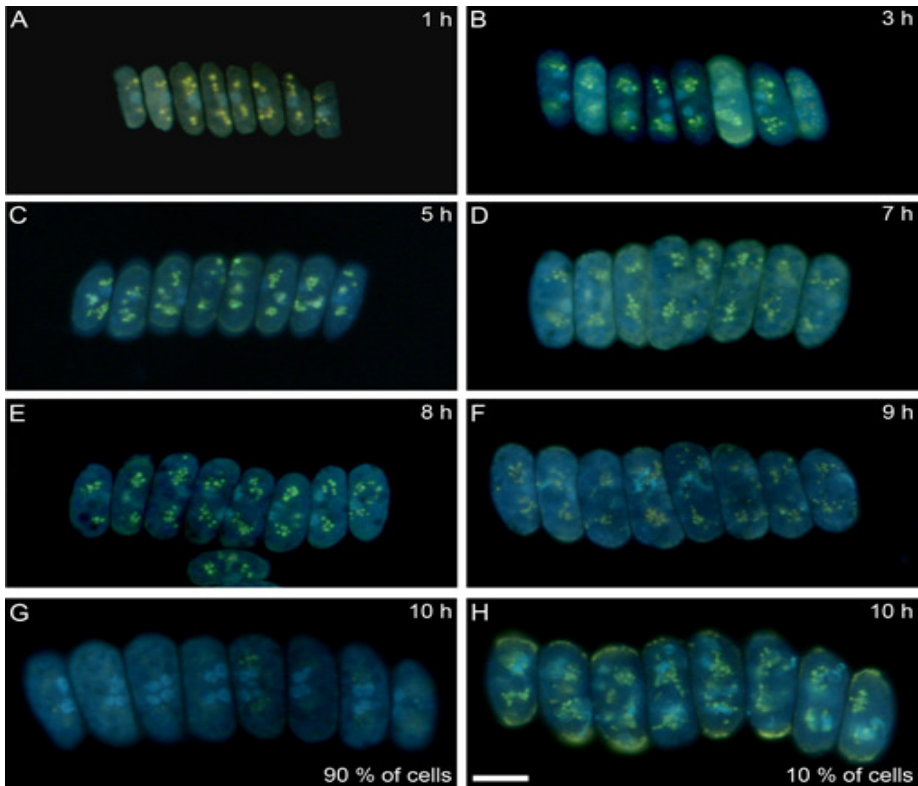


Figure 5-3: Fluorescence micrographs of coenobia stained by high concentration of 4',6-diamidino-2-phenylindole (DAPI) at different time points during the cell cycle. Polyphosphates are visible as yellow spots; the bluish spots are nuclei. Bar is 10 μm .

5.3.3 Raman estimates of cell volume and chemical composition

The biochemical analysis and the Raman experiments were not done on samples from the same cultures and from the same cultivations because of principal difference in sampling. The Raman microscopy was done immediately using living algal cells from aliquots taken during the cell cycle whereas the biochemical analysis was done on samples, which were accumulated and stored during the cycle. A practical reason for doing separate rather than simultaneous analysis was that the biochemical methods and Raman microscopy were done in different laboratories equipped in with different types of instrumentation.

The cultivation set-ups were the same for the two experimental methods, with the exception of light intensity, which was about three-fold lower for the Raman measurements. This led to changes in proportion of 4-celled and 8-celled coenobia within the population. The cultures used for biochemical experiments were composed exclusively of 8-celled coenobia, while the culture for Raman measurements contained both 4-celled and 8-celled coenobia. To overcome this limitation, the innermost two cells of randomly selected 8-celled coenobia were chosen for all the measurements. These cells are usually the largest ones within the coenobium and the most advanced in the cell cycle progression. This way we ensured that the two analyses were done on as similar cells as possible. Raman microscopy mapping was performed 35-times during the 24-hour cell cycle. All acquired Raman maps are presented in Figure 5-S1 in the Supplement. A subset of the maps is shown in Figure 4C, the age of the cells is schematically depicted in the figure is indicated in Figure 5-1 as well as in Figure 5-4A, B.

To verify the synchrony of the population used for Raman microscopy, number of coenobia per mL of the cell suspension (Figure 5-4A) and median volumes of the cells (Figure 5-4B) were obtained by Coulter counter measurement. To relate the bulk population analysis with the Raman microscopy results, cell volumes provided by the Coulter counter measurement were compared with Raman estimates of the volume of the two innermost cells of the mapped coenobium. These estimates were calculated as follows: the number of pixels belonging to the cells, identified according to carbon-hydrogen stretching band as described in *Material and methods*, was raised to the power of 1.5 and renormalized to fit the Coulter counter values in a least square sense. The number of pixels is directly proportional to the area of the cells' cross-section. As can be confirmed by Figure 5-4B, the Raman estimates of the volume, though of only two innermost cells of a randomly selected coenobium, fit well to the median volume determined for hundreds of thousands of cells by Coulter counter, indicating a good synchrony of the culture and justifying the simplifications.

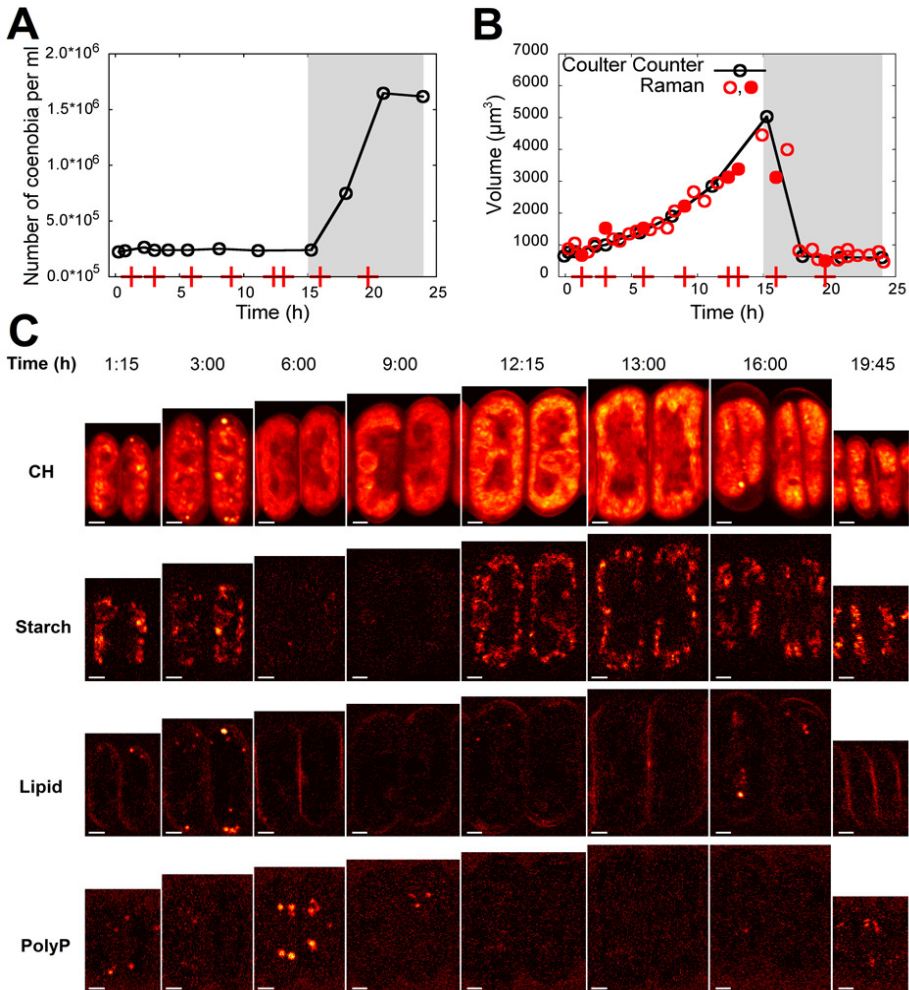


Figure 5-4: Time course of a number of coenobia in the cell culture of *D. quadricauda* as determined by Coulter counter (A). Time course of volumes of the coenobia determined by Coulter counter (black, median volume) and Raman microscopy (red) (B). For the time-point T = 18:05 h coinciding with the cell division of a majority of the cells, the Coulter counter volume of daughter cells is shown. The Raman microscopy volumes were estimated as a number of pixels belonging to both cells in coenobium (identified by the carbon-hydrogen stretching band) raised to the power of 1.5 and renormalized to fit the Coulter counter curve. The cells that are shown in panel (C) are indicated by filled circles. Raman maps showing the distribution of carbon-hydrogen (C-H) groups, starch, lipids, and polyphosphates in two innermost cells of eight-celled coenobia during the cell cycle (C). Time from

start of the cycle is indicated in the top row. For a given biomolecule, the color scale is the same for all Raman maps. The white bars correspond to 2 μm . The red crosses on the time axis in panels A, B indicate times at which the cells shown in panel C were taken from the culture. The grey area in panels A, B indicates the dark period of the cycle.

For all 35 samples taken during the 24 hour cycle for the Raman measurement, the distribution of starch, lipids and polyphosphate in the Raman maps were obtained by integrating the intensity of a Raman band characteristic for the given biomolecular species in each pixel spectrum, as described in section 5.2.8 from Materials and methods (supplementary Figure 5-S1). Additionally, the band of carbon-hydrogen (C-H) stretching vibrations was used to visualize the concentration of the total organic matter (proteins, carbohydrates, lipids, RNA, DNA) in the cells.

The distributions of carbon-hydrogen stretching vibrations, starch, lipids, and polyP are shown in Figure 5-4C for selected time-points where the cells exhibited some characteristic features. Those particular time-points are indicated in Figure 5-4A, B by red crosses on the horizontal axes and their cell volumes are indicated by filled circles in Figure 5-4B. For all the 35 samples measured here, the biomolecular distributions are shown in the supplementary Figure 5-S1.

As can be seen from Figure 5-4C and supplementary Figure 5-S1, the cells already contained some starch reserves and a few lipid and polyP bodies just after the dark phase of the previous cycle. The starch content was growing from the beginning of the light phase, reaching its first maximum at around $T = 2:15$ h after the light onset (supplementary Figure 5-S1), and then declining again. Lipid bodies, localized to the periphery of the cells, grew in number and lipid content with about 45 min delay behind the starch content. At last, the polyP content peaked at $T = 6:00$ h, when the cells contained multiple polyP bodies but exhibited nearly no starch nor lipids identifiable by Raman microscopy.

After $T = 6:00$ h, the polyP bodies slowly dissolved and nearly no starch and lipids were visible in the cells. The carbon-hydrogen vibrations visible in interiors of the cells thus come predominantly from proteins (Figure 5-4

and supplementary Figure 5-S2). At around $T = 10:30$ h, the cells started to accumulate starch again. The starch content and cell volume grew until the end of the light period at $T = 15:00$ h, when some of the cells were already dividing. Some lipid bodies can be seen in the cells even during the cell division (supplementary Figure 5-S2). The released daughter cells contained some starch and a few polyP bodies till the end of the cycle at $T = 24:00$ h. In some daughter cells, a few lipid bodies can be identified (supplementary Figure 5-S2).

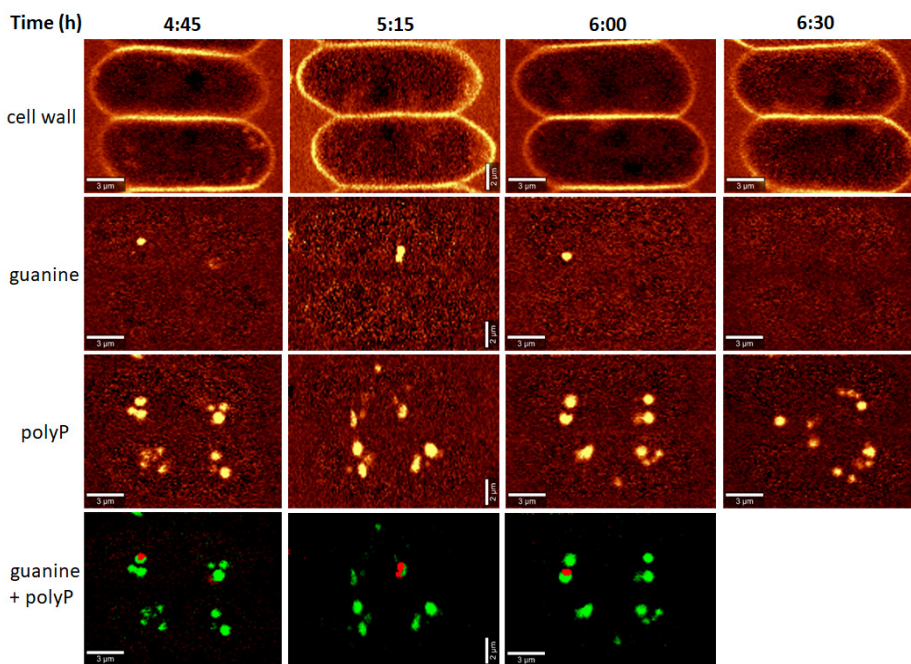


Figure 5-5: Raman maps showing the distribution of cell wall, guanine and polyphosphates (polyP) in two innermost cells of eight-celled coenobia during the early phase of cell cycle. Time from start of the cycle is indicated in the top row. For a given biomolecule, the color scale is the same for all Raman maps. The white bars correspond to $2 \mu\text{m}$ at Time = 5:15 h or $3 \mu\text{m}$ at other timepoints. The bottom panel shows an overlay of localization of guanine (red) and polyphosphates (green).

A more detailed sampling at the early phase of the cell cycle, prior to onset of DNA replication (between $T = 4:45$ h and $T = 6:30$ h) showed

guanine bodies coinciding and possibly co-localizing with the polyP granules (Figure 5-5), the cells exhibited between. Small guanine bodies of a lower signal intensity were observed also at T = 7:45 h, 9:45 h and 16:00 h (supplementary Figure 5-S2) but not in the daughter cells (Figure 5-S2).

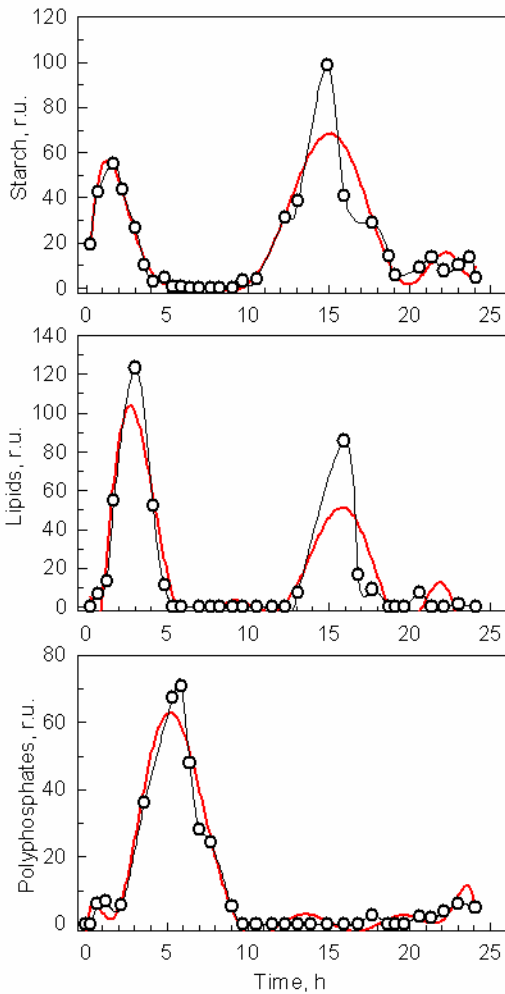


Figure 5-6: Time evolution of starch (top), lipids (middle) and polyphosphate (bottom) content of the cells during the cell cycle as determined from the Raman maps.

To show dynamics of the storage compounds (described qualitatively above) in a semi-quantitative way, Raman estimates of the starch, lipids and polyP content *per* single cell of the coenobium have been calculated by averaging contributions of both of the measured cells (for details see *Material and methods*) and are shown in Figure 5-6. Outlying values have

been excluded for the purpose of this figure and the data points were connected with splines to guide the eye.

5.3.4 Comparison of Raman and bulk biochemical analyses

Above, we present the results of cell content estimates by bulk biochemical methods and Raman mapping of individual cells in the synchronous cultures. The two methods differ in the biomolecules they are able to detect and quantify. The bulk biochemical methods can easily separate RNA, DNA and proteins (Figure 5-2) due to their different chemical properties. In contrast, Raman estimates of these three macromolecules are limited by a lack of intensive and specific spectral signatures as well as by their low concentration in the mapping voxels. On the other hand, Raman microscopy is very sensitive in detecting lipid droplets (Figure 5-4). The same size of lipid droplets is not detectable by conventional fluorescence microscopy with neutral lipids stained by a specific dye Nile Red (data not shown). Furthermore, we have tried to measure the lipid content by using a fluorescent plate reader and cells stained with Nile Red. This way, more cells are measured at the same time, thus multiplying the signal. Even then, we were unable to reliably detect any changes in lipid content. The changes detected were within few percents of the total lipid content, and not statistically significant (data not shown). Furthermore, Raman spectroscopy was able to detect guanine granules, for which there are no alternatives of in situ detection.

Both bulk methods and Raman estimates were able to detect starch and polyP. The bulk biochemical analysis identified a steady increase in starch amount from the beginning of the cell cycle till the cell darkening and start of cell division when starch started to be consumed. In contrast, Raman analyses detected increase in starch amount in the first three hours of the cell cycle followed by complete disappearance of starch. A new increase in synthesis was observed by about twelfth hour of the cell cycle, and it was followed by decrease of starch amount at the time of cell division and later on. Both Raman estimates and conventional fluorescence

microscopy revealed similar patterns of polyP localization in both space and time. Both of the methods detected two major groups of polyP granules on each side of a single nucleus or later on the outer side of the two newly formed nuclei. PolyP granules gradually disappeared by the time the cells completed divided their nuclei into four. The bulk biochemical analyses detected a rapid increase in both total and polyP content from the beginning of light period to about fifth hour of the cells cycle. Thereafter both total and polyP levels remained unchanged.

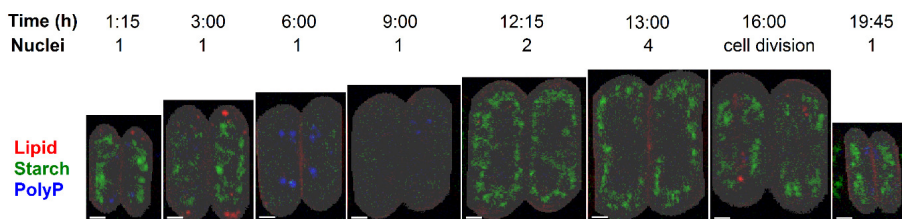


Figure 5-7: Raman maps showing the distribution of lipid droplets (red), starch bodies (green) and polyP granules (blue) in the same two innermost cells of eight-celled coenobia as presented in Figure 5-1C. The time counted from the beginning of the cell cycle and number of nuclei determined by DAPI staining of the culture is indicated in the top row. For a given biomolecule, the color scale is the same for all the maps. The white bars correspond to 2 μm .

5.4 Discussion

Synchronized cultures are a traditional tool for studies of cell cycle progression in different organisms. The cell cycle progression, encompassing growth and cell duplication and division events, has been routinely described by biochemical analyzes of macromolecules (RNA, protein, DNA, starch) composition. Such analyzes are rather time consuming, complicated and mostly require a large quantity of initial sample. Here, we have compared the bulk biochemical analyzes of biomolecules with Raman microscopy results. Raman microscopy visualizes distributions of the prevalent groups of biomolecules simultaneously,

without the need of artificial pre-processing of the sample and with a spatial resolution of a confocal microscope. As Raman microscopy shows intrinsic chemical content of the sample, even biochemical species not expected in the sample can be disclosed, provided they are present in a sufficient concentration and that their Raman spectra are correctly interpreted. This can be demonstrated on the example of guanine microcrystals that have been recently observed in two microalgal species (Moudříková et al. 2017) without previous knowledge of their existence. In the present study, the guanine microcrystals occurred regularly between approximately 5th and 7th hours of the cell cycle, *i. e.*, at the time of attainment of the second commitment point and completion of the first nuclear division, and then sporadically also during other cell cycle phases. The appearance of guanine microcrystals during a natural cell cycle of unstressed cells supports the tentative biological relevance of guanine microcrystals as effective depots of purines (Moudříková et al. 2017). Such biological functions can be related to their localization in the cells. Guanine crystals localized together with polyP granules, either in the vicinity of the newly formed nuclei, or in the place where nuclei are formed. The two possibilities are impossible to separate based on Raman microscopy, as the nuclei localization could not be detected in the algal cells. Both of the localizations would suggest guanine crystals can serve as purine deposits used (and spent) for nuclei formation.

Apart from identifying novel and/or otherwise undetectable biochemical species, Raman microscopy might be also more sensitive to low amount of biochemical species that can be detected and analyzed by fluorescence microscopy and/or bulk analytical techniques. This is demonstrated by the observed presence of lipid bodies at the periphery of some cells during the cell cycle (Figure 5-4 and supplementary Figure 5-S2). These lipid bodies could not be observed neither by fluorescence microscopy nor by bulk fluorescent measurements, as they do not increase the cellular lipid content enough to be detected separately.

Raman microscopy and fluorescent microscopy of polyphosphate bodies were in agreement (compare Figs 4 and 5). They visualized polyP

granules both in the places where new nuclei will be formed and near them, once they divided. This was particularly true for the first nuclear division. The localization of polyP granules (together with guanine crystals) close to nuclei could suggest they function as energy and phosphate store for nucleic acid synthesis. This localization is thus in an agreement with classical observation in green alga *Chlorella*, where polyP are preferentially used for the synthesis of DNA (and phosphoproteins), but not RNA (Miyachi and Tamiya 1961; Miyachi and Tamiya 1961; Miyachi et al. 1964). Both microscopy methods show a decrease in polyP granules after 8th hour of the cell cycle, *i.e.* at the time when exponential increase of DNA synthesis starts, further supporting a notion that polyP granules serve as a source for DNA synthesis. Interestingly, at the same time, the total phosphorus and polyP amounts, as determined by bulk biochemical analyses, plateau. The biochemical method that we used for total phosphorus and polyP was non-specific, and precipitated polyP granules together with DNA and RNA. This could explain the differences between the microscopy and biochemical method. Thus, from 8th hour, DNA is possibly newly made at the expense of polyP granules, and it gradually forms a larger portion of the biochemically detected polyP fraction.

The most striking difference was observed between the bulk biochemical and Raman analyses of starch. The bulk biochemical analysis showed a steady increase in starch, as has been established in the field (Bišová and Zachleder 2014; Zachleder et al. 2016; Juppner et al. 2018), whilst Raman microscopy showed a bimodal pattern with an initial increase in starch prior to attainment of the first CP followed by starch disappearance and another increase of starch amount by the time the cells reached third CP and completed the second nuclear division (Figures 5-1 and 5-6). This was really an intriguing observation, and we suspected it could be caused by combination of two factors, *i.e.* the difference in light intensities used for cultivation for the biochemical and Raman experiments and/or three dimensional structure of the cell. The light intensity is known to affect accumulation of starch, so that it increases with increasing light intensity (Vítová et al. 2011). At lower light intensity, less starch would be

synthesized, it would be continuously spent for general metabolism and no net starch granules will be visible by Raman microscopy. Despite its high sensitivity described above, Raman microscopy has, as any other method, a threshold detection limit depending on the experimental setup and Raman cross-section of the given biochemical species. Raman signal of a lower concentration than the limit might be covered by noise and/or signal of other content of the respective voxel. The other explanation stems from the fact that we acquired only two-dimensional maps of the cell cross-sections, since quantitative volumetric Raman imaging (Kallepitis et al. 2017) would be, under the current experimental setup using conventional Raman scattering, extremely time consuming. Thus, any cellular content that is situated on the bottom or top of the cells could escape detection. This would be especially true as the cell size increases, if the starch granules would be located near to the cell surface, while the Raman analysis would be performed in the cell center. To exclude such effects, we grew synchronized cells at higher light intensities corresponding to the biochemical experiments. In each of the cells, several stacks covering their entire volume were analyzed to avoid missing any starch granules located away from cell center. Even under such conditions, we were not able to detect any starch granules in the cells between fifth and tenth hour of the cell cycle (data not shown). This suggests that the starch present in the cells in this time period as detected by biochemical methods by us and others (Wanka 1975; Vítová et al. 2011; Juppner et al. 2018) is not in the form of localized granules but rather in some more soluble form readily available to the general metabolism but below the detection limit of Raman microscopy.

The graphical description of the time evolution of starch, lipid and polyphosphate content during cell cycle in Figure 5-4 should be treated as a semi-quantitative proxy. Although recent studies have shown that two-dimensional mapping can be used to quantitatively describe the amount of starch (Ji et al. 2014; Chiu et al. 2017), lipids (Hosokawa et al. 2014; Chiu et al. 2017) and polyphosphates (Moudříková et al. 2017) in microalgal cultures, these studies have averaged the results from Raman maps of

several to dozens of cells to obtain an accurate quantification when compared to bulk methods. On the other hand, as the cells in the present study were synchronous, the variability among the cellular culture should be much narrower than in a common non-synchronous culture. Furthermore, Raman signal is, by the nature of conventional Raman scattering, linearly proportional to the compound concentration in a given voxel.

The data presented here proved that Raman microscopy is capable of detecting relatively low concentrations of storage biomolecules present in a non-stressed *D. quadricauda* cells during a normal cell cycle. This is an improvement compared to current quantification studies such as (Hosokawa et al. 2014; Ji et al. 2014; Chiu et al. 2017), which worked with cells accumulating large amounts of the storage biomolecules. Although the merits of Raman microscopy have been shown here, it still possesses similar limitations as conventional fluorescence microscopy and bulk biochemical analyses. It is relatively low throughput and the parallelization is problematic, unless one possesses several Raman microscopes. To keep a sampling time of 30–45 minutes and a high spatial resolution of Raman mapping, it was not possible to measure more than two cells of *D. quadricauda* coenobium at a given time-point. Statistically more sound set of cells could be acquired only by compromising one or both of these requirements. However, lower spatial resolution would impair imaging and quantification of small biomolecular inclusions in Raman maps. On the other hand, increasing intervals between the samplings might lead to missing important phases in the cell cycle. Otherwise, there exists possibility to repeat the same experiment in multiplicates. However, the cell culture, although synchronous, is never exactly the same. Apart from the results presented here, we have performed the Raman mapping experiment during one another whole cell cycle with a lower spatial resolution. Additionally, we have performed Raman mapping of the first 8–9 hours of the cycle in three consecutive cell cycles with a slightly lower spatial resolution for the whole eight-celled coenobia of *D. quadricauda* (data not shown), with qualitatively the same results as presented here. As

microalgae possess photosynthetic apparatus that have to be photobleached prior to the Raman measurement, it was impossible to perform such a cell cycle study on exactly the same coenobium, as would be desirable. On the other hand, the photobleaching itself does not disqualify the results, as the consequent decay processes take longer time than needed for the Raman mapping (Moudříková et al. 2016).

5.5 Conclusions

We have compared the detection of energy-rich compounds (starch, lipid and polyphosphates) during the cell cycle of *Desmodesmus quadricauda* by two independent methodologies, conventional bulk biochemical analyzes and confocal Raman microscopy. The two methods were comparable in detection of polyphosphates. Fluorescence and Raman microscopies detected specific localization of polyphosphate granules near the nuclei until bi-nuclear stage. The two methods differed in detection of starch, possibly suggesting differences in starch localization and/or its solubility during the cell cycle. Raman microscopy was more sensitive in detecting lipids. It also detected guanine crystals; these were localized near polyphosphate granules and nuclei, suggesting their possible role in processes related to nuclear division. Confocal Raman microscopy is capable of detecting even low amounts of macromolecules naturally present in the cells during their vegetative development. It is especially suited for the detection of polyphosphates, lipids and guanine crystals within the cells. The differences in starch detection will require further experiments.

5.6 References

- An SS, Friedl T, Hegewald (1999) Phylogenetic relationships of *Scenedesmus* and *Scenedesmus*-like coccoid green algae as inferred from ITS-2 rDNA sequence comparisons. *Plant Biol* 1:418-428
- Bišová K, Zachleder V (2014) Cell-cycle regulation in green algae dividing by multiple fission. *J Exp Bot* 65:2585–2602

- Buchheim MA, Sutherland DM, Schlicher T, Forster F, Wolf M (2012) Phylogeny of Oedogoniales, Chaetophorales and Chaetopeltidales Chlorophyceae: inferences from sequence-structure analysis of ITS2. *Ann Bot* 109(1):109-116
- Butler HJ, Ashton L, Bird B, Cinque G, Curtis K, Dorney J, Esmonde-White K, Fullwood NJ, Gardner B, Martin-Hirsch PL, Walsh MJ, McAinsh MR, Stone N, Martin FL (2016) Using Raman spectroscopy to characterize biological materials. *Nature Protocols* 11(4):664-687
- Chiu LD, Ho SH, Shimada R, Ren N, Ozawa T (2017) Rapid in vivo lipid/carbohydrate quantification of single microalgal cell by Raman spectral imaging to reveal salinity-induced starch-to-lipid shift. *Biotechnol Biofuels* 10:9
- Decallonne JR, Weyns CJ (1976) A shortened procedure of the diphenylamine reaction for measurement of deoxyribonucleic acid by using light activation. *Anal Biochem* 74: 448-456
- Dieing TO, Hollricher T, Toporski O (2011) *Confocal Raman microscopy*, Springer.
- Donnan L, John PCL (1983) Cell cycle control by timer and sizer in *Chlamydomonas*. *Nature* 304:630-633
- Eaton JW, Bateman D, Hauberg S, Wehbring R (2015) GNU Octave version 4.0.0 manual: a high-level interactive language for numerical computations.
- Everall NJ (2009) Confocal Raman microscopy: Performance, pitfalls, and best practice. *Appl Spectrosc* 63(9):245a-262a
- Hlavová M, Vítová M, Bisova K (2016) Synchronization of green algae by light and dark regimes for cell cycle and cell division studies. *Plant Cell Division*. Caillaud MC. New York, Heilderberg, Dordrecht, London, Springer Science: 3-16
- Hosokawa M, Ando M, Mukai S, Osada K, Yoshiro T, Hamaguchi H, Tanaka T (2014) In vivo live cell imaging for the quantitative monitoring of lipids by using raman microspectroscopy. *Anal Chem* 86(16):8224-8230
- Huang YY, Beal CM, Cai WW, Ruoff R, Terentjev EM (2010) Micro-Raman spectroscopy of algae: composition analysis and fluorescence background behavior. *Biotechnol Bioeng* 105(5):889-898
- Jehlicka JH, Edwards GM, Oren A(2014) Raman spectroscopy of microbial pigments. *Appl Environ Microbiol* 80(11):3286-3295
- Ji Y, He Y, Cui Y, Wang T, Wang Y, Li Y, Huang WE, Xu J (2014) Raman spectroscopy provides a rapid, non-invasive method for quantitation of starch in live, unicellular microalgae. *Biotechnol J* 9(12):1512-1518

- Juppner J, Mubeen U, Leisse A, Caldana C, Wiszniewski A, Steinhauser D, Giavalisco P (2018) The target of rapamycin kinase affects biomass accumulation and cell cycle progression by altering carbon/nitrogen balance in synchronized *Chlamydomonas reinhardtii* cells. *Plant J* 93(2):355-376
- Kallepitis C, Bergholt MS, Mazo M, Leonardo V, Skaalure SC, Maynard SA, Stevens MM (2017) Quantitative volumetric Raman imaging of three dimensional cell cultures. *Nat Commun* 8:1-9
- Koch M, Zagermann S, Kniggendorf A, Wollweber M, Roth B (2017) Violaxanthin cycle kinetics analysed in vivo with resonance Raman spectroscopy. *J Raman Spectros* 48(5):686-691
- Li K, Cheng J, Ye Q, He Y, Zhou J, Cen K (2017) In vivo kinetics of lipids and astaxanthin evolution in *Haematococcus pluvialis* mutant under 15% CO₂ using Raman microspectroscopy. *Bioresour Technol* 244:1439-1444
- Lukavský J, Tetik K, Vendlova J (1973) Extraction of nucleic acid from the alga *Scenedesmus quadricauda*. *Archive für Hydrobiologie* 9(41):416-426
- Meksiarun P, Spiegazzini N, Matsui H, Nakajima K, Matsuda Y, Sato H (2015) In vivo study of lipid accumulation in the microalgae marine diatom *Thalassiosira pseudonana* using Raman spectroscopy. *J Appl Spectrosc* 69(1):45-51
- Miller GL (1959) Use of dinitrosalicylic acid reagent for determination of reducing sugar. *Anal Chem* 31(3):426-428
- Miyachi S, Kanai R, Mihara S, Miyachi S, Aoki S (1964) Metabolic roles of inorganic polyphosphates in *Chlorella* cells. *Biochim Biophys Acta* 93:625-634
- Miyachi S, Tamiya H (1961) Distribution and turnover of phosphate compounds in growing *Chlorella* cells. *Plant Cell Physiol* 2:405-414
- Miyachi S, Tamiya H (1961) Some observations on the phosphorus metabolism in growing *Chlorella* cells. *Biochim Biophys Acta* 46:200-202
- Moudříková Š, Mojzeš P, Zachleder V, Pfaff C, Behrendt D, Nedbal L (2016) Raman and fluorescence microscopy sensing energy-transducing and energy-storing structures in microalgae. *Algal Res* 16:224-232
- Moudříková Š, Nedbal L, Solovchenko A, Mojzeš P (2017) Raman microscopy shows that nitrogen-rich cellular inclusions in microalgae are microcrystalline guanine. *Algal Res* 23:216-222
- Moudříková S, Sadowsky A, Metzger S, Nedbal L, Mettler-Altmann T, Mojzeš P (2017) Quantification of polyphosphate in microalgae by raman microscopy and by a reference enzymatic assay. *Anal Chem* 89(22):12006-12013

- Ota S, Yoshihara M, Yamazaki T, Takeshita T, Hirata A, Konomi M, Oshima K, Hattori M, Bisova K, Zachleder V, Kawano S (2016) Deciphering the relationship among phosphate dynamics, electron-dense body and lipid accumulation in the green alga *Parachlorella kessleri*. *Sci Rep* 6:25731
- Palacky J, Mojzeš P, Bok J (2011) SVD-based method for intensity normalization, background correction and solvent subtraction in Raman spectroscopy exploiting the properties of water stretching vibrations. *J Raman Spectrosc* 42(7):1528-1539
- Samek O, Jonas A, Pikat Z, Zemanek P, Nedbal L, Triska J, Kotas P, Trtilek M (2010). Raman Microspectroscopy of Individual Algal Cells: Sensing Unsaturation of Storage Lipids in vivo. *Sensors (Basel)* 10(9):8635-8651
- Šetlík I, Berková E, Doucha J, Kubin S, Vendlova J, Zachleder (1972) The coupling of synthetic and reproduction processes in *Scenedesmus quadricauda*. *Arch Hydrobiol* 41(2)(41): 172-213
- Šetlík I, Zachleder V (1984) The multiple fission cell reproductive patterns in algae. *The microbial cell cycle*. P. Nurse and E. Streiblová. Boca Raton, Florida, USA, CRC Press Inc.:253-279
- Terashima M, Freeman ES, Jinkerson RE, Jonikas MC (2014) A fluorescence-activated cell sorting-based strategy for rapid isolation of high-lipid *Chlamydomonas* mutants. *Plant J* 81:147-159
- Tukaj Z, Kubínová A, Zachleder V (1996) Effect of irradiance on growth and reproductive processes during the cell cycle in *Scenedesmus armatus* (Chlorophyta) *J Phycol* 32:624-631
- Vítová M, Bišová K, Hlavova M, Kawano S, Zachleder V, Cizkova M (2011) *Chlamydomonas reinhardtii*: duration of its cell cycle and phases at growth rates affected by light intensity. *Planta* 233(1):75-86
- Vítová M, Hendrychová J, Cepak V, Zachleder V (2005) Visualization of DNA-containing structures in various species of Chlorophyta, Rhodophyta and Cyanophyta using SYBR green I dye. *Folia Microbiol* 50:333-340
- Vítová M, Zachleder V (2005) Points of commitment to reproductive events as a tool for analysis of the cell cycle in synchronous cultures of algae. *Folia Microbiologica* 50(2):141-149
- Wanka F, (1962) Die bestimmung der nucleinsäuren in *Chlorella pyrenoidosa*. *Planta* 58:594-619
- Wanka F, (1975) Possible role of the pyrenoid in the reproductional phase of the cell cycle of *Chlorella*. *Colloq Intern C.N.R.S.* 240:132-136
- Wu H, Volponi JV, Oliver AE, Parikh AN, Simmons BA, Singh S (2011) In vivo lipidomics using single-cell Raman spectroscopy. *Proc Natl Acad Sci U S A* 108(9):3809-14

- Xie B, Stessman D, Hart JH, Dong H, Wang Y, Wright DA, Nikolau BJ, Spalding MH, Halverson LJ (2014) High-throughput fluorescence-activated cell sorting for lipid hyperaccumulating *Chlamydomonas reinhardtii* mutants. *Plant Biotechnol journal* 12(7):872-882
- Zachleder V (1984) Optimization of nucleic acids assay in green and blue-green algae: Extraction procedures and the light-activated reaction for DNA. *Archiv für Hydrobiologie* 36: 313-328
- Zachleder V (1997) The course of reproductive events in the chloroplast cycle of the chlorococcal alga *Scenedesmus quadricauda* as revealed by using inhibitors of DNA replication. *Plant Cell Physiol* 38:56
- Zachleder V, Bišová K, Vitova M (2016) The cell cycle of microalgae. The physiology of microalgae. Borowitzka MA, Beardall J Raven JA. Dordrecht, Springer 6: 3-46
- Zachleder V, Bišová K, Vitova M, Kubin S, Hendrychova J (2002) Variety of cell cycle patterns in the alga *Scenedesmus quadricauda* (Chlorophyta) as revealed by application of illumination regimes and inhibitors. *Eur J Phycol* 37(3):361-371
- Zachleder V, Cepák V (1987) Visualization of DNA containing structures by fluorochrome DAPI in those algal cells which are not freely permeable to the dye. *Archiv für Hzdrobiologie* 47:157-168
- Zachleder V, Doucha J, Berkova E, Šetlík I (1975) The effect of synchronizing dark period on populations of *Scenedesmus quadricauda*. *Biol Plantarum* 17: 416-433
- Zachleder V, Schläfli O, Boschetti A (1997) Growth-controlled oscillation in activity of histone H1 kinase during the cell cycle of *Chlamydomonas reinhardtii* (Chlorophyta). *J Phycol* 33:673-681
- Zachleder V, Šetlík I (1982) Effect of irradiance on the course of RNA synthesis in the cell cycle of *Scenedesmus quadricauda*. *Biol Plantarum* 24(5): 341-353
- Zachleder V, Šetlík I (1988) Distinct controls of DNA-replication and of nuclear division in the cell-cycles of the chlorococcal alga *Scenedesmus quadricauda*. *J Cell Sci* 91:531-539
- Zachleder V, Šetlík I (1990) Timing of events in overlapping cell reproductive sequences and their mutual interactions in the alga *Scenedesmus quadricauda*. *J Cell Sci* 97:631-638
- Zachleder V, van den Ende H (1992) Cell-cycle events in the green alga *Chlamydomonas eugametos* and their control by environmental factors. *J Cell Sci* 102: 469-474

Appendix

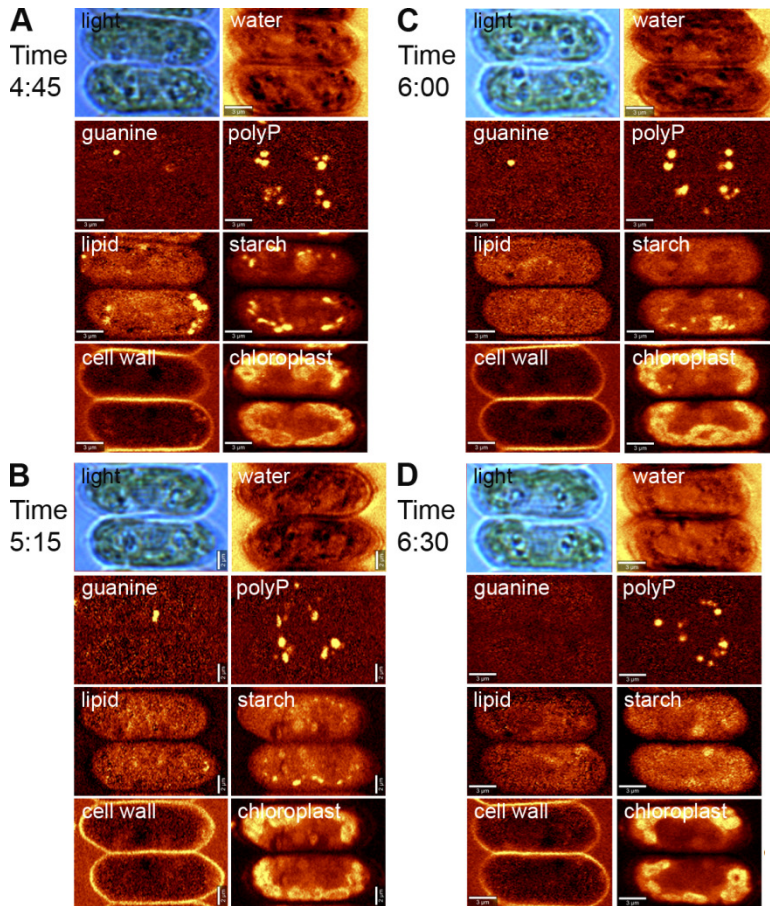
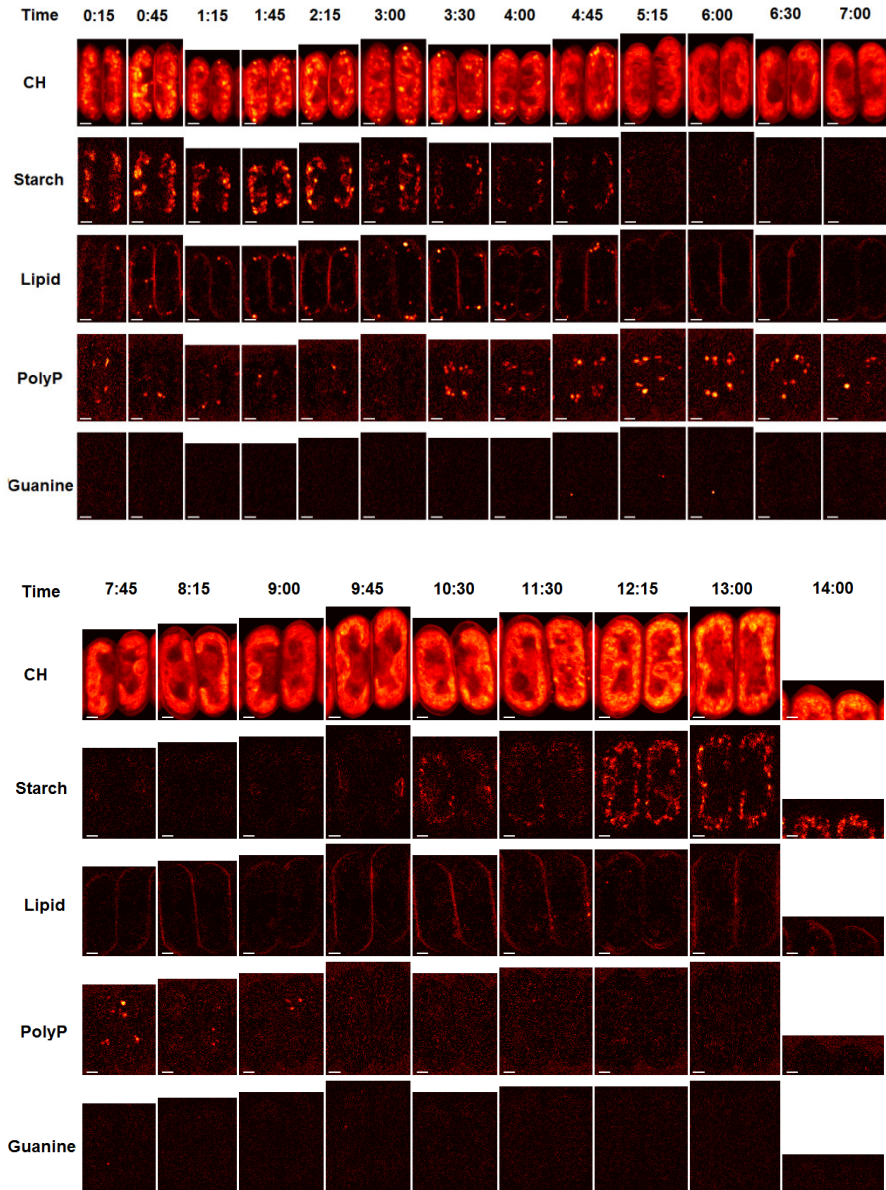


Figure 5-S1: Comparison of light microscopy and Raman maps showing distribution of water, guanine, polyP, lipids, starch, cell wall and chloroplasts in the same two innermost cells of eight-celled coenobia of *D. quadrica* at different time points of the cell cycle. Time shown is since the beginning of the cell cycle.



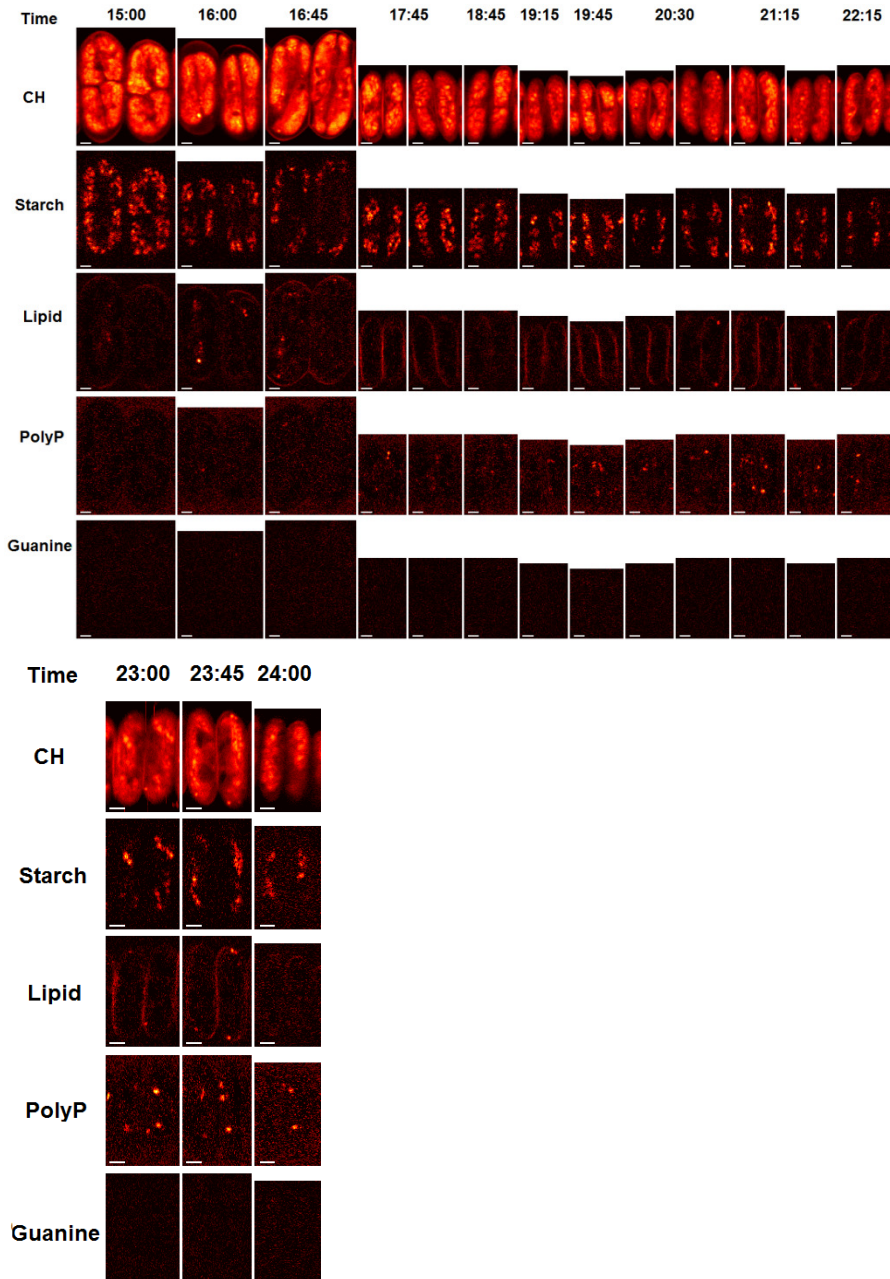


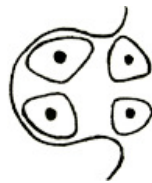
Figure 5-S2 (Continued from the previous page): Raman maps showing the distribution of carbon-hydrogen (C-H) groups, starch, lipids, and polyphosphates in two innermost cells of eight-celled coenobia during the cell cycle (C). Time from start of the cycle is indicated in the top row. For a given biomolecule, the color scale is the same for all Raman maps. The white bars correspond to 2 μm .

Coordination of growth and cell cycle progression in green algae

Chapter VIII

Summary

Ivan N. Ivanov



6.1 Goals and hypothesis

As we already discussed in chapters I and III the prevailing notion in the field of cell cycle research is that there is a supposed direct connection between growth and cell cycle progression. An immediate consequence of this hypothesis is the proposition of the existence of a mechanism for determination of a minimum cell size before the progression of the cell cycle can take place. This concept led to the development of a variety of models attempting to explain this putative connection between growth and cell cycle progression. However, the hypothesis of cell size (or any of its other determinants) being directly involved in controlling the progression of the cell cycle was rather unexpectedly called into question by our results in chapter IV. Our experiments with *D. quadricauda* revealed that temperature profoundly influenced cell size and cell cycle duration, with the cells grown at 20 °C having twice larger cell size and taking almost twice as long to complete their cell cycle compared to the cells at 30 °C, which were smaller and had a shorter cell cycle. The most intriguing were the results of the shift experiments, where cells grown in light at either 20 °C or 30 °C were transferred to darkness to prevent further growth, and then cultivated at the same or different temperature. If there was to be any direct connection between critical cell size and attainment of CP the cell cycle was expected to continue after the transfer, similarly to the control culture at the original temperature, albeit with different kinetics imposed by the difference in temperature. In contrast, if the opposite was true, namely that there is no direct connection between critical cell size and attainment of CP, then after the change of temperature the progression of the cell cycle should differ from that of the control culture. To our surprise the results confirmed the second hypothesis. Cells transferred from 30 °C in light to 20 °C in dark produced fewer nuclei and daughter cells, and some of them were unable to undergo cell division. Correspondingly, cells transferred from 20 °C in light to 30 °C in dark divided faster and into more daughter cells than the controls. These differences correlated with shifts in the CDK activity but they did not

correlate with cell size. This is in clear contradiction with the size hypothesis, which postulates that cell size determines the extent of cell cycle progression and suggests that in *D. quadricauda*, progression of the cell cycle is not cell size dependent. This suggests that in contrast to light, the role of temperature in timing of the cell cycle events goes beyond its effect on growth rate and metabolism.

To further investigate the effect of temperature on cell cycle events we conducted experiments with supraoptimal temperature - this time in the other model alga *C. reinhardtii*. The results presented in chapter V provide evidence that supraoptimal temperature causes the formation of abnormally large cells which have increased starch content. The supraoptimal temperature affected the ability of cells to divide in particular, but it did not seem to affect their synthetic processes. This was best illustrated by the complete lack of cell division at the supraoptimal temperature while in the same time growth appeared to be unaffected and was comparable to that at the optimal growth temperature. Furthermore, synthesis of nucleic acids and peaks in CDK activity were shifted in time, but they were still clearly present. This indicates that temperature does affect the cell cycle steps leading to DNA replication to an extent that causes their delay, however this cannot explain the complete absence of nuclear and cellular division observed at the supraoptimal temperature. In fact, our results point out that it is very likely that the cell cycle event which is inhibited by the supraoptimal temperature is related to the process of nuclear division. Be as it may, at this point we cannot provide further experimental evidence as to pinpoint the precise location of this supraoptimal temperature switch, thus a further inquiry in this direction is needed.

Another important feature of the cells treated with supraoptimal temperature was the accumulation of starch as a superfluous energy reserve due to the inhibition of cell division. This stems directly from the fact that both growth and carbon metabolism remained unaffected by the exposure to supraoptimal temperature facilitating the formation of formidable starch reserves when compared to the cultures grown at the

optimal temperature. An important observation here was the fact that the supraoptimal temperature effect could be negated by a subsequent transfer back to optimal growth temperature proving that up to a certain point temperature influence did not cause any permanent disruption of the cell cycle machinery or the growth related metabolism. However, both starch accumulation and growth rates were delayed after 18 hours at supraoptimal temperature hinting that prolonged exposure can have a detrimental impact on the cell. These intrinsic observations of the effect of supraoptimal temperature on the cell cycle and growth related processes in *C. reinhardtii* reaches beyond the field of fundamental research and can potentially have profound implications for applied research and in particular for microalgae derived biofuels.

In order to build upon these results, we next explored the implications of our thus far fundamental knowledge about the influence of temperature on the cell cycle from a biotechnological point of view. In chapter VI we investigated the potential of turning *C. reinhardtii* into a platform for commercial starch production. We made this attempt by exploiting the presumed connection between the inhibition of cell division by supraoptimal temperature and the over accumulation of starch. We demonstrated that this approach for starch synthesis can be successfully applied to large volumes of algal culture in conditions that are similar to a putative industrial production process. In doing so, we investigated the influence of culture density and hence light availability within the culture and we explored the possibility for recovery of the culture after the supra optimal temperature treatment. The results of our experiments indicated that the major bottleneck in such a production process lies within the ability to provide enough light per cell that can be converted into starch. This indicates that restrictions for the production process are not of physiological but rather of technical nature. Hence, engineering solutions directed at improving bioreactor design and light penetration within the algal culture are of vital importance for the economic viability of the process. Our experiments also demonstrated the prospect of culture recovery after the supraoptimal temperature treatment. Such an option

combined with the rapid starch accumulation can render our starch synthesis process with a competitive advantage over conventional starch producing provided that the previously mentioned technical challenges are met.

Much of the data in this thesis describing growth related processes was obtained by conventional biochemical analysis of macromolecules. However, such analysis is often time consuming, labour intensive and requires large sample volumes. In chapter VII we, in collaboration with our partners from the Institute of Physics of Charles University in Prague, investigated the use of confocal Raman microscopy as an alternative to conventional biochemical analysis. One of the big advantages of this technique is that it allows for the analysis of several compounds at the same time on a single cell level. Moreover, confocal Raman microscopy enables the study of compounds, such as guanine, that are otherwise impossible to detect by other means. With such tools the relation of molecule formation to cellular compartments can be determined and observed. Hence, confocal Raman microscopy can provide valuable information about the spatial localization of different molecules and their formation or degradation in the course of time. Another major advantage of confocal Raman microscopy is its high sensitivity for certain compounds when compared to biochemical analysis or fluorescence microscopy. This was illustrated during our experiments by the detection of lipid bodies at concentrations that otherwise could not be observed with conventional fluorescence microscopy.

6.2 Conclusions

In order to summarise the crucial messages of this work we will turn back to the combinations of working and null hypotheses that we formulated at the end of chapter II. In doing so we can state that:

According to our data we must **accept null hypothesis 1**. That is to say the cell cycle progression in *D. quadricauda* does not appear to be in direct

correlation with the cell growth processes and the attainment of critical cell size.

Extensive research in both laboratory and pilot scale experiments indicate that **working hypothesis 2** is to be **accepted**. Supraoptimal temperature does inhibit the cell cycle in *C. reinhardtii* causing cell cycle arrest leading to over accumulation of starch.

As demonstrated by our pilot scale experiments **working hypothesis 3** is **correct**. Production of starch through supraoptimal temperature in *C. reinhardtii* is possible in pilot scale. However, it must be stated that the economic viability of such a process can be vulnerable to technical challenges.

Our work of comparing confocal Raman microscopy with biochemical analyses reveals that **working hypothesis 4** is to be considered as **true**. Polyphosphates and a variety of other macromolecules in *D. quadricauda* can be successfully observed and quantified using confocal Raman microscopy. Not only that but the Raman technique provides a wealth of data that is unparalleled by any approach of biochemical analysis.

6.3 Looking forward

The current thesis presents studies on the mechanisms of mutual coordination between growth and cell cycle progression in green algae. It furthermore explores the practical application of some of the results and explores the use of confocal Raman microscopy as a novel technique for analysis of macromolecules in microalgae.

Future work may include efforts directed at unravelling the molecular mechanisms of coordination between growth processes, attainment of CP and cell cycle progression in *D. quadricauda*. Such work will be facilitated by the fact that the genome of *D. quadricauda* has already been fully sequenced and annotated (Nag Dasgupta et al. 2018). This will enable the

reconstruction of metabolic pathways associated with growth and cell cycle progression in this particular organism. Not only that, but having the complete genome sequence of *D. quadricauda* may allow for the location and study of cell cycle associated genes responsible for the attainment of CP and will enable the establishment of their regulatory pathways.

Another fascinating future research project will be to repeat the temperature shift experiments in another phylogenetically distant group of algae such as the phyla Rhodophyta. Although, as we have already established, the principles of cell cycle regulation have been conserved throughout much of the eukaryotic kingdom, some evolutionary conditioned differences can still occur. It will be extremely interesting to see whether our findings about the lack of direct connection between cell cycle progression and cell growth in *D. quadricauda* can be confirmed in another, evolutionary distant organism. A possible candidate for such experiments can be *C. merolae*. This single cellular red alga has a cell cycle that has been well studied and can be easily cultivated in synchronous cultures making it a suitable complement to *D. quadricauda* for future experiments (Fujiwara 2017; Suzuki et al. 1994).

For biotechnological applications, it might be interesting to study how supraoptimal temperature affects the accumulation and overall productivity of starch in other biotechnologically relevant microalgae such as *Chlorella* sp.. Although starch synthesis as a result of supraoptimal temperature treatment has been already described in *Chlorella vulgaris* no large scale cultivation attempts utilizing this method have been made so far (Šetlík et al. 1975). Furthermore, it might be also of interest to investigate the effect of supraoptimal temperature on the synthesis of other economically important compounds such as lipids as well as the use of more efficient cultivation models that can increase productivity and reduce production costs.

Overall, it may be said that the question of elucidating the mechanism for coordination between growth and cell cycle progression is so significant for our understanding of the natural world that in all probability research interests in this field will remain strong for the foreseeable future.

6.4 References

- Nag Dasgupta C, Nayaka S, Toppo K, Singh AK, Deshpande U, Mohapatra A (2018) Draft genome sequence and detailed characterization of biofuel production by oleaginous microalga *Scenedesmus quadricauda* LWG002611. *Biotechnol Biofuels* 11: 308
- Fujiwara T (2017) Cell Cycle and Organelle Division Cycle in *Cyanidioschyzon merolae*. In: Kuroiwa T. et al. (eds) *Cyanidioschyzon merolae*. Springer, Singapore
- Šetlík I, Zachleder V, Doucha J, Berková E, Bartoš J (1975) The nature of temperature block in the sequence of reproductive processes in *Chlorella vulgaris* Beijerinck. *Arch Hydrobiol Suppl* 49 *Algol Stud* 14:70–104
- Suzuki K., Ehara T., Osafune T., Kuroiwa H., Kawano S., Kuroiwa T. (1994): Behavior of mitochondria, chloroplasts and their nuclei during the mitotic cycle in the ultramicroalga *Cyanidioschyzon merolae*. *Eur J Cell Biol* 63:280–288

About the author

Ivan Nedyalkov Ivanov was born on April 22nd, 1985 in Dimitrovgrad, Bulgaria. He attended the „Ivan Vazov” High School of Mathematics and Natural Sciences where he obtained his diploma in 2004. In the following turbulent years, Ivan attended a number of universities including the „St. Kliment Ohridski” University of Sofia, the ”Carl von Ossietzky” University of Oldenburg and the University of Bremen. In 2009 he started his Bachelor of Science in Technical and Applied Biology at the Bremen University of Applied Sciences. During his studies he did an Erasmus stay at Linnaeus University and did an internship at the Laboratory of Algal Physiology and Biotechnology of Dr. Ladislav Nedbal at Czech Globe. During his bachelor thesis he worked at the Laboratory of Marine Biotechnology of Prof. Dr. Gerd Klöck. His work focused on the quality assurance aspects of a project which explored the potential of microalgal feed production in combination with bioremediation of aquaculture waste water. He obtained his B.Sc. in 2013 and continued with a Master of Science in Technical and Applied Biology at the Bremen University of Applied Sciences. For his M.Sc. thesis project Ivan moved to the Laboratory of Cell Cycle of Algae in Třeboň where he worked on the directed synthesis of storage lipids in the alga *Parachlorella kessleri*. He obtained his M.Sc. degree in 2014 and in 2015 he started his doctoral research at the Laboratory of Cell Cycle of Algae in Třeboň. During his Ph.D. project Ivan was awarded a travel fellowship which he spent at the Bioprocess Engineering group at Wageningen University and Research. The results of his Ph.D. research are described in this thesis.



Contact information: ivanov@alga.cz

List of publications

- I. Takeshita T, **Ivanov IN**, Oshima K, Ishii K, Kawamoto H, Ota S, Yamazaki T, Hirata A, Kazama Y, Abe T, Hattori M, Bišová K, Zachleder V, Kawano S (2018) Comparison of lipid productivity of *Parachlorella kessleri* heavy-ion beam irradiation mutant PK4 in laboratory and 150-L mass bioreactor, identification and characterization of its genetic variation. *Algal Res* 35:416-426 doi:10.1016/j.algal.2018.09.005
- II. Zachleder V, **Ivanov IN**, Vítová M, Bišová K (2019) Effects of cyclin-dependent kinase activity on the coordination of growth and the cell cycle in green algae at different temperatures. *J Exp Bot* 70(3):845-858 doi:10.1093/jxb/ery391
- III. Zachleder V, **Ivanov IN**, Vítová M, Bišová K (2019) Cell cycle arrest by supraoptimal temperature in the alga *Chlamydomonas reinhardtii*. *Cells* 8(10):1237 doi:10.3390/cells8101237
- IV. **Ivanov IN**, Vítová, M, Bišová K (2019) Growth and the cell cycle in green algae dividing by multiple fission. *Folia Microbiol* 64:663–672 doi:10.1007/s12223-019-00741-z
- V. Moudříková Š, **Ivanov IN**, Nedbal L, Zachleder V, Bišová K, Mojzeš P Raman microscopy shows the distribution of starch, lipids, polyphosphate and guanine during the cell cycle of *Desmodesmus quadricauda*. (Manuscript in preparation)
- VI. **Ivanov IN**, Vítová M, Zachleder V, Barbosa MJ, Bišová K Starch production in *Chlamydomonas reinhardtii* through supraoptimal temperature treatment cultivated in a pilot-scale photobioreactor. (Manuscript in preparation)

© for non-published parts Ivan Nedyalkov Ivanov

ivanov@alga.cz

Coordination of growth and cell cycle progression in green algae, Ph.D. Thesis Series, 2020, No. 17

All rights reserved
For non-commercial use only

Printed in the Czech Republic by Typodesign
Edition of 20 copies

University of South Bohemia in České Budějovice
Faculty of Science
Branišovská 1760
CZ-37005 České Budějovice, Czech Republic

Phone: +420 387 776 201
www.prf.jcu.cz, e-mail: sekret-fpr@prf.jcu.cz